

Progress in
10 Clinical Biochemistry
and Medicine

Ruthenium and Other Non-Platinum Metal Complexes in Cancer Chemotherapy

With contributions by

E. Alessio, W. M. Attia, M. R. Berger, V. Brabec,
J.-L. Butour, A. M. Casazza, M. Calligaris, S. Cauci,
M. J. Clarke, M. Defais, L. Dolzani, H. Flechtner,
N. Farrell, M. E. Heim, M. Henn, N. P. Johnson,
U. M. Juhl, B. K. Keppler, P. Köpf-Maier, B. H. Long,
L. G. Marzilli, L. F. Mausner, H. A. Meinema,
G. Mestroni, C. Monti-Bragadin, R. Niebl, S. Pacor,
V. Pierson, F. Quadrifoglio, G. Sava, J. E. Schurig,
E. V. Scott, S. C. Srivastava, M. Tamaro, K. Timmer,
G. Villani, F. E. Wagner, F. L. Wimmer, G. Zon,
S. Zorzet

With 99 Figures



Springer-Verlag Berlin Heidelberg New York
London Paris Tokyo Hong Kong

ISBN-13:978-3-642-74762-5 e-ISBN-13:978-3-642-74760-1
DOI: 10.1007/978-3-642-74760-1

The Library of Congress has cataloged this serial title as follows:

Progress in clinical biochemistry and medicine.
1 — Berlin; New York: Springer-Verlag, [c1984—, v. : ill. ; 25 cm.
Irregular. Title from cover.
ISSN 0177-8757 = Progress in clinical biochemistry and medicine.
1. Clinical biochemistry — Collected works.
I. Title: Clinical biochemistry and medicine.
[DNLM: 1. Biochemistry — periodicals. 2. Medicine — periodicals. W1PR668EM]
RB112.5.P76 610'.5 — dc19 86-644052 AACR 2 MARC-S
Library of Congress [8701]

This work is subject to copyright. All rights are reserved, whether the whole or part of the material is concerned, specifically the rights of translation, reprinting, reuse of illustrations, recitation, broadcasting, reproduction on microfilms or in other ways, and storage in data banks. Duplication of this publication or parts thereof is only permitted under the provisions of the German Copyright Law of September 9, 1965, in its version of June 24, 1985, and a copyright fee must always be paid. Violations fall under the prosecution act of the German Copyright Law.

© Springer-Verlag Berlin Heidelberg 1989
Softcover reprint of the hardcover 1st edition 1989

The use of registered names, trademarks, etc. in this publication does not imply, even in the absence of a specific statement, that such names are exempt from the relevant protective laws and regulations and therefore free for general use.

2151/3020-543210 — Printed on acid-free paper

Preface

This volume contains the plenary lectures of a symposium on "Ruthenium and Other Non-Platinum Metal Complexes in Cancer Chemotherapy" sponsored by the University of Trieste, the Italian Chemical Society and the Regione Autonoma Friuli-Venezia Giulia. Professors G. Mestroni and G. Sava and Dr. E. Alessio of the University of Trieste and E. Quadrifoglio of the University of Udine, were particularly responsible for its efficient organization and the gracious atmosphere under which the meeting was conducted.

Owing to the remarkable success of the platinum-containing anticancer drug cisplatin (*cis*-dichlorodiammineplatinum(II)), an introductory paper by Neil P. Johnson detailing the mechanism of this and related platinum pharmaceuticals opens the volume. As is suggested in the second paper, the initial site of attack of platinum and ruthenium chemotherapeutic agents is likely to be the same. However, the exact mechanism of the two are probably different. Indeed, as is pointed out in the paper by Bernhard K. Keppler, ruthenium compounds are often active against platinum-resistant tumors. Likely reasons for this are the differences in the geometric structure of the generally square-planar platinum compounds and the ruthenium species, which are nearly always octahedral. Moreover, the ruthenium compounds investigated so far are much more likely to undergo changes in oxidation state *in vivo* than the platinum(II) drugs. On the other hand, correlations may yet emerge between the few octahedral platinum(IV) compounds now in testing and active ruthenium(III) compounds.

The relatively low toxicity of ruthenium compounds is well illustrated in Giovanni Mestroni's contribution, which introduces the chemical intricacies in the dimethylsulfoxide class of ruthenium antitumor agents. An alternative approach to cancer therapy is presented by Nicholas Farrell, who has begun to achieve success in using metal complexes to coordinate radiosensitizing agents to the DNA target molecule. Synergisms between the metal complex and ligands, which are themselves radiosensitizers, may increase the effectiveness of ionizing radiation in treating inoperable cancers. The use of ruthenium radioisotopes as a means of imaging internal organs and visualizing their functioning in real time is discussed in the article by Suresh C. Srivastava. The useful chemical and radiophysical properties of ^{97}Ru make it especially promising as the gamma-emitting nuclide of choice in the development of agents to mark, locate and size tumors to diagnose the stage of progression of cancer or to indicate the efficacy of treatment.

The use of elements other than those in the platinum group is introduced by Petra Köpf-Maier, whose variety of complexes with cyclopentadienyl ligands has

opened an entirely new front in the development of metal-containing anticancer pharmaceuticals. The following paper by Luigi Marzilli presents an exciting new approach to ascertaining the effects of anticancer drugs at the molecular level by illustrating the first use of a paramagnetic metal complex to determine the mode of binding of drugs to DNA by NMR spectroscopy. The contribution by John Schurig suggests that phosphine ligands may be especially useful in the design of some anticancer pharmaceuticals, and the final paper by M. E. Heim and B. K. Keppler presents the initial clinical results of a budotitane, which is the first titanium anticancer drug to be tested on humans.

Following each paper presented at the meeting, there were enthusiastic discussions concerning: the mechanism of action of ruthenium and other metal complexes now in testing, indications of clinical activity through in vitro and in vivo screening procedures, the desirability of particular pharmacological properties in new complexes, the role of different types of ligands in various drugs, methods of optimizing drug efficacy and reducing toxicity on both the molecular and clinical levels, and many other aspects of chemistry, biochemistry, biology and oncology in an effort to determine the best approaches toward the design of metal-containing anticancer pharmaceuticals. It is our hope in producing this volume that these papers will stimulate a similar interest and discussion among those already in this field or considering entering it.

Chestnut Hill, Massachusetts
March, 1989

Michael J. Clarke

Editorial Board

- Prof. Dr. Etienne Baulieu* Université de Paris Sud, Département de Chimie
Biologique, Faculté de Médecine de Bicêtre,
Hôpital de Bicêtre, F-94270 Bicêtre/France
- Prof. Dr. Donald T. Forman* Department of Pathology, School of Medicine,
University of North Carolina
Chapel Hill, NC 27514/USA
- Prof. Dr. Magnus
Ingelman-Sundberg* Karolinska Institutet Institutionen för
Medicinsk Kemi Box 60400
S-104 01 Stockholm/Sweden
- Prof. Dr. Lothar Jaenicke* Universität Köln, Institut für Biochemie
An der Bottmühle 2
D-5000 Köln 1/FRG
- Prof. Dr. John A. Kellen* Sunnybrook Medical Centre, University
of Toronto, 2075 Bayview Avenue
Toronto, Ontario, Canada M4N 3M5
- Prof. Dr. Yoshitaka Nagai* Department of Biochemistry, Faculty
of Medicine, The University of Tokyo
Bunkyo-Ku, Tokyo/Japan
- Prof. Dr. Georg F. Springer* Immunochemistry Research, Evanston Hospital
Northwestern University, 2650 Ridge Avenue,
Evanston, IL 60201/USA
- Prof. Dr. Lothar Träger* Klinikum der Johann Wolfgang Goethe-
Universität, Gustav-Embden-Zentrum
Theodor Stern Kai 7
D-6000 Frankfurt a. M. 70/FRG
- Prof. Dr. Liane Will-Shahab* Akademie der Wissenschaften der DDR
Zentralinstitut für Herz- und Kreislauf-Forschung
Lindenberger Weg 70
DDR-1115 Berlin-Buch
- Prof. Dr. James L. Wittliff* Hormone Receptor Laboratory, James Graham
Brown Cancer Center, University of Louisville
Louisville, KY 40292/USA

Table of Contents

Metal Antitumor Compounds: The Mechanism of Action of Platinum Complexes N. P. Johnson, J.-L. Butour, G. Villani, F. L. Wimmer, M. Defais, V. Pierson, V. Brabec	1
Ruthenium Chemistry Pertaining to the Design of Anticancer Agents M. J. Clarke	25
New Ruthenium Complexes for the Treatment of Cancer B. K. Keppler, M. Henn, U. M. Juhl, M. R. Berger, R. Niebl, F. E. Wagner . . .	41
Chemical, Biological and Antitumor Properties of Ruthenium(II) Complexes with Dimethylsulfoxide G. Mestroni, E. Alessio, M. Calligaris, W. M. Attia, F. Quadrifoglio, S. Cauci, G. Sava, S. Zorzet, S. Pacor, C. Monti-Bragadin, M. Tamaro, L. Dolzani . . .	71
Metal Complexes as Radiosensitizers N. Farrell	89
Radioruthenium-Labeled Compounds for Diagnostic Tumor Imaging S. C. Srivastava, L. F. Mausner, M. J. Clarke	111
The Antitumor Activity of Transition and Main-Group Metal Cyclopentadienyl Complexes P. Köpf-Maier	151
NMR Relaxation Footprinting: The $[\text{Cr}(\text{NH}_3)_6]^{3+}$ Cation as a Probe for Drug Binding Sites on Oligonucleotides E. V. Scott, G. Zon, L. G. Marzilli	185
Antitumor Activity of Bis[Bis(Diphenylphosphino)Alkane and Alkene] Group VIII Metal Complexes J. E. Schurig, H. A. Meinema, K. Timmer, B. H. Long, A. M. Casazza	205
Clinical Studies with Budotitane — A New Non-Platinum Metal Complex for Cancer Therapy M. E. Heim, H. Flechtner, B. K. Keppler	217
Author Index Volumes 1–10	225

Metal Antitumor Compounds: The Mechanism of Action of Platinum Complexes

Neil P. Johnson¹, Jean-Luc Butour¹, Giuseppe Villani¹, Franz L. Wimmer¹,
Martine Defais¹, Veronique Pierson¹, and Viktor Brabec²

¹ Laboratoire de Pharmacologie et de Toxicologie Fondamentales, CNRS, 205, Route de Narbonne, Toulouse 31077, France

² Institute of Biophysics, Czechoslovak Academy of Sciences, Brno 12, Kralovopolska 135, Czechoslovakia

Cisplatin (*cis*-diamminedichloroplatinum(II)) is widely used in the treatment of testicular and ovarian cancers. A number of biological and biochemical results indicate that the reaction of cisplatin with DNA is responsible for the cytotoxic action of this drug. The effect of platinum compounds on the conformation and stability of DNA has been investigated and several platinum-DNA adducts have been identified *in vitro* and *in vivo*. Preliminary experiments have quantified the effect of these different lesions on DNA replication, their capacity to induce mutations and their susceptibility to DNA repair processes. Additional DNA damage may be created by platinum(IV) compounds, perhaps during their reduction to platinum(II) compounds by the cell.

1 Introduction	2
2 The Target	2
2.1 The Drug Binds to DNA at Pharmacological Doses	3
2.2 Selective and Irreversible Inhibition of DNA Synthesis	3
2.3 Higher Toxicity in Cells which are Deficient in DNA Repair	3
2.4 Structure Activity Relations	5
2.5 Synergism and Antagonism	6
2.6 Summary	8
3 The Reaction of Cisplatin with DNA <i>in vitro</i>	9
3.1 Physical Chemical Studies of Platinum-DNA Complexes	10
3.2 Platinum-DNA Adducts	12
4 Biological Effects of Platinum-DNA Adducts	15
4.1 Effect of Platinum-DNA Adducts on DNA Replication <i>in vitro</i>	15
4.2 Repair of Platinum-DNA Adducts	16
4.3 Mutagenic Platinum-DNA Adducts	17
5 Metal Oxidation State and Antitumor Activity	17
6 Acknowledgements	20
7 References	20

1 Introduction

Cisplatin, *cis*-diamminedichloroplatinum(II), is a transition metal complex whose introduction in the clinic 10 years ago has reversed the prognosis of testicular cancer. It is also active against ovarian carcinoma and responses of bladder cancer and head and neck cancer have been reported¹⁾. However, the drug has a number of undesirable side effects including nephrotoxicity, vomiting and nausea, myelosuppression and neurotoxicity. In addition, the development of resistance by tumors previously treated with cisplatin is a serious clinical problem. As a result, hundreds of platinum derivatives have been synthesized and tested. Of a dozen potential second generation compounds, carboplatin entered clinical trials in the hope of overcoming some of the toxic effects of the parent compound²⁾. Several review articles on the mechanism of action of this compound are available³⁻¹¹⁾.

Antitumor activity is a complex phenomenon for which various aspects such as biodistribution, toxicity, cytotoxicity and resistance may have different targets and mechanisms of action. For example, the available cisplatin is limited by its complexation with blood proteins which inactivate the drug¹²⁾. The dose-limiting nephrotoxicity of cisplatin is probably a consequence of interactions between the drug and specialized cells of the kidney¹³⁾. We will restrict this article to the cytotoxic effect of cisplatin.

This topic can be divided into three parts: first, identifying the cellular target of the drug; second, the chemical nature of the drug-target interaction; and third, mechanisms by which the modified target molecules produce the cytotoxic effect. In addition, we have examined the influence of platinum redox reactions and their resulting DNA lesions on the cytotoxic effect of cisplatin.

2 The Target

The target may be defined as a site within the cell which is altered by the drug and whose modification leads to cell death. Transition metal complexes are often electrophilic and may react with many cellular components. Only a few of these lesions, those which lead to cell death, would be considered the target.

Cisplatin covalently binds to cellular DNA and the platinum-DNA complex can be isolated¹⁴⁾. It has numerous genotoxic effects which are characteristic of drugs which cause DNA damage. For example, the compound is mutagenic in bacteria^{15, 16)} and mammalian cells^{17, 18)} where it also produces chromosomal abnormalities¹⁹⁻²²⁾. It inhibits bacteriophages²³⁾ and transforming DNA²⁴⁻²⁶⁾. It activates SOS functions such as bacterial filamentation²⁷⁾ and prophage induction^{28, 29)}. (The SOS response is caused by DNA lesions which block the replication fork³⁰⁾.) Although it is clear from these results that cisplatin binds to DNA, it is less evident whether or not DNA-binding is responsible for the cytotoxic activity of the drug. Couldn't binding at another target, e.g., a protein or membrane, cause the pharmacological effect of this compound?

The following paragraphs summarize a number of key experiments which suggest that platinum-DNA lesions are the critical lesions which inhibit replication and kill the tumor cell.

Table 1. Platinum molecules bound to macromolecules when survival of HeLa cells is reduced to $1/e$ ¹⁴⁾

	<i>cis</i> -DDP	<i>trans</i> -DDP
DNA	22	125
mRNA	1/8	2.5
rRNA	1/30	1/2
tRNA	1/1500	1/70
protein	1/1500	nd

2.1 The Drug Binds to DNA at Pharmacological Doses

After treatment of CHO cells with toxic doses of cisplatin, only about 10% of the intracellular platinum binds to DNA ¹⁷⁾. This might suggest that DNA-binding is a relatively unimportant event. It is instructive, however, to compare the fixation of cisplatin to various macromolecules after treatment with a dose which produces one mean lethal event per cell (Table 1). Cisplatin binds to RNA and proteins as well as to DNA ¹⁴⁾. Assuming random binding at the various nucleophilic sites, DNA is the only macromolecule for which the entire population has reacted with the drug. This is not a consequence of greater reactivity of DNA, but rather of its size. Any proposal that another type of macromolecule, e.g. a protein, is responsible for the cytotoxicity would require a mechanism for selective reaction of cisplatin with the target.

2.2 Selective and Irreversible Inhibition of DNA Synthesis

Painter ³¹⁾ has suggested that persistent inhibition of DNA synthesis might indicate that an antimetabolic drug acts by binding to DNA. Drugs which act by another mechanism, such as depletion of an essential precursor, would inhibit replication until the cell synthesizes the missing ingredient, after which replication can continue. In this case, S phase is prolonged until the limiting factor can be replaced by the cell.

DNA, RNA and protein synthesis are inhibited following treatment of mammalian cells with cisplatin ^{32, 33)} (Fig. 1). However, Thd incorporation decreases before Urd or Leu. Furthermore, RNA and protein synthesis recover after several hours whereas DNA synthesis remains depressed. Selective and persistent inhibition of DNA synthesis suggests that inhibition of replication is responsible for cell death. Similarly, the toxicity of cisplatin toward bacteria seems to be associated with the inhibition of replication rather than the inhibition of RNA or protein synthesis ³⁴⁾.

2.3 Higher Toxicity in Cells which are Deficient in DNA Repair

This approach uses genetics to detect the target responsible for cytotoxicity. It consists of introducing a mutation which alters the manner in which the cell processes

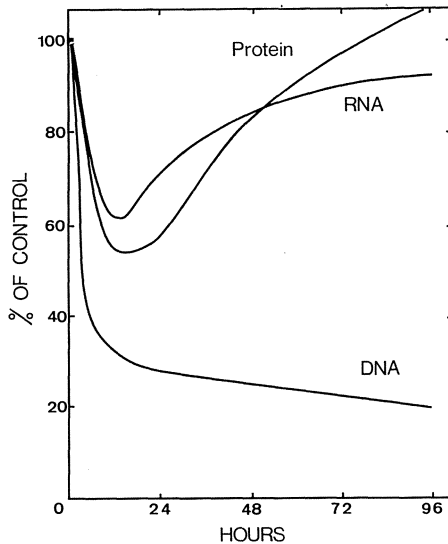


Fig. 1. DNA, RNA and protein synthesis by Ehrlich ascites tumor cells. The tumor was implanted in mice and treated with a single intraperitoneal dose of cisplatin. Cells were subsequently removed at various times and incorporation was measured in vitro (from ³²)

the lesion. For example, the persistence of DNA adducts depends on the capacity of cells to repair the damage. A point mutation is introduced in a gene for one of the proteins necessary for the repair of DNA. Other cellular properties such as the uptake of the drug or its reactions in the cytoplasm are unchanged. Hence, the desired modification is the only variable introduced and the effect of a drug can be compared in several mutant strains for which intracellular concentrations and DNA-binding are unchanged.

Bacteria which are deficient in DNA repair are more sensitive to killing by cisplatin ^{34, 35}. For example, mutants with defective excision repair (*uvrA*) or SOS repair (*recA*) are, respectively, 3 and 15 times more sensitive to cisplatin than wild type bacteria while the double mutant (*uvrArecA*) is the most sensitive (Table 2). Similar results are observed in mammalian cells. *Xeroderma pigmentosum* cells which are deficient in excision repair are more sensitive to cisplatin than human fibroblasts ^{36, 37}. These results show that the cell must remove or bypass DNA lesions if it is to survive cisplatin treatment and imply that unrepaired DNA damage is responsible for its cytotoxicity.

Table 2. Concentrations of cisplatin which reduce survival of various repair-deficient bacteria to 1/e ³⁹

Strain	Genotype	μM
AB1157	wild-type	40
AB1886	<i>uvrA</i>	15
AB1885	<i>uvrB</i>	15
AB2463	<i>recA</i>	3
AB2480	<i>uvrArecA</i>	2

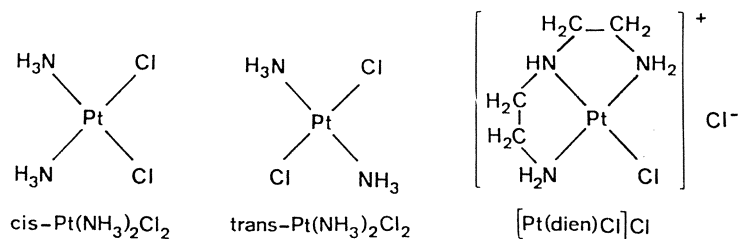


Fig. 2. Structures of three platinum(II) complexes. Only cisplatin is an active antitumor agent

2.4 Structure Activity Relations

Structure-activity studies have shown that antitumoral platinum complexes must have two labile ligands in a *cis* conformation³⁸. Inactive compounds such as *trans*-DDP and $[\text{Pt}(\text{dien})\text{Cl}]\text{Cl}$ (dien = diethylenetriamine) (Fig. 2) have been widely used to investigate the mechanism of action of cisplatin. In this approach, one searches for differences between active and inactive compounds which may be responsible for the pharmacological effect. These three types of molecules cause different changes in DNA conformation and stability, and DNA replication, mutagenicity and repair (see below).

In addition, the relative antitumor activities of these molecules are correlated with their cytotoxicities. Cisplatin is an order of magnitude more toxic toward bacteria and mammalian cells than the *trans* isomer while $[\text{Pt}(\text{dien})\text{Cl}]\text{Cl}$ is not toxic^{14, 17, 39, 40}. Hence, these molecules can be used as probes to determine the cellular target of cisplatin which is responsible for its cytotoxicity. Active compounds should either have a larger concentration on the cellular target molecule than inactive ones or a greater effect per lesion.

Table 3. Relative biological and biochemical effects of DNA lesions caused by different platinum compounds. Data are from bacterial studies with about 10^{-4} platinum per nucleotide. Data have been normalized to results of treatment by *trans*-DDP

	Cisplatin	<i>trans</i> -DDP	$[\text{Pt}(\text{dien})\text{Cl}]\text{Cl}$
Toxicity ^a	10	1	0
Mutagenicity ^b	10	1	0
Repair			
— Excision ^a	100	1	0
— SOS ^c	4	1	0.4
Inhibition of DNA synthesis			
— <i>E. coli</i> ^a	12	1	0
— Cell-free Extract ^d	5	1	nd

a 39), b 6) and unpublished data, c 41), d 42)

A lesion caused by *trans*-DDP on the DNA of *E. coli* is an order of magnitude less toxic than a molecule of cisplatin and the DNA adducts caused by [Pt(dien)Cl]Cl do not seem to be lethal (Table 3). Similar results are observed in mammalian cells (Table 1). The lower toxicity of these compounds in bacteria is not caused by lower DNA-binding or by greater repair of the DNA lesions. The inactive compounds bind to bacterial DNA at least as well as cisplatin and bacteria treated with *trans*-DDP and [Pt(dien)Cl]Cl undergo less excision repair³⁹⁾ and less SOS repair⁴¹⁾ than bacteria treated with cisplatin. Nevertheless, both *cis*- and *trans*-DDP kill bacteria by inhibiting DNA synthesis. The relative sensitivities of repair-deficient bacteria to these compounds are the same and increased toxicity in these strains is always inversely proportional to Thd incorporation³⁹⁾. Furthermore, *in vitro* replication of platinated T7 DNA by a crude bacterial extract shows that *trans*-DNA lesions are 5 to 10 times less inhibitory than lesions caused by *cis*-DDP⁴²⁾. These results indicate that the DNA lesions formed by *trans*-DDP and [Pt(dien)Cl]Cl block replication less effectively than those formed by *cis*-DDP. Hence, the structure-activity effects which are observed for the cytotoxicity of these platinum compounds are also present at the level of their effect on DNA replication.

The most striking difference between the DNA lesions caused by *cis*- and *trans*-DDP is their mutation induction. The correlation between the mutation induction of a series of platinum compounds and their antitumor activity^{16, 43, 44)} might suggest that mutagenesis and antitumor activity are caused by the same biochemical event. However, *cis*-DDP induces mutations in Chinese hamster ovary cells at low frequencies, e.g., less than 200 hypoxanthine-guanine phosphoribosyl transferase (HGPRT) mutants per 10⁶ cells¹⁷⁾. The HGPRT locus is on the X chromosome and it is functionally hemizygotic⁴⁵⁾. If we assume that lethal mutations would occur with the same frequency as mutations at the HGPRT locus, then the inactivation of both copies of an essential gene product would occur with a probability on the order of 10⁻⁸. In contrast, the cytotoxic event must occur at a high frequency. For example, a mouse will die of cancer after the injection of a single L1210 leukemia cell⁴⁶⁾. It seems unlikely that the cytotoxic effect of cisplatin is the result of lethal mutants.

The structure-activity approach is a particularly powerful technique for testing putative mechanisms of action. For example, cisplatin is known to block the polymerization of tubulin *in vitro*. However, the *trans* isomer has a larger effect⁴⁷⁾. Since *trans*-DDP is more chemically reactive than the *cis* isomer⁴⁸⁾, this phenomenon is probably the result of platinum complexation at protein sulfhydryl groups and not associated with antitumor activity.

2.5 Synergism and Antagonism

Certain agents which have synergistic effects when used in combination with cisplatin may influence its interaction with DNA. For example, pretreatment with cisplatin increases the cytotoxic effect of ionizing radiation. Similarly, the effect of ionizing radiation on the conformation of platinum-DNA complexes is greater than its effect on DNA alone⁴⁹⁾.

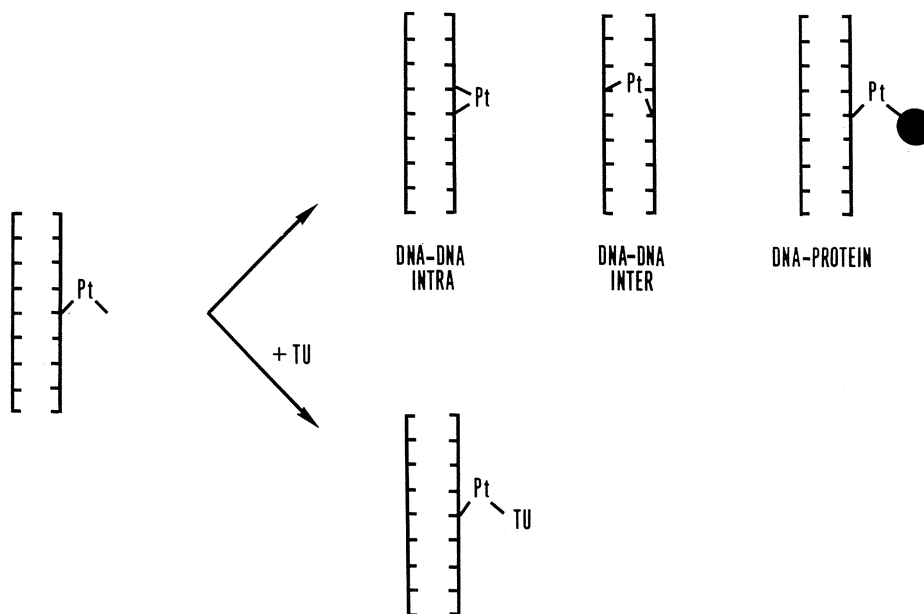


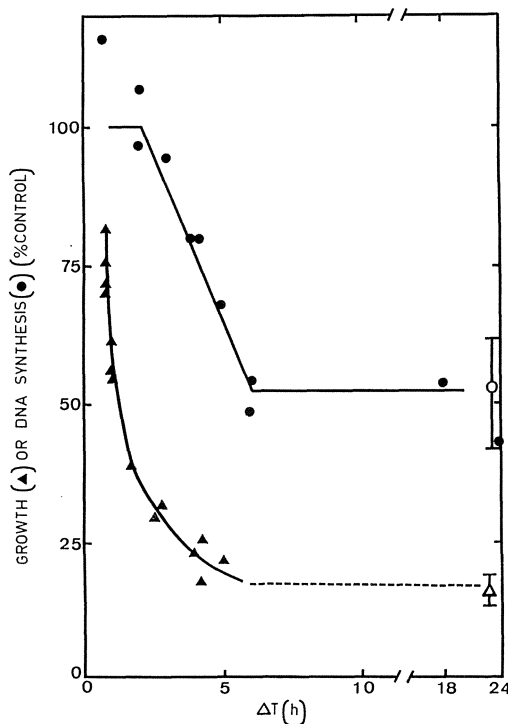
Fig. 3. Monoadduct quenching (from ⁵²)

Thiourea, a strong nucleophile, antagonizes the antitumor and cytotoxic effects of cisplatin. If it is administered prior to cisplatin, the drug loses its antitumor effect, probably because it is trapped by thiourea before it can reach the cellular target. If thiourea is administered immediately after treating cultured mammalian cells with cisplatin, the toxicity and mutagenicity of the drug are suppressed. However, if cells are incubated after treatment before adding thiourea, the antagonism diminishes and after several hours of incubation thiourea has no effect ^{50, 51}). These results suggest that a thiourea-sensitive lesion is fixed during the hours which follow cisplatin treatment to form thiourea-insensitive toxic and mutagenic lesions.

Zwelling ⁵²) proposed a mechanism called monoadduct quenching to explain thiourea antagonism (Fig. 3). Thiourea is supposed to react with monofunctional platinum-DNA adducts and prevent the formation of bifunctional lesions which are responsible for the toxicity and mutagenicity of cisplatin. The reaction of thiourea with monofunctional platinum-DNA lesions has been observed *in vitro* ⁵³). Thiourea also blocks, but does not reverse, the formation of interstrand crosslinks and DNA-protein crosslinks during the 6 to 12 hours following treatment of cultured mammalian cells with cisplatin ⁵⁰).

If cisplatin acts by inhibiting DNA replication, then thiourea should also antagonize the inhibition of DNA synthesis. Furthermore, thiourea should lose its antagonistic effect during post-treatment incubation with the same kinetics for DNA synthesis and toxicity. In order to test this hypothesis, we measured Thd incorporation and cell

Fig. 4. Effect of thiourea on Thd incorporation and cell proliferation. Cells were treated for 2 hours with 18 μM cisplatin, washed and resuspended in culture media for various times, ΔT , before exposure to a 1 hour pulse of 50 mM thiourea. That incorporation was measured 24 hours after cisplatin treatment and cell proliferation was determined after 48 hours. *Open symbols* are the inhibitory effect of cisplatin without the addition of thiourea



inhibits cytotoxicity, restores DNA replication (Fig. 4) and blocks the formation of bifunctional platinum-DNA lesions.

Taken together these results are compelling evidence that cisplatin binds to cellular DNA and inhibits its replication, thereby leading to cell death. These approaches are perfectly general and can be used to determine if DNA is the target of other drugs. Furthermore, they are applicable to other targets than DNA.

3 The Reaction of Cisplatin with DNA in vitro

Cisplatin undergoes hydrolysis to form positively charged monoquo and diaquo species (Fig. 5). The rate constants for the loss of the first and second chloride at 25° are 2.5×10^{-5} and $3.3 \times 10^{-5} \text{ sec}^{-1}$ (54). The aquo ligand is in equilibrium with its deprotonated hydroxo form. The pK_A values are 5.6 for the diaquo species and 7.3 for the monoaquomonohydroxo and monoaquomonochloride species (55–57). The hydroxo moiety forms a stable bond with platinum while water is a good leaving group. As a result, the monoaquomonohydroxo species condenses under appropriate conditions to form bridged hydroxy dimers and trimers (58, 59).

The neutral species (Fig. 5) and oligomers do not react with DNA in vitro. The aquated forms $[\text{Pt}(\text{NH}_3)_2(\text{H}_2\text{O})_2]^{2+}$ and $[\text{Pt}(\text{NH}_3)_2\text{Cl}(\text{H}_2\text{O})]^+$, bind covalently to

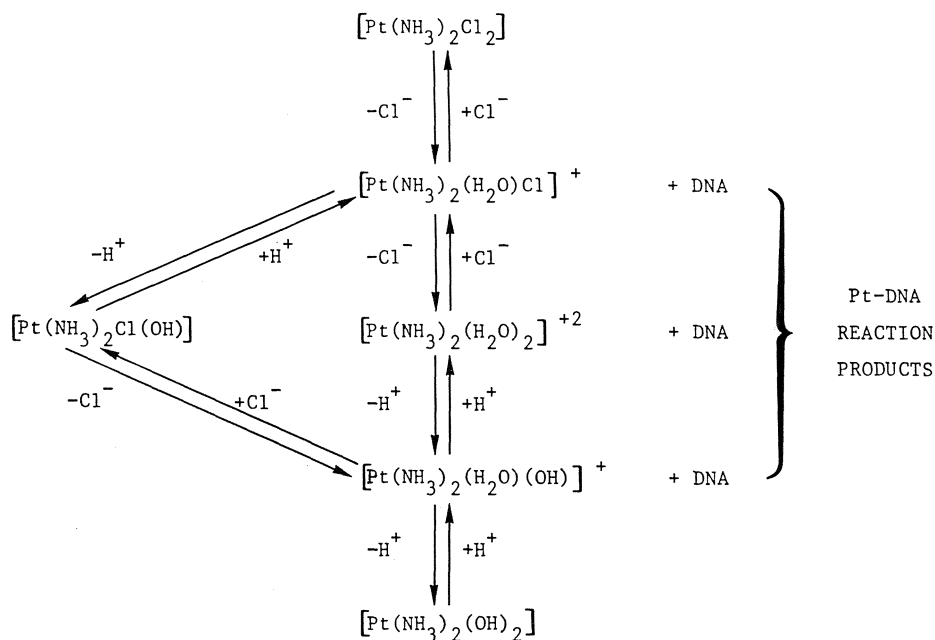


Fig. 5. Aquation of cisplatin and reaction of aquated species with DNA

the polynucleotide in two kinetically distinct reactions which are pseudo-first-order with respect to platinum concentration⁶⁰. Under these conditions, the half-life of the reaction of the diaquo species with 10^{-4} M DNA in 5 mM NaClO_4 at 25° pH 5–6 is 0.8 min while the half-life of the mono-aquomonochloro species is 6 h. $[\text{Pt}(\text{NH}_3)_2(\text{H}_2\text{O})(\text{OH})]^+$ reacts with the same kinetics as the diaquo species. If freshly dissolved solutions of platinum compound are added to DNA, formation of the mono-aquo species is the rate limiting step^{61, 62}. The half-life of this reaction in water is 4 h at 37° .

3.1 Physical Chemical Studies of Platinum-DNA Complexes

Physical chemical studies reveal that complexation of platinum compounds with DNA disrupts the structure and stability of the polynucleotide (Table 4). These studies were carried out at low levels of DNA-binding, molar ratio of platinum bound per nucleotide (r_b) 0.005 to 0.05, which are the limits of detection for these techniques. It is assumed that the observed alterations are also present around the platinum lesion at biological levels of DNA binding where the r_b is 10^{-4} to 10^{-6} .

Platinum compounds disrupt base stacking and destabilize DNA. Bifunctional platinum-DNA lesions prevent the intercalation of planar dye molecules between adjacent nucleotide bases. For example, fixation of one molecule of *cis*- or *trans*-DDP on DNA prevents the intercalation of one ethidium ion while $[\text{Pt}(\text{dien})\text{Cl}]\text{Cl}$ has no effect⁶³. In addition, complexation of cisplatin on DNA increases the UV absorption at

Table 4. Alterations of structure and stability of DNA by fixation of Pt(II)chloroamines in vitro, $r_b = 0.01$

	<i>cis</i> -DDP	<i>trans</i> -DDP	[Pt(dien)Cl]Cl
DNA	0	0	0
Strand breaks ^a			
S1-sensitive Single-stranded DNA ^a	0	0	0
Interstrand Crosslinks (crosslink per Pt) ^b	(1/30)	nd	0
DNA shortening ^c	+	+	—
Disruption Base stacking			
— Exclusion of Intercalating Agents ^d	+	+	—
— Increased CD at 275 nm ^e	+	—	—
ΔTm^c	—2.4°	1.3°	3.3°

a 4); b 69); c 66); d 63); e 64)

260 nm and the positive CD band at 275 nm, which indicates that the drug disrupts electronic interactions between adjacent bases^{64, 65}). Structural changes are also indicated by decreases in the viscosity and the length of DNA which is complexed with cisplatin or *trans*-DDP but not [Pt(dien)Cl]Cl^{65, 66}). These structural changes may destabilize the polynucleotide. For example, fixation of 5 cisplatin molecules per 1000 nucleotides decreases the melting temperature of T7 DNA by 1.7°⁶⁶).

Cis- and trans-DDP form interstrand crosslinks. The reaction of cisplatin and its *trans* isomer with DNA produces interstrand crosslinks, judging from the appearance of high molecular weight DNA in denaturing conditions^{14, 67}), enhanced thermal renaturation⁶⁶), and diminished rate of alkaline elution⁶⁸). Interstrand crosslinks are relatively minor lesions which represent about 1% of the platinum-DNA lesions⁶⁹).

Time-dependent physical chemical changes. The above results concern physical chemical measurements of the complex which is formed at the end of the reaction between cisplatin and DNA. Recently, experiments studying earlier times in the reaction have uncovered dynamic processes which may correspond to the passage of monoadducts to bifunctional lesions (see below). Schaller and Holler⁷⁰) have reported time-dependent changes in the UV spectrum of DNA following its reaction with [Pt(NH₃)₂(H₂O)₂]²⁺. Kleinwachter et al.⁷¹) have observed time-dependent changes in the circular dichroism (CD) spectra of DNA following cisplatin binding. During the reaction of cisplatin with DNA, the CD band at 280 nm decreased and then increased. When unreacted cisplatin was removed after several minutes of reaction, the CD band at 280 nm continued to increase for 6 h. Control experiments with [Pt(dien)Cl]Cl indicate that monofunctional binding may be responsible for the initial decrease of the CD spectrum. Formation of bifunctional lesions from monoadducts

probably results in the characteristic increase of the positive CD band and the kinetics of this process may be followed by CD spectroscopy.

Finally, exposure of either purified DNA or DNA in mammalian cells to cisplatin produces 1 crosslink per 150 platinum lesions. In both cases the number of crosslinks increases to 1/30 when the platinum-DNA complex is stored in buffer at 37° for 24 h after treatment⁶⁹⁾.

3.2 Platinum-DNA Adducts

Cisplatin reacts with DNA at the N⁷ position of Guo to form a monofunctional adduct. This monoadduct has been observed in the X-ray structure of a platinated dodecanucleotide⁷²⁾. It has been isolated from DNA by two methods and identified by comparison with model compounds of known structure. In the first, the reactive site on the monoadduct is substituted by thiourea⁵³⁾ or NH₃^{7, 3)} thereby preventing further complexation with a second purine base. The substrate is then digested by nucleases and the adducts separated using column chromatography. Alternatively, protonation of the platinum-DNA complex blocks the N⁷ position of the purine bases. At the same time acid conditions cleave the sugar-base bond and liberate platinum-base adducts which can be characterized by paper chromatography⁷⁴⁾ or HPLC (unpublished data).

We have determined the kinetics of formation of bifunctional lesions from the monoadduct using two independent methods. Cisplatin was reacted with DNA for 2 h at 37° and the unreacted platinum removed. In one experiment the monoadduct was quantified during post-treatment incubation by acid hydrolysis⁷⁴⁾ and in the other by its reaction with radioactive Guo⁷⁵⁾. Both experiments show that the monoadduct disappears in a biphasic reaction. The first step involves the majority of the lesions and is complete during the 2 h reaction with *cis*-DDP. The second reaction concerns 5 to 10% of the lesions which disappear at 37° in 10 mM NaClO₄ with a half-life of 20 ± 5 h.

At the end of the reaction *cis*-[Pt(NH₃)₂{dGpG}], represents 60 to 65% of the platinum-DNA adducts⁷⁶⁾. Similar results are observed for [Pt(en)Cl₂] (en = ethylenediamine)⁵³⁾. This adduct has been characterized as a dinucleotide and in oligonucleotides using NMR^{7, 10, 77-87)} and the crystal structure of the dinucleotide complex has been determined^{88, 89)} (Fig. 6). Gua base stacking is disrupted by Pt binding to the N⁷ position of both bases. The two Guo are in the *anti-anti* configuration. The 5'-nucleoside has the *N* (C3'-*endo*) conformation while the 3'-nucleoside conformation is more flexible. There is a hydrogen bond between the amine ligand and the 5'-phosphate group.

The stereochemical constraints introduced by complexation have surprisingly little effect on the structure and stability of adjacent nucleotides. For example, NMR studies of oligonucleotides show that platination of the GpG sequence dissociates only a single base pair adjacent to the lesion^{86, 90)}. These NMR results also suggested that cisplatin introduces a kink in the DNA structure which has subsequently been observed by retardation gel technique⁹¹⁾. These conformational changes seem to be sufficient to account for the CD spectral changes and the decreased thermal stability summarized above^{83, 85, 90)}.

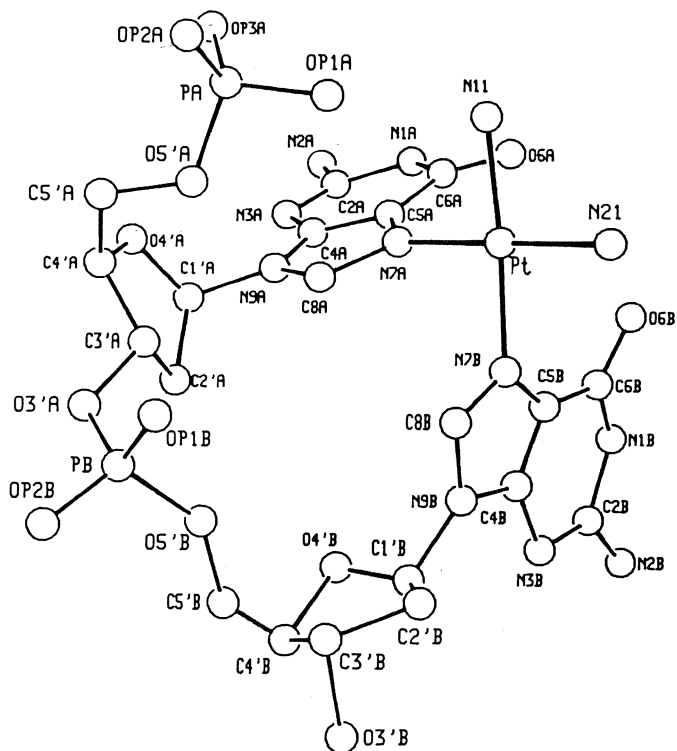


Fig. 6. X-ray structure of the major platinum-DNA adduct *cis*-[Pt(NH₃)₂{d(GpG)}] (from ⁸⁸) Copyright 1985 by the AAAS)

cis-[Pt(NH₃)₂{dApG}] represents 20% of the platinum-DNA lesions under these conditions. Structural characterization of the adduct by NMR shows that the platinum is bound to the N⁷ position of the purine bases ⁷⁶). The corresponding adduct with dGpA is not observed. Although the reaction of aquated cisplatin with ApG is kinetically preferred to GpA ^{92, 93}), steric constraints of the double helical DNA conformation may also contribute to the observed sequence specificity ⁹⁴).

Finally, 5 to 10% of the platinum-DNA adducts are isolated as *cis*-[Pt(NH₃)₂-(5'-dGMP)₂] after enzymatic digestion ^{53, 76}). These are believed to result from two types of lesions. Interstrand DNA-DNA crosslinks represent about 1% of the platinum-DNA lesions *in vitro* ⁶⁹). These adducts involve Guo bases on opposite strands of DNA and form during several h post-treatment incubation *in vitro* ^{75, 95}). The remaining [Pt(NH₃)₂-(5'-dGMP)₂] adducts are believed to be intrastrand crosslinks on non-nearest neighbor Guo bases. Complexes between cisplatin and nucleotide sequences GpXpG, where X is any base, have been reported for trinucleotides and in oligonucleotides ⁹⁶⁻¹⁰¹). Alternatively, cisplatin might complex Guo bases separated by longer sequences of nucleotides to form microloops.

All of these adducts have been detected in cultured cells treated with cisplatin ¹⁰²). In addition protein-DNA crosslinks are observed *in vivo*. Judging from alkaline elution studies the quantity of protein-DNA crosslinks formed by *cis*-DDP is on the

same order as DNA-DNA crosslinks. The concentrations of DNA-DNA and protein-DNA crosslinks in cultured cells increases during post-treatment incubation^{50, 102}.

The labile ligands of *trans*-DDP are sterically disposed in such a way that this isomer can not complex the N⁷ positions of adjacent purine bases. On the other hand, complexes of *trans*-DDP with trinucleotides such as dGdCdG have been reported¹⁰. After a short reaction with DNA, *trans*-DDP forms greater than 80% monofunctional adducts^{75, 103}. These disappear over several h to form *trans*-[Pt(NH₃)₂(5'-dGMP)(5'-dXMP)] adducts where X = Guo, Ctd, or Ado¹⁰⁴. Little data is available on the relative concentrations of the various interstrand or intrastrand crosslinks. *Trans*-DDP forms more protein-DNA crosslinks *in vitro*¹⁰⁵ and *in vivo*⁶⁸) than *cis*-DDP, probably as a result of the high concentration and stability of monofunctional adducts.

The kinetics of formation of bifunctional lesions by *trans*-DDP^{75, 103}) are reminiscent of the production of interstrand crosslinks by cisplatin⁶⁹). They contrast

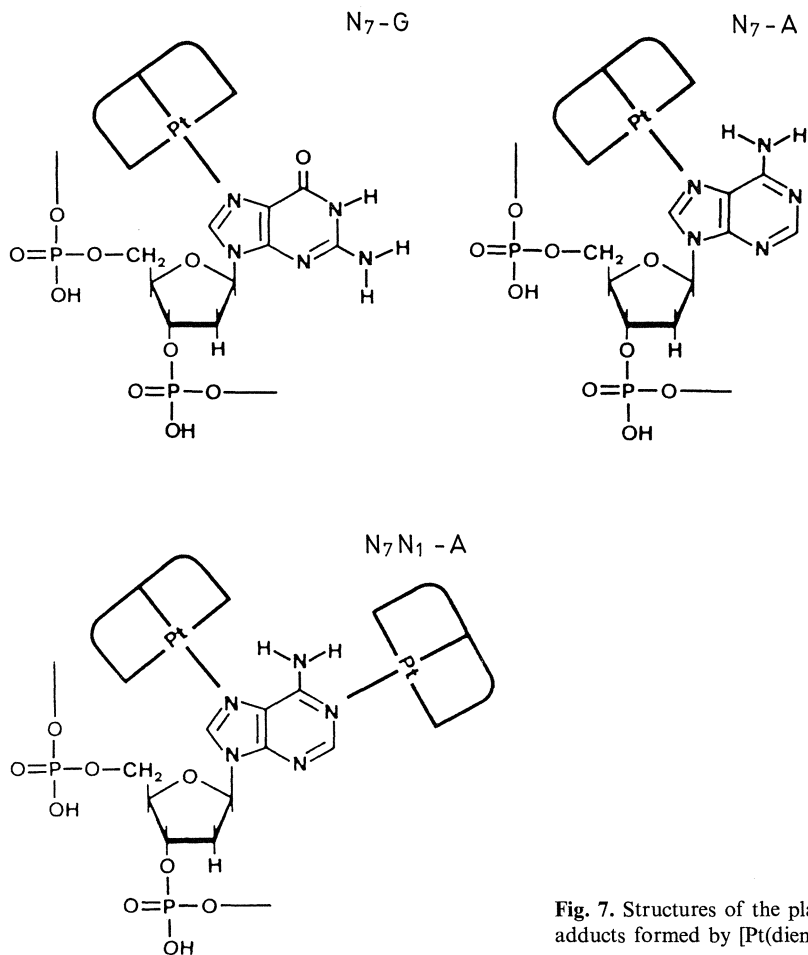


Fig. 7. Structures of the platinum-DNA adducts formed by [Pt(dien)Cl]Cl

dramatically with the kinetics of reaction of *cis*-DDP with adjacent nucleotides and may characterize the reaction of monofunctional platinum-DNA adducts with non-nearest neighbor bases ^{74, 75}.

The DNA lesions formed by the reaction of [Pt(dien)Cl]Cl with DNA *in vitro* have been characterized after cleavage from the polymer by acid hydrolysis ¹⁰⁶ (Fig. 7). At levels of DNA damage of less than 0.1 lesion per nucleotide, platinum binds exclusively to the N⁷ position of Guo. At higher levels, [Pt(dien)Cl]Cl also reacts at the N⁷ position of adenine. When more than 0.3 platinum per nucleotide are bound, denaturation of the DNA exposes the N¹ position of Ade and 1,7-[[Pt(dien)]₂Ade]²⁺ is formed.

Different chemical and spectroscopic changes are observed after alkylation or platination of the N⁷ position of Guo. For example, both substituents lower the pK of the N¹ proton although the effect of an alkyl group (pK_a = 7.1 ¹⁰⁷) is somewhat greater than [Pt(dien)] (pK_a = 8.0 ¹⁰⁶). Methylation of Guo changes its absorption spectra ¹⁰⁸) and raman scattering ¹⁰⁹) more than platination. N⁷-methyl-Guo is less stable in acid than the corresponding platinum compound ¹⁰⁶). Finally the alkylated imidazole ring opens at high pH to give a formamido pyrimidine derivative ¹¹⁰) whereas the imidazole ring of the platinated nucleoside is stable under these conditions ¹⁰⁶). The glycosyl linkage at the N⁹ position of Guo is weakened by a positive charge on the imidazole ring after protonation of the N⁷ position or formation of N⁷-alkyl-Guo ¹¹¹). These results suggest that alkylation or protonation of a nucleic acid base would alter its electron distribution more than the corresponding platinum complex.

4 Biological Effects of Platinum-DNA Adducts

4.1 Effect of Platinum-DNA Adducts on DNA Replication *in vitro*

In the past ten years several laboratories have investigated the effect of platinum compounds on *in vitro* DNA synthesis by a variety of DNA polymerases. Harder et al. ¹¹²) studied DNA synthesis by partially purified α and β DNA polymerases. For relatively high levels of DNA modification, $r_b = 0.01$, *cis*-DDP inhibited DNA synthesis more than the *trans* isomer. This study used partially digested salmon sperm DNA as a substrate. The observed DNA synthesis fills the single stranded gaps in double stranded DNA which may explain the relatively high r_b value necessary for the inhibition of replication. We have studied the *in vitro* replication of T7 DNA by a crude bacterial extract ⁴²). Replication in this system was inhibited at levels of DNA binding on the order of 10^{-4} platinum per nucleotide which corresponds to the concentration of cisplatin necessary to inhibit bacterial replication *in vivo* ³⁹). When normalized to the number of platinum atoms on the DNA, the inhibition of DNA synthesis *in vitro* was 5 times more effective for *cis*- than for *trans*-DDP.

More recently Pinto and Lippard ¹¹³) have studied the *in vitro* conversion of platinated M13 phage DNA to double stranded form by the Klenow fragment of *Escherichia coli* DNA polymerase I. The sites at which platinum lesions block replication were determined using DNA sequencing techniques. They concluded that *cis*-DDP inhibited DNA synthesis at sequences which contained dG_n ($n \geq 2$). *Trans*-

DDP also inhibits DNA synthesis, although the sequence dependence of this inhibition appears to be less regular than for *cis*-DDP. Monofunctional adducts formed by [Pt(dien)Cl]Cl on DNA did not inhibit DNA synthesis at the ratios of drug/nucleotide employed. In an extension of this study¹¹⁴⁾, we have compared the replication of platinated single stranded M13 DNA by *Escherichia coli* DNA polymerase I Klenow fragment with highly purified eukaryotic DNA polymerase α from *Drosophila melanogaster* embryos and from calf thymus. Cisplatin blocked the eukaryotic DNA polymerases at essentially the same sequences as *Escherichia coli* polymerase I. However, inhibition was observed not only at dG_n sequences but also at other sites which may represent putative *cis*-DDP-DNA adducts.

Hence, a consensus seems to exist on the capacity of bifunctional platinum-DNA lesions to inhibit DNA synthesis in vitro. The mechanism of inhibition is unknown although there are some intriguing experimental results. The lesions block replication enzymes which lack 3'-5' "proofreading" exonuclease activity so that excising mispaired bases at the site of the lesion does not appear to play a major role in the pattern of arrest sites which is observed¹¹⁴⁾. A recent kinetic study of the replication of partially digested double stranded DNA by the Klenow fragment of *Escherichia coli* polymerase I indicates that the platinum lesion decreases the association constant between the enzyme and the template¹¹⁵⁾. Platinum compounds may block replication by destabilizing the complex formed between the replicase and its substrate. In this case, the processivity of the enzyme would be an important factor in determining the capacity of DNA damage to block replication¹¹⁶⁾. It should be pointed out that with the exception of the T7 DNA replication system, all of the other polymerases employed in the studies cited above have fairly distributive modes of DNA replication in vitro.

4.2 Repair of Platinum-DNA Adducts

The biochemical processes which remove platinum adducts from DNA have been most thoroughly studied in *Escherichia coli*. Excision repair is of particular interest because it has been shown to be the major pathway responsible for the survival of bacteria treated with platinum compounds^{34, 39)}. Nucleotide excision repair in *Escherichia coli* is mediated by the ABC excinuclease which is composed of three subunits, the UvrA, UvrB and UvrC proteins. The enzyme incises on both sides of the modified nucleotide(s), hydrolyzing the eighth phosphodiester bond in the 5' direction and the fourth or fifth phosphodiester bond in the 3' direction from the platinum-DNA adduct^{117, 118)}. Platinum adducts at GpG sequences are a good substrate for ABC excinuclease in vitro¹¹⁸⁾. A recent study¹¹⁹⁾ using a 43 base pair oligonucleotide containing a single platinum adduct at a predetermined site indicated that Agp lesions are a better substrate for the ABC excinuclease than GpG adducts. Finally, DNA damage produced by *cis*-DDP is recognized better by the ABC excinuclease in vitro than adducts formed by *trans*-DDP^{118, 120)}. Similar results have been reported in vivo where density gradient experiments show that lesions formed in *Escherichia coli* by *cis*-DDP are excised to a greater extent than those formed by the *trans* isomer³⁹⁾.

Platinum-DNA lesions induce the SOS repair system in bacteria. Lesions formed by *cis*-DDP induce 4 times more RecA protein than those formed by *trans*-DDP⁴¹⁾. Finally, the mismatch repair mechanism may be implicated in the repair of platinum-DNA lesions¹²¹⁾. Data on the repair of particular adducts by this mechanism are not yet available.

Excision of platinum¹²²⁾ and the disappearance of specific platinum-DNA adducts^{123, 124)} have been observed in mammalian cells. Initial reports that DNA lesions formed by *trans*-DDP are better repaired in mammalian cells than those formed by *cis*-DDP¹²⁵⁾ have not been confirmed¹²⁶⁾, unpublished results.

4.3 Mutagenic Platinum-DNA Adducts

Mutagenesis by platinum compounds has been reported in bacteria^{15, 16)} and mammalian cells^{17, 18)}. When the mutation frequency is normalized to the number of DNA lesions, cisplatin appears to be a weak mutagen in mammalian cells, three orders of magnitude less mutagenic than *N*-ethyl-*N*-methyl-nitrosourea. Platinum-DNA adducts formed by *cis*-DDP are two orders of magnitude more mutagenic than those formed by *trans*-DDP¹⁷⁾.

An early report¹²⁷⁾ detected the existence of "hot spots" for mutagenesis at GpCpG and GpApG sequences in the *lacI* gene of *Escherichia coli*. However, the *lacI* gene mutation assay is limited in that among all of the induced mutants, only mutations leading to nonsense codons can be detected. By using a forward mutation assay which is sensitive to other mutations, it has recently been shown that both ApG and GpG adducts are mutagenic, the ApG site having a higher mutagenic potential¹²⁸⁾.

SOS mediated error-prone repair is implicated in the mutagenesis of both *Salmonella typhimurium* and *Escherichia coli* by *cis*-DDP^{25, 129-131)}. The best evidence for this involvement is the necessity of the *umuC, D* gene products for the expression of cisplatin induced mutagenesis^{129, 131-133)}. However, mutagenesis by *cis*-DDP in *Escherichia coli* is strongly reduced or abolished in either *uvrA* or *uvrB* mutants^{25, 127, 130, 133)} while mutagenesis by classical SOS inducers such as ultraviolet irradiation are increased in *uvr* deficient strains³⁰⁾. Thus it appears that the excision repair system, ABC excinuclease, which is normally error-free, may play a role in mutation induction by cisplatin.

5 Metal Oxidation State and Antitumor Activity

Many transition metal complexes can be easily oxidized and reduced. The various oxidation states have different chemical properties. In its most common oxidation states platinum forms square planar Pt(II) or octahedral Pt(IV) compounds. Platinum substitution reactions generally take place by an axial attack of the incoming ligand and, as a result of their d⁶ electronic configuration, Pt(IV)

complexes are characteristically unreactive^{48, 135}). Consequently, one might expect the pharmacological effects of transition metal complexes to vary with their oxidation state. In this section we will examine the role of redox reactions and the oxidation state in the antitumor activity of platinum compounds.

Surprisingly, platinum compounds in both oxidation states have similar pharmacological effects. Antitumor activity against rodent tumor models has been reported for Pt(II) and Pt(IV) complexes¹³⁶⁻¹⁴⁵). Two Pt(IV) complexes, iproplatin (*cis*-dichloro-*trans*-dihydroxo-bis-isopropylamineplatinum(IV)) and tetraplatin (diaminocyclohexanetetrachloroplatinum(IV)), are currently undergoing clinical or pre-clinical studies¹⁴⁶⁻¹⁴⁸). In addition, platinum compounds in both oxidation states have similar toxic effects¹⁴⁷⁻¹⁵⁰).

Pt(IV) compounds were included in some early studies of the mechanism of action. The observation of filamentous bacterial growth (which led to the discovery of the antitumor activity of cisplatin) was first reported for Pt(IV) chloroammines²⁷). The genotoxic effects of platinum complexes in both oxidation states have been subsequently compared in bacteria¹⁵¹) and mammalian cells^{18, 20, 40, 152}). Results show that for complexes in both oxidation states the *trans* isomers are less toxic and mutagenic than the corresponding *cis* isomers or inactive. As in the case of Pt(II) compounds, Pt(IV) complexes selectively and persistently inhibit DNA synthesis³³). Consequently DNA-binding is thought to be responsible for the cytotoxic effect of Pt(IV) compounds.

There is some evidence for the covalent binding of Pt(IV) compounds to nucleotides *in vitro*. In particular, cisplatin and oxoplatin (*cis*-diamminedichloro-*trans*-dihydroxyplatinum(IV)) form different platinum-DNA adducts. They produce different effects on thermal denaturation and renaturation, circular dichroism and differential pulse polarography when they are compared at equal levels of DNA binding¹⁵³). Furthermore, antibodies against DNA which has been modified by cisplatin do not cross-react with oxoplatin-DNA complexes (Brabec, unpublished data). Finally, the reaction of Pt(IV) compounds with 9-methyl-hypoxanthine and 5'-GMP gives products in both oxidation states^{154, 155}). The greater electron withdrawing capacity of Pt(IV) compounds may destabilize the glycosyl linkage of Guo more than Pt(II) adducts¹⁵⁶).

As might be expected from their chemical properties, Pt(IV) chloroammines react more slowly with DNA *in vitro* than the corresponding Pt(II) compounds^{67, 142, 157}). However, complexes in both oxidation states bind well to the DNA of cultured cells and form similar numbers of interstrand crosslinks^{14, 18, 67}).

In order to explain the rapid fixation of Pt(IV) complexes on cellular DNA, it has been proposed that they might be reduced *in vivo* to the corresponding *cis*-Pt(II) compounds which would be responsible for the biological activity^{38, 139}).

The most abundant intracellular reducing agent is glutathione. This compound facilitates the reaction of tetraplatin with DNA *in vitro*. The reduction of tetraplatin is rapid and loss of the chloride leaving group from the resulting *cis*-diaminocyclohexanedichloro platinum(II) is the rate-limiting step for the reaction with DNA¹⁵⁸). Pt(IV) compounds may also bind to nucleotides in the presence of reducing agents such as ascorbic acid and cysteine-containing peptides^{144, 145, 154, 159}). These *in vitro* studies suggest that Pt(IV) complexes would be rapidly reduced in the intracellular media to form Pt(II) reduction products.

Several pharmacological results support the bioreduction hypothesis. Antitumor activity in animal models is only observed for Pt(IV) compounds which have active Pt(II) reduction products^{141, 143, 149, 160}. Since equatorial geometry is conserved in redox reactions^{48, 135}, these structure-activity results are consistent with the reduction of a *cis*-Pt(IV) "prodrug" to an active *cis*-Pt(II) species. Furthermore, Pt(II) reduction products are among the metabolites found in patients treated with Pt(IV) antitumor drugs. For example, *cis*-[Pt(II)Cl₂(NH₂CH(CH₃)₂)₂] has been found in the plasma and urine of patients treated with iproplatin (*cis, trans, cis*-[Pt(IV)Cl₂(OH)₂(NH₂CH(CH₃)₂)₂]¹⁴⁷). Finally, platinum-DNA adducts in cells treated with oxoplatin are recognized by antibodies against *cis*-DDP-DNA complexes (Brabec, unpublished data).

In order to test the bioreduction hypothesis, we have compared the genotoxic effects of *cis*-diamminetetrachloro platinum(IV) (*cis*-DTP) with its reduction product *cis*-diamminedichloroplatinum(II) (*cis*-DDP)¹⁶¹. If *cis*-DTP is reduced *in vivo* to *cis*-DDP prior to its reaction with DNA, then an equal number of DNA lesions formed by either compound should produce identical genotoxic effects.

After exposure of bacteria to equal concentrations of the two drugs, the intracellular concentration of *cis*-DTP was an order of magnitude greater than *cis*-DDP. At equal intracellular concentrations (50 to 500 ng Pt/mg protein), twice as much *cis*-DDP as *cis*-DTP bound to bacterial DNA. The high level of DNA binding observed for *cis*-DTP is consistent with its reduction to *cis*-DDP in the bacteria.

The quality of the DNA lesions formed by the two compounds was evaluated by comparing the survival or mutagenicity of cells with identical numbers of DNA adducts. The survival of bacteria exposed to *cis*-DTP or *cis*-DDP was identical for equal levels of DNA damage. For both compounds, increasing DNA binding to 10⁻³ Pt/nucleotide, decreased survival to 10% of control cultures; log survival was a linear function of the number of platinum-DNA lesions. However, mutagenic lesions occurred at a lower frequency for the Pt(IV) compounds. When mutagenicity (as measured by *his* reversion) was expressed as a function of the number of platinum-DNA lesions, a given number of *cis*-DDP molecules on the bacterial genome caused 7 ± 3 times more mutants than the same number of *cis*-DTP adducts. Mutagenesis of platinum compounds in *Escherichia coli* is a consequence of the induction of the SOS repair^{25, 129-131} which is triggered when *Escherichia coli* is exposed to agents or conditions which interfere with its replication³⁰. The induction of the SOS system can be quantified by measuring the concentration of protein *recA*⁴¹. When *recA* induction levels were compared at equal levels of DNA-binding, *cis*-DDP induced the synthesis of 3.5 ± 0.5 times more *recA* protein than *cis*-DTP¹⁶¹.

Although the reaction of *cis*-DTP with bacterial DNA is consistent with its bioreduction to *cis*-DDP, the capacity of equal levels of DNA damage to cause different levels of mutagenesis and *recA* protein indicates that these compounds do not form identical DNA lesions. Similar conclusions were reached by Elespuru and co-workers who measured the induction of prophage lambda in bacteria exposed to a series of Pt(II) and Pt(IV) ethylenediamine compounds¹⁶². Likewise, an equal number of DNA lesions formed by Pt(IV) compounds and their reduction products are reported to produce different genotoxic effects in CHO cells¹⁸. Hence, the fixation of Pt(II) reduction products is not the only mechanism by which Pt(IV) compounds damage DNA *in vivo*.

The molecular bases for these differences can only be speculated. Part of the Pt(IV) compound may react directly with DNA as observed *in vitro* (see above). In addition, it has been proposed that bioreduction of Pt(IV) compounds might cause DNA strand breaks. However, initial reports that Pt(IV) but not Pt(II) compounds cause strand breaks *in vitro*^{163,164} now seem to be the result of hydrogen peroxide contaminant^{144,165}.

We are currently studying the formation of strand breaks in bacteria by two Pt(IV) antitumor compounds, iproplatin and *cis*-DTP, as well as the Pt(II) antitumor compound *cis*-DDP. In one experiment, a new bacterial test which permits the detection of DNA strand breaks by their induction of the SOS response has been employed^{166,167}. In a second experiment, strand breaks were measured directly by gel electrophoresis of plasmid DNA extracted from bacteria which had been treated with these drugs. Preliminary results indicate that Pt(IV) but not Pt(II) antitumor compounds cause DNA strand breaks in bacteria (Defais et al., unpublished).

In summary, there is much evidence that Pt(IV) antitumor compounds are reduced *in vivo*. Both *cis*-Pt(II) and *cis*-Pt(IV) compounds are antitumoral and have similar toxicities. DNA binding seems to be responsible for the cytotoxic effect in both cases. Nevertheless, some evidence suggests that the DNA lesions formed by Pt(IV) compounds and their Pt(II) analogues may have different genotoxic effects. It is possible that Pt(IV) antitumor compounds may resemble certain antibiotics where bioreductive activation leads to both the covalent reaction of the drug with DNA and the formation of DNA strand breaks¹⁶⁸. Hence Pt(IV) antitumor compounds might possess a mechanism of action and pharmacological activity different from their Pt(II) analogues which would resemble natural product antitumor agents such as bleomycin and neocarzinostatin.

6 Acknowledgements

This project was supported in part by grants from Sanofi Recherche, Fédération Nationale des Groupements des Entreprises Françaises dans la Lutte Contre le Cancer, Fédération Nationale des Centres de Lutte Contre la Cancer and Association pour la Recherche sur le Cancer.

7 References

1. Prestayko AR, Crooke ST, Carter SK (eds) (1980) Cisplatin current status and new developments. Academic, New York
2. Harrap KR (1985) *Cancer Treat. Revs.* 12: 21
3. Roberts JJ, Thomson AJ (1979) *Prog. Nucl. Acid Res. Mol. Biol.* 22: 71
4. Macquet JP, Butour JL, Johnson NP (1983) in: S. J. Lippard (ed) Platinum, gold and other metal chemotherapeutic agents: chemistry and biochemistry. American Chemical Society, Washington, p 75
5. Pinto AL, Lippard SJ (1985) *Biochim. Biophys. Acta* 780: 167

6. Johnson NP, Lapetoule P, Razaka H, Villani G (1986) In: McBrien DCH, Slater TF (eds) *Biochemical mechanisms of platinum antitumor drugs*. IRL, Oxford, p 1
7. Reedijk J, Fichtinger-Schepman AMJ, van Oosterom AT, van de Putte P (1987) *Structure and Bonding* 67: 53
8. Eastman A (1987) *Pharmac. Ther.* 34: 155
9. Roberts JJ, Friedlos F (1987) *Pharmac. Ther.* 34: 215
10. Sherman SE, Lippard SJ (1987) *Chem. Rev.* 87: 1153
11. Lippert B (1988) *Gaz. Chim. Ital.* 118: 153
12. Manaka RC, Wolf W (1978) *Chem.-Biol. Interact.* 22: 353
13. McBrien DCH, Slater TF (eds) (1986) *Biochemical mechanisms of platinum antitumor drugs*. IRL, Oxford
14. Pascoe JM, Roberts JJ (1974) *Biochem. Pharmacol.* 23: 1345
15. Monti-Bragadin C, Tamaro M, Banfi E (1975) *Chem.-Biol. Interact.* 11: 469
16. Lecoite P, Macquet JP, Butour JL, Paoletti C (1977) *Mutation Res.* 48: 139
17. Johnson NP, Hoeschele JD, Rahn RO, O'Neill JP, Hsie AW (1980) *Cancer Res.* 40: 1463
18. Plooy ACM, van Dijk M, Lohman HM (1984) *Cancer Res.* 44: 2043
19. van den Berg HW, Roberts JJ (1975) *Mutation Res.* 33: 279
20. Bonatti S, Lohman PHM, Berends F (1983) *Mutation Res.* 116: 149
21. Brodberg RK, Lyman RF, Woodruff RC (1983) *Environ. Mutagen.* 5: 285
22. Tandon P, Sodhi A (1985) *Mutation Res.* 156: 187
23. Shooter KV, Howse R, Merrifield RK, Robins AB (1972) *Chem.-Biol. Interact.* 5: 289
24. Munchausen LL (1974) *Proc. Natl. Acad. Sci. USA* 71: 4519
25. Villani G, Lherisson C, Defais M, Johnson NP (1987) *Mutation Res.* 183: 21
26. Knox RJ, Lydall DA, Friedlos F, Basham C, Roberts JJ (1987) *Biochim. Biophys. Acta* 908: 214
27. Rosenberg B, van Camp L, Grimley EB, Thomson AJ (1967) *J. Biol. Chem.* 242: 1347
28. Reslova S (1971/72) *Chem.-Biol. Interact.* 4: 66
29. Lecoite P, Macquet JP, Butour JL (1979) *Biochem. Biophys. Res. Comm.* 90: 209
30. Walker GC (1984) *Microbiol. Rev.* 48: 60
31. Painter RB (1977) *Nature* 265: 650
32. Howle JA, Gale GR (1970) *Biochem. Pharmacol.* 19: 2757
33. Harder HC, Rosenberg B (1970) *Int. J. Cancer* 6: 207
34. Beck DJ, Brubaker RR (1973) *J. Bact.* 116: 1247
35. Drobnik J, Urbankova M, Krekulova A (1973) *Mutation Res.* 17: 13
36. Fraval HNA, Rawlings CJ, Roberts JJ (1978) *Mutation Res.* 51: 121
37. Roberts JJ, Fraval HNA (1978) *Biochimie* 60: 869
38. Cleare MJ (1974) *Coord. Chem. Rev.* 12: 349
39. Alazard R, Germanier M, Johnson NP (1982) *Mutation Res.* 93: 327
40. Plooy ACM, Lohman PHM (1980) *Toxicology* 17: 169
41. Salles B, Lesca C (1982) *Biochem. Biophys. Res. Comm.* 105: 202
42. Johnson NP, Hoeschele JD, Kummerle NB, Masker WE, Rahn RO (1978) *Chem.-Biol. Interact.* 23: 267
43. Beck DJ, Brubaker RR (1975) *Mutation Res.* 27: 181
44. Beck DJ, Fisch JE (1980) *Mutation Res.* 77: 45
45. Caskey CT, Kruh GD (1979) *Cell* 16: 1
46. Skipper HE, Schabel FM, Wilcox WS (1964) *Cancer Chemother. Rep.* 35: 1
47. Wright M, Lacorre-Arescaldino I, Macquet JP, Daffe M (1984) *Cancer Res.* 44: 777
48. Hartley FR (1973) *The chemistry of platinum and palladium*. Applied Science, London.
49. Vrana O, Brabec V (1986) *Int. J. Radiat. Biol.* 50: 995
50. Zwelling LA, Filipiski J, Kohn KW (1979) *Cancer Res.* 39: 4989
51. Bradley MO, Patterson S, Zwelling LA (1982) *Mutation Res.* 96: 67
52. Zwelling LA (1983) In: S. J. Lippard (ed) *Platinum, gold and other metal chemotherapeutic agents: chemistry and biochemistry*. American Chemical Society, Washington, p 27
53. Eastman A (1986) *Biochem.* 25: 3912
54. Reishus JW, Martin DS Jr. (1961) *J. Am. Chem. Soc.* 83: 2457
55. Lim MC, Martin RB (1976) *J. Inorg. Nucl. Chem.* 38: 1911
56. Perumareddi JR, Adamson AW (1968) *J. Phys. Chem.* 72: 414

57. Jensen KA (1939) *Z. Anorg. Allg. Chem.* 242: 87
58. Rosenberg B (1978) *Biochimie* 60: 859
59. Faggiani R, Lippert B, Lock CJL, Rosenberg B (1978) *Inorg. Chem.* 17: 1941
60. Johnson NP, Hoeschele JD, Rahn RO (1980) *Chem.-Biol. Interact.* 30: 151
61. Horacek P, Drobnik J (1971) *Biochim. Biophys. Acta* 254: 341
62. Green M (1987) *Transition Met. Chem.* 12: 186
63. Butour JL, Macquet JP (1977) *Eur. J. Biochem.* 78: 455
64. Macquet JP, Butour JL (1978) *Eur. J. Biochem.* 83: 375
65. Macquet JP, Butour JL (1978) *Biochimie* 60: 901
66. Butour JL, Macquet JP (1981) *Biochim. Biophys. Acta* 653: 305
67. Pascoe JM, Roberts JJ (1974) *Biochem. Pharmacol.* 23: 1359
68. Zwelling LA, Anderson T, Kohn KW (1979) *Cancer Res.* 39: 365
69. Roberts JJ, Friedlos F (1982) *Chem.-Biol. Interact.* 39: 181
70. Schaller W, Holler E (1988) in: Nicolini, M. (ed) *Platinum and other metal coordination compounds in cancer chemotherapy*. Martinus Nijhoff, Boston, p 132
71. Kleinwachter V, Vrana O, Brabec V, Johnson NP (1988) *Studia Biophys.* 123: 85
72. Wing RM, Pjura P, Drew HR, Dickerson RE (1984) *EMBO J.* 3: 1201
73. Fichtinger-Schepman AMJ, van der Veer JL, Lohman PHM, Reedijk J (1984) *J. Inorg. Biochem.* 21: 103
74. Johnson NP, Mazard AM, Escalier J, Macquet JP (1985) *J. Am. Chem. Soc.* 107: 6376
75. Butour JL, Johnson NP (1986) *Biochem.* 25: 4534
76. Fichtinger-Schepman AMJ, van der Veer JL, den Hartog JHJ, Lohman PHM, Reedijk J (1985) *Biochem.* 24: 707
77. Marcelis ATM, Canters GW, Reedijk J (1981) *Recueil J. Royal Neth. Chem. Soc.* 100: 391
78. den Hartog JHJ, Altona C, Chottard JC, Girault JP, Lallemand JY, de Leeuw FAAM, Marcelis ATM, Reedijk J (1982) *Nucl. Acids Res.* 10: 4715
79. Girault JP, Chottard G, Lallemand JY, Chottard JC (1982) *Biochem.* 21: 1352
80. Girault JP, Chottard JC, Guittet ER, Lallemand JY, Huynh-Dinh T, Igolen J (1982) *Biochem. Biophys. Res. Comm.* 109: 1157
81. Caradonna JP, Lippard SJ (1982) *J. Amer. Chem. Soc.* 104: 5793
82. Reedijk J, Fichtinger-Schepman AMJ, den Hartog JHJ (1983) *Inorg. Chim. Acta* 79: 252
83. den Hartog JHJ, Altona C, van Boom JH, van der Marel GA, Haasnoot CAG, Reedijk J (1984) *J. Amer. Chem. Soc.* 104: 1528
84. Neumann JM, Tran-Dinh S, Girault JP, Chottard JC, Huynh-Dinh T, Igolen J (1984) *Eur. J. Biochem.* 141: 465
85. van Hemelryck B, Guittet E, Chottard G, Girault JP, Huynh-Dinh T, Lallemand JY, Igolen J, Chottard JC (1984) *J. Amer. Chem. Soc.* 106: 3037
86. den Hartog JHJ, Altona C, van Boom JH, Reedijk J (1984) *FEBS Lett.* 176: 393
87. den Hartog JHJ, Altona C, van der Marel GA, Reedijk J (1985) *Eur. J. Biochem.* 147: 371
88. Sherman SE, Gibson D, Wang AHJ, Lippard SJ (1985) *Science* 230: 412
89. Admiraal G, van der Veer JL, de Graaff RAG, den Hartog JHJ, Reedijk J (1987) *J. Amer. Chem. Soc.* 109: 592
90. van Hemelryck B, Guittet E, Chottard G, Girault JP, Herman F, Huynh-Dinh T, Lallemand JY, Igolen J, Chottard JC (1986) *Biochem. Biophys. Res. Comm.* 138: 758
91. Rice JA, Crothers DM, Pinto AL, Lippard SJ (1988) *Proc. Natl. Acad. Sci. USA* 85: 4158
92. van Hemelryck B, Girault JP, Chottard G, Valadon P, Laoui A, Chottard JC (1987) *Inorg. Chem.* 26: 787
93. Laoui A, Kozelka J, Chottard JC (1988) *J. Amer. Chem. Soc.* 27: 2751
94. Dewan JC (1984) *J. Amer. Chem. Soc.* 106: 7239
95. Eastman A (1985) *Biochem.* 24: 5027
96. van der Veer JL, van den Elst H, den Hartog JHJ, Fichtinger-Schepman AMJ, Reedijk J (1986) *Inorg. Chem.* 25: 4657
97. Marcelis ATM, den Hartog JHJ, Reedijk J (1982) *J. Am. Chem. Soc.* 104: 2664
98. Marcelis ATM, den Hartog JHJ, van der Marel GA, Wille G, Reedijk J (1983) *Eur. J. Biochem.* 135: 343
99. den Hartog JHJ, Altona C, van Boom JH, Marcelis ATM, van der Marel GA, Rinkel LJ, Wille-Hazeleger G, Reedijk J (1983) *Eur. J. Biochem.* 134: 485

100. Inagaki K, Kidani Y (1984) *Inorg. Chim. Acta* 92: L9
101. den Hartog JHJ, Altona C, van den Elst H, van der Marel GA, Reedijk J (1985) *Inorg. Chem.* 24: 986
102. Plooy ACM, Fichtinger-Schepman AMJ, Schutte HH, van Dijk M, Lohman PHM (1985) *Carcinogenesis* 6: 561
103. Eastman A, Barry MA (1987) *Biochem.* 26: 3303
104. Eastman A, Jennerwein MM, Nagel DL (1988) *Chem.-Biol. Interact.* 67: 71
105. Lippard SJ, Hoeschele JD (1979) *Proc. Natl. Acad. Sci. USA* 76: 6091
106. Johnson NP, Macquet JP, Wiebers JL, Monsarrat B (1982) *Nucl. Acids Res.* 10: 5255
107. Sober H (ed) (1970) *Handbook of Biochemistry*, 2nd ed. The Chemical Rubber Co., Cleveland.
108. Theophanides T, Ganguli PK, Bertrand MJ (1981) *Anticancer Res.* 1: 383
109. Chu GYH, Mansy S, Duncan RE, Tobias S (1978) *J. Am. Chem. Soc.* 100: 593
110. Lawley PD, Brookes P (1963) *Biochem. J.* 89: 127
111. Zoltewicz JA, Clark FD, Sharpless TW, Grahe G (1970) *J. Am. Chem. Soc.* 92: 1741
112. Harder HC, Smith RG, Leroy AF (1976) *Cancer Res.* 36: 3821
113. Pinto AL, Lippard SJ (1985) *Proc. Natl. Acad. Sci. USA* 82: 4616
114. Villani G, Hubscher U, Butour JL (1988) *Nucl. Acids Res.* 16: 4407
115. Bernges F, Holler E (1988) *Biochem.* 27: 6398
116. Livneh Z (1986) *J. Biol. Chem.* 261: 9526
117. Sancar A, Rupp WD (1983) *Cell* 33: 249
118. Beck DJ, Popoff S, Sancar A, Rupp WD (1985) *Nucl. Acids Res.* 13: 7395
119. Page JD, Husain I, Chaney SG, Sancar A. (1988) In: Nicolini, M. (ed) *Platinum and other metal coordination compounds in cancer chemotherapy*. Martinus Nijhoff, Boston, p 115
120. Popoff SC, Beck DJ, Rupp WD (1987) *Mutation Res.* 183: 129
121. Fram RJ, Cusick PS, Wilson JM, Marinus MG (1985) *Mol. Pharmacol.* 28: 51
122. Pera MF, Rawlings CJ, Roberts JJ (1981) *Chem.-Biol. Interact.* 37: 245
123. Bedford P, Fichtinger-Schepman AMJ, Shellard SA, Walker MC, Masters JRW, Hill BT (1988) *Cancer Res.* 48: 3019
124. Eastman A, Schulte N (1988) *Biochem.* 27: 4730
125. Ciccarelli RB, Solomon MJ, Varshavsky A, Lippard SJ (1985) *Biochem.* 24: 7533
126. Roberts JJ, Friedlos F (1987) *Cancer Res.* 47: 31
127. Brouwer L, van de Putte P, Fichtinger-Schepman AMJ, Reedijk J (1981) *Proc. Natl. Acad. Sci. USA* 78: 7010
128. Burnouf D, Daune M, Fuchs RPP (1987) *Proc. Natl. Acad. Sci. USA* 84: 3758
129. Venturini S, Monti-Bragadin C (1978) *Mutation Res.* 50: 1
130. Konishi H, Usui T, Sawada H, Uchino H, Kidani Y (1981) *Gann* 72: 627
131. Jarosik GP, Beck DJ (1984) *Chem.-Biol. Interact.* 51: 247
132. Fram RJ, Cusick PS, Marinus MG (1986) *Mutation Res.* 173: 13
133. Johnson NP, Razaka H, Wimmer F, Defais M, Villani G (1987) *Inorg. Chim. Acta* 137: 25
134. Brouwer J, Vollebregt L, van de Putte P (1988) *Nucl. Acids Res.* 16: 7703
135. Mason WR (1972) *Coord. Chem. Rev.* 7: 241
136. Rosenberg B, van Camp L (1970) *Cancer Res.* 30: 1799
137. Braddock PD, Connors TA, Jones M, Khokhar AR, Melzack DH, Tobe ML (1975) *Chem.-Biol. Interact.* 11: 145
138. Beaumont KP, McAuliffe CA, Cleare MJ (1976) *Chem.-Biol. Interact.* 14: 179
139. Tobe ML, Khokhar AR (1977) *J. Clin. Hematol. Oncol.* 7: 114
140. Rose WC, Schurig JE, Huftalen JB, Bradner WT (1982) *Cancer Treat. Rep.* 66: 135
141. Rotondo E, Fimiani V, Cavallaro A, Ainis T (1983) *Tumori* 69: 31
142. Macquet JP, Butour JL (1983) *J. Natl. Cancer Inst.* 70: 899
143. Brandon RJ, Dabrowiak JC (1984) *J. Med. Chem.* 27: 861
144. Blatter EE, Vollano JF, Krishnan BS, Dabrowiak JC (1984) *Biochem.* 23: 4817
145. Vollano JF, Al-Baker S, Dabrowiak JC, Schurig JE (1987) *J. Med. Chem.* 30: 716
146. Bramwell VHC, Crowther D, O'Malley S, Swindell R, Johnson R, Cooper EH, Thatcher N, Howell A (1985) *Cancer Treat. Rep.* 69: 409
147. Pendyala L, Cowens JW, Chheda GB, Dutta SP, Creaven P (1988) *Cancer Res.* 48: 3533
148. Rahman A, Roh JK, Wolpert-DeFilippes MK, Goldin A, Venditti JM, Woolley PV (1988) *Cancer Res.* 48: 1745

149. Leonard BJ, Eccleston E, Jones D, Todd P, Walpole A (1971) *Nature* 234: 43
150. Berenbaum MC (1971) *Br. J. Cancer* 261: 208
151. Mattern IE, Cocchiarella L, van Kralingen CG, Lohman PHM (1982) *Mutation Res.* 95: 79
152. Poll EHA, Arwert H, Joenje H, Eriksson AW (1982) *Human Genet.* 61: 228
153. Vrana O, Brabec V, Kleinwachter V (1986) *Anti-Cancer Drug Design* 1: 95
154. van der Veer JL, Peters AR, Reedijk J (1986) *J. Inorg. Biochem.* 26: 137
144. van der Veer JL, Ligetvoet GJ, Reedijk J (1987) *J. Inorg. Biochem.* 29: 217
156. Astashkina TG, Vlasov VV, Kazakov SA, Cvetkov IV (1988) *Dokl. Akad. Nauk. SSSR* 301: 234
157. Brabec V, Vrana O, Kleinwachter V (1986) *Studia Biophysica* 114: 199
158. Eastman A (1987) *Biochem. Pharmacol.* 36: 4177
159. Kuroda R, Neidle S, Ismail IM, Sadler PJ (1983) *Inorg. Chem.* 22: 3620
160. Rosenberg B, van Camp L, Trosko JE, Mansour VH (1969) *Nature* 222: 385
161. Razaka H, Salles B, Villani G, Johnson NP (1986) *Chem.-Biol. Interact.* 60: 207
162. Das Sarma B, Daley SK, Elespuru RK (1983) *Chem.-Biol. Interact.* 46: 219
163. Mong S, Huang CH, Prestayko AW, Crooke ST (1980) *Cancer Res.* 40: 3313
164. Mong S, Eubanks DC, Prestayko AW, Crooke ST (1982) *Biochem.* 21: 3174
165. Vollano JF, Blatter EE, Dabrowiak JC (1984) *J. Am. Chem. Soc.* 106: 2732
166. Salles B, Defais M (1984) *Mutation Res.* 131: 53
167. Salles B, Germanier M, Defais M (1987) *Mutation Res.* 183: 213
168. Neidle S, Waring MJ (eds) (1983) *Molecular aspects of anticancer drug action*, Chemie, Weinheim.

Ruthenium Chemistry Pertaining to the Design of Anticancer Agents

Michael J. Clarke

Department of Chemistry, Boston College, Chestnut Hill, MA 02167/USA

Ruthenium compounds hold particular promise in the design of new anticancer agents, including: a) chemotherapeutic drugs, b) radiopharmaceuticals for diagnostic imaging, and, c) most recently, radiosensitizers for radiotherapy. With regard to chemotherapeutic agents, complexes with nitrogen ligands and anionic leaving groups appear to be the most active as cytotoxic agents, with nuclear DNA usually assumed as the target site. Binding to DNA may occur in a variety of modes with ion-pairing and covalent bonding probably being the most important for active agents, often with the former occurring before the latter. After injection as a Ru(III) prodrug, selective localization in the tumor may take place by *in vivo* reduction to the more actively binding Ru(II) complex. Transferrin may also mediate the transfer of some ruthenium complexes to the tumor site. At least in the case of $[(\text{H}_2\text{O})(\text{NH}_3)_5\text{Ru}]^{2+}$, coordination to DNA occurs initially at G⁷ sites in the major groove of the DNA. However, higher concentrations appear to cause uncoiling with subsequent binding to the exocyclic amines of A and C. On coordination to nucleosides, ammineruthenium ions can migrate between nitrogen sites or exist as rotamers on exocyclic amines. Such metal ion movements can be choreographed by controlling the pH and electrochemical potential of the media. Square-wave voltammetry promises to be a sensitive method for probing the redox chemistry of ruthenium both on free nucleosides and on DNA, and for monitoring isomerization reactions following electron transfer. At high pH, Ru(III) induces the rapid autoxidation of nucleosides, in a manner reminiscent of xanthine oxidase, to yield 8-keto-purines. The anticancer activities of some selected ruthenium compounds are surveyed as to possible mechanisms consistent with their chemistry.

1 Introduction	26
2 Chemistry	26
3 Binding to Nucleic Acids	28
4 Terpsichorean Movements	30
5 Effects of Ru Coordination	34
6 Antitumor Activity	35
7 Acknowledgement	37
8 References	37

1 Introduction

Ruthenium compounds with nitrogen ligands have not only shown good antitumor activity in screening studies¹⁻⁶⁾ but many also localize in tumor tissue^{7,8)}. Since selective uptake of radioactive isotopes provides one means of visualizing tumors by modern scintigraphic imaging techniques⁷⁻⁹⁾, the development of ruthenium-containing anticancer pharmaceuticals may proceed along either chemotherapeutic or radiodiagnostic lines. Tumor localization can aid selective tumor toxicity, so that, in the case of ruthenium, the two types of pharmaceutical activities may be related. Moreover, the target molecule for most metal-containing anticancer agents appears to be DNA, which is also the target for anticancer radiotherapy and most radiosensitizing agents. As discussed elsewhere in this volume, Farrell has recently used ruthenium complexes to help localize radiosensitizing agents onto cellular DNA by employing them as ligands in platinum group metal complexes¹⁰⁾.

While these three areas now constitute the foci of research into ruthenium-containing anticancer pharmaceuticals, ruthenium(II) complexes with ammine or imine ligands are also capable of binding to specific sites on protein surfaces and altering their activity. Consequently, investigations into the medicinal uses of this metal may be useful whenever interrupting the function of nucleic acids or some types of proteins would result in therapeutic effects. In particular, since virus particles consist of little more than a nucleic acid code encased in a protein coat, it is reasonable to consider that ruthenium-based drugs may be developed against at least some types of human viruses.

2 Chemistry

In aqueous solution with nitrogen and acido ligands the Ru^{II}, Ru^{III} or Ru^{IV} oxidation states usually prevail. The majority of nitrogen ligands when bound to any of the three specified ions are often inert to substitution¹¹⁻¹³⁾. Ruthenium(IV) compounds require a number of acido, oxo^{14,15)} or sulfido ligands for stabilization¹⁶⁾, while ruthenium(II) species will remain unoxidized in air only if good π -acceptor ligands are present. Unlike the platinum anticancer drugs, which (in their active form) are square-planar in geometry, these ruthenium ions are usually six coordinate with octahedral structures. The two additional coordination sites may allow new modes of binding to nucleic acids, and, with some ligands, provide for chirality in the complexes and so in their interactions with the DNA helix¹⁷⁾.

The reduction potentials of ruthenium complexes are strongly modulated by the ligands. For example, E° values vary from -0.08 V with L = hydroxide to 1.1 V with dinitrogen¹⁸⁾. Anionic, σ -donor ligands usually lower the reduction potential, while neutral or cationic, π -acceptor ligands raise it. Owing to small bond distortions between Ru^{II} and Ru^{III}, redox reactions involving Ru^{II,III} couples are often rapid^{11,10)}. Ligand substitution in ammine-ruthenium(II) ions is solvent-mediated in aqueous solution and so is controlled by the rate of water exchange ($k_{ex} = 5-10$ s⁻¹)¹²⁾. In most complexes with the specified ruthenium ions, the bonds to ammonia or other nitrogen ligands are sufficiently strong to remain intact following electron transfer^{11,12)}.

Drugs which selectively localize in tumors should exhibit enhanced toxicity to tumor cells. If they contain a γ -emitting isotope, such pharmaceuticals may also be useful in imaging and locating the tumor. An approach, that may accomplish both objectives, involves ammine-ruthenium(III) ions as prodrugs and does not require the presence of specific receptor sites. Since ruthenium(III) ions are relatively "hard" and have a high attraction for halides and anionic oxygen ligands, these ligands are retained for fairly long periods. Conversely, ruthenium(II) ions are relatively "soft" and have little affinity for these ligands. In general, prodrugs introduced into an organism as Ru(III) or Ru(IV) with nitrogen and acido ligands would be expected to remain fairly stable to substitution as long as these oxidation states are maintained. Upon reduction to a lower oxidation state, the metal would immediately lose the acido ligand and engage in rapid exchange of water molecules at the open site. Consequently, tissue binding is expected to be favored in areas low in oxygen and high in reductants, such as the reducing, hypoxic environment prevalent in many tumors²⁰, where reduction, but not reoxidation, of the ruthenium should produce a higher Ru(II)/Ru(III) ratio than in the surrounding, more aerated tissue.

Being directly below Fe in the periodic table and existing in both the di- and tripositive oxidation states in aqueous solution, there is evidence that absorption of $\text{RuCl}_3 \cdot 3 \text{H}_2\text{O}$ into the body parallels that of iron. It is concentrated by the villi of the small intestines and then widely distributed, with a maximum blood concentration occurring within 12 hr²¹. A portion remains in the blood for a relatively long period and may be taken up by transferrin. Like Fe(III), Ru(III) has a high affinity for phenolate ligands²², which are involved in the transferrin Fe-binding site²³, so that it is not surprising that Ru also has a high affinity for this plasma protein. Release of Ru(III) from transferrin may be facilitated by cellular reduction to Ru(II)²⁴, which then separates and binds to cellular structures, while the transferrin is free to migrate back out of the cell. When large ligands, such as proteins, are involved, localization is usually dependent on the nature of the biochemical moiety. For example, tumor localization resulting from protein labelling occurs with ^{103}Ru -transferrin, whose uptake by EMT-6 sarcoma in mice is almost twice as high as that of the most widely used tumor-imaging agent^{25,26}. Rapidly growing cells, such as those in neoplasms, have a high iron requirement and, consequently, a large number of receptors for the Fe-transport protein, transferrin.

Bleomycin, an iron-requiring antibiotic which is often used successfully as an adjuvant to cisplatin, has been complexed with Ru in hopes of taking advantage of the tumor-localizing properties of this drug. Direct combination with $\text{RuCl}_3 \cdot 3 \text{H}_2\text{O}$ yields a product that retains a level of toxicity to cells in tissue culture identical with free bleomycin and exhibits similar *in vivo* uptake by rat tumors²⁷. Meares has reported on the photo-induced nicking of DNA in the presence of air by a Ru(II)-bleomycin, which was prepared by reduction of $\text{RuCl}_3 \cdot 3 \text{H}_2\text{O}$ in basic ethanol at 200 °C²⁸. Also, $[(\text{H}_2\text{O})(\text{NH}_3)_5\text{Ru}^{\text{II}}]^{2+}$ has been combined with bleomycin at room temperature to yield a mixture of products in which $[(\text{NH}_3)_5\text{Ru}^{\text{III}}]$ is coordinated to an imidazole ring nitrogen or to the exocyclic amine of the pyrimidine moiety in somewhat variable ratios⁵. These complexes are cytotoxic, but unlike iron-bleomycin, failed to show any increased ability to cleave DNA in the presence of oxygen and a reductant. The ruthenium ion appeared to be released upon electrochemical reduction and yielded $[\text{Cl}(\text{NH}_3)_5\text{Ru}]\text{Cl}_2$ on acid hydrolysis. Preli-

minary studies indicated the complex selectively localized in tumors, but no significant chemotherapeutic activity was evident.

Aside from uptake owing to nonspecific causes such as increased blood perfusion and higher cell permeability in tumors, overall it is likely that tumor accumulation of simple ammineruthenium complexes proceeds by two pathways. First, rapid tumor uptake proceeds through activation of the Ru^{III}-prodrug toward binding by reduction in the tumor. Since small ions are excreted fairly readily by the kidneys, this mode of binding should decrease rapidly with time. A second, slower mode of tumor binding, which may occur for many days following injection, is probably mediated by transferring.

Effective radio-imaging agents for the liver have been developed using radio-ruthenium(III) with iminodiacetato ligands containing lipophilic groups, which facilitate uptake by the biliary tract^{29,30}). Several lipophilic ruthenocene derivatives are excreted in both urine and bile following hydroxylation in the liver and formation of a glucuronide conjugate³¹) and some ruthenocene derivatives have been designed to localize in the adrenals and other organs^{32,33}). The complex [(pyal)(NH₃)₅Ru^{III}]³⁺ (pyal = b-(4-pyridyl)-a-alanine) shows good uptake by the pancreas³⁴). Complexes with phosphate and phosphonates tend to localize in bone³⁵). Ruthenium red³⁶) binds in vitro and in vivo to cell surfaces high in acidic glycoproteins and has been used to image tumors^{2-4,37,38}). Hexaammineruthenium(III) causes the elimination of pBR322 and pBR329 plasmids from *E. coli*³⁹).

3 Binding to Nucleic Acids

While it is possible for Ru(III) complexes to bind directly to nucleic acids⁴⁰), coordination by Ru(II) is usually considerably faster, so that reduction Ru(III) or Ru(IV) ions in the body is probably central to the mechanism of activity of these agents. Microsomal enzymes rapidly reduce ammineruthenium(III) ions when NADH is used as a reductant, as do mitochondria, but much more slowly⁴¹). Whole mitochondria will not oxidize [(NH₃)₆Ru]²⁺, but cyt-b₅₆₂ on the inner face of submitochondrial particles and cytochrome oxidase will^{42,43,44}). This complex is also reduced by the transmembrane electron transport system, which has been present in all cells tested²⁴). In general, these rates are rapid, if the electron-transfer site on the protein is near the surface. If the redox site is deeply buried within the protein matrix, the rates are several orders of magnitude slower⁴⁵).

A number of metalloprotein adducts prepared by the reaction of [(H₂O)(NH₃)₅-Ru^{II}]²⁺ with proteins have been used in studies of electron-transfer through the protein matrix^{46,47,48}). This metal ion tends to complex histidyl imidazoles, especially those relatively exposed on the surface, with a surprisingly high degree of selectivity^{49,50}). While coordination of [(H₂O)(NH₃)₅Ru^{II}]²⁺ to amine groups on proteins, such as surface lysines, might be expected to occur, this appears to be inhibited by competition from protons, and the affinity of this ion for carboxylate moieties is inherently low⁵¹).

Coordination of [(H₂O)(NH₃)₅Ru^{II}]²⁺ to DNA occurs somewhat more rapidly than might be expected. At higher [Ru]/[P_{DNA}] ratios, this reaction exhibits biphasic kinetics, the second phase of which probably has to do with the Ru(II) attacking

new sites made available on unpairing of the DNA strands. The initial reaction is relatively independent of DNA concentration in the millimolar range of $[P_{\text{DNA}}]$. At low $[\text{Ru}]/[P_{\text{DNA}}]$, coordination is almost exclusively at the N7 of guanine (G^7), which is relatively exposed in the major groove of B-DNA. Since the metal ion is a dication, it undergoes a fairly strong electrostatic attraction for the polyanionic DNA, entering into an ion-pairing equilibrium. This pre-equilibrium step increases the efficiency of the complexation reaction. Since $[(\text{H}_2\text{O})(\text{NH}_3)_5\text{Ru}^{\text{II}}]^{2+}$ is known to react by dissociative mechanisms, rapid binding probably follows loss of the water molecule. The rate law for this reaction is as follows:

$$\frac{d[\text{Ru}-\text{G}]}{dt} = \frac{f_{\text{G}}k_3k_2K_{\text{ip}}}{(k_2 + k_3)(1 + K_{\text{ip}}[G_{\text{DNA}}])} [P_{\text{DNA}}] [\text{Ru}^{\text{II}}]$$

where k_2 is the rate of water dissociation from $[(\text{H}_2\text{O})(\text{NH}_3)_5\text{Ru}^{\text{II}}]^{2+}$, while k_{-2} is the reassociation rate, k_3 is the rate at which the five-coordinate intermediate binds to guanine sites, and $[G_{\text{DNA}}]$ is the effective DNA nucleotide concentration capable of binding, i.e., that fraction of sites which are G, $[G_{\text{DNA}}] = f_{\text{G}} \times P_{\text{DNA}}$. K_{ip} is a function of the ionic strength of the monocations in the solution and can be estimated to be around 200 at $\mu = 0.1$ and 900 in Tris-Acetate (TA) buffer ⁵².

A second set of coordination sites becomes evident spectroscopically when $[\text{Ru}^{\text{II}}]/[P_{\text{DNA}}] > 0.5$ or when single-stranded DNA is used, which arise from coordination to the exocyclic amines, N6 of adenine and N4 of cytosine ⁵³. K_{assoc} for helical calf thymus DNA has been determined to be 5.1×10^3 and is 7.8×10^3 for single-stranded DNA. Binding at low $[\text{Ru}^{\text{II}}]/[P_{\text{DNA}}]$ causes a linear decrease in T_m and a decrease in the circular dichroism spectrum, which suggest a weakening or unwinding of the DNA helix. This work also provided the first direct measurement of a reduction potential for a metal ion coordinated to DNA, $E^\circ = 48 \text{ mV}$ for $[G_{\text{DNA}}^7(\text{NH}_3)_5\text{Ru}^{\text{III}}]^{53}$.

Binding of $[\text{Cl}(\text{NH}_3)_5\text{Ru}^{\text{III}}]^{2+}$ to both DNA ⁵⁴ and RNA ⁴⁰ has been observed, but is quite slow. Sundarlingham et al. showed that the reaction of $[\text{Cl}(\text{NH}_3)_5\text{Ru}^{\text{III}}]^{2+}$ with phenylalanine transfer RNA produced both ion-paired and covalently bound adducts ⁴⁰. Direct coordination was observed at the N7 of G_{15} , which was further stabilized by hydrogen bonding between ammine protons and phosphate oxygens on P_{14} and P_{15} . Additional N7 binding occurred at G_1 and G_{18} . The G_{15} and G_{18} sites are in non-helical regions, where their N7's are well exposed and the phosphate charge density is high ⁴⁰.

Barton has shown that chiral Ru(II) complexes with large, bidentate aromatic ligands interact with nucleic acids in ways that are largely dependent on the overall shape of the complex. Planar ligands which extend well out from the metal ion tend to intercalate into DNA to a degree dependent on their chirality and that of the nucleic acid ⁵⁵. Smaller complexes or ones with shapes unsuitable for intercalation are more likely to attach to the surface of the DNA either through electrostatic or van der Waals forces. Enantiomers of $[(\text{DIP})_3\text{Ru}]^{2+}$, where DIP = 4,7-diphenylphenanthroline, distinguish between right- and lefthanded DNA helices, with the D-enantiomer preferentially binding to right-handed B-DNA. While both enantiomers bind equally to left-handed Z-DNA, space-filling models suggest that a left-

handed DNA with a tighter helix should preferentially bind the Λ -enantiomer ⁵⁶. Direct coordination (probably at G⁷) has been proposed with similar complexes such as *cis*-[Cl₂(phen)₂Ru^{II}]; in this case, the Λ -enantiomer selectively binds B-DNA ⁵⁶. Binding proceeds somewhat slowly ($t_{1/2} = 1.5$ h) and is probably preceded by intercalation through the *o*-phenanthroline rings.

4 Terpsichorean Movements

Movement of pentaammineruthenium between different sites on the same purine or pyrimidine ligand can occur as a result of changes in the ruthenium oxidation state or by altering the charge distribution on the ligand. Deprotonation from N1 of 7-methylhypoxanthine leaves a negative charge on the pyrimidine ring causing coordination at the N3 of the same ring to be stable; however, neutralization of this charge by protonating N1 induces the metal ion to move to the nearby N9 site with a half-life of about 1.5 hr ⁵⁷.

Stable complexes of pentaammineruthenium(III) with adenosine and related ligands are easily isolated, in which the Ru(III) is coordinated to the somewhat unusual position of the exocyclic amine ⁵⁸. With this as a starting material, it is possible to investigate metal ion movements on these sorts of ligands using NMR and electrochemical techniques. As shown in Fig. 1, the presence of the paramagnetic Ru(III) ion induces large shifts in the ¹H-NMR resonances of the protons at C2

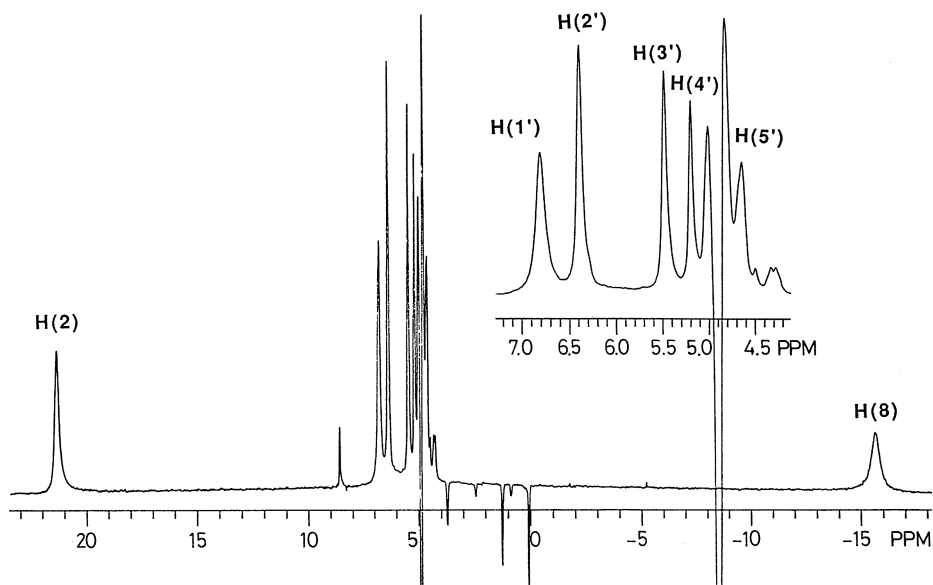


Fig. 1. ¹H-NMR spectrum of 6-[5'-AMP(NH₃)₅Ru^{III}] in D₂O at pH 1.23 showing large shifts in resonances due to the paramagnetism of Ru(III). The peak at 8.6 ppm is due to free ligand. Inverted peaks arise from TSP owing to suppression of the HOD peak, which has a similar relaxation time

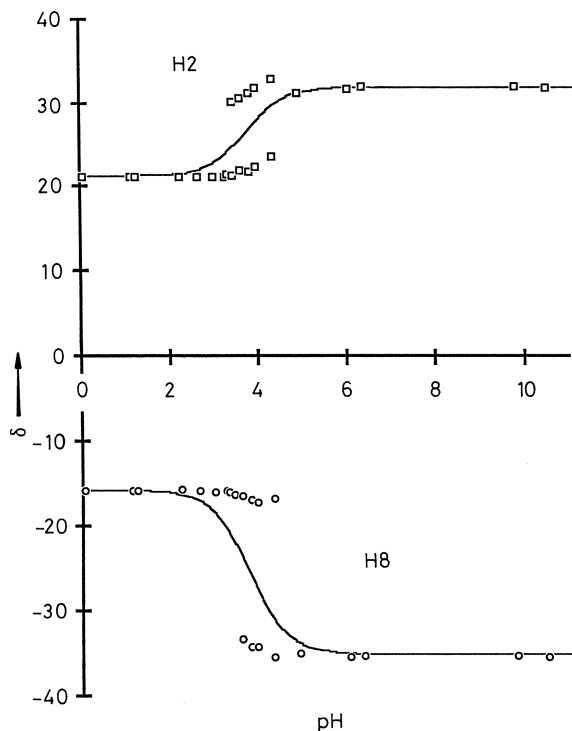


Fig. 2. Plot of NMR chemical shift (δ) versus pH for H2 and H8 on 6-[Ado(NH₃)₅Ru^{III}]. Fitted line assumes spectrophotometrically determined pK_a. Divergence is attributed to the presence of pH-dependent rotameric forms

and C8 on the adenine ring with the former being shifted downfield 12–25 ppm and the latter moved upfield by 25–35 ppm. Figure 2 shows the changes in these resonances as a function of pH with the *solid lines* representing fits using the spectrophotometrically determined pK_a value of 3.15⁵⁶). Obviously, many of the points do not lie close to the fitted lines but diverge in a manner suggesting pK_a values significantly greater or less than the spectrophotometric measurement. In fact, these data indicate that there are two different isomers in equilibrium, each with a different spectrum and acidity.

In this case, the isomers are rotamers, which interconvert depending upon whether the N1 site is protonated or not. When deprotonated, hydrogens on coordinated ammine ligands can form hydrogen-bonds with the lone pair available on N1, so that the metal ion resides on the N1 side of the ligand (E-form). However, when a proton resides at this position, H-bonding is negated and a steric repulsion is set up inducing the metal ion to swing around the C–N axis to the imidazole side of the purine. In this, the Z-form, H-bonding becomes possible between the amines and N7. Similar rotamerizations are seen in cytosine derivatives.

The existence of two rotameric forms is also evident in the electrochemistry of these complexes. Figure 3 illustrates a series of square-wave voltammograms of [(Ado)(NH₃)₅Ru^{III}] taken on a mercury electrode at three different voltage scan rates. Computer simulated scans, which were calculated by the algorithm developed by Prock⁵⁹), are also given in this figure. Comparison of the two shows that rate

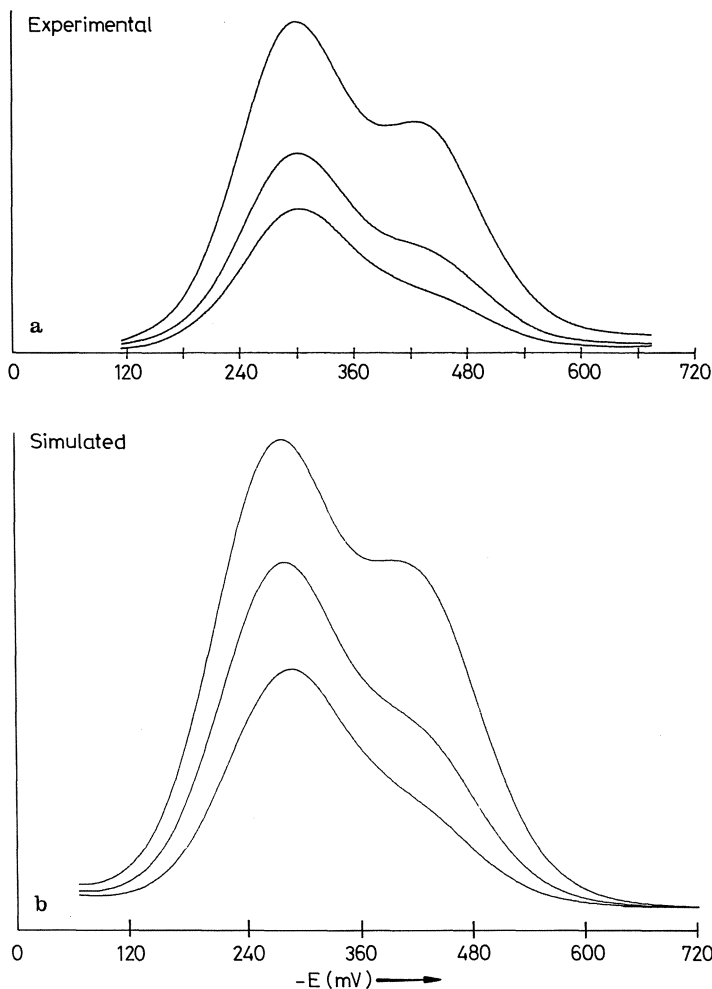


Fig. 3a. Square-wave voltammograms of a 6-[(5'-AMP)(NH₃)₅Ru^{III}] on Hg electrode showing changing E/Z rotameric ratio with varying scan rate, which are 500, 250 and 125 mV/s. The experiment is run from an initial potential of +100 mV (versus Ag/AgCl, note abscissa is $-E$) and scanned negatively in steps of 2 mV to -700 mV, with a square wave amplitude of 50 mV, and then back positively. Scan rates are varied by changing the staircase frequency. The scans traced are for the reverse (anodic) scans. **b** Computer simulations were made with the following rate constants: $k_{\text{exo-endo}} = 0.91 \text{ s}^{-1}$, $k_{\text{endo-exo}} = 10.0 \text{ s}^{-1}$, and $k_{\text{E-Z}} = 4.65 \text{ s}^{-1}$. Potential scale is relative to the Ag/AgCl electrode

constants for first-order reactions following electron transfer can be extracted from square-wave experiments of this type. The two voltammetric peaks correspond to the two rotameric forms in which the Ru is on the N1 side (*E*-form) and on the N7 side (*Z*-form) of the adenosine. In the *E*-form, the Ru(III) is placed closer to the anionic charge residing on the deprotonated N1, and so is more difficult to reduce than the other rotamer. In the *Z*-form, the metal ion is more distant from the ligand's

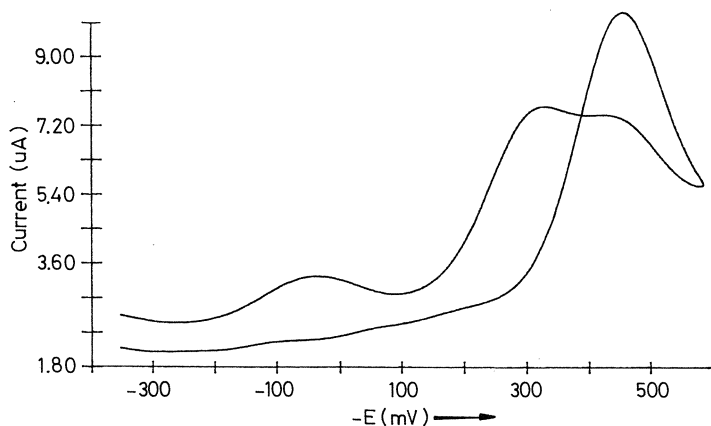


Fig. 4. Square-wave voltammetry scans of a 6-[(5'-AMP)(NH₃)₅Ru^{III}] on carbon paste electrode showing the appearance of the endocyclic isomer in the reverse scan. Potential scale is relative to the Ag/AgCl electrode

negative charge and has the higher reduction potential. Upon reduction of the Ru(III), protonation at N1 also occurs, since this site is rendered less acidic on reduction of the charge of the metal ion, which is proximal to the ionization site. As already indicated, protonation at this site favors the *Z*-rotamer, so that a change in the *E* and *Z* current peaks takes place. The slower the scan rate, the more time the complex has to rotamerize following reduction, so that the relative size of the two peaks is a function of the rate of the voltage change.

A second type of isomerization occurs on reducing the Ru(III) to Ru(II), which involves the movement of the metal ion from the exocyclic amine to the adjacent ring nitrogen at N1. Coordination at the latter position is preferred by Ru(II), since backbonding from the metal ion to the endocyclic imine occurs to form a partial

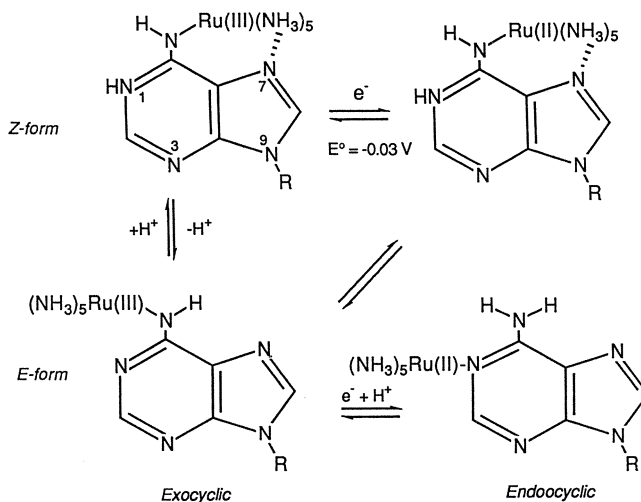


Fig. 5. Summary of various isomeric forms possible with [(Ado)(NH₃)₅Ru]

π -bond, which is evident in the significantly higher reduction potential (around 300 mV in Fig. 4). Re-oxidation to Ru^{III} facilitates deprotonation of the adjacent exocyclic ammine, N(6), making this the more attractive binding site, so that the metal ion can easily move back to form an amide complex, in which substantial π -bonding from N6 to the Ru(III) occurs⁴). Since the movement of the metal ion occurs in either direction, depending on the oxidation state of the ruthenium, the relative change in peak heights between the waveforms for the *endo*- and *exocyclically* bound complexes as a function of scan rate can be used to estimate the rates of linkage isomerization in both directions. The various movements of ruthenium as a function of metal oxidation state and protonation state of the ligand are summarized in Fig. 5. Square-wave voltammetric studies of $[(\text{NH}_3)_5\text{Ru}]_n$ -DNA show behavior similar to that seen in Fig. 4, with the wave for electron transfer involving $[\text{dG}^7(\text{NH}_3)_5\text{Ru}^{\text{III}}]$ superimposed around 48 mV (vs. NHE).

5 Effects of Ru Coordination

Due to the relative selectivity of ammineruthenium ions for the N7 of purines, it is likely that these ions may concentrate in nuclear chromatin and so interfere with nucleic acid metabolism. Indeed, *in vitro* studies demonstrate that Ru^{II} and Ru^{III} compounds are active in inhibiting DNA synthesis⁶⁰ and possess mutagenic activity in the Ames and related assays⁶¹). Among the possible mechanisms for interfering with DNA metabolism following binding to G⁷ sites are: 1) failure of replicating enzymes to recognize the metallated G; 2) additional metal binding following or inducing helix disruption; 3) subsequent protein-, intra-, or interstrand crosslinking by the metal; 4) chemical reactions of the guanine residue induced by the presence of the metal ion; and, 5) Fenton's chemistry taking place at the metal ion to generate radicals capable of strand cleavage.

Replication enzymes are sensitive to the ionic environment, so that even simple outer-sphere ion-pairing or hydrogen bonding may cause replication errors to be made. This may be especially so if such binding induces a local change in DNA conformation. Local helix disruption might be caused by a) the sheer bulk of the metal ion, b) weakening of the hydrogen bonding and π -stacking abilities of the base through polarization of electron density toward the metal cation, which is accentuated in the case of Ru^{III} by π -bonding effects, and c) O(6) and phosphate hydrogen bonding to ammine protons. Additionally, the linkage isomerization reactions already discussed may allow the metal to migrate on the surface of the DNA. The effect of $[(\text{NH}_3)_5\text{Ru}^{\text{III}}]$ on purine and pyrimidine acidity, which would probably affect base pairing, has been shown to vary in a predictable inverse-square fashion^{2-4,57}).

The relatively high charge of Ru^{III} sometimes makes apparent chemical effects resulting from electronic polarization that are often not observable with dipositive metal ions. One example is the lysing of the sugar-purine bond in $[(\text{dG}^7)(\text{NH}_3)_5\text{Ru}^{\text{III}}]$, which occurs with a half-life of 1.5 days at 56 °C and pH 7⁶²). A reaction unobserved with other metal ions is the air oxidation of the nucleosides to 8-hydroxy-nucleosides when coordinated to $[(\text{NH}_3)_5\text{Ru}^{\text{III}}]$ at the N7 position. The donation of π -electron density from the nucleoside to the metal ion facilitates an initial deprotonation step,

which probably involves C8, and electron transfer to O₂⁶⁵. This autoxidation reaction of [(dG)(NH₃)₅Ru^{III}] proceeds with a half-life of about 1.8 hr at 56 °C and pH 7.56.

The autoxidation of 7-[(Ino)(NH₃)₅Ru]³⁺ and 7-[(1 MeIno)(NH₃)₅Ru]³⁺ also proceeds rapidly at high pH to yield the corresponding 8-keto complexes. These reactions have been studied as a function of pH and oxygen concentration and obey the rate law: $d[(8\text{-O-Ino})\text{Ru}]/dt = k_1 k_2 [(\text{Ino})\text{Ru}][\text{O}_2] / \{k_{-1}[\text{H}^+] + k_2[\text{O}_2]\}$. The reaction with 7-[(Ino)(NH₃)₅Ru]³⁺ exhibits a secondary kinetic isotope effect of $k_{\text{H}}/k_{\text{D}} = 1.6 \pm 0.3$. Running the reaction in H₂¹⁸O resulted in 80% substitution of ¹⁸O in the oxidized product. At 25° the specific rates for the Ino and MeInb complexes respectively are: $k_1 k_2 / k_{-1} = (7 \pm 2) \times 10^{-11}$ and $(9 \pm 2) \times 10^{-10} \text{ s}^{-1}$, and $k_1 = (6 \pm 1) \times 10^{-4}$ and $(4 \pm 1) \times 10^{-4} \text{ s}^{-1}$. Activation parameters are $\Delta H^* = 54 \pm 4 \text{ kJ/mol}$, and $\Delta S^* = -120 \pm 21 \text{ J/mol } ^\circ\text{K}$, for the Ino complex. The rate law, kinetic isotope effect and isotopic labeling are consistent with a mechanism involving proton ionization at the C8 position followed by autoxidation as the rate limiting step.

The cleavage of DNA via autoxidation of small transition metal ion complexes in the presence of a reductant is now a well known phenomenon^{63,64}. In such systems, it is generally thought that hydroxyl radicals are ultimately generated (Fenton's chemistry) and that these rapidly attack sugar groups on the DNA⁶⁶. In some cases, it is more efficient to use hydrogen peroxide, rather than molecular oxygen, as the oxidant. Abstraction of hydrogen atoms by the hydroxy radicals initiates sugar fragmentation and strand scission. A number of ruthenium complexes have been shown to cleave DNA, presumably through generation of Fenton's chemistry⁵⁴. However, when [(NH₃)₅Ru^{III}] is bound directly to G⁷ sites little or no strand cleavage occurs. This may be due to the fact that the concentration of ruthenium cations around the polyanionic DNA is substantially higher than those which covalently bind. Consequently, when the free ruthenium ions are removed, relatively little strand cleavage results from the fraction that remain. No evidence for strand cleavage that should follow hydrolysis of the sugar-purine bond or oxidation of the C⁸ of guanine has yet been observed⁵⁴. Recently, Barton and coworkers have shown that a ruthenium complex, Ru(DIP)₂MACRO]ⁿ⁺, where DIP = 4,4'-diphenyl-1,10-phenanthroline, and MACRO = DIP modified with a disulfonamide-TREN chelating group at the 4 position on each phenyl group, catalytically hydrolyzes the phosphodiester groups on DNA in the presence of a second metal ion, which is directly responsible for the hydrolysis. The ruthenium complex binds to the DNA through intercalation and its chelating ligands then concentrate hydrolytic metal ions, such as Cu(II) and Zn(II), near the phosphate backbone of the DNA. When low concentrations of the second metal are added, single-strand scission is effected; when higher concentrations are present, both strands are cleaved⁶⁵.

6 Antitumor Activity

Ruthenium compounds present a particularly promising and versatile path toward the development of new chemotherapeutic drugs. Table 1 lists screening results for a selected number of ruthenium complexes. In general, a high percentage of the ruthenium coordination complexes tested show presumptive antitumor activity and are

Table 1. Antitumor Activity of Selected Ruthenium Complexes^a

Compound	Dose (mg/kg)	T/C (%)	Ref.
<i>fac</i> -[Cl ₃ (NH ₃) ₃ Ru ^{III}]	50	189	Clarke ²⁾
[Cl ₃ (1,5-dimethyltetrazole) ₃ Ru ^{III}]	80	179	Keller, Keppler ⁶⁶⁻⁶⁹⁾
[CH ₃ CH ₂ COO(NH ₃) ₅ Ru ^{III}] ⁺ ClO ₄ ⁻	12.5	163	Clarke ²⁾
(ImH) ₂ [Cl ₃ ImRu ^{III}] (Im = imidazole)	72.8	162.5	Keppler ⁷³⁾
(1,2,4-triazolium)[Cl ₄ (1,2,4-triazole) ₂ Ru ^{III}]	45.1	161	Keller, Keppler ⁶⁶⁻⁶⁹⁾
<i>cis</i> -[Cl ₂ (NH ₃) ₄ Ru ^{III}]Cl	12.5	157	Clarke ²⁾
Ru ^{IV} (PDTA-H ₃)	120	152	González-Vilchez ⁷⁰⁾
[(C ₄ O ₄)(NH ₃) ₅ Ru ^{III}](F ₃ CSO ₃)	21.2	140	Pell, Clarke ⁷²⁾
<i>cis</i> -[Cl ₂ (DMSO) ₄ Ru ^{II}]	565	125	Sava, et al. ⁷⁴⁾
[Cl(NH ₃) ₅ Ru ^{III}]Cl	1.5	116	Armor ²⁾
[Ox(bipy) ₂ Ru]	3.13	101	Clarke ²⁾
[(Asc)(NH ₃) ₅ Ru ^{II}](F ₃ CSO ₃)	10	96	Pell, Clarke ⁷²⁾
[Cl ₂ (phen) ₂ Ru ^{II}] ⁺ ClO ₄ ⁻	6.25	90	Clarke ²⁾

^a T/C values are expressed as the 100 times the ratio of the lifetime of animals treated with the ruthenium drug to that for the untreated animals. Values listed are for the most common initial screens, i.e., P388, L1210 or Sarcoma 180. In some cases, T/C values on other screens were considerably higher or lower.

less toxic than cisplatin, but require a higher therapeutic dose. While still in need of verification by *in vivo* experiments, Ru-containing chemotherapeutic agents designed on the basis of the "activation by reduction" hypothesis often yield good results. In particular, it will be necessary to determine the modes of tumor uptake and DNA binding by ruthenium complexes in actual biological organisms.

The compound, *fac*-[Cl₃(NH₃)₃Ru], showed excellent activity in several tumor screens; however, its poor solubility precludes it from adequate formulation as a drug. Recognizing this, Keppler has successfully opted to pursue complexes with one or two fewer nitrogen ligands and one or two more halides, arriving at species which are more soluble due to their anionic charge ^{66,67,68,69)}. It is likely that such complexes are transported, at least in part, to the tumor site by transferrin, since the halides should be fairly easily displaced at the transferrin binding site. Initial results indicate that the nitrogen heterocycles on these types of ions may also be easily substituted ⁶⁶⁾. Of particular interest is the Ru(IV)-PDTA complex ⁷⁰⁾, which is likely to undergo reduction to Ru(III) or Ru(II) *in vivo*. Ruthenium(III) complexes with EDTA type ligands often substitute rapidly owing to the labilizing effect of a pendant carboxylate ligand ⁷¹⁾. The more active complexes appear to be monomeric with octahedral structures. At this point, it is not definitively known whether DNA is the target molecule for these complexes, and no studies are yet available on their possible modes of binding.

The activity of pentaammineurethenium complexes suggests that intrastrand G⁷—G⁷ crosslinking is not important in ruthenium anticancer agents as it is in the platinum drugs. Indeed, space-filling models indicate appreciable steric hindrance to the *cis*-coordination of guanine residues. However, crosslinks to other than adjacent sites remain a possibility and ammine ligands can be replaced by suitable attacking groups on either Ru(II) or Ru(III). In particular, if transferrin does transport

some ruthenium species to tumor sites, it is likely that several of the original ligands are displaced upon fixing Ru(III) in the iron binding site of the protein. This is likely to deliver a more aquated species into the cell, assuming that the metal ion is released intracellularly by reduction to Ru(II).

The lack of antitumor activity evident when mice bearing 180A sarcomas were treated with $[(\text{Asc})(\text{NH}_3)_5\text{Ru}](\text{CF}_3\text{SO}_3)$ contrasts with the results obtained in the NCI antitumor panel, where the structurally similar compound, $[\text{Sqr}(\text{NH}_3)_5\text{Ru}]\text{Cl} \cdot \text{H}_2\text{O}$, proved to be effective against the mouse P388 lymphocytic leukemia tumor with a best T/C of 140%. Against L1210 lymphocytic leukemia a T/C of 130% at a nontoxic dose of 25 mg/kg was obtained. Against a melanoma, the compound exhibited a T/C of 126% at 6.25 mg/kg, with all animals surviving. However, the compound showed no effect against an MXI, transplanted human mammary tumor, nor against the M5076 sarcoma.

Since the squarate and ascorbate complexes have the same charge and overall structure, it is surprising that one shows good activity and the other does not. Assuming the target site to be chromatin nucleic acids, neither of these complexes would likely bind to these sites without ligand loss opening up a coordination position. The electrochemical results show that both ascorbate and squarate ligands are rapidly lost on reduction of the ruthenium center⁷²). However, to be active in vivo, the complexes must have biologically accessible reduction potentials. Indeed, the $\text{Ru}^{\text{III,II}}$ couple for the squarate complex is quite accessible at 16 mV; however, that for the ascorbate species (-300 mV) is at or below the limit available in a biological system. The difference between these reduction potentials indicates that it is much more likely that the squarate complex will be reduced in vivo than the ascorbate. Consequently, the squarate complex will produce a much greater quantity of $[\text{H}_2\text{O}(\text{NH}_3)_5\text{Ru}^{\text{II}}]^{2+}$ to actively bind to nucleic acids and other molecules.

At this point, a relatively small number of ruthenium compounds have been tested for antitumor activity and relatively little is known of actual mechanisms of action. However, it is clearly desirable to synthesize and test a wider range of derivatives with the general formulations: *cis*- $[\text{X}_2\text{L}_4\text{Ru}]\text{X}$, $[\text{X}_3\text{L}_3\text{Ru}]$, and $\text{M}[\text{X}_4\text{L}_4\text{Ru}]$, where X = Cl or Br, L = NH_3 or nitrogen heterocycle and M = any monocationic cation, since these types of compounds have shown the most promise thus far. Use of large, aromatic ligands, capable of intercalating into the DNA and possibly forming H-bonds to the bases should increase the specificity of these complexes for the target molecule. For reasons mentioned previously, complexes prepared with these desired properties should also be screened against selected human viruses.

7 Acknowledgement

This work was supported by PHS Grant GM26390.

8 References

1. Dwyer FP, Mayhew E, Roe EMF, Shulman A (1965) *Brit J Cancer* 19: 195, and references therein
2. Clarke MJ (1980) *Metal ions in Biological Systems* 11: 231, and references therein
3. Clarke MJ (1980) In: Martell AE (ed) *Inorganic chemistry in biology and medicine*, ACS Symposium Series #190, American Chemical Society, Washington, D.C. p 157

4. Clarke MJ (1983) In: Lippard SJ (ed) *Platinum, gold and other chemotherapeutic agents*, ACS Symposium Series #209, American Chemical Society, Washington, D.C. p 335
5. Margalit R, Gray HB, Podbielski L, Clarke MJ (1986) *Chemico-Biological Interactions* 59: 231
6. Clarke MJ (1986) In: Zysk EE and Bonucci JA (eds) *Proceeding of the Ninth International Precious Metals Conference*, Int Precious Metals Inst, Allentown, PA, p 369
7. Srivastava SC, Mausner LF (1988) *Prog Clin Biochem Med* XX:XX
8. Schachner ER, Gil MC, Atkins HL, Som P, Srivastava SC, Badia J, Sacker DF, Fairchild R, Richards P (1981) *J Nucl Med* 6: 403. Taube M (1976) *Radioisotopes* 25: 44
9. Clarke MJ (1987) *Coord. Chem. Rev.* 78: 253
10. Farrell N (1988) *Prog. Clin. Biochem. Med.* XX: XX
11. Taube H (1973) *Surv. Prog. Chem.* 6: 1
12. See citations in reference 2
13. Shepherd R, Taube H (1973) *Inorg. Chem.* 12: 1392
14. Takeuchi KJ, Samuels GJ, Gersten SW, Gilbert JA, Meyer TJ (1983) *Inorg. Chem.* 22: 1407. Seok WK, Meyer TJ (1988) *J. Am. Chem. Soc.* 110: 7358 and references therein
15. Khan MMT, Ramachandiraiah G (1982) *Inorg. Chem.* 21: 2109
16. Koch SA, Millar M (1983) *J. Am. Chem. Soc.* 105: 3362
17. Mei HY, Barton JK (1985) *Proc. Natl. Acad. Sci., USA*, 85: 1339
18. Dowling MG, Clarke MJ (1983) *Inorg. Chim. Acta* 78: 153
19. Taube H (1979) *Pure Appl. Chem.* 51: 901
20. Gullino PM (1976) *Adv. Exp. Biol. Med.* 75: 521
21. Bruce RS, Carr TEF, Collins ME (1962) *Health Phys.* 8: 397
22. Pell SD, Salmonsens RB, Abelleira A, Clarke MJ (1984) *Inorg. Chem.* 23: 385
23. Que L (1983) *Coord. Chem. Rev.* 50: 73
24. Sun IL, Crane FL, Chou JY (1986) *Bio&em. Biophys. Acta* 886: 327
25. Srivastava SC, Richards P, Meinken GE, Larson SM, Grunbaum Z (1981) In: Spencer RP (ed) *Radiopharmaceuticals*, Grune & Stratton, New York, p 207
26. Som P, Oster ZH, Matsui K, Gugliemi G, Persson B, Pellettieri ML, Srivastava SC, Richards P, Atkins HL, Brill AB (1983) *Eur. J. Nucl. Med.* 8: 491
27. Stern PH, Halpern SE, Hagan PL, Howell S, Dabbs JE, Gordon RM (1981) *J. Nat. Canc. Inst.* 66: 807-11
28. Subramanian R, Meares CF (1985) *Biochem. Biophys. Res. Commun.* 133: 1145
29. Schachner ER, Gil MC, Som P, Oster ZH, Atkins HL, Subramanian G, Badia J, Srivastava SC, Richards P, Treves S (1983) *Nucl. Med. Commun.* 4: 94
30. Schachner ER, Gil MC, Som P, Oster ZH, Atkins HL, Subramanian G, Badia J, Srivastava SC, Richards P, Treves S (1981) *J. Nucl. Med.* 22: 352
31. Taylor AJ, Wenzel M (1978) *Biochem. J.* 172: 77
32. Herken R, Wenzel M (1985) *Eur. J. Nucl. Med.* 10: 56
33. Wenzel M, Park IH (1986) *Int. J. Appl. Radiat. Isot.* 37: 491
34. Meyer CD, Davis MA, Periana CJ (1983) *J. Med. Chem.* 26: 737
35. Srivastava SC, Som SC, Meinken GE, Sewatkar A, Ku TH (1978) *Abstracts: Proc. Sec. Intl. Cong. World Fed. Nucl. Med. & Bio., Washington D.C.,* p 19
36. Carrondo CT, Griffith WP, Hall JP, Skapski AC (1980) *Biochim. Biophys. Acta* 627: 332
37. Iozzo RVJ (1984) *Cell. Biol.* 99: 403
38. Anghileri LJ, Marchal C, Matrat M, Crone-Escanye MC, Robert J (1986) *Neoplasma* 33: 603
39. Reddy G, Shridhar P, Polasa H (1986) *Curr. Microbiol.* 13: 243
40. Rubin JR, Sabat M, Sundarlingam M (1983) *Nucl. Acid Res.* 11: 6571
41. Clarke MJ, Bittle S, Rennert D, Buchbinder M, Kelman AD (1980) *Journal of Inorganic Biochemistry* 12: 79
42. Kunz WS, Konstantinov A (1984) *FEBS Lett.* 175: 100, and Kunz WS, Konstantinov A, Tsofina L, Liberman EA (1984) *FEBS Lett.* 172: 261
43. Tsofina L, Liberman EA, Vygodina TV, Konstantinov AA (1986) *Biochem. Intl.* 12: 103
44. Moroney PM, Scholes TA, Hinkle PC (1984) *Biochem.* 23: 4991
45. Cummins D, Gray HB (1977) *J. Am. Chem. Soc.* 99: 5158
46. Isied SS, Kuehn C, Worosila G (1984) *J. Am. Chem. Soc.* 106: 1722
47. Toi H, LaMar GN, Margalit R, Che CM, Gray HB (1984) *J. Am. Chem. Soc.* 106: 6213
48. Jackman MP, McGinnis J, Pows R, Salmon GA, Sykes AG (1988) *J. Am. Chem. Soc.* 110: 5880

49. Matthews CR, Recchia J, Froebe CL (1981) *Analyt. Biochem.* 112: 329. Matthews CR, Recchia J, Rhee MJ, Horrocks WD (1982) *Biochim. Biophys. Acta* 702: 105. Matthews CR, Erickson PM, Froebe CL (1980) *Biochim. Biophys. Acta* 624: 499
50. Gray HB (1986) *Chem. Soc. Rev.* 15: 17
51. Kuehn C, Taube H (1976) *J. Am. Chem. Soc.* 98: 689
52. Manning GS (1978) *Q. Rev. Biophys.* 11: 179
53. Clarke MJ, Buchbinder M, Kelman AD (1978) *Inorganica Chimica Acta* 27: L27
54. Clarke MJ, Jansen B, Marx KA, Kruger R (1986) *Inorganica Chimica Acta* 124: 13
55. Barton JK, Basile LA, Danishefsky A, Alexandrescu A (1984) *Proc. Natl. Acad. Sci. USA* 81: 1961. Barton JK (1988) *Chem. & Eng. News*, Sept. 26, 30–42
56. Barton JK, Lolis E (1985) *J. Am. Chem. Soc.* 107: 708
57. Kastner MK, Coffey KF, Clarke MJ, Edmonds SE, Eriks K (1981) *J. Am. Chem. Soc.* 103: 5747
58. Clarke MJ (1980) *Inorg. Chem.* 19: 1103
59. Prock A, Clarke MJ, Galang R (1988) (unpublished work)
60. Kelman AD, Clarke MJ, Edmonds SD, Peresie HJ (1977) *Journal of Clinical Hematology and Oncology* 7: 274
61. Yasbin RE, Matthews CR, Clarke MJ (1980) *Chemical and Biological Interactions* 30: 355
62. Clarke MJ, Morrissey PE (1983) *Inorg. Chim. Acta* 80: L69
63. Hertzberg RP, Dervan PB (1984) *Biochemistry* 23: 3934
64. Barton JK, Raphael AL (1984) *J. Am. Chem. Soc.* 107: 2466
65. Basile LA, Barton JK (1987) *J. Am. Chem. Soc.* 109: 7548. Basile LA, Raphael AL, Barton JK (1987) *J. Am. Chem. Soc.* 109: 7550
66. Keller HJ, Keppler BK, PCT Int. Appl. WO 8600,904
67. Keller HJ, Keppler BK, PCT Int. Appl. WO 8600,905
68. Keppler BK (1988) *Prog. Clin. Biochem. Med.* XX: XX
69. Keppler BK, Wehe D, Endres H, Rubp W (1987) *Inorg. Chem.* 26: 844 and 26: 4366
70. Vilaplana R, Basallote MG, González-Vilchez F (1988) *Am. Chem. Soc., Abstracts Natl. Meeting*, INOR 332
71. Matsubara T, Creutz CA (1979) *Inorg. Chem.* 18: 1956

New Ruthenium Complexes for the Treatment of Cancer

B. K. Keppler¹, M. Henn¹, U. M. Juhl¹, M. R. Berger², R. Niebl¹, and F. E. Wagner³

¹ Anorganisch-Chemisches Institut der Universität Heidelberg, Im Neuenheimer Feld 270, 6900 Heidelberg, FRG

² Institut für Toxikologie und Chemotherapie am Deutschen Krebsforschungszentrum, Im Neuenheimer Feld 280, 6900 Heidelberg, FRG

³ Physik-Department E15, Technische Universität München, 8046 Garching, FRG

The aim of developing new tumor-inhibiting ruthenium complexes, in particular compounds which act against tumors that have been chemoresistant up to now, has led us to the synthesis of different classes of ruthenium complexes. These were selected for further evaluation on the basis of increase in survival time in the P388 tumor model and water-solubility. The water-soluble ruthenium complexes coordinated with heterocycle ligands in *trans*-position, $\text{HB}(\text{RuB}_2\text{Cl}_4)$, and the corresponding pentachloro derivatives, $(\text{HB})_2(\text{RuBCl}_5)$, were identified as being the most active ones. Their chemical properties were investigated by means of x-ray analyses, Mössbauer spectra, NMR spectra, and other methods. Their galenic formulation was relatively easy to establish owing to their solubility in water or in physiological saline. Stability of the complexes turned out to be sufficient for infusion therapy. Antitumor activity of such compounds was confirmed not only in the P388 tumor model but also in the Walker 256 carcinosarcoma, the Stockholm Ascitic tumor, the subcutaneously growing B 16 melanoma, the intramuscularly growing sarcoma 180 and the AMMN-induced colorectal tumors of the rat.

In particular, the two compounds $\text{ImH}(\text{RuIm}_2\text{Cl}_4)$ and $\text{IndH}(\text{RuInd}_2\text{Cl}_4)$, Im = Imidazole, Ind = Indazole, turned out to be highly active against these tumor models, with the emphasis on activity against AMMN-induced colorectal tumors. This is a strong indication of future clinical activity against such adenotumors. The toxicological target organs turned out to be the kidneys and the liver. In addition, erythropenia and an increase in both creatinine and liver enzymes were observed. Nevertheless, in chronic application at therapeutic doses, toxicity is well tolerated. On account of these promising properties, the two compounds were selected for further toxicological studies, which are the prerequisites for the beginning of clinical studies.

1 Introduction	42
2 Synthesis, Characterization and Stability of New Cancerostatic Ruthenium Species	47
3 Tumor-inhibiting and Toxicological Properties of the New Ruthenium Compounds	59
4 Conclusions	66
5 Acknowledgements	67
6 Abbreviations	68
7 References	68

1 Introduction

Malignant neoplasms are responsible for about 25 % of total mortality in the western world today. Numerous efforts are being made to improve the efficacy of surgery, radiation, and chemotherapy — the three “weapons” against cancer.

The development of new tumor-inhibiting ruthenium complexes is a field of major interest in recent cancer research. Scientists’ efforts to find such substances can best be understood by going back, first of all, to Rosenberg’s investigations into platinum complexes^{1,2,3)}.

In 1969, Rosenberg discovered the pharmacological activity of *cis*-diamminedichloroplatinum(II), INN: cisplatin. With the help of this drug, testicular carcinomas, a disease which until the late 1970s had almost always been incurable, can be cured in the majority of cases today. Cisplatin is now widely and more or less successfully used against various types of tumors in the clinic, but the spectrum of indication, in terms of high cure rates and major increases in lifespan, is rather limited^{4,5,6)}.

Figure 1 shows the spectrum of indication of cisplatin. Obviously cisplatin is highly active against testicular carcinomas, ovarian tumors, tumors of the head and neck, bladder tumors and osteosarcoma, but it is not active against the slowly growing tumors with a high incidence, such as lung adenocarcinomas and adenocarcinomas of the colon and rectum. These are responsible for about 30 % of cancer mortality and cannot be treated sufficiently with cisplatin and other antitumor agents. Nevertheless, the development of cisplatin indicates that metal complexes can serve to achieve high cure rates in particular types of cancer.

Thus the development of new tumor-inhibiting metal complexes is aimed at expanding the rather narrow spectrum of indication of cisplatin by developing metal complexes which act successfully against the most common tumors such as adenocarcinomas of the type mentioned above.

In order to reach this aim a large number of direct derivatives of cisplatin have been synthesized and tested against different types of tumors. Just a few of these complexes have reached the stage of clinical studies. The most important example

Spectrum of indication of Cisplatin

In combination with other chemotherapeutic agents, surgery and radiation.

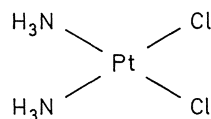
Main activity with curative success in the majority of cases: testicular carcinoma

High activity in terms of lifespan prolongation and cures in some cases: ovarian tumors, tumors of the head and neck, bladder tumors, osteosarcoma

Minor activity with a minor lifespan prolongation and, in rare cases, cures in a few other tumors such as: small cell lung carcinoma

No or insufficient activity in adenotumors such as: lung adenocarcinomas, adenocarcinomas of the colon and rectum

Fig. 1. Spectrum of indication of cisplatin



cis-Diamminedichloroplatinum(II)
INN: Cisplatin

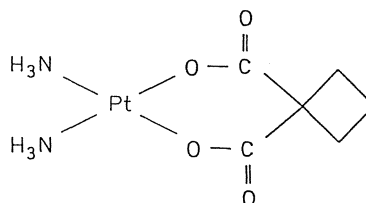


Fig. 2. Structures of Cisplatin and Carboplatin

cis-Diammine-1,1-cyclobutanedicarboxylatoplatinum(II)
Carboplatin

is carboplatin, which, besides *cisplatin*, is available in several countries for routine clinical use ⁷⁾.

Fig. 2 shows the structures of both *cisplatin* and carboplatin.

Unfortunately, direct derivatives of *cisplatin* have failed to act successfully against those types of tumors that do not respond to *visplatin*, but side effects could be reduced to a considerable extent. Nephrotoxicity thus is no longer a major problem. Myelotoxicity, however, remains the dose-limiting side effect, and some of the new derivatives are even more myelotoxic than *cisplatin* itself.

In consequence, the only way to achieve some success in the treatment of *cisplatin*-resistant tumors is to synthesize non-platinum compounds. For this reason much scientific work has already been done in the field of non-platinum complexes with anticancer properties.

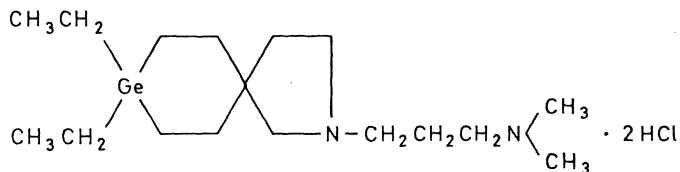
Fig. 3 shows the non-platinum metal complexes which have qualified for a clinical stage of development besides *cisplatin* and its derivatives.

The two germanium compounds — Spirogermanium and Germanium-132 — and galliumnitrate have reached clinical phase II studies by now, but, unfortunately, no really promising field of indication has been detected to date ^{8, 9, 10)}.

The clinical phase I studies with budotitane are almost completed by now, and subsequent phase II studies will prove the clinical value of this new drug, which has exhibited promising activity against adenotumors in preclinical studies ¹¹⁾.

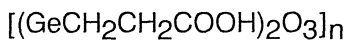
Unfortunately, ruthenium complexes have so far remained in the field of preclinical investigation, despite the fact that very interesting research into this metal has already been done.

The reason why this is so may be that, in biological experiments, ruthenium complexes were hardly ever investigated in realistic and sophisticated tumor models. Ruthenium complexes are practically always compared with *cisplatin* in the P388 leukemia model, and, due to the fact that this model is highly sensitive to platinum



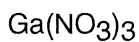
Spirogermanium

N-(3-Dimethylaminopropyl)-2-aza-8,8-diethyl-8-germaspiro(4,5)decanedihydrochloride

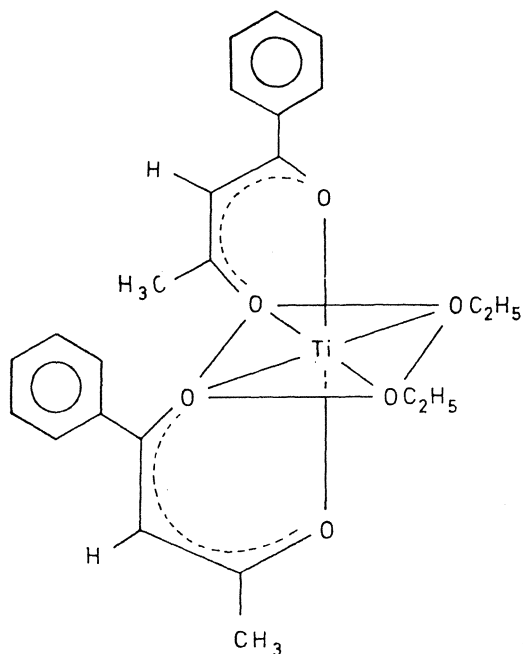


Germanium-132

Carboxyethylgermaniums sesquioxide



Galliumnitrate



Budotitane

Diethoxybis(1-phenylbutane-1,3-dionato)titanium(IV)

Fig. 3. Metal Complexes which have reached a clinical stage of development, excluding cisplatin

compounds, ruthenium compounds usually fail to show a better effect than cisplatin does. In our opinion, the P388 model and other routine screening models are suited for separating active ruthenium complexes from inactive ones. There is, however, no need for a ruthenium compound likely to qualify for clinical evaluation to surpass cisplatin in the P388 model.

As a consequence of the results of the P388 screening, ruthenium compounds are rather infrequently investigated in other, more sophisticated tumor systems which represent different organ tumors that do not respond to cisplatin. A good example of these would be selected autochthonous tumors and xenografts. Our experiments have shown that it is necessary to carry out such investigations in order to arrive at a new approach to cancer therapy.

In order to understand the following description of tumor-inhibiting properties, it is necessary to explain the evaluation of the antitumor activity of particular

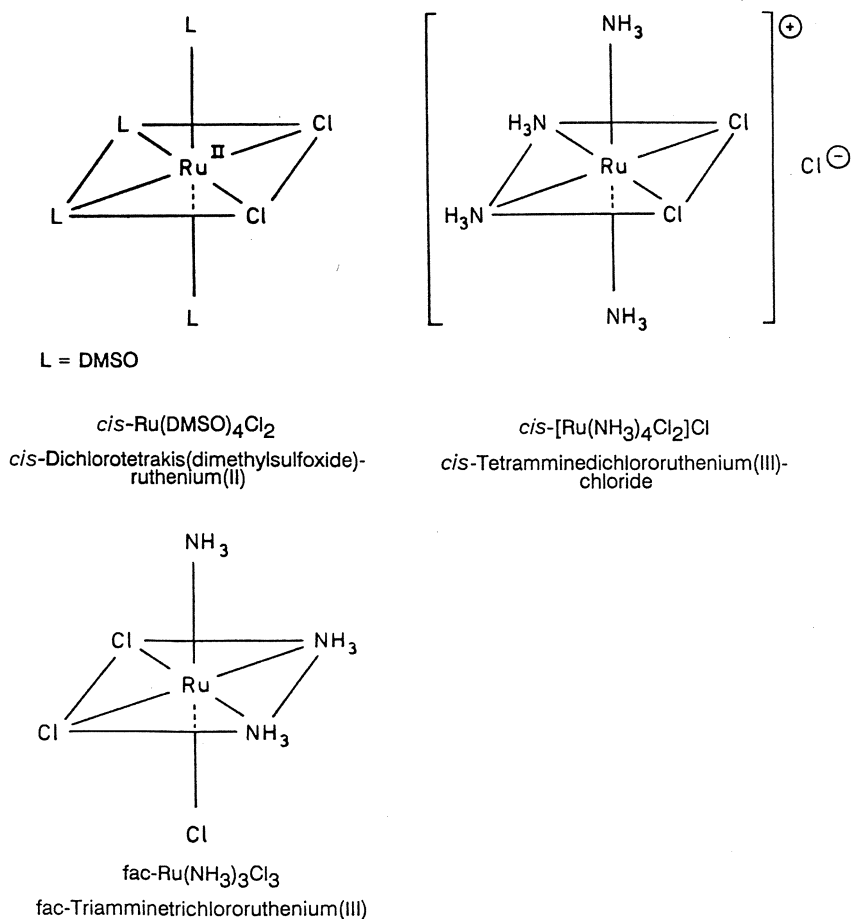


Fig. 4. Three ruthenium complexes with known antitumor activity

complexes. The parameters used can be either survival time or tumor weight. A value is calculated, termed T/C value, which represents the median survival time/tumor weight of treated (=T) animals versus the median survival time/tumor weight of control (=C) animals $\times 100$. This gives antitumor activity in percent. When survival time is taken as parameter, high T/C values, exceeding 125%, indicate good antitumor activity, owing to the increase in lifespan of the animals.

When tumor weight serves as parameter, T/C values must be low for evidence of good antitumor activity. This is due to the reduction in tumor mass. Values should fall below 45% in this case.

One of the best-known tumor-inhibiting ruthenium complexes is *cis*-Dichlorotetrakis(dimethylsulfoxide)ruthenium(II), *cis*-Ru(DMSO)₄Cl₂. It is shown, together with two other ruthenium complexes, in Fig. 4^{12,13}.

This complex, which is easy to dissolve in water, exhibits only marginal activity against the P388 leukemia, but it is highly active in some other tumor systems such as the Lewis Lung tumor. Promising activity of the corresponding *trans*-compound was also detected, by Mestroni et al.^{12,13}.

One of the other two complexes shown in Fig. 4 is *cis*-Tetraamminedichlororuthenium(III)chloride, *cis*-[Ru(NH₃)₄Cl₂]Cl. This complex is active against the P388 leukemia, reaching T/C values of about 160%. It is well soluble in water¹⁴.

The last complex is *fac*-Triamminotrichlororuthenium(III), *fac*-Ru(NH₃)₃Cl₃. It exhibits higher activity against the P388 leukemia than the tetrammine complex, but, unfortunately, it is insoluble in water¹⁴.

A good water-solubility is highly advantageous for applying metal complexes in the clinic, because the addition of solubilizers and the carrying out of complicated galenic procedures with water-insoluble metal complexes create major problems with analytics for registration at the national drug administrations. In addition, such galenic procedures and the use of solubilizers often fail to succeed in solubilizing the drug, or accelerate decomposition of the metal complexes used, or lead to adducts of the compounds with solubilizers that are difficult to characterize.

The activity of the three ruthenium complexes just described against transplatable leukemias is illustrated in Fig. 5, along with data concerning Ruthenium red, which is rather inactive.

	Solubility in water	Dose		Treat- ment on days	T/C* (%)	Tumor system
		mmol/kg	mg/kg			
<i>fac</i> -Ru(NH ₃) ₃ Cl ₃	—	0.19	50	1, 5, 9	189**	P 388
		0.1	26	1, 2, 3	144	P 388
<i>cis</i> -[Ru(NH ₃) ₄ Cl ₂]Cl	+	0.045	12.5	1, 5, 9	157**	P 388
		0.09	25	1	154	L 1210
<i>cis</i> -Ru(DMSO) ₄ Cl ₂	+	1.17	565	1, 5, 9	125**	L 1210
Ruthenium red [(NH ₃) ₅ RuORu(NH ₃) ₄ ORu(NH ₃) ₅]Cl ₆	+	0.01	9	1, 5, 9	115	P 388

Fig. 5. Antitumor activity of ruthenium complexes. * Evaluation parameter: survival time. ** The results indicated with two asterisks are in accordance with Ref. 14). All other results were obtained in our own laboratories.

These complexes and their derivatives are typical representatives of tumor-inhibiting ruthenium complexes synthesized up to now.

2 Synthesis, Characterization and Stability of New Cancerostatic Ruthenium Species

The complexes synthesized and tested by us are summarized in Fig. 6, along with the three active ruthenium complexes mentioned before, which were used as reference substances. The complexes are listed in order of increasing T/C values obtained in P388 leukemia.

The first three types of complexes in Fig. 6 are by-products, which we obtained during our efforts to synthesize other ruthenium complexes (see Fig. 12). These by-products — ruthenium hexachlorides in the oxidation stages III and IV and oxygen-bridged ruthenium chlorides with different protonized heterocycles as cation — turned out to be inactive (T/C < 125%).

The synthesis of derivatives of $\text{Ru}(\text{DMSO})_4\text{Cl}_2$ (Fig. 3), aimed at obtaining compounds of the type $\text{Ru}(\text{DMSO})_{4-n}\text{B}_n\text{Cl}_2$, B = heterocycle, was successful only in the case of some pyridine and pyrazine derivatives. $\text{Ru}(\text{DMSO})_4\text{Cl}_2$, or the corresponding TMSO (tetramethylenesulfoxide) complex, were used as adducts. The results of the antitumor activity tests were not very encouraging, with T/C values falling below 125%.

The next two types shown in Fig. 6, in terms of structure, are derivatives of the *fac*- $\text{Ru}(\text{NH}_3)_3\text{Cl}_3$ complex. These two types of complexes are as insoluble in water as is the original compound. In one case, thioethers are used as ligand, and in the other, nitrogen heterocycles. The two thioether complexes of the general formula RuB_3Cl_3

	Solubility in water	T/C (%) ¹
$\text{Ru}^{\text{III}}\text{Cl}_6(\text{HB})_3$	+	100–120
$(\text{Ru}^{\text{IV}}\text{Cl}_6)(\text{HB})_2$	+	100–120
$(\text{Ru}_2^{\text{IV}}\text{OCl}_{10})(\text{HB})_4$	+	100–120
$\text{Ru}^{\text{II}}(\text{DMSO})_4\text{Cl}_2$	+	125
$\text{Ru}^{\text{II}}(\text{DMSO})_{4-n}\text{B}_n\text{Cl}_2$	+	100–125
$\text{Ru}^{\text{III}}(\text{RSR})_3\text{Cl}_3$	—	130–135
$\text{Ru}^{\text{III}}\text{B}_3\text{Cl}_3$	—	100–130
$\text{Ru}_2^{\text{III}}(\text{O}_2\text{CR})_4\text{Cl}$	+	125–135
<i>cis</i> - $[\text{Ru}^{\text{III}}(\text{NH}_3)_4\text{Cl}_2]\text{Cl}$	+	160 ²
<i>fac</i> - $\text{Ru}(\text{NH}_3)_3\text{Cl}_3$	—	190 ²
<i>trans</i> - $[\text{Ru}^{\text{III}}\text{B}_2\text{Cl}_4]\text{HB}$	+	140–200
$[\text{Ru}^{\text{III}}\text{BCl}_3](\text{HB})_2$	+	140–200

Fig. 6. Comparison of the activity of Ruthenium complexes in the P388 tumor system. B = nitrogen heterocycle, R = organic ligand, n = 1–4. ¹ Evaluation parameter: survival time, ² under consideration of Ref. ¹⁴⁾

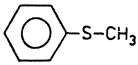
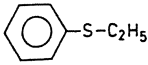
RuB ₃ Cl ₃ B =	Dose		Treatment on days	T/C ¹⁾ (%)	Tumor model
	mmol/kg	mg/kg			
NH ₃	0.19	50	1,5,9	189 ²⁾	P 388
	0.1	26	1,2,3	144	P 388
 3)	0.16	93	1	130	P 388
Phenylmethylsulfide					
 3)	0.16	100	1	134	P 388
	0.16	100	1	300	S 180
Phenylethylsulfide					

Fig. 7. Antitumor Activity of Ruthenium compounds with the formula RuB₃Cl₃, Part I. ¹⁾ Evaluation parameter: survival time. ²⁾ In accordance with Ref. ¹⁴⁾. ³⁾ Synthesis in accordance with Ref. ²⁸⁾

can be obtained by reaction of the organic ligand with RuCl₃. A phenylmethylthioether and the corresponding ethyl derivatives were used as ligands. The products obtained are insoluble in water, as is the corresponding ammine compound, too. Both compounds are active against the P388 tumor system and against the sarcoma 180 system (see Fig. 7).

The T/C values of about 130% obtained in the P388 tumor model are significant but not promising. Much better results were obtained when using the sarcoma 180 ascitic tumor model, but this model is more sensitive to chemotherapeutic agents than the P388 leukemia. In our investigations, it turned out to be highly sensitive to insoluble ruthenium compounds, which are only marginally active in other tumor systems. Such models, which produce high activities for many ruthenium compounds, are not eligible for distinguishing between more active complexes and less active ones. This high sensitivity, however, is not the same for every metal. The situation may change according to the metal used. In our investigations with titanium-β-diketonato complexes the sarcoma 180 proved to be a good model for distinguishing between complexes with varying activities, because this model was not very sensitive to titanium compounds in general.

The complexes with the general formula RuB₃Cl₃, shown in Fig. 8, were obtained by reaction of the thioether complexes, given in Fig. 7, with different nitrogen heterocycles. The antitumor activity of all these compounds is not very promising. Only the complexes with 4-dimethylaminopyridine, pyridine-4-aldehyde and pyridazine do reach a value of 125%, which indicates biological significance. None of the compounds reaches the high T/C value of the Trisammineruthenium complex used as reference.

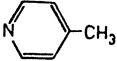
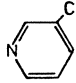
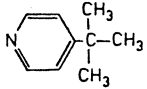
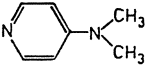
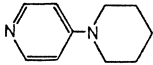
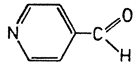
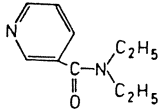
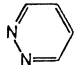
RuB ₃ Cl ₃ B =		Dose		Treatment on days	T/C (%)
		mmol/kg	mg/kg		
4-Methylpyridine		0.16	78	1	83
3-Methylpyridine		0.16	78	1	83
4- <i>tert.</i> Butylpyridine		0.16	110	1	110
4-Dimethylamino-pyridine		0.16	92	1	125
4-(1-Piperidyle)-pyridine		0.06	42	1,5,9	103
Pyridine-4-aldehyde		0.06	32	1,5,9	127
3-Diethylamino-carbonylpyridine		0.06	45	1,5,9	106
Pyridazine		0.06	27	1,5,9	127

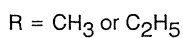
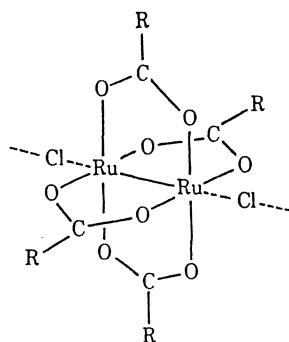
Fig. 8. Antitumor activity of Ruthenium compounds with the formula RuB₃Cl₃, Part II. All values were obtained in the P 388 tumor model

In addition, the results obtained with water-insoluble metal complexes such as these in an ip/ip model like the P388 leukemia must be evaluated very cautiously. The activity may unrealistically increase due to a “depot effect” of the insoluble compound at the site of the tumor.

An attempt was made to synthesize complexes with improved water-solubility. An example of these is given by the binuclear carboxylates of ruthenium (Fig. 6 and Fig. 9).

These complexes were designed in analogy to the binuclear carboxylates of rhodium and rhenium, which both are active against experimental tumor systems^{15,16}.

The structures of the two ruthenium complexes synthesized are given in Fig. 9. These have acetic acid and propionic acid as ligand. Both complexes are water-soluble



	Dose		Days of treatment	T/C (%)	Tumor system
	mmol/kg	mg/kg			
Ru ₂ (OOCCH ₃) ₄ Cl*	0.21	100	1	125	P 388
Ru ₂ (OOCCH ₂ CH ₃) ₄ Cl*	0.16	85	1	125	P 388
	0.06	32	1,5,9	133	P 388

Fig. 9. Antitumor Activity of Dirutheniumtetracarboxylates. * Synthesis according to Ref. 29)

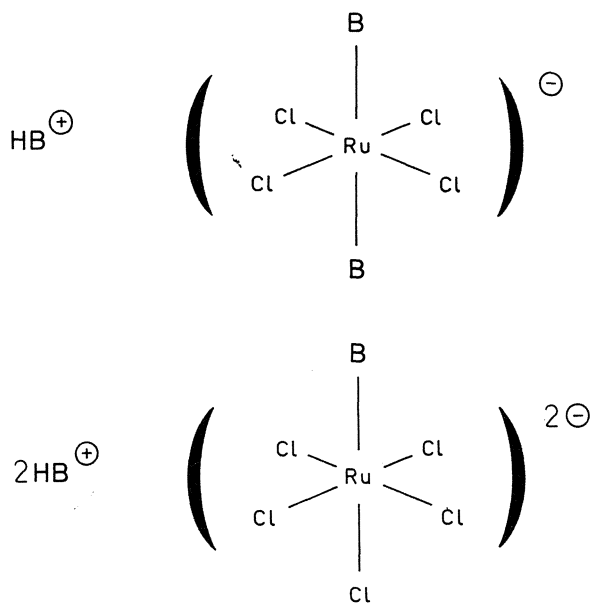


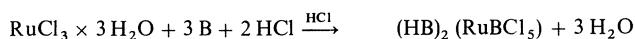
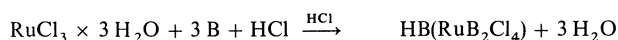
Fig. 10. General structure of the antitumor-active Ruthenium compounds HB(RuB₂Cl₄) and (HB)₂(RuBCl₅). B = Nitrogen Heterocycle

and slightly, but significantly, active in the P388 leukemia system, reaching T/C values of 125 and 133 %, respectively.

The most active, and water-soluble, complexes we synthesized were the two ruthenium species with the general formulas $\text{HB}(\text{RuB}_2\text{Cl}_4)$ and $(\text{HB})_2(\text{RuBCl}_5)$ (Fig. 10), which reach T/C values of 140–200 % in the P388 leukemia (see Fig. 6) ^{17–21}.

Methods 1a, 1b, and 1c:

commercial “ $\text{RuCl}_3 \times 3 \text{H}_2\text{O}$ ” $\xrightarrow{\text{HOEt, HCl}}$ solution of Ru^{III}



1a = 1 N HCl; 1b = conc. HCl; 1c = HCl/abs. ethanol

Method 2:

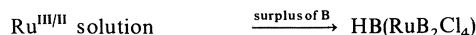
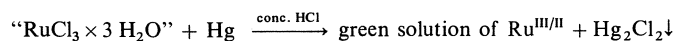


Fig. 11. Preparation of the Ruthenium species $\text{HB}(\text{RuB}_2\text{Cl}_4)$ and $(\text{HB})_2(\text{RuBCl}_5)$

Ligand B	Methods*				By-products of methods 1a–c or 2
	1a	1b	1c	2	
Imidazole	I,II	—	—	II	
1-Methylimidazole	I,II	—	—	—	
2-Methylimidazole	I,II	—	—	—	$(\text{HB})_4(\text{Ru}_2^{\text{IV}}\text{OCl}_{10})$, 1a
4-Methylimidazole	I,II	—	—	—	$(\text{HB})_4(\text{Ru}_2^{\text{IV}}\text{OCl}_{10})$, 1a
1-Ethylimidazole	I	—	—	—	
4-tert. Butylimidazole	I	—	—	—	
Benzimidazole	I	—	—	—	$(\text{HB})_3\text{Ru}^{\text{III}}\text{Cl}_6$, 1a
Pyrazole	(I)	I	—	—	$\text{Ru}^{\text{III}}\text{B}_3\text{Cl}_3$, 1a $(\text{HB})_2\text{Ru}^{\text{IV}}\text{Cl}_6$, 1b
3,5-Dimethylpyrazole	I	—	II	—	
3,5-Diethylpyrazole	I	—	—	—	
Indazole	I	—	—	—	
1,2,4-Triazole	I	—	—	—	
2-Aminothiazole	I	—	—	—	
Pyridine	—	—	—	I	
2-Methylpyridine	—	—	—	I	
3-Methylpyridine	—	—	—	I	
4-Methylpyridine	—	—	—	I	
Chinoline	I	—	—	I	

Fig. 12. Methods of preparing the ruthenium compounds $\text{HB}(\text{RuB}_2\text{Cl}_4)$ [=I] and $(\text{HB})_2(\text{RuBCl}_5)$ [=II]. * Methods: 1a = 1 N HCl; 1b = conc. HCl; 1c = HCl/abs. ethanol; 2 = Hg, B = Nitrogen Heterocycle

These anionic complexes are characterized by, in most cases, *trans*-standing heterocycles. The complexes that are coordinated with only one heterocycle are usually a little less active than their biscoordinated counterparts.

The active complexes can be prepared by two methods (Fig. 11). Method 1 involves the use of commercially available RuCl_3 . This is impurified by small amounts of Ru^{IV} , nitroso complexes and others. That is why it is refluxed with ethanol and hydrochloric acid for purification.

The solution obtained of pure $\text{Ru}(\text{III})$ then reacts with the heterocycle and different amounts of hydrochloric acid to give the two different products with one or two heterocycles coordinated. The use of method 1a involves 1 N HCl, 1b conc. HCl, and method 1c involves hydrochlorine in absolute ethanol.

In method 2, the commercially available RuCl_3 solution was reduced and purified with mercury to obtain a green solution of $\text{Ru}(\text{III})$ with small amounts of $\text{Ru}(\text{II})$. The green colour is due to the $\text{Ru}(\text{II})$ impurities. This solution is then

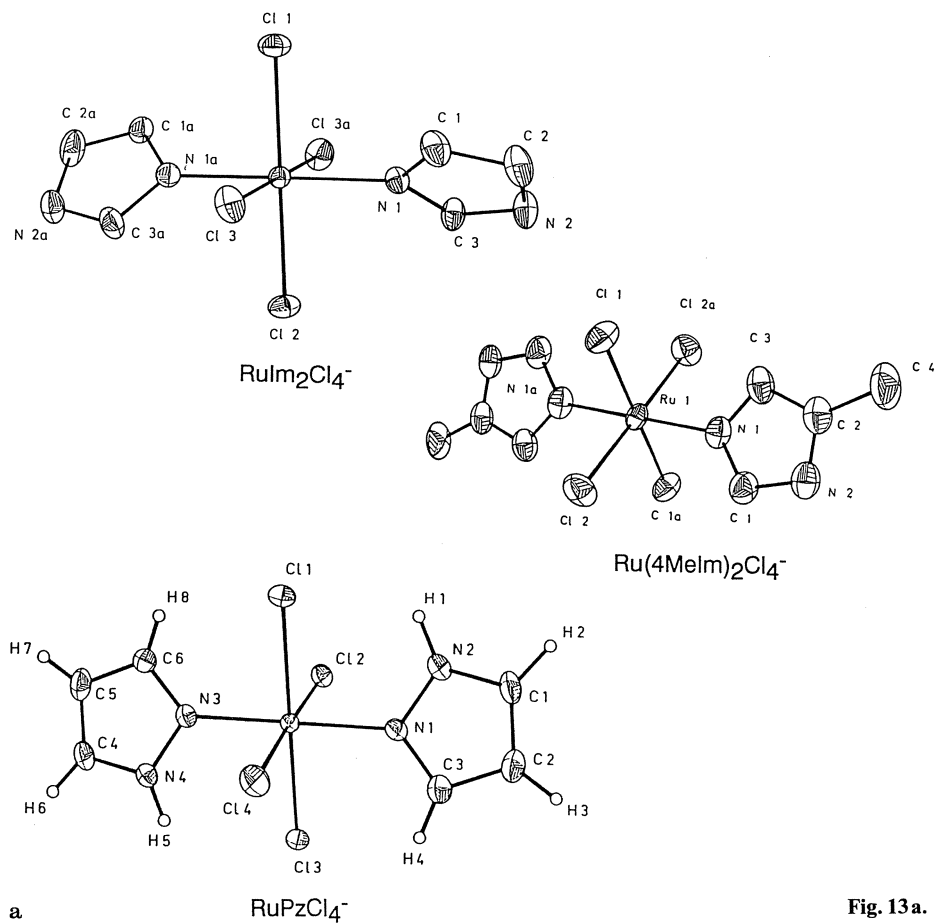
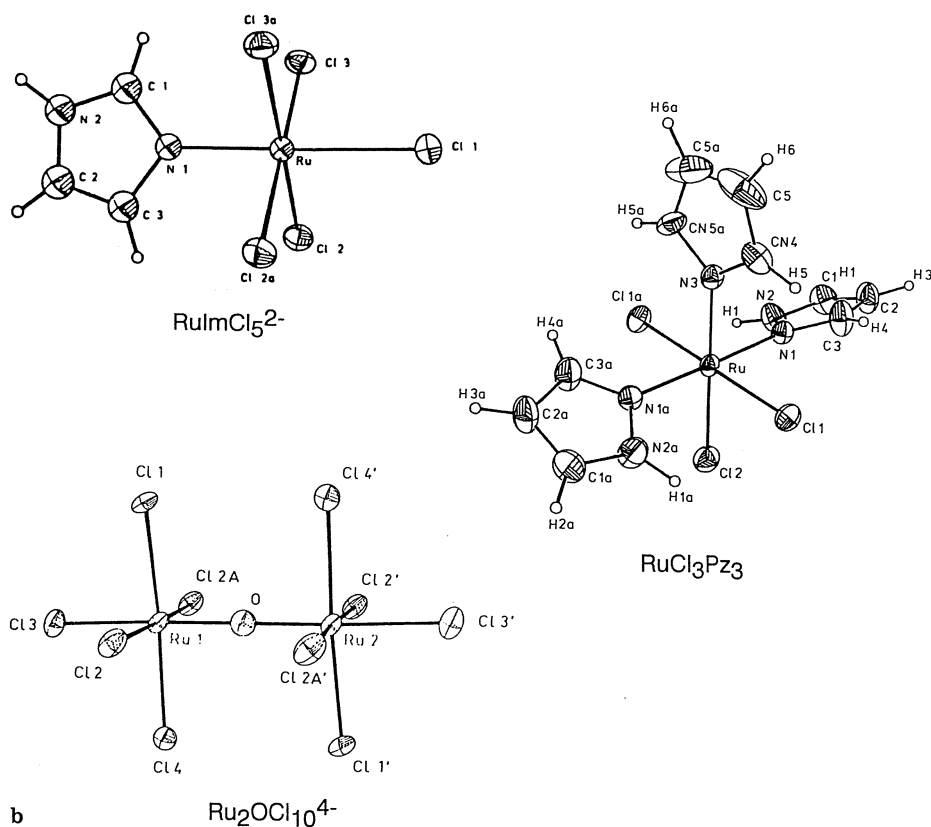


Fig. 13a.

subjected to reaction with a surplus of B to obtain the *trans*-, heterocycle coordinated ruthenium complexes.

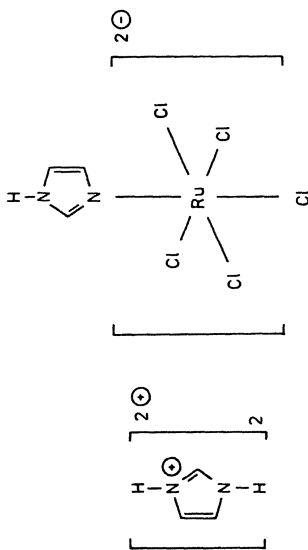
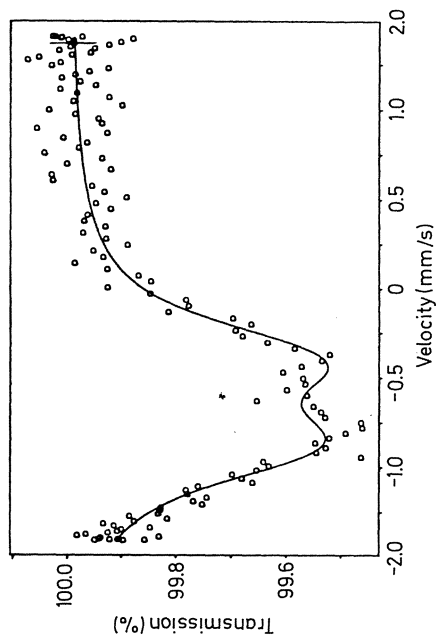
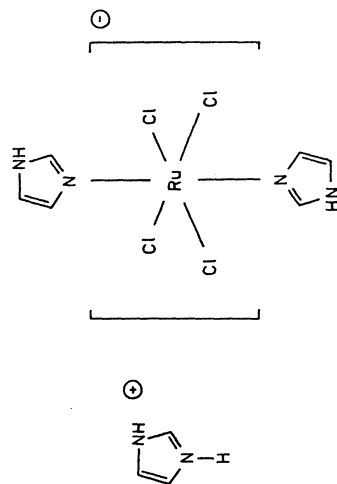
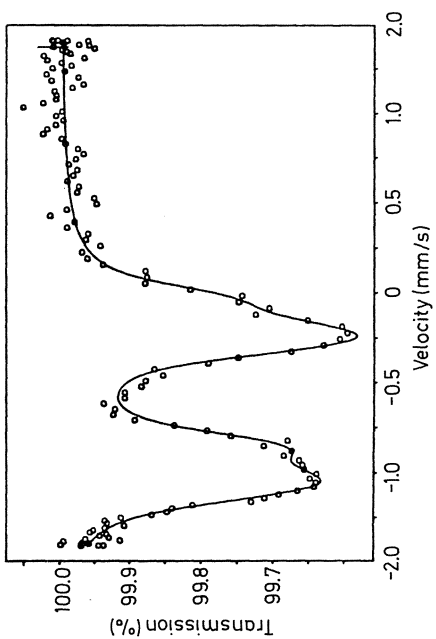
We have synthesized a series of these complexes with different heterocycles, which are listed in Fig. 12.

Most of the compounds can be produced by means of Method 1 a. It should be pointed out that this method produced some 100 g of $\text{ImH}(\text{RuIm}_2\text{Cl}_4)$ and



b

Fig. 13a. Molecular structures of the *trans*-configured anions in $\text{ImH}(\text{RuIm}_2\text{Cl}_4)$, *trans*-Imidazolium-bisimidazoletetrachlororuthenate(III), in $(4\text{MeImH})[\text{Ru}(4\text{MeIm})_2\text{Cl}_4]$, *trans*-4-Methylimidazolium-tetrachlorobis(4-methylimidazole) ruthenate(III), and in $\text{PzH}(\text{RuPz}_2\text{Cl}_4)$, *trans*-Pyrazolium-bispyrazoletetrachlororuthenate(III). All these *trans*-configured ruthenium species and their derivatives show marked tumor-inhibiting properties. **b.** Molecular structures of the anion in $(\text{ImH})_2 \cdot (\text{RuImCl}_5)$, Bisimidazolium[pentachloroimidazoleruthenate(III)], of RuCl_3Pz_3 , Trichlorotripyrazoleruthenium(III), and of the anion in $(3,5\text{-DiMePzH})_4[\text{Ru}_2\text{OCl}_{10}]$, Tetrakis(3,5-dimethylpyrazolium)- μ -oxobis(pentachlororuthenate(IV)). The compound $(\text{ImH})_2(\text{RuImCl}_5)$ is active in several tumor systems, but to a lesser degree than the bis-coordinated, *trans*-configured counterpart shown in Fig. 13a. The other two compounds, which form as byproducts during the synthesis of the *trans*-configured compounds (cf. Fig. 12), are not or only marginally active.

 $(\text{ImH})_2(\text{RuImCl}_5)$  $\text{ImH}(\text{RuIm}_2\text{Cl}_4)$

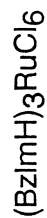
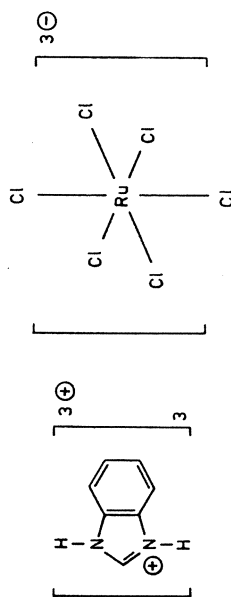
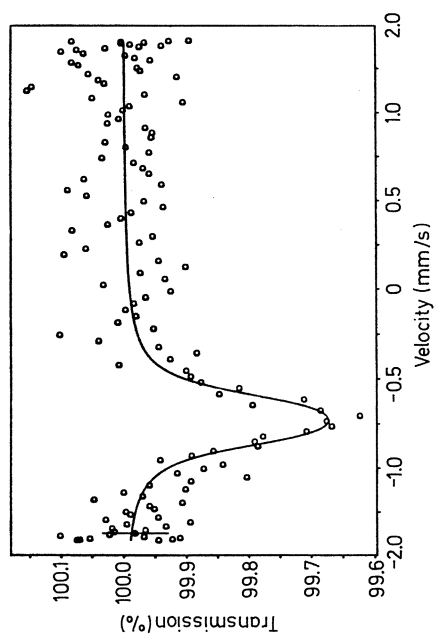


Fig. 14. Möbbaauer spectra of *trans*-Imidazolium-bisimidazolium-tetrachlororuthenate(III), ImH(RuIm₂Cl₄), ICR, Bisimidazolium[pentachloroimidazolineruthenate(III)], (ImH)₂(RuImCl₅), and Tris(benzimidazolium)rutheniumhexachloride, (BzImH)₃RuCl₆

$\text{IndH}(\text{RuInd}_2\text{Cl}_4)$, which we needed for the investigations described later on. This quantity produced showed a high, reproducible degree of purity, and the yield ranged between 20 and 50 %.

The pyridine complexes can only be obtained by means of Method 2. Methods 1b and 1c have to be used in the case of pyrazole and its 3,5-dimethyl derivative.

In some cases, by-products are formed, such as oxygen-bridged ruthenium chloride, ruthenium chlorides in the oxidation stages III or IV, and ruthenium complexes of the type RuB_3Cl_3 .

The molecular structures of several of these compounds were investigated, using x-ray methods. The structures are listed in Fig. 13 and were obtained by the following general procedure: Crystals were mounted on top of glass capillaries and data collections were carried out at room temperature with monochromated Mo-K α radiation (graphite monochromator). Crystal quality, cell dimensions and space groups were determined first by Weissenberg photographs and then from the setting angles of a number of reflections centered on a Nicolet Syntex-R3 4-circle-diffractometer. This was used together with its commercial software. An empirical absorption correction was performed with a SHELXTL routine ²²⁾.

Structure solution was carried out by locating the Ru and some of the Cl positions from Patterson maps and completed by Fourier syntheses with the SHELXTL or SHELX86 routines ²²⁾. Heavy and light atoms were refined with anisotropic temperature factors. H atoms were inserted at calculated positions or could be found by Difference-Fourier-Syntheses. Refinement was carried out by blockmatrix least squares on a Nova 3 or an Eclipse-computer from Data General (using scattering factors from International Tables ²³⁾ and taking anomalous dispersion into account). The function minimized was $\Sigma w^{1/2} (|F_o| - |F_c|)$ with weights $w = 1/\sigma^2(F)$, σ being taken from counting statistics. R and R_w are defined accordingly. The graphical representations were made on a Tektronix or a Nicolet Zeta-plotter with SHELXTL running on a Nova 3 computer.

These methods served to confirm the *trans*-configuration of the active complexes. The structure of the pentachloro compound is as was expected from routine methods. The by-product RuCl_3Pz_3 is meridionally configured. The oxygen-bridged complex has an eclipsed configuration.

Another useful method of characterizing such ruthenium complexes is Mössbauer spectroscopy with the 89 keV Γ -rays of ⁹⁹Ru (see, e.g. ²⁴⁾), which gives information on oxidation state of the ruthenium and on the ligands to which the ruthenium is coordinated. As an example, spectra of ruthenium chlorine complexes coordinated in different ways with three nitrogen heterocycles are shown in Fig. 14. These spectra were measured at 4.2 K with a source of ⁹⁹Rh in Ru metal. The small splitting of the Mössbauer emission line arising from the electric quadrupole interaction in the hexagonal Ru matrix ²⁵⁾ was taken into account in the least square fits of the Mössbauer spectra. The Mössbauer transition in ⁹⁹Ru takes place between an excited nuclear state with spin 3/2 and the ground state with spin 5/2. Electric quadrupole interactions result in six-line spectra that are, in practically all cases, only partly resolved. The strength of the electric quadrupole interaction, which is a measure of the deviations of the surrounding charges from cubic symmetry, is usually given as the splitting ΔE_Q of the excited state. For the isomer shift S, i.e. the displacement of the centroid of the Mössbauer pattern from zero velocity, certain regions have been

established²⁶⁾ for compounds with ruthenium in different oxidation states and with different ligands.

The first of the spectra shown in Fig. 14 is of $\text{ImH}(\text{RuIm}_2\text{Cl}_4)$, a complex in which the ruthenium is coordinated with two heterocycles in *trans*-position and four chlorine ligands, while the third heterocycle is protonated and serves as a cation. This compound exhibits a quadrupole splitting of $\Delta E_Q = -0.82 \pm 0.01$ mm/s, one of the largest splittings so far found for compounds of trivalent ruthenium, while the isomer shift of -0.587 ± 0.005 mm/s places it well within the region established for Ru^{3+} compounds²⁶⁾.

The second spectrum of Fig. 14 represents $(\text{ImH})_2(\text{RuImCl}_5)$, where the ruthenium is coordinated to only one heterocycle, the other two being protonated and serving as cations outside the coordination sphere of the metal. The Mössbauer spectrum of this compound exhibits a substantial line broadening, presumably because of slow paramagnetic relaxations of the spin of the $4d^5$ electron configuration of Ru^{3+} . When fitted with a broadened quadrupole pattern, this spectrum yields a smaller quadrupole splitting ($\Delta E_Q = 0.49 \pm 0.02$ mm/s) than that of $\text{ImH}(\text{RuIm}_2\text{Cl}_4)$. The sign of the electric quadrupole splitting cannot be determined in this case, but presumably it is negative like in $\text{ImH}(\text{RuIm}_2\text{Cl}_4)$. The electric quadrupole interactions can thus be used to distinguish between complexes of the general formula *trans*- $\text{HB}(\text{RuB}_2\text{Cl}_4)$, which exhibit very large quadrupole interactions, and complexes of the type $(\text{HB})_2(\text{RuBCl}_5)$ with their substantially smaller quadrupole splittings. The isomer shift of $(\text{ImH})_2(\text{RuImCl}_5)$ ($S = -0.64 \pm 0.01$ mm/s) is more negative than in the case of $\text{ImH}(\text{RuIm}_2\text{Cl}_4)$, where two heterocycles are bound to the ruthenium. This behavior is in agreement with the systematics of isomer shifts in compounds of Ru^{3+} ²⁶⁾, which have shifts near -0.70 mm/s when the ruthenium is coordinated to six Cl atoms, and more positive values when chlorine is replaced by other ligands.

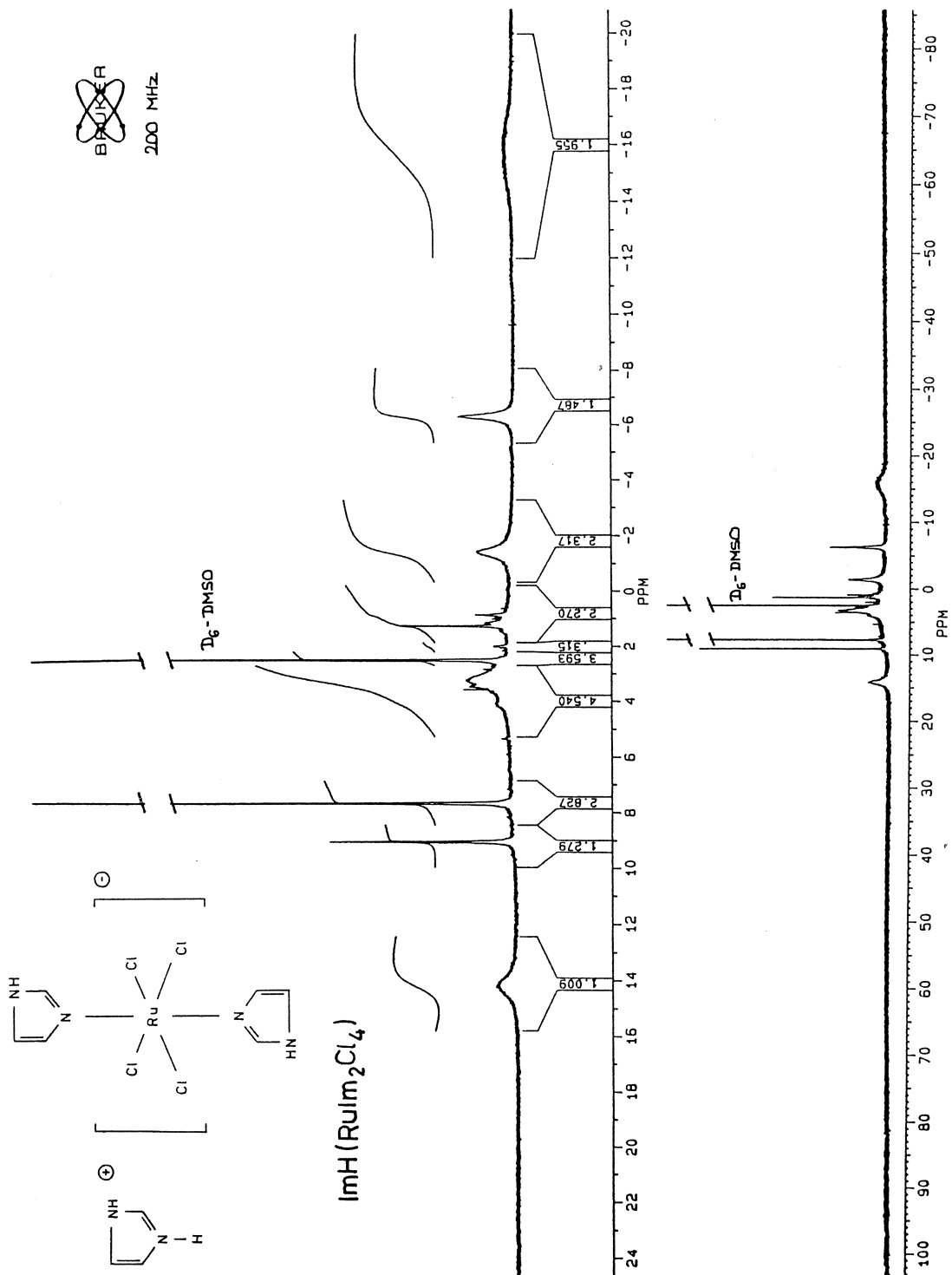
The third spectrum shown in Fig. 14 represents $(\text{BzImH})_3\text{RuCl}_6$, a case where the ruthenium is coordinated to six chlorine atoms, while all three heterocycles serve as cations. While the isomer shift of this compound ($S = -0.73 \pm 0.01$ mm/s) has the expected value, the electric quadrupole splitting ($\Delta E_Q = 0.14 \pm 0.03$ mm/s) is very small, as is expected for the basically cubic ligand environment of the ruthenium.

Yet another useful method of characterizing ruthenium complexes is NMR spectroscopy. Fig. 15 provides an example of a characteristic NMR spectrum of $\text{ImH}(\text{RuIm}_2\text{Cl}_4)$.

Owing to the paramagnetic properties of Ru(III) , the signals of the protons of the heterocycles, which are bonded directly to the ruthenium, are shifted into the high field of the NMR.

This way a distinction can easily be drawn between coordinated and uncoordinated heterocycle ligands.

Finally, a point of major interest for clinical use is the investigation of the stability of the galenic formulation of ICR and its derivatives. This was examined by means of high pressure liquid chromatography (Fig. 16). Samples of 20 μl of the solutions to be investigated were chromatographed, under isochratic conditions, with acetonitrile/phosphate buffer pH 4.5 (a ratio of 85/15) on a LiChrosphere 100 Diolcolumn (5 μm , $l = 125$ mm, $d = 4.6$ mm, MERCK) at a rate of flow of 1 ml/min. UV detection was carried out at 220 nm²⁷⁾.



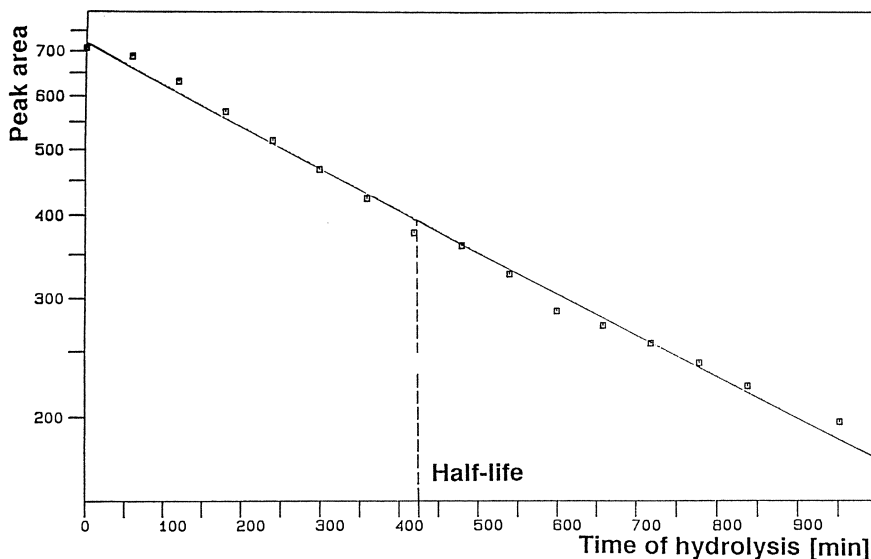


Fig. 16. HPLC investigation of the decomposition of Imidazolium-bisimidazoletetrachlororuthenate(III), ImH(RuIm₂Cl₄), ICR, in physiological saline

The half-life of the compound, calculated from the linear regression of lg peak area against time, is about 400 minutes, that is to say, that during the first hour more than 95% of the complex remains undecomposed. This is good enough for infusion therapy in the clinic.

3 Tumor-inhibiting and Toxicological Properties of the New Ruthenium Compounds

The two types of ruthenium complexes of major interest, HB(RuB₂Cl₄) and (HB)₂(RuBCl₅), exhibit marked and significant activity against the P388 leukemia. Fig. 17 gives the results of a number of compounds, compared with the clinically established drugs *cis*platin and 5-fluorouracil.

A T/C value of about 200% was reached applying ImH(RuIm₂Cl₄), ICR, compared to a T/C value of about 180% with *cis*platin and one of about 150% with 5-fluorouracil. The T/C values of the other substances are in the range between 130% for the aminothiazole compound and 160% for the chinoline compound.

When comparing the different possible dose schedules, it seems that treatment on the days 1, 5 and 9 after tumor transplantation is more favorable than the others.

◀ Fig. 15. NMR spectrum of *trans*-Imidazolium-bisimidazoletetrachlororuthenate(III), ImH(RuIm₂Cl₄), ICR

	Dose	Treatment on the days	T/C (%)	Range
Control animals	—	—	100	(100–137)
cisplatin	3 mg/kg 0.01 mmol/kg	1, 5, 9	175	(100–275)
5-FU	60 mg/kg 0.46 mmol/kg	1, 5, 9	144	(115–179)
ICR, ImH(RuIm ₂ Cl ₄)*	209.3 mg/kg 0.45 mmol/kg	1	156	(138–200)
	69.8 mg/kg 0.15 mmol/kg	1, 5, 9	194	(138–262)
	23.3 mg/kg 0.05 mmol/kg	1–9	163	(138–225)
(ImH) ₂ (RuImCl ₅)*	218.5 mg/kg 0.45 mmol/kg	1	150	(100–150)
	72.8 mg/kg 0.15 mmol/kg	1, 5, 9	163	(150–163)
	24.3 mg/kg 0.05 mmol/kg	1–9	156	(150–163)
(1MeImH) ₂ - [Ru(1MeIm)Cl ₅]	52.4 mg/kg 0.1 mmol/kg	1, 5, 9	144	(78–144)
(4MeImH)- [Ru(4MeIm) ₂ Cl ₄]*	73.5 mg/kg 0.15 mmol/kg	1, 5, 9	133	(122–155)
(BzImH)[Ru(BzIm) ₂ Cl ₄]*	60.7 mg/kg 0.1 mmol/kg	1, 2, 3	155	(144–178)
(BzImH) ₂ (RuBzImCl ₅)	100.7 mg/kg 0.15 mmol/kg	1, 5, 9	133	(122–144)
(PzH)[RuPz ₂ Cl ₄]	44.8 mg/kg 0.1 mmol/kg	1, 2, 3	144	(144–156)
(DiMePzH)- [Ru(DiMePz) ₂ Cl ₄]	53.2 mg/kg 0.1 mmol/kg	1, 2, 3	133	(111–189)
(IndH)[RuInd ₂ Cl ₄]*	91.1 mg/kg 0.15 mmol/kg	1, 5, 9	133	(133–144)
TrH(RuTr ₂ Cl ₄)	73.1 mg/kg 0.15 mmol/kg	1, 5, 9	138	(115–150)
(ChinH)[RuChin ₂ Cl ₄]	64.0 mg/kg 0.1 mmol/kg	1, 2, 3	160	(130–270)
(2AmiThiazolH)- [Ru(2AmiThiazol) ₂ Cl ₄]*	54.4 mg/kg 0.1 mmol/kg	1, 2, 3	130	(130–130)

Fig. 17. Antitumor Activity of selected Ruthenium Compounds with the general formulas HB(RuB₂Cl₄) and (HB)₂(RuBCl₅) against the P388 leukemia, compared with cisplatin and 5-fluorouracil. All T/C values are statistically significant from control according to the Steel Test. * In addition, some of the compounds above have meanwhile been tested by the NCI, and activity in the P388 leukemia has been confirmed

Figure 18 gives a summary of the results of ICR against different experimental tumor models. The column in the middle gives evaluation parameters, survival time or tumor weight, respectively. T/C values must be interpreted accordingly (see above).

ICR, in addition to the promising increase in survival time of the treated animals bearing the P388 leukemia, reached a T/C value of about 250% in the Walker 256

Tumor model	Evaluation parameter ¹	Optimum T/C value (%)
P 388 leukemia	ST	200
Walker 256 carcinosarcoma	ST	250
Stockholm Ascitic Tumor	ST	150
B 16 melanoma, s.c. growing	TW	15
Sarcoma 180, i.m. growing	TW	45
AMMN ² -induced colorectal tumors of the rat	TW	10

Fig. 18. Survey of the test results of ICR in experimental tumor models. ¹ ST = Survival time, TW = Tumor weight; ² AMMN = Acetoxymethylmethylnitrosamine

carcinosarcoma model, and a T/C value of about 150% in the Stockholm ascitic tumor.

The subcutaneously transplanted B 16 melanoma and the intramuscularly growing sarcoma 180, which are both solid tumors, were treated intravenously. Treatment with ICR resulted in a significant reduction of tumor weight of up to 15%, compared to control animals (100%), and up to 45%, respectively.

The last tumor model given in Fig. 17, the AMMN-induced colorectal tumor of the rat, is a valuable model for the development of new anticancer agents. The tumors produced by the carcinogen Acetoxymethylmethylnitrosamine (AMMN), macroscopically and microscopically, are very similar to those found in humans.

Figure 19 conveys an impression of this type of tumors, at the same time showing the structure of AMMN.

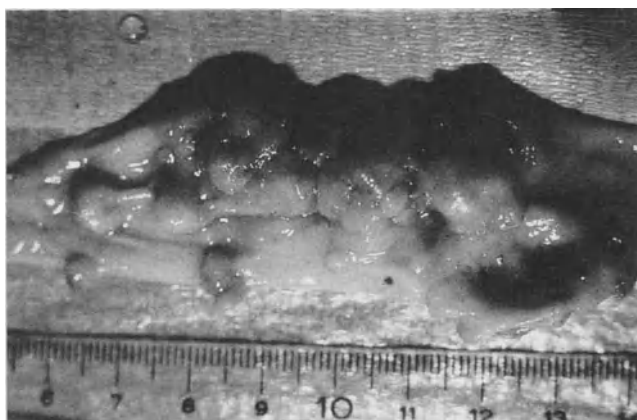
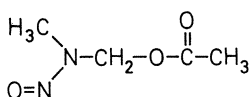


Fig. 19. Structure of Acetoxymethylmethylnitrosamine, and the tumors this carcinogen induces in the colon of rats

The sensitivity of these animal tumors to chemotherapeutic agents is also virtually the same as that of their human counterparts. They are not sensitive to *cis*platin or alkylating agents such as cyclophosphamide. To date, 5-fluorouracil has been the only substance to produce significant effects in terms of decrease in tumor volume. It is also the only compound that can be used in the clinic against this type of tumors, but with only a minor degree of efficiency. Thus, the results obtained by the use of the animal model are highly predictive for the clinical situation.

Apart from ICR, several derivatives were tested in this model. The compound which produced the best improvement, compared to ICR, is *trans*-Indazolium-bisindazoletrichlororuthenate(III), $\text{IndH}(\text{RuInd}_2\text{Cl}_4)$. The results obtained with both these compounds are illustrated in Fig. 20. These are compared to the activity of 5-fluorouracil and *cis*platin in the same model. The inactivity of *cis*platin in this experimental model could be confirmed, as could be expected from the clinical situation. Besides, as the column for *cis*platin is obviously higher than that for control animals, it is evident that tumor growth was slightly stimulated, as is often the case when treatment is carried out with ineffective compounds.

The above mentioned positive effect of 5-fluorouracil in the clinic could be reproduced in the tumor model. The tumor volume decreased to 40%, compared to the control group.

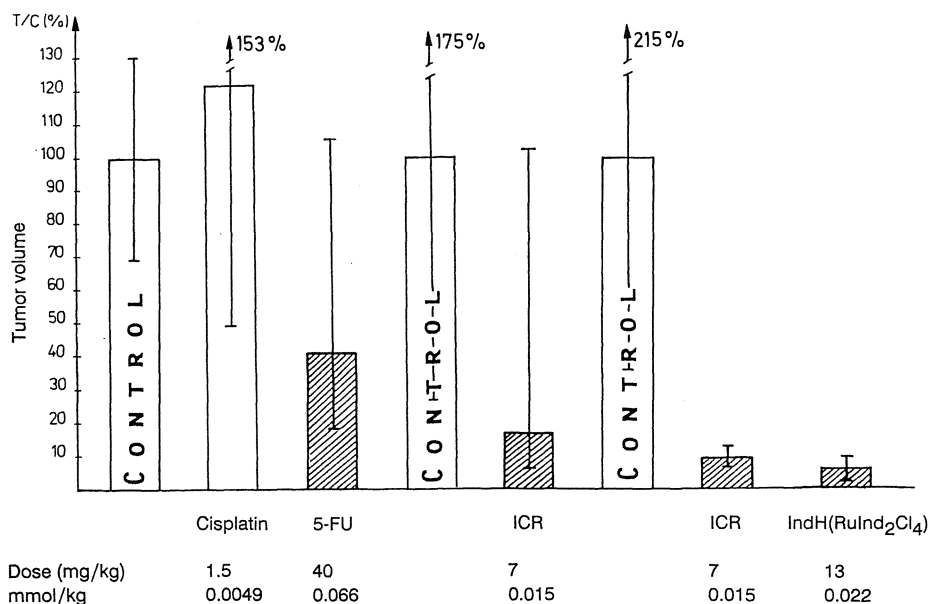


Fig. 20. Survey of the test results of Ruthenium compounds against autochthonous colorectal tumors, compared to cisplatin and 5-FU. 5-FU = 5-fluorouracil; ICR = $\text{ImH}(\text{RuIm}_2\text{Cl}_4)$. Three different experiments are summarized. For each, the control group is given, which represents 100% of tumor volume. Doses were applied twice per week over ten weeks. Shaded columns indicate statistical significance

ICR was given at a dose of 7 mg/kg twice a week over ten weeks. Tumor volume was reduced to 20% in one experiment and to 10% in the other, compared to the control groups.

The indazole compound, IndH(RuInd₂Cl₄), which is less toxic in chronic applications, was given at a higher dose and reduced the tumor volume up to 5%. This corresponds to a reduction of tumor mass of 95%.

Fig. 21 given more information on the last experiment in Fig. 20. In particular, details are given concerning weight loss, mortality, and total tumor volume.

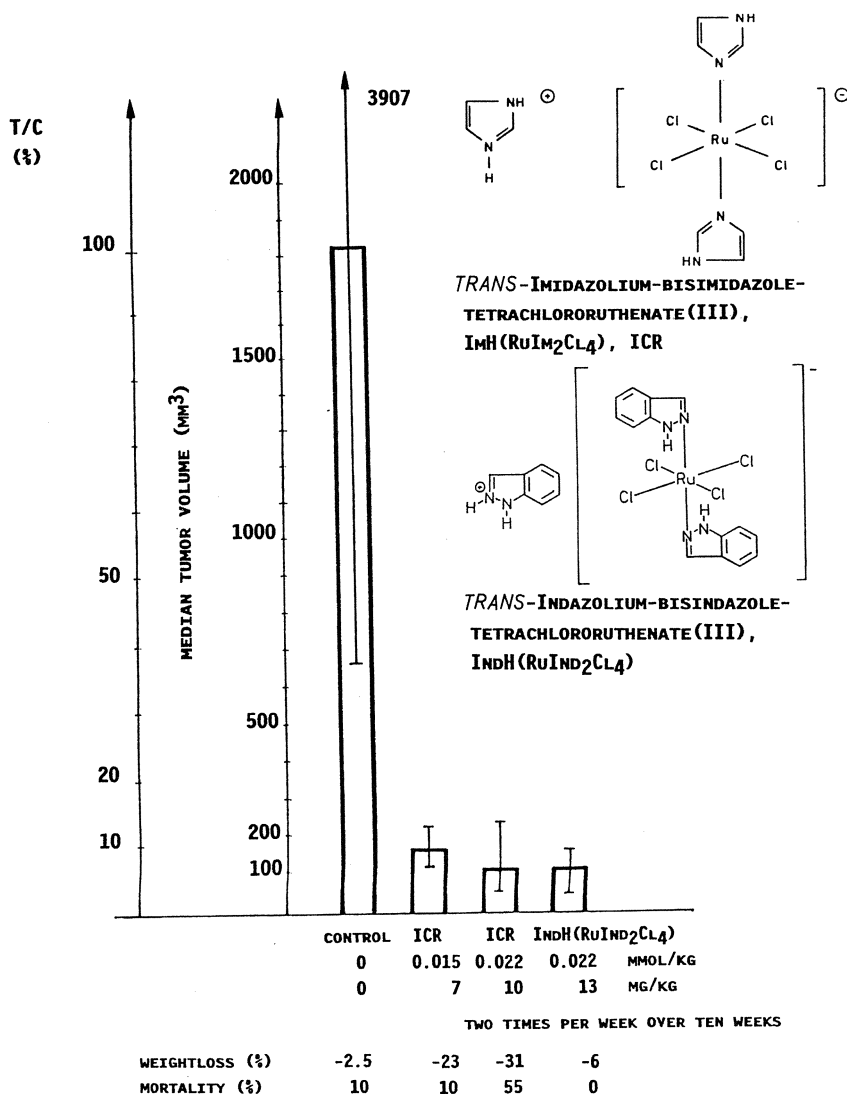


Fig. 21. Activity of two ruthenium compounds in autochthonous colorectal tumors in the rat

Mortality and weight loss in the control groups are due to the invasively growing tumors. Treatment with ICR resulted in a 90% reduction of tumor weight, accompanied by the same mortality as in the control group, but more loss in body weight. This therapeutic effect with its barely tolerable toxicity could not be further improved by applying higher doses of ICR.

The application of 10 mg/kg of ICR two times per week over ten weeks resulted in a weight loss of 40% and a mortality of 55%.

Most surprising was the effect of the derivative $\text{IndH}(\text{RuInd}_2\text{Cl}_4)$, which produced a 95% reduction of tumor weight without any mortality (0%) and without any considerable weight loss (6%). This implies a non-toxic treatment of colorectal tumors.

This is most encouraging, because *cisplatin* is completely inactive in this model, and because colorectal tumors account for a high share of total human cancer mortality. Thus, it can be assumed that this compound possesses promising properties for clinical use.

A comparison of the results of the two compounds in the autochthonous tumor model and in the P388 leukemia shows clearly that a parallelism in activity is not necessarily implied. The indazole compound is more active in the highly developed model, and the imidazole compound in the screening model. This could mean that the value of the screening model lies more in the separation of active from inactive ruthenium complexes rather than in the decision as to which ruthenium complex from a particular number belonging to the same general structure is the most promising for clinical development.

The toxicological data for ICR, $\text{ImH}(\text{RuIm}_2\text{Cl}_4)$, and $\text{IndH}(\text{RuInd}_2\text{Cl}_4)$ is summarized in the following (Fig. 22).

The single dose mortality study with ICR resulted in a LD_{50} of about 125 mg/kg (Fig. 22). The dose was applied in 2 ml of physiological saline per 100 g of mouse.

Mortality, single dose, for $\text{ImH}(\text{RuIm}_2\text{Cl}_4)$, ICR.

60 mg/kg	1/10	$\text{LD}_{50} = 125 \text{ mg/kg}$
80 mg/kg	2/10	Method: Litchfield-Wilcoxon
110 mg/kg	4/10	
160 mg/kg	5/10	
210 mg/kg	10/10	

Each dose was applied in 2 ml of physiological saline per 100 g of mouse.

Dependence of mortality on the volume of solubilizer applied

1. $\text{ImH}(\text{RuIm}_2\text{Cl}_4)$

Dose (mg/kg)	2 ml/100 g Mortality (%)	8 ml/100 g Mortality (%)
100	40	0
200	100	25

2. $\text{IndH}(\text{RuInd}_2\text{Cl}_4)$

Dose (mg/kg)	2 ml/100 g Mortality (%)	8 ml/100 g Mortality (%)
50	50	0
100	100	50

Fig. 22. Toxicological studies with $\text{ImH}(\text{RuIm}_2\text{Cl}_4)$, ICR, and $\text{IndH}(\text{RuInd}_2\text{Cl}_4)$, in NMRI mice

Histological findings:

Liver: single cell necroses, swelling of Kupffer's cells

Kidneys: tubular necroses

Spleen: cell proliferation in red and white pulp

Stomach: hyperplasia and hyperkeratosis of the border fold

Intestine: no change

Lung: no change

Major hematological findings: erythropenia, increase in liver enzymes, increase in creatinine

Fig. 23. Histological and hematological findings with ImH(RuIm₂Cl₄), ICR, at a dose of 110 mg/kg, in NMRI mice. The compound was applied in 2 ml of physiological saline per 100 g of mouse

	ImH(RuIm ₂ Cl ₄), ICR	IndH(RuInd ₂ Cl ₄)
period of treatment	7 weeks	8 weeks
no. of applications per week	2	2
single dose	0.022 mmol/kg 9.8 mg/kg	0.022 mmol/kg 13.3 mg/kg
total dose	0.308 mmol/kg 138 mg/kg	0.352 mmol/kg 213.8 mg/kg
mortality	0 %	0 %
change in bodyweight during treatment		
treated group	+ 38 %	+ 80 %
control group	+ 50 %	+ 53 %

Graphic representation of bodyweight change during treatment

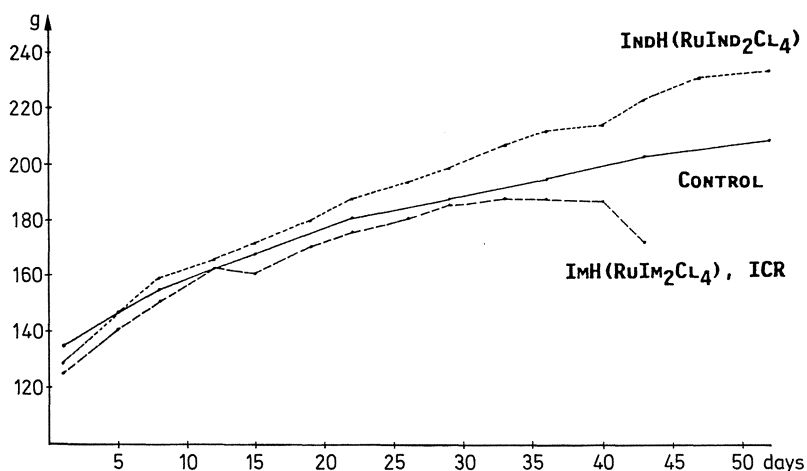


Fig. 24. Chronic Toxicity of ImH(RuIm₂Cl₄), ICR, and IndH(RuInd₂Cl₄), in SD rats

In later experiments, a high dependence of mortality on the volume of solubilizer applied was detected. A dose of 100 mg/kg of ICR causes mortality of 40% when 2 ml of solubilizer are given, but mortality could be reduced to 0% when 8 ml of solubilizer per 100 g of mouse were applied. The dose of 200 mg/kg of ICR, which normally results in 100% mortality, was reduced to 25% by the same procedure. A similar effect could be observed with the indazole compound, where the LD₅₀ could be increased from 50 mg/kg to 100 mg/kg by using the higher volume of solubilizer (Fig. 22). These data suggest that the nephrotoxicity of the two compounds can be considerably reduced by the administration of physiological saline.

The histological findings at a dose of 110 mg/kg and 2 ml/100 g of mouse are summarized in Fig. 23. The main target organs of toxicity are the liver and the kidneys. The major hematological findings include erythropenia and an increase in both creatinine and liver enzymes.

In studies of the chronic toxicity of the imidazole and indazole compounds, both were given at equimolar doses two times per week (Fig. 24). ICR was applied at a dose of about 10 mg/kg two times per week for seven weeks, and the indazole compound at a dose of about 13 mg/kg two times per week for eight weeks. No mortality at all was observed during this experiment for both compounds. The animals treated with ICR lost body weight to a significant extent during the last two weeks, which indicates toxicity, and, as a result, the experiment had to be discontinued after the seventh week.

By contrast, treatment with the indazole compound turned out to be non-toxic until the eighth week of treatment. The lower degree of toxicity of the indazole compound, which was obvious from the experiment with colorectal tumors (Fig. 21), could be confirmed in this experiment.

4 Conclusions

The most serious problem of cancer chemotherapy is to find new substances that will act selectively against particular types of cancer. In view of the fact that there are more than 100 different types of human cancer, it is obvious that no "universal anticancer agent" can be found. Experience in the development of anticancer agents that are under clinical use today has confirmed this fact.

Cisplatin is a good example for such selective anticancer agents in that it has a curative effect in testicular carcinomas, at least in most cases, and is highly active against ovarian carcinomas, bladder tumors, and tumors of the head and neck.

The success of the so-called "rational design" of new anticancer agents, which is aimed at synthesizing derivatives of known tumor-inhibiting structures, is rather limited. This can be gathered, for example, from the limited success achieved in the synthesis and biological testing of thousands and thousands of platinum complexes, which have not really contributed anything to improve the clinical activity of *cisplatin*, despite improvements regarding the reduction of side effects. A new breakthrough in cancer therapy, which the development of *cisplatin* itself had meant, cannot be achieved this way.

Thus, in finding new antineoplastic agents with genuine success in chemoresistant tumors, the “old-fashioned” empirical way of cancer research, synthesizing, testing and establishing structure-activity relationships for new compounds, has to be followed. The structure-activity relation valid for cisplatin, with *cis*-configuration, etc., can not even be transferred to other metals, not to mention the mechanism of action, which is not really clear even for cisplatin, and not at all for other tumor-inhibiting metal complexes. Thus, it does not represent any useful tool for developing new anticancer agents. Even the assumption that an increase in cell uptake of the drug would also increase activity cannot be confirmed for most anticancer agents. Cisplatin, in particular, does not show any marked parallelism between uptake in specific organs and antitumor activity.

Screening systems such as the P388 leukemia, the sarcoma 180, or the Walker 256 carcinosarcoma, among others, are under much controversial discussion, but they are the only useful tools we have in separating a major number of active compounds from inactive ones.

In following this way we have been led to a new class of tumor-inhibiting ruthenium complexes, of the general formulas $\text{HB}(\text{RuB}_2\text{Cl}_4)$ and $(\text{HB})_2(\text{RuBCl}_5)$. Activity was found in transplantable screening tumors such as the P388 leukemia, the intramuscularly transplanted sarcoma 180, the Walker 256 carcinosarcoma, the B16 melanoma, and the Stockholm Ascitic tumor. Positive results obtained in the intravenous treatment of tumors like the B16 melanoma or the sarcoma 180 are necessary to confirm the systemic activity of the drug when it is not applied at the site of the tumor, as is the case in ip/ip models. Of all modes of treatment, the intravenous application simulates clinical application best.

Positive results obtained in such screening systems indicate cancerostatic activity in general, but they do not point to any clear field of indication against different organ tumors. Thus it is necessary to test compounds with positive results against experimental tumor models with a higher predictivity for the clinical situation, e.g. selected autochthonous tumors, which are chemically induced, and treated with the substance after the establishment of the tumor in the particular organ, and which are useful tools in predicting clinical activity. We chose AMMN-induced tumors for this investigation.

Positive results in this tumor model and others, along with tolerable toxicity, lay the foundations for a further development of this class of drugs, in particular of the two representatives $\text{ImH}(\text{RuIm}_2\text{Cl}_4)$ and $\text{IndH}(\text{RuInd}_2\text{Cl}_4)$.

In further studies, we will complete the pharmacological and toxicological profile of $\text{ImH}(\text{RuIm}_2\text{Cl}_4)$ and $\text{IndH}(\text{RuInd}_2\text{Cl}_4)$, in order to render possible the beginning of clinical studies.

5 Acknowledgements

We thank the Gesellschaft for Kernforschung, Karlsruhe, FRG, for preparing the Mössbauer source. The Mössbauer studies were funded by the German Federal Ministry for Research and Technology.

This article was supported by the Deutsche Krebshilfe, Dr. Mildred-Scheel-Stiftung für Krebsforschung.

6 Abbreviations

AMMN	Acetoxymethylmethylnitrosamine
Im	imidazole
ICR	trans-Imidazolium-bisimidazoletetrachlororuthenate(III)
1MeIm	1-methylimidazole
4MeIm	4-methylimidazole
BzIm	benzimidazole
Pz	pyrazole
DiMePz	3,5-dimethylpyrazole
Ind	indazole
Tr	1,2,4-triazole
Chin	chinoline
2AmiThiazol	2-aminothiazole

7 References

- Rosenberg B, VanCamp L, Krigas Th (1965) *Nature* 205: 698
- Rosenberg B, VanCamp L, Trosko JE, Mansour V (1969) *Nature* 222: 385
- Rosenberg B (1978) *Interdiscipl Sci Rev* 3; 2: 134
- Seeber S, Schmidt CG, Nagel G, Achterrath W (eds) (1980) *Cisplatin. Derzeitiger Stand und neue Entwicklungen in der Chemotherapie maligner Neoplasien*. Karger, Basel (Beiträge zur Onkologie, vol 18)
- Prestayko AW, Crooke ST, Carter SK (eds) (1980) *Cisplatin — Current status and new developments*. Academic, New York
- Nicolini M (ed) (1988) *Proc 5th Int. Symp. on Platinum and other metal coordination complexes in cancer chemotherapy*. Martinus Nijhoff, Boston
- Dabrowiak JC, Bradner WT (1987) *Progress Med. Chem.* 24: 129
- Slavik M, Blanc O, Davis J (1983) *Invest. New Drugs* 1: 225
- Hopkins SJ (1980) *Drugs of the Future V*; 11: 545
- Ward SG, Taylor RC (1988) In: Gielen MF (ed) *Metal-based anti-tumour drugs*. Freund, London
- Keppler BK, Heim ME (1988) *Drugs of the Future, Vol 13, No. 7*, 637
- Alessio E, Attia W, Calligaris M, Cauci S, Dolzani L, Mestroni C, Monti-Bragadin G, Nardin G, Quadrifoglio F, Sava G, Tamaro M, Zorzet S (1988) In: Nicolini M (ed) *Proc. 5th Int. Symp. on Platinum and Other Metal Coordination Compounds in Cancer Chemotherapy* Martinus Nijhoff, Boston
- Mestroni C et al (1988) this volume
- Clarke MJ (1980) In: Sigel H (ed) *Metal ions in biological systems*, New York, Vol 11, p 231
- Kadish KM, Das K, Howard R, Dennis A, Bear JL (1978) *Bioelectrochem. and Bioenergetics* 5: 741
- Eastland GW, Yang G, Thompson T (1983) *Meth and Find Exptl Clin Pharmacol* 5 (7): 435
- Keppler BK, Rupp W (1986) *J Cancer Res Clin Oncol* 111: 166
- Keppler BK, Balzer W, Seifried V (1987) *Drug Res.* 37 (II) 7: 770
- Keppler BK, Wehe D, Endres H, Rupp W (1987) *Inorg. Chem.* 26 (6): 844
- Garzon FT, Berger MR, Keppler BK, Schmähl D (1987) *Cancer Chemother Pharm* 19: 347
- Keppler BK, Rupp W, Endres H, Niebl R, Balzer W (1987) *Inorg. Chem.* 26: 4366

22. Sheldrick GM (1984) "SHELXTL"; University of Göttingen: Göttingen, FRG
23. International Tables for X-Ray Crystallography (1974) Vol. IV; Kynoch: Birmingham, UK
24. Gütlich Ph, Link R, Trautwein A (1978) *Inorgan. Chem. Concepts* Vol. 3. Springer, Berlin Heidelberg New York
25. Kotthaus J, Vianden R (1983) *Hyperfine Interactions* 14: 99
26. Wagner FE, Wagner U (1978) In: Shenoy GK, Wagner FE (eds) *Mössbauer Isomer Shifts* North Holland, Amsterdam, p 431
27. Krüger U (1988) personal communication
28. Chatt J, Leigh GJ, Storace AP (1971) *J. Chem. Soc. (A)*, 1380
29. Stephenson TA, Wilkinson G (1966) *J. Inorg. Nucl. Chem.* 28: 2285

Chemical, Biological and Antitumor Properties of Ruthenium(II) Complexes with Dimethylsulfoxide

Giovanni Mestroni,¹ Enzo Alessio,¹ Mario Calligaris,² Wahib M. Attia,³ Franco Quadrifoglio,⁴ Sabina Cauci,⁴ Gianni Sava,⁵ Sonia Zorzet,⁵ Sabina Pacor,⁵ Carlo Monti-Bragadin,⁶ Marisa Tamaro,⁶ and Lucilla Dolzani⁶

Two ruthenium(II)-dimethylsulfoxide complexes, *cis*- and *trans*-RuCl₂(DMSO)₄ are shown to possess antitumor and, in particular, antimetastatic activity against several murine tumor models. The complexes interact both *in vitro* and *in vivo* with DNA, which seems to be their most likely target. The synthesis and chemical behavior of the two complexes are described and related to their interactions with DNA and their antitumor properties. A tentative scheme of the mechanism of action of the two isomers is also reported.

1	Introduction	72
2	Chemical Properties	72
2.1	Reaction Mechanism and Intermediates	72
2.2	Synthesis and Structure of <i>trans</i> -RuCl ₂ (DMSO) ₄	74
2.3	Chemical Behaviour of <i>cis</i> - and <i>trans</i> -RuCl ₂ (DMSO) ₄ in Aqueous Solution	74
3	Toxicity and Antitumor Activity of <i>cis</i> - and <i>trans</i> -RuCl ₂ (DMSO) ₄	77
4	Interaction of <i>cis</i> - and <i>trans</i> -RuCl ₂ (DMSO) ₄ with O- and N-donor Ligands	79
5	Interaction of <i>cis</i> - and <i>trans</i> -RuCl ₂ (DMSO) ₄ with DNA <i>in Vitro</i>	81
5.1	Reactions of <i>cis</i> -RuCl ₂ (DMSO) ₄ with DNA	81
5.2	Reactions of <i>trans</i> -RuCl ₂ (DMSO) ₄ with DNA	82
6	Proposed Schemes of Mechanism	83
7	Interaction of <i>cis</i> - and <i>trans</i> -RuCl ₂ (DMSO) ₄ with DNA <i>in Vivo</i>	85
8	Concluding Remarks	86
9	Acknowledgement	86
10	List of Symbols and Abbreviations	86
11	References	87

¹ Department of Chemical Sciences, University of Trieste, Piazzale Europa 1, 34127 Trieste, Italy

² Department of Chemistry, University of Pavia, 27100 Pavia, Italy

³ Department of Physics, Suez Canal University, Ismailia, Egypt

⁴ Institute of Biology, University of Udine, 33100 Udine, Italy

⁵ Institute of Pharmacology, University of Trieste, 34100 Trieste, Italy

⁶ Institute of Microbiology, University of Trieste, 34100 Trieste, Italy

1 Introduction

The search for non-platinum antitumor metal complexes, which should possibly be active against a broader tumor panel and present a lower host toxicity than the clinically used *cis*-PtCl₂(NH₃)₂, is an item of major research interest.

Among other transition metal derivatives, several ruthenium complexes have been shown to possess a promising antitumor activity ¹⁾.

In the early seventies we chose, among others, a known ruthenium(II)-dimethylsulfoxide complex, *cis*-RuCl₂(DMSO)₄ (*I*) ²⁻⁴⁾, for biological and antineoplastic evaluation. Despite its octahedral geometry and the absence of amino ligands, this complex presented some interesting analogies with *cis*-PtCl₂(NH₃)₂ (cisplatin), that is neutrality, two *cis*-chloride ligands, high stability of the 2+ oxidation state and high affinity for nitrogen donor ligands. Moreover, dimethylsulfoxide is known to cross the cell membranes easily and the complex is fairly soluble in water.

The complex was first tested against *E. Coli* bacterial strains and the results suggested its interaction with DNA in vivo. In fact, in analogy with *cis*-DDP, *cis*-RuCl₂(DMSO)₄ induced filamentous growth and λ profage as well as inhibiting bacterial strains with defective repair systems ⁵⁾.

Thereafter, the complex was tested against several model tumors. Cisplatin was always used as positive control. *cis*-RuCl₂(DMSO)₄ was found to have a toxicity at least three orders of magnitude lower than that of *cis*-DDP. Working at the maximum tolerated dose with daily treatment for 14 days, *cis*-RuCl₂(DMSO)₄ showed activity against both the primary tumor and the metastases in mice bearing Lewis lung carcinoma or MCa mammary carcinoma. In certain cases its activity was comparable to that of *cis*-DDP with the same treatment schedule ⁶⁾. Moreover the ruthenium complex had an overall less pronounced host toxicity than cisplatin.

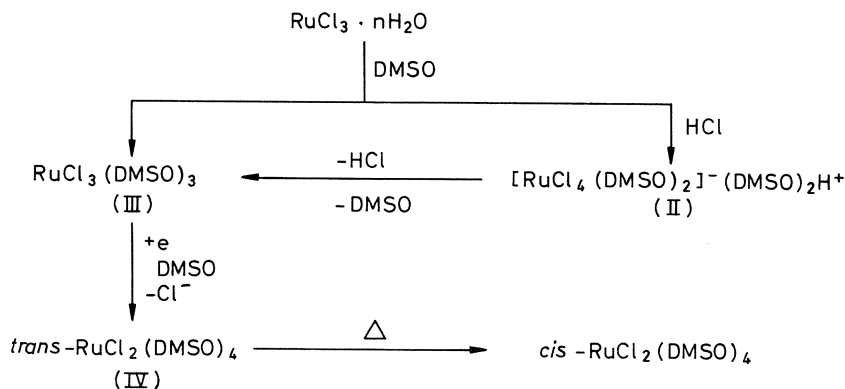
These results prompted us to undertake a systematic study of ruthenium(II)-dimethylsulfoxide complexes. The research project can be roughly divided into three parts: a) a detailed study of the synthesis of *cis*-RuCl₂(DMSO)₄, in order to find out reaction intermediates and possible isomers of the final product; b) interactions of the complexes with DNA in vitro, assuming that, as in the case of *cis*-DDP, it is the intracellular main target; c) synthesis of new ruthenium-dimethylsulfoxide derivatives and test of their biological activity.

2 Chemical Properties

2.1 Reaction Mechanism and Intermediates

The synthesis ^{2,3)} and crystal structure ⁴⁾ of *cis*-RuCl₂(DMSO)₄ have been known for several years. The synthesis is easily accomplished with high yields by heating commercial hydrated RuCl₃ in dimethylsulfoxide. The complex has an octahedral structure, with two *cis*-chlorine atoms. Three DMSO molecules are bonded through the sulfur atom in facial configuration, while the last one is O-bonded.

In the course of our study, in addition to some conformers of *I* ^{7,8)}, we have been able to isolate and characterize some reaction intermediates. Accordingly, the following reaction scheme can be proposed:



The first detected intermediate is the anionic ruthenium(III) complex *trans*-[RuCl₄(DMSO)₂]⁻ (II), whose structure is shown in Fig. 1⁹⁾. The complex has four chlorine atoms in the equatorial plane (Ru—Cl bond distance = 2.354(1) Å) and two S-bonded DMSO molecules in *trans* position (Ru—S bond distance = 2.3474(8) Å). The yield of this complex can be enhanced by the presence of a chloride excess. Interestingly, this Ru(III) derivative is isostructural and isoelectronic with *trans*-bis(imidazole)tetrachlorouranate(III), whose promising antitumor properties have been recently reported by Keppler et al.¹⁰⁾. The comparison between the chemical and biological properties of the two complexes will help to shed light on the influence of the axial ligands on their antitumor properties.

In dimethylsulfoxide solution, *trans*-[RuCl₄(DMSO)₂]⁻ can react further to give the neutral derivative III⁹⁾, which should undergo a monoelectronic reduction to the product isomer, *trans*-RuCl₂(DMSO)₄ (IV). Under the synthesis conditions the *trans* complex IV readily isomerize to the thermodynamically more stable *cis*-RuCl₂(DMSO)₄⁸⁾.

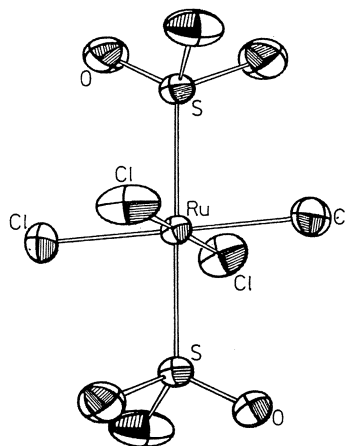


Fig. 1. ORTEP drawing of *trans*-[RuCl₄(DMSO)₂]⁻ with the atom labeling scheme

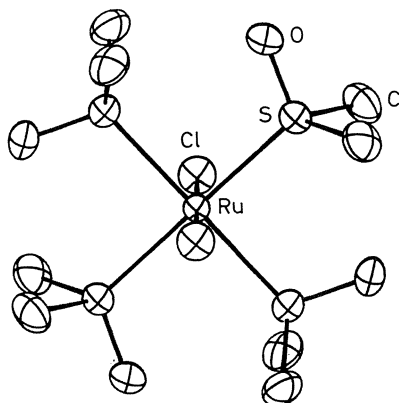


Fig. 2. ORTEP drawing of *trans*-RuCl₂(DMSO)₄ with the atom labeling scheme

2.2 Synthesis and Structure of *trans*-RuCl₂(DMSO)₄

trans-RuCl₂(DMSO)₄ can be obtained in high yields through a photochemical isomerization of *cis*-RuCl₂(DMSO)₄ in dimethylsulfoxide at room temperature⁸⁾. Beside the chlorides disposition, the *trans* complex remarkably differs from the *cis* isomer also in the DMSOs coordination mode (Fig. 2). In fact, in *IV* all the four DMSO molecules are S-bonded in the octahedral equatorial plane. The sensibly longer Ru—S bond distance in the *trans* isomer (2.35 Å versus an average of 2.26 Å in *I*) is indicative of both an enhanced π backbonding competition among the S-bonded DMSOs and of their steric crowding in the equatorial plane.

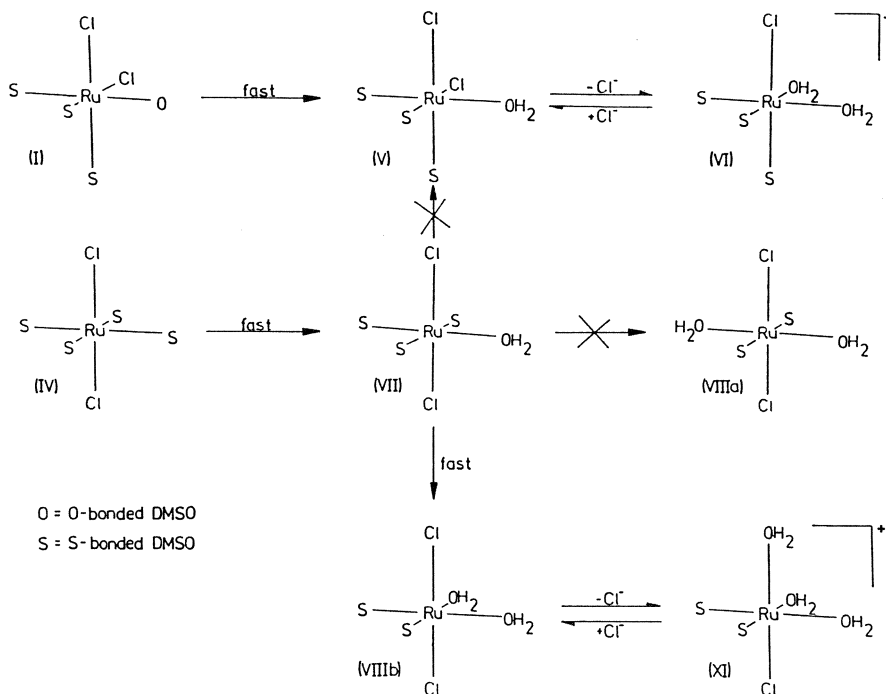
The remarkably different structures of the two RuCl₂(DMSO)₄ isomers will involve a different behavior in solution and, consequently, different biological properties.

2.3 Chemical Behavior of *cis*- and *trans*-RuCl₂(DMSO)₄ in Aqueous Solution

The chemical behavior of the two isomers in aqueous solution has been studied by means of NMR and UV-vis spectroscopy and conductivity measurements. It is reported in Scheme 2.

Upon dissolution *cis*-RuCl₂(DMSO)₄ immediately releases the O-bonded DMSO to give the neutral monoaquo derivative *V*. This step is followed by the slow dissociation of a chloride anion (about 3 h at 37 °C) to form the cationic derivative *VI* with two *cis*-water molecules^{3,8,11,12)}. While the chloride dissociation ([Ru] = 1 mM) is almost complete in water or in 3 mM Cl⁻ solution (intracellular chloride concentration), it is completely suppressed in 150 mM Cl⁻ (extracellular chloride concentration). The same chloride dependent dissociation equilibrium has been found in the case of *cis*-PtCl₂(NH₃)₂¹³⁾.

As mentioned above, the *trans* isomer shows rather different behavior⁸⁾. Once dissolved in water, *trans*-RuCl₂(DMSO)₄ rapidly releases one DMSO molecule to give a neutral monoaquo derivative *VII* with the three remaining DMSOs in a



meridional configuration. This intermediate is not detectable being quite unstable. However it does not isomerize to the stable facial isomer *V* but rather rapidly releases a second DMSO ligand. This second step might, in principle, lead to two different products, *VIIIa* and *VIIIb*, according to whether the second released DMSO is *trans* or *cis* to the water molecule, respectively. Steric reasons would favour *VIIIa* while electronic considerations, that is the strong *trans* effect of S-bonded DMSO, would rather favour isomer *VIIIb*. Unfortunately the NMR data do not allow us to distinguish between the two possible isomers since both of them would have equivalent DMSO ligands.

Recently however we have synthesized, under similar conditions, the corresponding diamino derivative *trans*-RuCl₂(DMSO)₂(NH₃)₂ (*IX*), whose structure is reported in Fig. 3⁹). As can be seen, the diamino complex has the two ammonia molecules in *cis* position, *trans* to the S-bonded remaining DMSOs. The remarkable shortening of the Ru—S bond length (2.24 Å in the diamino derivative versus 2.35 Å in *trans*-RuCl₂(DMSO)₄) is indicative of a particular good stability of two DMSO molecules in *cis* position and *trans* to σ donor ligands. Under the same experimental conditions *cis*-RuCl₂(DMSO)₄ gives a monoamino derivative, *cis*-RuCl₂(DMSO)₃(NH₃) (*X*), by substitution of the O-bonded DMSO ligand⁹).

The structure of the diamino derivative *IX* strongly suggests that also in the case of the diaquo derivative a similar *cis* arrangement should be preferred. The neutral *trans*-dichloro *cis*-diaquo *cis*-bis(dimethylsulfoxide)Ru(II) species *VIIIb* further releases one chloride anion to give the cationic complex *XI* with three water molecules

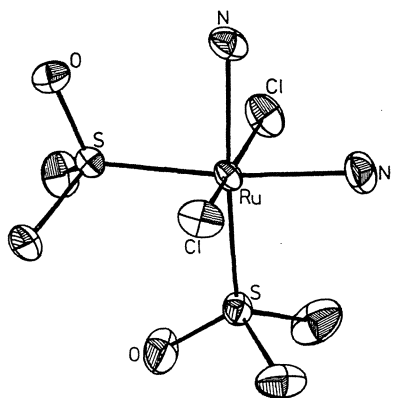


Fig. 3. ORTEP drawing of *trans*-RuCl₂(DMSO)₂(NH₃)₂ with the atom labeling scheme

in facial configuration. This dissociation is again inhibited in 150 mM Cl⁻ solution ([Ru] = 1 mM). In agreement with the lower *trans* effect of Cl with respect to DMSO, the chloride dissociation in *VIIIb* is slower than in *V* (about 8 h at 37 °C).

It is interesting to note that, under the same experimental conditions, both isomers show a chloride dissociation rate comparable to that of *cis*-DDP (Fig. 4).

Assuming that the coordinated water molecules have a labile nature, while the *cis* neutral derivative *V* has only one labile position, the corresponding derivative from the *trans* isomer, *VIIIb*, has two. After chloride dissociation, *VI* has two equivalent coordination sites, while the *trans* derivative *XI* has three available positions in facial configuration. By raising the pH, at least one of the coordinated water molecules should undergo deprotonation to give neutral hydroxo-aquo species.

The aqueous species *V* and *VI* show a considerable higher steric hindrance than the corresponding *VIIIb* and *XI*, due to the presence of the third DMSO molecule.

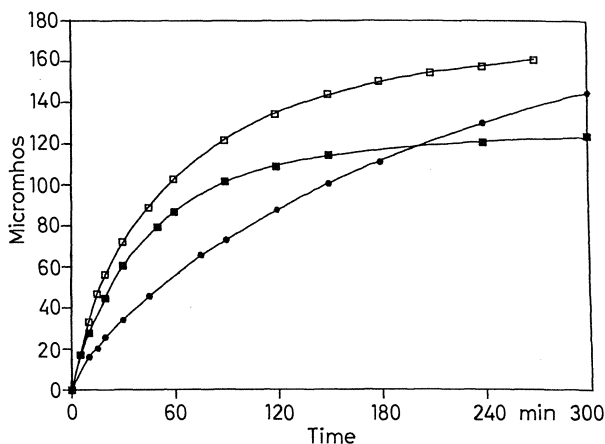


Fig. 4. Conductivity of 1 mM solutions of *cis*-RuCl₂(DMSO)₄ (■), *trans*-RuCl₂(DMSO)₄ (●) and *cis*-PtCl₂(NH₃)₂ (□) versus time.

According to these considerations *trans*-RuCl₂(DMSO)₄ is expected to have a remarkably higher reactivity than the *cis* isomer in aqueous solution.

3 Toxicity and Antitumor Activity of *cis*- and *trans*-RuCl₂(DMSO)₄

The effects of *cis*- and *trans*-RuCl₂(DMSO)₄ on primary tumor growth and on the formation of lung metastases were studied in mice bearing Lewis lung carcinoma. The tumor line, maintained in C57B1 female mice of 20 g, was propagated in BDSF1 female hybrids. Tumor inocula were made by *s.c.* implantation of tumor fragments or by *i.v.* inoculation of tumor cells of a single cell suspension. Primary tumor growth and formation of lung metastases were evaluated according to already reported procedures⁶).

The treatment schedule chosen for the study of the antitumor activity consists of daily *i.p.* injections for 14 consecutive days, starting 24 h after tumor implantation. The dosage employed for each complex is the maximum tolerated dose and corresponds to the LD_{0.05}.

On a molar basis, *trans*-RuCl₂(DMSO)₄ shows a significantly higher toxicity than the *cis* isomer (LD₅₀ of 84 mg/kg d⁻¹ vs 890 mg/kg d⁻¹). The difference is even more evident when the LD_{0.05} values of *I* and *IV* are compared (37 vs 700 mg/kg d⁻¹).

The effects of equitoxic dosages of both isomers and *cis*-DDP on primary tumor growth and on the formation of polmonary metastases, are reported in Table 1.

The treatment has no statistically significant effects on the growth of primary tumor. A significant reduction of the primary tumor growth to 50% (determined on day 17 from tumor implantation) is obtained with the *trans* isomer when a reduced tumor inoculum (50 μl instead of 100 μl) is used.

Table 1. Comparison of the antineoplastic action of *cis*- and *trans*-RuCl₂(DMSO)₄ and *cis*-DDP in mice bearing Lewis lung carcinoma

Compound	Dose (mg/kg/day)	Primary tumor weight (mg) ^a		Lung metastases ^b			
				Number		Weight (mg)	
		Mean ± S.E.	%I	Mean ± S.E.	%I	Mean ± S.E.	%I
Controls	—	2513 ± 275	—	41 ± 3	—	216 ± 32	—
<i>cis</i> -RuCl ₂ (DMSO) ₄	700	1809 ± 352	28	22 ± 2*	46	104 ± 17*	52
<i>trans</i> -RuCl ₂ (DMSO) ₄	37	1960 ± 226	22	18 ± 2*	57	62 ± 11*	71
<i>cis</i> -PtCl ₂ (NH ₃) ₂	0.52	1608 ± 420	36	14 ± 4*	66	47 ± 9*	78

^a Measured on day 14 from tumor implantation;

^b measured on day 21 from tumor implantation.

* Mean statistically different from the corresponding value of the control group, Student-Newmann-Keuls test, p = 0.05;

%I: means percent inhibition compared to the value obtained in the control group.

Groups of 8 BD2F1 mice, inoculated *s.c.* with 100 mm³ of Lewis lung carcinoma fragments on day 0, were given *i.p.* the reported compounds on days 1–14

Table 2. Treatment schedule dependence of the effects of *cis*-DDP on the formation of artificial metastases in mice bearing *i.v.* Lewis lung carcinoma

	Treatment schedule	
	Lung metastases	
	number	weight
0.52 mg/kg/day on days 1–10	4	13
2.5 mg/kg/day on days 1–5	64*	96*
10 mg/kg on day 1	75*	93*

* Means significantly different from the controls, Mann-Whitney „U“ test for a two-tailed comparison, $p < 0.05$;

S.E. are omitted for clarity.

Groups of 7 BD2F1 mice, inoculated *i.v.* with 10^5 Lewis lung carcinoma cells on day 0, were given *i.p.* the reported dosages of *cis*-DDP. Each value is expressed as percent inhibition over controls

In contrast, all the complexes exhibit a significant antimetastatic activity. *cis*- $\text{RuCl}_2(\text{DMSO})_4$ reduces the number and weight of spontaneous lung metastases by 46% and 52%, respectively. The *trans* isomer is slightly more active than the *cis* one with an inhibition of 57% and 71%, respectively. The antimetastatic activity of *cis*-DDP is only slightly more pronounced than that of *trans*- $\text{RuCl}_2(\text{DMSO})_4$.

The antitumor efficacy of cisplatin presently observed is below the known potentialities of this drug, and can be attributed to the length of the treatment schedule used. Indeed, the use of a shorter treatment schedule, with higher daily doses, allows one to obtain an overall higher efficacy.

The effects of *cis*-DDP on the formation of artificial metastases in mice bearing *i.v.* Lewis lung carcinoma, confirm this hypothesis (Table 2). In fact, the effects of cisplatin on the reduction of the number and weight of artificial metastases are negligible with the 10 day treatment, but they can be reverted by using a shorter schedule, with reduction of the average number and weight of lung tumor colonies higher than 60% and 90%, respectively. While a similar study is not possible with *cis*- $\text{RuCl}_2(\text{DMSO})_4$, mainly because of its low toxicity, it could be done with the *trans* isomer and better results than those here reported could be reasonably obtained. Preliminary data on artificial lung metastases seem to confirm such hypothesis.

The therapeutic potentials of *cis*- and *trans*- $\text{RuCl}_2(\text{DMSO})_4$ have been compared with that of *cis*-DDP in mice bearing Lewis lung carcinoma and undergoing surgical removal of the primary tumor. Data reported in Table 3 show that the postsurgical treatment with *I* and *IV* causes a statistically significant prolongation of the survival time of the treated animals as compared to the drug-untreated controls.

The effects of *cis*-DDP are much less impressive. The use of an equitoxic treatment with $0.52 \text{ mg/kg d}^{-1}$ for 10 days is completely devoid of statistically significant effects on the life span of the treated animals. A shorter treatment schedule, with 2.5 mg/kg d^{-1} for 5 days, is necessary to cause effects intermediate between those of *cis*- and *trans*- $\text{RuCl}_2(\text{DMSO})_4$. These results seem to suggest that the use of shorter treatment

Table 3. Effects of *cis*- and *trans*-RuCl₂(DMSO)₄ and *cis*-DDP on the survival time of mice bearing *i.m.* Lewis lung carcinoma and undergoing surgical removal of primary tumor

Complex	Treatment schedule	% Survivals ^a
—	Controls	0
<i>cis</i> -RuCl ₂ (DMSO) ₄	700 mg/kg/day on days 1–10	23
<i>trans</i> -RuCl ₂ (DMSO) ₄	37 mg/kg/day on days 1–10	38*
<i>cis</i> -DDP	0.52 mg/kg/day on days 1–10	15
<i>cis</i> -DDP	2.5 mg/kg/day on days 1–4	25

^a The percentage of survivals reflects the situation in each group when no survivors in the control group are available (day 17 from surgery);

* 1/15 cured.

Groups of 13–17 BD2F1 mice, inoculated *i.m.* with 100 mm³ of Lewis lung carcinoma fragments and undergoing surgical amputation of the tumor bearing leg 9 days later, were given the reported dosages starting 24 h after surgery

schedules, and higher daily doses, could further increase the percentage of survivals actually obtained with *trans*-RuCl₂(DMSO)₄.

These data, in their overall meaning, stress the interesting antineoplastic action of ruthenium(II)-dimethylsulfoxide derivatives. In particular, it emerges that ruthenium complexes presently being studied exhibit antitumor potentialities comparable to those of cisplatin, at least in the murine models actually tested. Of particular importance seems to be the effect on the postsurgical survival time which, unlike cisplatin, for the ruthenium complexes is significant at the same doses active on lung metastasis formation.

4 Interactions of *cis*- and *trans*-RuCl₂(DMSO)₄ with O- and N-donor Ligands

In order to better understand the interactions of *cis*- and *trans*-RuCl₂(DMSO)₄ with DNA *in vitro* and to postulate a tentative mechanism of their action we recently began to study the reactivity of the two isomers towards small molecules of particular biological interest. Some preliminary results concerning their interactions with inorganic phosphate (Pi) and imidazole are reported below. Pi is an example of a biologically important oxygen donor ligand which is present in rather high concentration in the cell, while imidazole is the N-donor moiety of a wide class of biologically important molecules.

Spectroscopic data suggest that, upon addition of a phosphate buffer to a solution of *cis*- or *trans*-RuCl₂(DMSO)₄, not only are the acid-base equilibria altered but also covalent interactions between Pi and the complexes probably occur. Proposed products of the covalent bonding are chelates *XII* and *XIII*, respectively (Fig. 5). Assuming that Pi preferably interacts with cationic species, the rate of formation of chelate *XIII* should be considerably slower than that of *XII*, due to the slower chloride dissociation rate in the *trans* isomer *IV*. Moreover, chelate *XIII* is not coordinatively saturated, still having one labile site which can further react with other ligands.

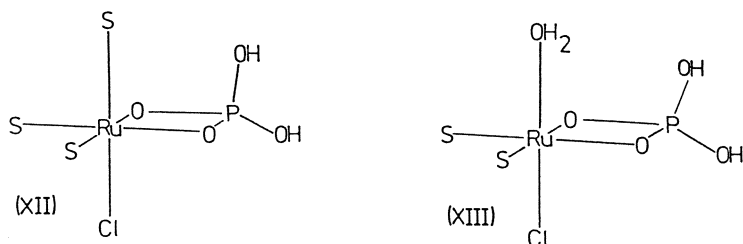


Fig. 5. Proposed products of the reaction of *cis*- and *trans*- $\text{RuCl}_2(\text{DMSO})_4$ with inorganic phosphate

The reactions of both complexes with imidazole have been carried out in 150 mM Cl^- , in order to inhibit the chloride dissociation. The results are schematically reported in Fig. 6. The *trans* derivative *VIIIb* undergoes, at room temperature, a fast substitution of both the coordinated water molecules to give the *trans*-dichloro *cis*-bis(dimethylsulfoxide) *cis*-bis(imidazole)ruthenium(II) complex (*XIV*), which has been isolated under similar conditions and spectroscopically characterized. As evidenced by the trend of conductivity versus time, the chloride dissociation rate in this product is much slower than that of the starting complex *VIIIb*. Therefore, due to the lack of available coordination sites, it will probably be biologically inactive.

The behavior of the *cis* derivative is more complex. The first step is the formation of a mono-imidazole derivative by substitution of the coordinated water. This reaction is about 100 times slower than that with the *trans* isomer. Also this *cis*-dichloro mono-imidazole complex (*XV*) has been isolated under similar conditions and spectroscopically characterized. Despite the presence of the chloride excess, it can further react with imidazole to give uncharacterized cationic species.

In conclusion *trans*- $\text{RuCl}_2(\text{DMSO})_4$ turns out to be considerably more reactive than the *cis* isomer towards N-donor ligands.

The study of the interaction of the complexes with S-donor ligands is in progress.

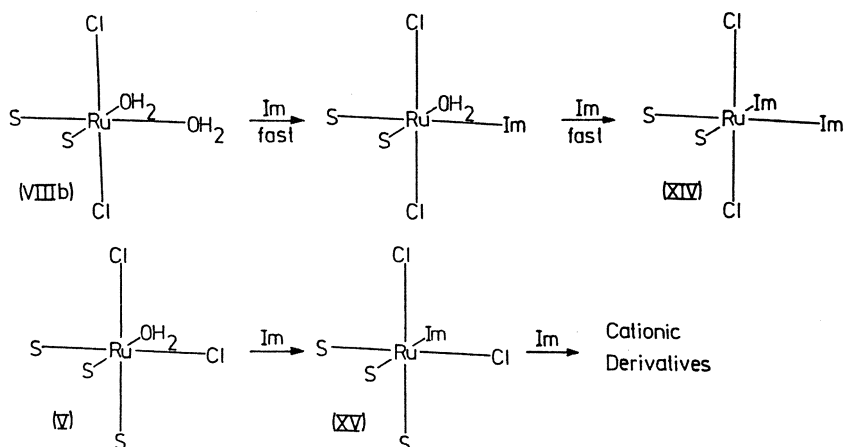


Fig. 6. Reaction schemes of *trans*- and *cis*- $\text{RuCl}_2(\text{DMSO})_4$ with imidazole in aqueous solution

5 Interactions of *cis*- and *trans*-RuCl₂(DMSO)₄ with DNA *in Vitro*

5.1 Reactions of *cis*-RuCl₂(DMSO)₄ with DNA

When calf thymus DNA is incubated with *cis*-RuCl₂(DMSO)₄ in equimolar amounts in pseudo-intracellular conditions (3 mM NaCl, 1 mM phosphate buffer, pH = 7.2, 37 °C), the UV spectrum of the ultrafiltered DNA solutions shows modifications which are related to the incubation time and to the amount of *cis*-RuCl₂(DMSO)₄ covalently bound as determined by atomic absorption spectroscopy (Fig. 7). The reaction is not very fast, r_b being about 0.05 after ten hours of incubation.

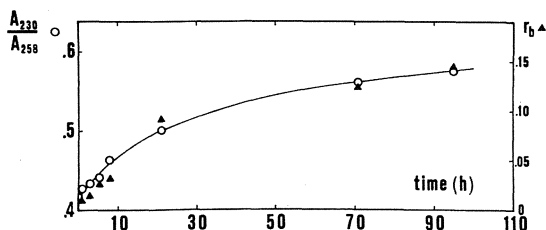
A comparison between the rate of chloride dissociation and that of DNA bonding suggests that the main reactive species is the cationic ruthenium derivative VI.

The binding of the complex to the DNA chain increases its stability toward thermal denaturation and does not affect significantly its B conformation, as deduced by CD spectral measurements. On the contrary, the same reaction carried out with poly(dGdC) in the presence of low ionic strength, induces a B to Z transition in the polymer which is complete within about ten hours (Fig. 8). This results strongly suggests that a major target for the ruthenium complex is N7 of guanine, whose *syn* conformation is stabilized by the presence of a bulky group covalently bound to N7 or C8. In fact, in the alternated Z conformation the purine residues must assume the *syn* form of the glycosidic bond. N7 of adenine is also a possible target for the complex. However, the experimental higher reactivity of the complex toward 5'-dGMP with respect to 5'-dAMP, which is in agreement with the higher nucleophilicity of guanine N7, suggests that the latter site is the main target on double stranded DNA.

The reaction of the complex monoamino derivative, X, with poly(dGdC) was also examined. This reaction produces the same conformational changes observed with *cis*-RuCl₂(DMSO)₄, but at a lower rate (midpoint of the B—Z transformation at 7 hours instead of 4). As the two complexes show almost the same rate for Cl⁻ dissociation, the slower reaction of the monoamino derivative with the polymer is probably due to the presence of only one available coordination site instead of the two aquated sites provided by VI. The obtainment of the Z conformation with the monoamino derivative indirectly confirms that also in the case of *cis*-RuCl₂(DMSO)₄ a monoadduct could be formed. This conclusion does not necessarily imply that *cis*-RuCl₂(DMSO)₄ is not able to form bifunctional adducts with DNA chains. The experimental evidences so far collected, however, suggest that such a possibility is not relevant, at least for the incubation times examined.

Fig. 7. Binding of *cis*-RuCl₂(DMSO)₄ to ctDNA.

(○) 230/258 nm absorbance ratio of DNA spectra versus incubation time. Unreacted ruthenium was removed by ultrafiltration. (▲) Amount of ruthenium bound as determined by A.A.S. on the same DNA solutions



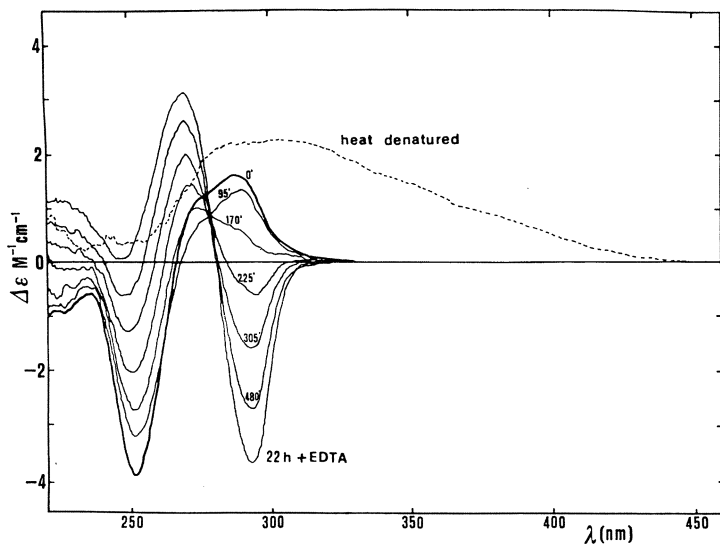


Fig. 8. CD spectra of poly(dGdC) reacted with equimolar *cis*-RuCl₂(DMSO)₄ as a function of reaction time (2×10^{-4} NaClO₄, 37 °C). The heat denatured reacted polymer (— —) does not renature

5.2 Reactions of *trans*-RuCl₂(DMSO)₄ with DNA

trans-RuCl₂(DMSO)₄, when incubated with ctDNA under the same experimental conditions as the *cis* isomer, covalently binds to it with a markedly higher reaction rate (Fig. 9). As expected, the B—Z transformation of poly(dGdC) is also much faster, with a midpoint of about 50 minutes, compared with the 4 hours of the *cis* isomer. Again the data with poly(dGdC) and with mononucleotides suggest N7 of guanine as the main target.

In the case of *trans*-RuCl₂(DMSO)₄, even after a few hours of incubation, the reaction with ctDNA produces a marked modification of the DNA structure as re-

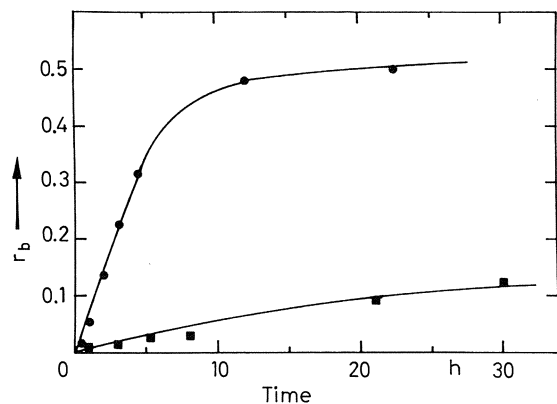


Fig. 9. Amount of ruthenium bound to ctDNA (per phosphate group) versus incubation time, as determined by A.A.S.: (■) *cis*-RuCl₂-(DMSO)₄, (●) *trans*-RuCl₂-(DMSO)₄

vealed by the intensity decrease of CD bands. This spectral change, which can be attributed to a progressive destruction of the ordered DNA structure, could be related to the formation of bifunctional adducts along the chain.

The reaction of the diamino complex *IX* with poly(dGdC) has also been examined. The very low reaction rate observed is probably due to the negligible Ru—Cl bond dissociation rate and to the inertness of the coordinated ammonia molecules.

6 Proposed Schemes of Mechanism

On the basis of the chemical behavior of *cis*- and *trans*- $\text{RuCl}_2(\text{DMSO})_4$ and of their interactions with chloride, inorganic phosphate, imidazole and DNA, a first scheme of their mechanism of action *in vivo* can be tentatively proposed.

The scheme for *cis*- $\text{RuCl}_2(\text{DMSO})_4$ is reported in Fig. 10. Due to the high extracellular chloride concentration, the main species present outside the cell should be the neutral monoquo derivative *V*. In agreement with its reported behavior, it will slowly react with the various ligands present *in vivo* to give coordinatively saturated neutral and cationic species.

Because of its relative inertness, *V* should be able to reach the cell membrane

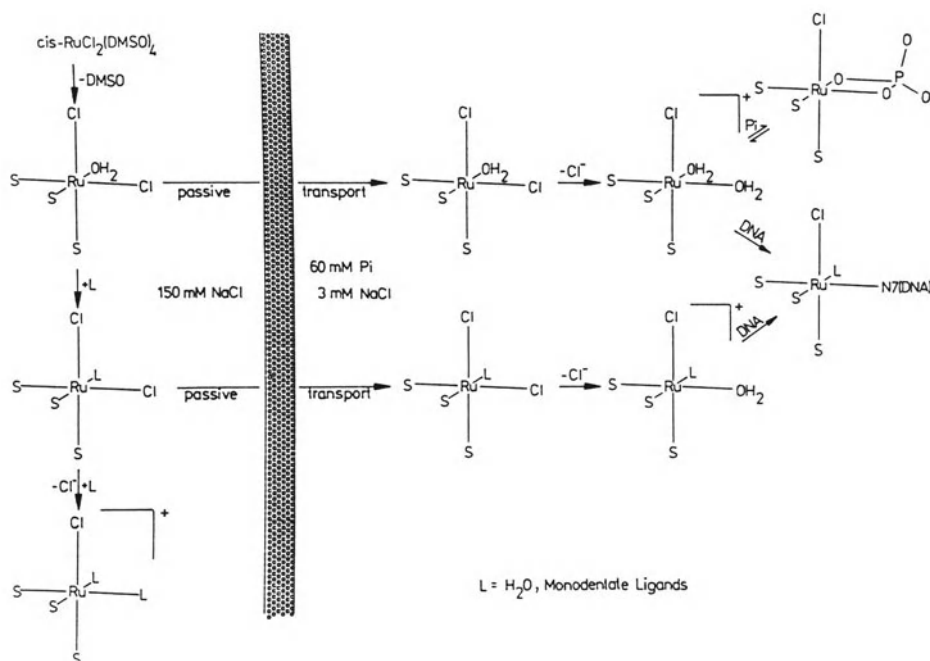


Fig. 10. Proposed scheme of action for *cis*- $\text{RuCl}_2(\text{DMSO})_4$ *in vivo*

in rather good amounts and cross it, probably through a passive transport mechanism. Once inside the cell it can release a chloride anion to give the cationic diaquo species *VI* which, in turn, should slowly react with DNA. Assuming that the first DNA target is guanine N7 and considering that the complex has two reactive sites, the possible products of the covalent interaction are monofunctional adducts, N7-O6 chelates or even bifunctional adducts. The complex can of course react with other components inside the cell, including inorganic phosphate (*vide supra*).

The corresponding monoamine derivative *X* has no free coordination sites in a high Cl^- environment and therefore it should not react outside the cell. On the basis of their strict analogies, closely similar behavior between complexes *V* and *X* in crossing the cell membrane can be reasonably hypothesized. Once inside the cell *X* can dissociate the Ru—Cl bond and interact with DNA to give only monofunctional adducts.

The schematic mechanism proposed for *trans*- $\text{RuCl}_2(\text{DMSO})_4$ is reported in Fig. 11. For the same considerations exposed above, in this case the main species outside the cell should be the neutral diaquo *VIIIb*. It will react easily, much faster than the corresponding *cis* derivative *V*, with the ligands present in the extracellular medium to give coordinatively saturated species. Accordingly, only a rather small fraction of the administered complex should be able to reach the cell membrane and cross it, probably again through a passive transport mechanism. Having crossed the cell membrane it can release a Cl^- and interact with DNA. Due to the lower steric hindrance, in this case the probability of bifunctional adducts formation should be higher than with the *cis* derivatives.

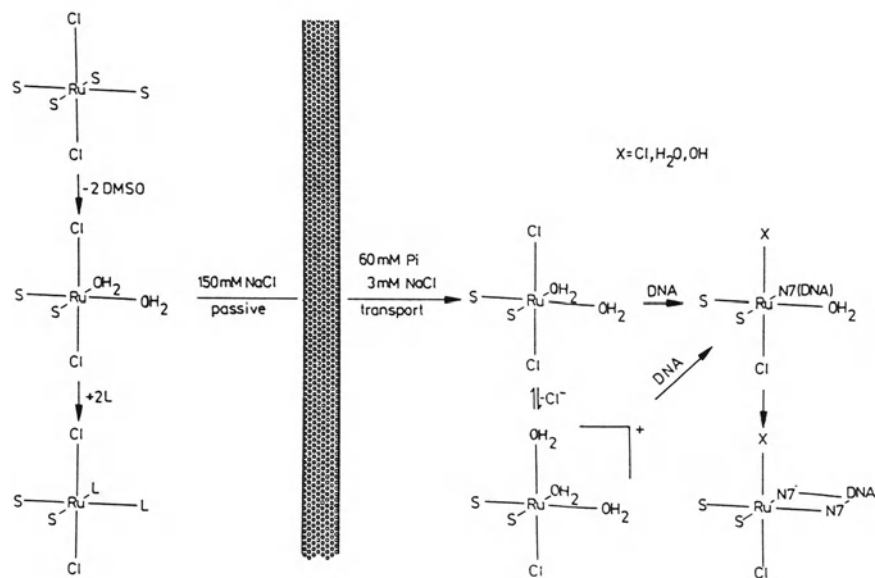


Fig. 11. Proposed scheme of action for *trans*- $\text{RuCl}_2(\text{DMSO})_4$ in vivo

7 Interaction of *cis*- and *trans*-RuCl₂(DMSO)₄ with DNA *in Vivo*

cis-RuCl₂(DMSO)₄ shows mutagenic activity against two series of bacterial strains, *S. Typhimurium* and *E. Coli*. The activity strongly depends on the concentration of the inorganic phosphate in the culture medium. A decrease of mutagenic activity and an increase of the MIC values occur as the Pi concentration or the preincubation time are increased. This behavior clearly suggests that the complex interacts with DNA and that inorganic phosphate acts as an inhibitor. The complex low toxicity could be, at least in part, due to its interaction with Pi¹⁴.

trans-RuCl₂(DMSO)₄ shows a very low mutagenic activity when tested on the same bacterial strains¹⁴. These results could be ascribed to the higher chemical reactivity of the *trans* isomer in comparison with the *cis* one. In fact the neutral diaquo complex *VIIIb* should rapidly interact outside the cells with some compounds of the medium to give inert complexes and therefore only a small fraction of the original complex can reach its intracellular target, DNA.

On the other hand the *trans* isomer shows a higher cytotoxicity and mutagenic activity than the *cis* one when tested against an eukariotic system, the V79 Chinese hamster lung cells in culture (Fig. 12). In particular in the range 0–400 µg/ml, in which both complexes are non toxic, *IV* shows a good mutagenic activity, while *I* is almost inactive.

The same type of cells have been treated with equimolar doses of both isomers, their DNA extracted and the amount of ruthenium bound determined by A.A.S. The results summarized in Table 4 show that an approximatively five fold amount

Fig. 12. Lethal and mutagenic effects of *cis*- (△) and *trans*-RuCl₂(DMSO)₄ (○) on V79 Chinese hamster lung cells. After 24 h of incubation with the ruthenium complexes dissolved in culture medium, the cells were subcultured for evaluation of survival (Panel A) and mutagenesis (Panel B). The latter was detected after an expression period of 6 days: mutants defective in the purine salvage enzyme hypoxanthine-guanine phosphoribosyl transferase (HGPRT) were selected by adding 6-thioguanine to a final concentration of 5 µg/ml. Each point represents the mean of three independent experiments

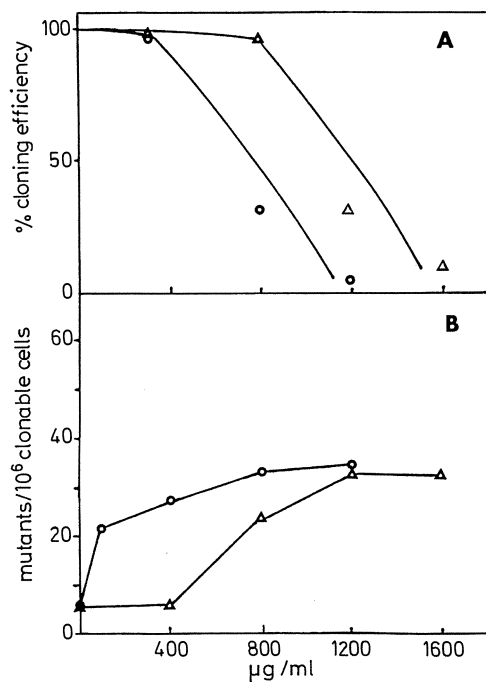


Table 4. Percentage of Ruthenium bound to DNA extracted from V79 Chinese hamster lung cells treated with equimolar amounts of *cis*- and *trans*-RuCl₂(DMSO)₄

Complex	r _b
<i>cis</i> -RuCl ₂ (DMSO) ₄	5.6 × 10 ⁻⁴
<i>trans</i> -RuCl ₂ (DMSO) ₄	2.8 × 10 ⁻³

V79 cells were incubated for 2.5 h at 37 °C with 5 mg/ml of the two complexes

of ruthenium is found in the case of *trans*-RuCl₂(DMSO)₄, suggesting that the mutagenicity is related to this parameter.

The overall data suggest that both isomers interact *in vivo* with DNA.

8 Concluding Remarks

The pharmacological tests reported show that the two isomers *cis*- and *trans*-RuCl₂(DMSO)₄ have antitumor and, in particular good, antimetastatic activity. In the case of the *trans* isomer the activity can be probably increased by using shorter treatment schedules.

Several new ruthenium-DMSO derivatives, including some chiral compounds, have been synthesized and are now under investigation. Some complexes with promising antitumor activity have already been identified.

DNA seems to be an important target also for these complexes and the cationic derivative *fac*-[RuCl(H₂O)₃(DMSO)₂]⁺ (*XI*) is probably the most reactive species.

The ruthenium(II) complexes with dimethylsulfoxide and related ligands, due to the high stability of the +2 oxidation state, can be considered as useful models to study the interactions of octahedral complexes with DNA and related molecules.

9 Acknowledgement

Financial support from Ministry of Public Instruction (40% Grant) and Boehringer Biochemia Robin is gratefully acknowledged. The authors would also like to thank Mr. R. Nardini (U.S.L. 7, Udine, Italy) for the atomic absorption measurement.

10 List of Symbols and Abbreviations

- DMSO = Dimethylsulfoxide
cis-DDP = *cis*-PtCl₂(NH₃)₂, cisplatin
s.c. = Subcutaneous
i.v. = Intravenous
 ctDNA = Calf thymus DNA

- Pi = Inorganic phosphate
r_b = Amount of ruthenium bound to DNA per phosphate group
MIC = Minimum inhibiting concentration
A.A.S. = Atomic absorption spectra

11 References

1. Clarke MJ (1980) in: Siegel H (ed) *Metal ions in biological systems*, vol 11, Marcel Dekker, New York, p 231; Clarke MJ (1983) in: Lippard SJ (ed) *Platinum, gold and other chemotherapeutic agents*, ACS symposium series, vol 209. American Chemical Society, Washington D.C., p 335; Clarke MJ, Galang RD, Rodriguez VM, Kumar R, Pell S, Bryan DM (1988) in: Nicolini M (ed) *Platinum and other metal coordination compounds in cancer chemotherapy*. Martinus Nijhoff, Boston, p 582
2. James BR, Ochiai E, Rempel GL (1971) *Inorg. Nucl. Chem. Lett.* 7: 781
3. Evans IP, Spencer A, Wilkinson G (1973) *J. Chem. Soc. Dalton Trans.*: 204
4. Mercer A, Trotter J (1975) *J. Chem. Soc. Dalton Trans.*: 2480
5. Monti-Bragadin C, Ramani L, Samer L, Mestroni G, Zassinovich G (1975) *Antimicrob. Agents Chemother.* 7: 825; Monti-Bragadin C, Giacca M, Dolzani L, Tamaro M (1987) *Inorg. Chim. Acta* 137: 31
6. Sava G, Zorzet S, Giraldi T, Mestroni G, Zassinovich G (1984) *Eur. J. Cancer Clin. Oncol.* 20: 841
7. Attia WM, Calligaris M (1987) *Acta Crystallogr., Sect. C: Cryst. Struct. Commun.* C43: 1426
8. Alessio E, Mestroni G, Nardin G, Attia WM, Calligaris G, Sava G, Zorzet S (1988) *Inorg. Chem.* 27: 4099
9. Alessio E, Mestroni G, Calligaris M, Attia WM (unpublished results)
10. Keppler BK, Rupp W (1986) *J. Cancer Res. Clin. Oncol.* 111: 166; Keppler BK, Rupp W, Juhl UM, Endres H, Niebl R, Balzer W (1987) *Inorg. Chem.* 26: 4366
11. Barnes JR, Goodfellow RJ (1979) *J. Chem. Res. (M)*: 4301
12. Farrel N, De Oliveira NG (1980) *Inorg. Chim. Acta* 44: L225
13. Howe-Grant ME, Lippard SJ (1980) in: Siegel H (ed) *Metal ions in biological systems*, vol 11. Marcel Dekker, New York, P 63
14. Alessio E, Attia WM, Calligaris M, Cauci S, Dolzani L, Mestroni G, Monti-Bragadin C, Nardin G, Quadrifoglio F, Sava G, Tamaro M, Zorzet S (1988) in: Nicolini M (ed) *Platinum and other metal coordination compounds in cancer chemotherapy*. Martinus Nijhoff, Boston, p 617

Metal Complexes as Radiosensitizers

Nicholas Farrell

Department of Chemistry, University of Vermont, Burlington, VT 05405, USA

Many classes of transition metal complexes enhance cellular radiation damage both *in vitro* and *in vivo*. The radiosensitization of hypoxic cells is of clinical relevance due to the inherent radioresistance of a tumor hypoxic fraction. Selective attack on hypoxic cells may also be achieved by development of hypoxic cytotoxins and chemosensitizers, which may act by enhancing the hypoxic toxicity of other agents. In radiosensitization three principal mechanisms by which metal complexes act are by DNA-binding with subsequent consequences to repair processes, thiol depletion, and by an electron-affinic mechanism, implying reduction of the metal complex and subsequent fixation of damage on the intracellular target of radiation, DNA. The types of complexes shown to act by the above mechanisms are summarized.

1	Introduction	90
2	Interaction of Radiation and Biological Tissue	91
2.1	Chemistry of Radiation Sensitization	91
2.2	Survival Curves and Radiation Dose	92
2.3	Chemical Modification of Radiation Damage	93
3	Metal Complexes as Radiosensitizers	94
3.1	Platinum-Amine Complexes as Potentiators of Radiation Damage	95
3.2	Radiosensitization by Thiol Depletion	96
3.3	Radiosensitization by Electron Affinity	97
3.3.1	Targeted Radiosensitizers	97
3.3.2	Metal Complexes as Redox Centres	103
4	Metal Chemistry Relevant to Radiosensitization	106
5	Summary	107
6	Acknowledgements	107
7	References	107

1 Introduction

Many tumors contain necrotic areas usually separated some distance (150–200 μm) from the vascular system. This situation is explained by the fact that the disordered nature of tumor cell replication and the subsequent requirements of oxygen metabolism produce an oxygen gradient rendering the cells farthest from the capillaries hypoxic (oxygen-deficient). In the treatment of cancer, the presence of these hypoxic areas may lead to an inherent resistance to drug action ¹⁾.

The problem of hypoxic resistance is especially acute in radiation treatment. The fact that tumor cells showed diminished radiation sensitivity in the absence of oxygen had been known for some time and the full relevance of this physico-chemical effect in therapy was demonstrated in classic studies by Gray and co-workers ^{2,3)}. The hypoxic cells, which may represent up to 30% of the total tumor mass, are inherently radioresistant but may become aerobic upon termination of treatment. In this case tumor growth would recommence.

Chemical compounds with some hypoxic cell selectivity belong in three major categories:

- i) *Radiosensitizers and Radiopotentiators*. Compounds which enhance radiation kill, preferably in hypoxic cells.
- ii) *Hypoxic Cytotoxins*. Compounds which are toxic to cells in absence of radiation (i.e., chemotherapeutic selectivity).
- iii) *Chemosensitizers*. Compounds which enhance toxicity of chemotherapeutic agents, again preferentially in hypoxic cells.

Under the overall term of chemical modification of radiation damage, three general mechanisms of radiosensitization may also be distinguished as

- ia) *DNA-incorporation (binding)*. Agents which disrupt DNA function may place a much greater stress on repair processes etc. in conjunction with radiation damage.
- ib) *Thiol Depletion*. Thiols radioprotect, therefore thiol depletion, either by chemical means or through biochemical manipulation of radioprotectant thiols such as glutathione, sensitizes.
- ic) *Use of Oxygen-mimetic (electron-affinic) compounds*. Compounds which act like oxygen may “substitute” for oxygen in hypoxic cells and thus sensitize. The mechanism is identical to that of oxygen, involving electron transfer from a radiation-damaged target, DNA, to the sensitizer with resultant fixation of the damaged lesion (strand break) on the DNA ⁴⁾.

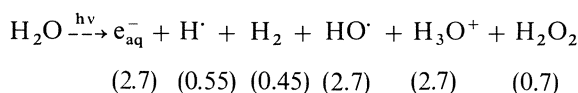
The vast majority of mechanistic work and drug development in these areas has concentrated on organic compounds, yet metal complexes meet many of the criteria commonly considered as prerequisites for hypoxic cell selectivity. Our own work has, over the years, identified classes of metal complexes toxic to hypoxic cells by all three mechanisms (i–iii) and, indeed, these actions may be related. Further, metal complexes have been shown to interact with radiation by each of the mechanisms (ia–ic). This contribution summarizes especially the field of metal complexes as radiosensitizers and is intended to complement earlier reviews ^{5,6)}.

2 Interaction of Radiation and Biological Tissue

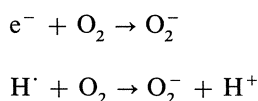
2.1 Chemistry of Radiation Sensitization

An excellent source on the chemical basis of radiobiology is to be found in the book by von Sonntag ⁷⁾ and a compendium on radiation effects on DNA also covers many basic chemical aspects ⁸⁾.

The radiolysis reaction of oxygenated aqueous solutions may be written, with the yields (G-values) for X-rays in parentheses ⁴⁾:



The formation of both HO^\cdot and e_{aq}^- is complete in 10^{-11} s with molecule formation from recombination or chemical reaction complete in 10^{-8} s. Both e^- and H^\cdot react at diffusion controlled rates with oxygen giving superoxide:



The hydroxyl radical is by far the most reactive, and thus damaging, of the water radiolysis products. The target of radiation damage is overwhelmingly accepted to be DNA. Damage may be either direct (by direct interaction with radiation with the target itself suffering a localized polarization) or indirect (through some radiolysis product, such as hydroxyl radical, which may act by H-abstraction or $\cdot\text{OH}$ addition). The relative contributions in oxygenated solutions have been calculated as 60% indirect and 40% direct ⁹⁾. Independent of mode of damage, subsequent chemical rearrangement “fixes” the lesion. Enzymatic repair takes place on a time scale of 10^{-1} to 10^4 s. The molecular lesions are classified as: a) double-strand breaks, b) single-strand breaks, c) base damage and d) cross-linking ¹⁰⁾. Hydroxyl radicals cause strand breaks, of which double-strand breaks are considered most difficult to repair ¹¹⁾.

Oxygen may be considered to be the classic dose-modifying agent or sensitizer and must be present during delivery of radiation, at least for all practical purposes, to exert its sensitizing effect. One possible mechanism is considered to be electron acceptance from target radicals generated by the radiation:



These R^\cdot (DNA) radicals have a very short lifetime and may undergo chemical changes; reaction of a product with oxygen to give an organic peroxide is non-reversible and results in biological damage by fixation of a lethal lesion on the target, i.e., DNA, as stated. In the absence of oxygen, fewer peroxides are formed and thus more are repaired. Detailed studies on the chemical products of radiation damage to DNA in presence of O_2 indicate a complicated mechanism of chemical change for

the RO_2 radical, once formed, and strand breaks resulting from nucleoside excision, altered sugar on the 3' end and base loss upon alteration of sugar have been recognized¹²⁾.

2.2 Survival Curves and Radiation Dose

The effectiveness of cell kill by radiation, either in vitro or in vivo, is measured by the cell-survival or dose-survival curve¹³⁾. In Fig. 1 are represented the typical curves for cells exposed to X-radiation under N_2 and under O_2 . A number of mathematical models have been used to describe these curves and these have been compared¹⁴⁾. Most models converge at high doses but they give disparate results at low doses. This is of importance because, whereas doses of 300 to 3000 rads are routinely used to construct these curves for X-rays, the clinically relevant doses are up to 200 rads, with multiple doses over the period of treatment. Accurate description of the survival curve at low dose is essential for prediction of clinical behaviour and the importance of the oxygen effect at low doses has been discussed¹⁵⁾.

The major point to note for our purposes is that the dose required to obtain a given effect (i.e., same cell kill) is approximately three times greater in deoxygenated, or hypoxic, cells than in normal aerobic cells. This ratio, which varies with the type of radiation but which, for any given radiations, is generally independent of survival level is called the Oxygen Enhancement Ratio (OER), and is the ratio of hypoxic to aerated doses needed to produce a given effect. The concentration of oxygen required for full sensitization is 2% (30 μM) so most normal tissues ($[\text{O}_2]$ between 2–5%) have sufficient oxygen for the full radiation effects to be observed. For agents other than oxygen, ER or dose-modifying factor (DMF) is used to describe the effect

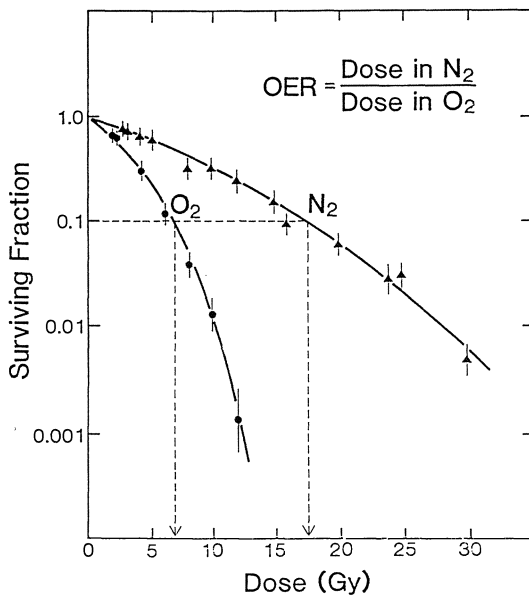


Fig. 1. Typical survival curve for Chinese Hamster Ovary (CHO) cells in O_2 and N_2 showing the Oxygen Enhancement Ratio

of the agent vs. N_2 . Thus, an ER of 1 means little or no effect and a compound approaching the efficiency of oxygen should be >2 .

A further point worth mentioning at this stage is the relationship between chromosome volume and radiosensitivity — the smaller the chromosomal volume, the larger the dose required to inhibit growth of that particular organism by the random damage induced by radiation¹⁶⁾. This is relevant because both bacterial and mammalian cell lines have been used for in vitro studies of radiosensitization. Radiation doses, however, are significantly higher in bacterial systems than in mammalian systems. Extrapolation of mechanism between the two systems should be made with great caution — the radiation chemistry of metal complexes may not be the same at the different doses employed.

2.3 Chemical Modification of Radiation Damage

Approaches to chemical modification include use of “electron-affinic” sensitizers which act as oxygen mimics; thiol-binding agents which increase the effective concentration of oxygen by competitive reactions with endogenous reducing thiols, and DNA-binding agents which may alter template activity either by incorporation or inhibition of repair processes. These may be considered to be the major mechanisms of radiosensitization. The concepts outlined briefly above can be found in more detail in some relatively recent reviews^{1, 17, 18)}. The electron-affinic theory was originally developed in 1963 by Adams and Dewey¹⁹⁾ and refined later²⁰⁾ to that depicted in Fig. 2. Essentially this states that electron transfer from a locally polarized DNA molecule to a more “electron-affinic” molecule (oxygen or a radiosensitizer in the absence of oxygen) can result in greater probability of fixation of damage at that site.

Electron transfer from a damaged molecule to a more electron-affinic molecule results in higher probability of irreversible chemical change.

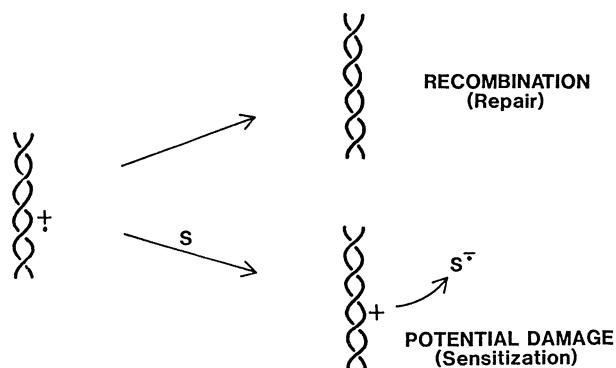


Fig. 2. Schematic representation of possible fixation of damage induced by a sensitizer upon reaction with radiation-damaged DNA

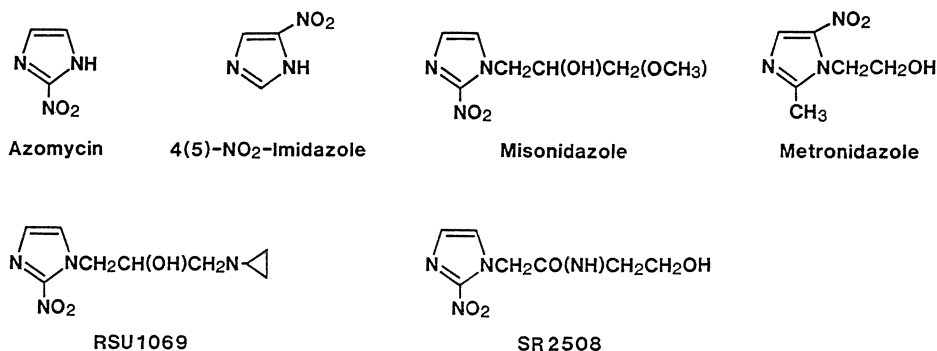


Fig. 3. Structures of nitroimidazoles of interest as radiosensitizers

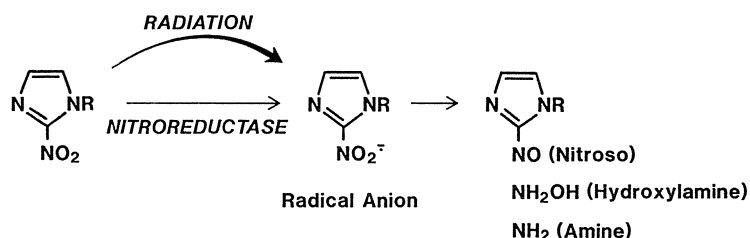


Fig. 4. Activation of nitroimidazoles by either radiation or metabolic pathways

Development of the electron affinity theory produced many molecules with sensitizing activity. Currently the species of clinical interest are the nitroimidazoles and the principal examples to be discussed here are shown in Fig. 3. The leading candidate for clinical use was misonidazole but clinical trials have shown unacceptable toxic side-effects especially neurotoxicity, at useful doses for radiosensitization. Recently attention has turned to a nitroimidazole with a peptide side linkage and structure similar to misonidazole (SR 2508 or etanidazole). This and others are so far unproven in clinical trials and the need for efficient non-toxic radiosensitizers is as acute as ever.

Electron transfer to a nitroimidazole leads to initial production of the nitro-radical anion which eventually decays to the amine. Metabolic reduction in the absence of radiation can lead to hypoxic toxicity by initial production of the radical anion and so compounds, such as misonidazole, may have both properties of radiosensitizer and hypoxic cytotoxin²¹). The activation of nitroimidazoles by both radiation and metabolic pathways is shown in Fig. 4.

3 Metal Complexes as Radiosensitizers

Table 1 shows those metals whose complexes, independent of structure, have demonstrated radiosensitizing ability and the possible mechanisms by which they act.

Table 1. Summary of some radiosensitizing metal complexes

Complex	System	Possible mechanism	Refs.
<i>cis/trans</i> -[PtCl ₂ (NH ₃) ₂]	Mammalian	DNA Repair	22)
	Bacterial	Radiolysis products?	25)
Hg Carboxylates	Bacterial	Thiol depletion	31)
Rh Carboxylates	Mammalian	Thiol depletion	35)
	Bacterial	Radiolysis products	37)
Ferricyanide	Bacterial	Thiol depletion	34)
Targeted sensitizers	Mammalian	Electron-affinic, DNA?	44)
Co amines	Mammalian	Reduction?	65)
Cu salts	Mammalian	Reduction	73)
	Bacterial	Reduction	72)
Co, Cu porphyrins	Mammalian	DNA, Reduction	66)
Ferricenium ion	Mammalian	Reduction	69)
Hydroxynaphthoquinone chelates of Ni	Mammalian	Electron-affinic	76)

A point to be clarified here is the distinction between sensitization, implying an oxygen-mimetic mechanism, and potentiation, which implies modification of radiation damage by other pathways such as DNA binding or incorporation. In view of the lack of mechanistic detail on the action of most metal complexes, sensitization is a valid concept and will be used throughout for non-platinum complexes.

A clear requirement for an efficient radiosensitizer is good electron affinity and the ability to undergo a one-electron reduction reaction. An ideal radiosensitizer would be non-toxic to aerobic cells and thus be selective to hypoxic regions; pharmacokinetic parameters such as rate of metabolism and ability to reach sufficiently high concentrations eventually dictating the overall efficacy. Metal complexes would appear to represent ideal candidates for systematic studies but few such studies have been carried out. We will summarize the actions of metal complexes under the mechanistic headings discussed at the beginning of the chapter.

3.1 *Platinum-Amine Complexes as Potentiators of Radiation Damage*

The clinical utility of the platinum amines makes their interaction with radiation of particular interest, from the point of view of their inherent ability to modify radiation damage, their interaction with sensitizers such as the nitroimidazoles and their potential clinical use in combined chemotherapy/radiation treatment regimens. Cisplatin, *cis*-[PtCl₂(NH₃)₂], is showing interesting results in combination with radiation in the clinic, especially with head and neck and bladder cancer, although no definitive statements as to its utility can yet be made²²⁾. This latter review on the clinical status updates earlier ones by Nias²³⁾ and Douple and Richmond²⁴⁾. Because of its clinical use as a second-generation analog of cisplatin the interactions

of CBDCA with radiation are of interest and initial results indicate promising activity in both bacterial and mammalian systems²⁵⁾.

The exact mechanism by which this and other platinum complexes enhance radiation damage and the mechanisms of inhibition of cellular repair processes after radiation is at present not clear but is most probably related to their DNA-binding. A true sensitizing action for platinum complexes is likely to require a reduction to Pt(I). The rate constants for reaction of *cis*-[PtCl₂(NH₃)₂] with e_{aq}⁻ and ·OH have been calculated as 1.8×10^{10} and $2.0 \times 10^9 \text{ M}^{-1} \text{ s}^{-1}$, respectively²⁶⁾. A reaction rate with the hydrated electron of $1.3 \times 10^{10} \text{ M}^{-1} \text{ s}^{-1}$ for the *trans* isomer has also been calculated²⁷⁾. The reduction potentials of both *cis* and *trans*-[PtCl₂(NH₃)₂] are $< -1.0 \text{ V}$ and therefore the complexes are extremely poor electron scavengers (compare $E^1_7 \text{ O}_2/\text{O}_2^- = -155 \text{ mV}$)²⁶⁾. Therefore, any mechanism involving electron acceptance from target radicals (such as DNA) must also be eliminated from consideration. These points also explain the semantic differences between a modifier or potentiator of radiation damage (by whatever mechanism) and a sensitizer (implying oxygen-mimetic or electron accepting mechanisms); although the literature is not always consistent on this point.

For platinum-amine complexes it is important to note that there is no correlation between chemotherapeutic activity and enhancement of radiation damage—particularly relevant is the fact that *trans*-[PtCl₂(NH₃)₂] is as effective a radiosensitizer as the *cis* isomer²⁸⁾. Considering the now well-defined differences in DNA-binding between the *cis* and *trans* isomers, the implication is that the lesions responsible for cytotoxicity are not necessarily identical to those involved in radiosensitization. The survival curves show that at 100 μM the *trans* isomer is as effective as 10 μM of the *cis*, with a Dose Modifying Factor of 1.3 to 1.4; the higher dose for the *trans* isomer is allowed because of the reduced toxicity. So, from purely in vitro considerations, the complexes are only moderately active. More recently, the results of low dose irradiation of both the *cis* and *trans* isomers indicate greatly increased enhancement ratios over those previously reported²⁹⁾. The *trans* isomer gave an ER of 1.5 at 75 μM (at a survival level of 0.8, See Fig. 1) while the *cis* complex gave an ER of 1.7 at 1 μM (also at a survival level of 0.8)³⁰⁾. These interesting results may indicate general utility for metal complexes in the critical low dose region.

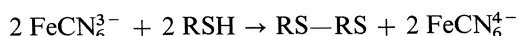
3.2 Radiosensitization by Thiol Depletion

The radioprotecting properties of thiols and amino-thiols have been known for some time and this is generally attributed to quenching of radiation-induced radicals such as O₂⁻. Compounds which remove endogenous thiols thus increase radical lifetime and can have sensitizing properties. This mechanism contributes to the action of, for instance, *N*-ethylmaleimide³¹⁾ and any thiol depletion by artificial means should indeed produce enhancement of sensitization³²⁾.

The great affinity of mercuric salts for thiols led to their examination as sensitizers³³⁾. In bacteria, phenylmercuric acetate (PMA), was found to sensitize under both aerobic and anaerobic conditions, the dose-modifying factor being twice as great

under nitrogen. Studies with *p*-hydroxymercuribenzoate (HMB) have also been reported and activity in various strains, including radioresistant ones, correlated with thiol binding. Treatment of bacteria with PMA or HMB after irradiation did not result in sensitization. A brief report on *p*-chlormercuribenzoate in mice claimed some sensitizing action.

The known use of ferricyanide as a thiol-labelling group also prompted its examination, and excellent sensitization in bacteria was found³⁴⁾ and attributed to the reaction:



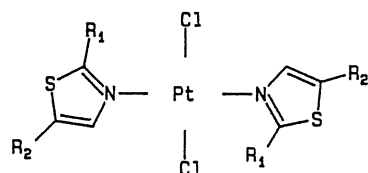
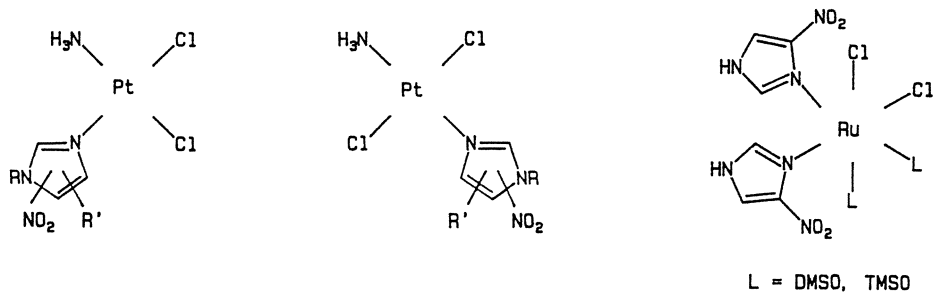
The number of possibilities for reaction of these species with radiation-induced radicals is large and the exact mechanism may be different to that suggested by the above reaction. In recent results the *in vitro* sensitizing action of rhodium carboxylates, $[\text{Rh}_2(\text{O}_2\text{CR})_4]$, has been attributed to their thiol-binding capacity³⁵⁾. The *in vitro* sensitizing efficiency of the carboxylates follows the order butyrate > propionate > acetate > methoxyacetate, which parallels the antitumor effect and is related to the intracellular uptake. The sensitization, except for the butyrate, is greater under hypoxic conditions. Unfortunately, essentially no sensitization was seen *in vivo*. The results are of interest because the mechanism of the antitumor effect of the rhodium carboxylates also involves thiol interactions³⁶⁾.

The points made earlier about lack of correlation between results in mammalian and bacterial systems is particularly relevant here and underlines the need for systematic comparison of metal complexes. The mechanism of action of the rhodium complexes in bacteria seems more likely to be due to radiation-induced products rather than thiol depletion³⁷⁾. Similarly an E.R. of only 1.1 was found for ferricyanide in the CHO mammalian cell line³⁸⁾.

3.3 Radiosensitization by Electron Affinity

3.3.1 Targeted Radiosensitizers

Consideration of DNA as the target of radiation damage by “oxygen mimics” prompts the question as to how potential drugs with both DNA-binding and radiosensitizing properties may be designed. The strong binding of platinum and ruthenium, in their complexes, to purines and pyrimidines suggested that the metal atom could carry the nitroimidazole to DNA, the purported site of action. A more efficient radiosensitizer could translate into lower clinical doses with concomitant reduction of toxic side-effects. The presence of potential donor atoms in nitroimidazoles and nitrothiazoles prompted the study of the modification of the properties of these molecules by metallation. The structures of some of the complexes of interest are given in Fig. 5.



$R_1 = \text{NO}_2, R_2 = \text{H}$ (2 - NT)

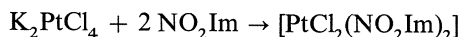
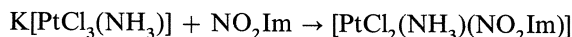
$R_1 = \text{NH}_2, R_2 = \text{NO}_2$ (ANT)

Fig. 5. Structures of some targeted radiosensitizers of platinum and ruthenium

i) Platinum-Nitroimidazole Complexes

Chemistry of Platinum-Radiosensitizer Complexes

The platinum complexes of interest may be made by standard reactions^{39,40,41,42)}

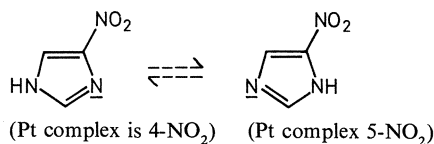


Analogous bis(imidazole) complexes have been prepared⁴³⁾. Initial studies with bis(nitroimidazole) complexes $[\text{PtCl}_2(\text{NO}_2\text{Im})_2]$ proved disappointing²³⁾ and currently the series of interest is the mono(nitroimidazole) series $[\text{PtCl}_2(\text{NH}_3)(\text{NO}_2\text{Im})]$. The chemistry and biology of these complexes have been reviewed recently⁴⁴⁾, and only the principal points will be summarized here.

The nitro group may substitute in the imidazole ring in any of three possible positions, 2-, 4- or 5- (see Fig. 3). The chemistry is quite different depending on the substitution position. The presence of the nitro group would indicate that the nitroimidazole is less reactive than imidazole due to the lower basicity of the coordinating nitrogen and the deactivating nature of the nitro group is also reflected in the slower reactions of 2 and 4-substituted ligands compared to the 5-substituted isomer. In parallel, 5-nitroimidazole complexes are also more stable with respect to dissociation than their 2-nitro counterparts. Chemical aspects of relevance to the biological activity of the nitroimidazole complexes include geometry of the complexes, possible formation of

linkage isomers, reduction potential and planarity or otherwise of the nitro group.

In principle, the effects of different modes of targeting i.e., DNA-binding, may be studied by synthesis of complexes with different geometry capable of either monodentate or bidentate lesions. A crystal structure of the complex $[\text{PtCl}_2(\text{NH}_3)(\text{Etanidazole})]$ confirms the initial *cis* configuration of the mono complexes⁴⁵. The free ligand 4(5)-nitroimidazole exists in tautomeric equilibrium:



The 4-tautomer predominates at room temperature⁴⁶ but we have found evidence for linkage isomers in both $[\text{PtCl}_2(\text{NH}_3)(\text{NO}_2\text{Im})]$ and $[\text{PtCl}_2(\text{NO}_2\text{Im})_2]$ ⁴⁷. One example of enhancement of radiosensitization of the platinated ligand in comparison to free ligand in the series *cis*- $[\text{PtCl}_2(\text{NH}_3)(\text{NO}_2\text{Im})]$ (See below) is in fact 4(5)-Nitroimidazole and thus an exact description of the structure of the complexes is essential. The 4-NO₂Im complex was structurally determined and other complexes assigned by spectroscopy.

Effect of Platinum on Nitro Group

One feature worth noting from the structural determinations so far carried out on Pt-nitroimidazole complexes is the planarity or otherwise of the NO₂ group with respect to the plane of the imidazole ring:

Nitro Group Out Of Plane	Nitro Group Coplanar
<i>trans</i> - $[\text{PtCl}_2(\text{Misonidazole})_2]$ {45.6°}	<i>cis/trans</i> - $[\text{PtCl}_2(\text{Metronidazole})_2]$
<i>cis</i> - $[\text{PtCl}_2(\text{Etanidazole})(\text{NH}_3)]$ {31°}	<i>cis</i> - $[\text{PtCl}_2(4\text{-NO}_2\text{Im})_2]$

The 2-nitroimidazole complexes have the NO₂ group bent out of the plane. Since 2- and 4-nitroimidazoles have the nitro group on the carbon adjacent to the binding nitrogen, one would expect similar chemistry but the structure of the 4-NO₂ complex shows the nitro group also coplanar with the imidazole ring. The reasons for this difference between 2- and 4-nitroimidazoles are not clear — steric effects should be the same. The concept of targeting implies electron transfer at some point to the nitro group — presumably this is facilitated if this group is planar, stabilizing the nitro-radical anion.

Metallation of nitroimidazoles causes an increase in reduction potential of the NO₂ group which, other factors being equal, should make for more effective sensitization, as observed for the free ligands⁴⁸. A correlation between the polarographic reduction potential and electron affinity has also been confirmed for free nitroimidazoles and thus the use of polarography as an initial indicator of electron affinity is valid⁴⁹. The increase in reduction potential upon platination is, in general, approximately 0.15–0.25 V. The variation of ligands should allow for fine tuning in any particular set of complexes. This is relevant because stability and steric considerations outlined above indicate that 5-NO₂-substituted complexes are most

suited as targeting complexes — they also have the most negative reduction potentials.

Biological Studies of Platinum-Nitroimidazole Complexes

DNA-Binding

Concurrent with initial evaluations of cytotoxicity and radiosensitization a relatively easy and semiquantitative assay, which examines complexes for their inhibition of restriction enzyme activity was developed to study DNA binding⁵⁰. In this assay inhibition of the activity of the restriction enzymes Bam HI (recognition sequence CCTAG/G) and Eco RI (recognition sequence CTTAA/G) on a linearized pSV2-gpt plamid DNA is examined. Binding of the metal complex at or near the restriction site inhibits DNA cleavage by the enzyme. Those compounds which inhibit are then further assessed by titration of the inhibition, giving the degree of inhibition with increasing concentration to compare relative binding by the complexes.

Within the series the order is misonidazole > metronidazole > etanidazole > 5-NO₂Im > 4-NO₂Im. Of the free ligands only 4(5)-NO₂-imidazole showed slight inhibition. The 5-NO₂Im complex inhibits more effectively than its 4-NO₂Im linkage isomer at equal concentrations. This is probably related to the fact that the axial interactions of the NO₂ group in *cis*-[PtCl₂(NH₃)(4-NO₂Im)] will slow down any substitution reaction involving association and thus what we are seeing is the fact that the less sterically hindered 5-NO₂Im complex reacts faster than the 4-NO₂Im species. Indeed, until we have quantitated the binding by measurement of DNA-bound Pt, the assay as used reflects kinetic effects in a series of complexes. In the present case the use of this assay parallels the incubation period (1 h.) of radiosensitization. The point here is that the position of the NO₂ group does affect the DNA-binding in closely related complexes. The bis complexes *cis*-[PtCl₂(metronidazole)₂] and *trans*-[PtCl₂(misonidazole)₂] do not inhibit at equal concentrations.

Radiosensitization

The results may be summarized⁵¹, as in Table 2.

- i) The complexes [PtCl₂(NH₃)(NO₂Im)] are uniformly better radiosensitizers than [PtCl₂(NO₂Im)₂], and bind to DNA better than their bis counterparts. For misonidazole, when normalized for mole of radiosensitizer ligand, the mono complexes are approximately as efficient as free ligand (1.25 and 1.3 at 100 μM respectively).
- ii) In the case of 5-NO₂Im, the complex is more effective than free ligand and is more effective both in radiosensitization and in DNA-binding than its 4-NO₂ linkage isomer.
- iii) The order of radiosensitizing ability for nitroimidazole complexes is misonidazole > 5-NO₂-Imidazole > metronidazole ~ 4-NO₂-Imidazole.
- iv) The radiosensitization is uniformly greater in hypoxia than in air.

Toxicity

The proposal of targeting a nitroimidazole to DNA for radiosensitization implies some form of “non-toxic” binding since we require the nitroimidazole to do the lethal

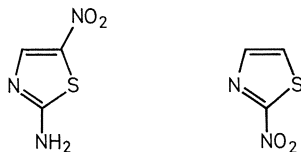
chemistry. However, for targeted compounds, increased DNA-binding (independent of any contribution from radiolytic or metabolic nitro group reduction) may result in inherent toxicity due to that binding. Some of the complexes, especially both isomers of $[\text{PtCl}_2(\text{NH}_3)(\text{Misonidazole})]$, are more toxic to hypoxic cells, unlike $[\text{PtCl}_2(\text{NH}_3)_2]$, and thus may have chemotherapeutic potential in their own right as hypoxic cytotoxins, particularly in conjunction with vasoactive agents which selectively increase tumor hypoxia⁵²⁾. An explanation for this behavior is that the Pt-DNA binding is responsible for the “normal” toxicity in air whereas reduction of the nitroimidazole in hypoxia results in increased toxicity. In this sense, the complexes are formally analogous to the nitroimidazole analogs such as RSU1069 which contain a DNA-alkylating moiety (aziridine ring) on the N-alkyl side-chain (Fig. 3)⁵³⁾. In principle, different toxicities should be expected for platinum complexes capable of monodentate, *cis*-bidentate or *trans*-bidentate lesions.

ii) Ruthenium-Nitroimidazole Complexes

The stability, and therefore integrity in solution, of metal-bound nitroimidazole will be a major factor in determining overall efficacy. The relative inertness of Ru complexes prompted the study of species based on the moderately antitumor active *cis*- $[\text{RuCl}_2(\text{DMSO})_4]$ ⁵⁴⁾. Both DMSO and TMSO(tetramethylene sulfoxide) have been used and the basic structure is of the form *cis,cis,cis*- $[\text{RuCl}_2(\text{L})_2(\text{NO}_2\text{Im})_2]$ (L = sulfoxide). The synthesis, structural characterization and radiosensitizing properties have been reported^{55,56)}. Interestingly, in some cases such as Etanidazole (SR 2508, Fig. 3) and N-Me4-NO₂Imidazole the NO₂ group acts as a chelate ligand using the ring nitrogen and an oxygen of the nitro group giving complexes of formula $[\text{RuCl}_2(\text{L})_2(\text{NO}_2\text{Im})]$. Some selected results are also summarized in Table 2. Of note is the fact that the Etanidazole complex is significantly more active than free ligand. The radiosensitization achieved in some cases is much more promising than the corresponding Pt complexes and, in contrast to those of Pt, the Ru complexes do not show much toxicity. The lesser toxicity of Ru complexes, previously observed in their survey as chemotherapeutic agents⁵⁷⁾, would therefore be advantageous in designing a “genuine” radiosensitizer while the properties of Pt complexes due to DNA-binding renders them of interest as hypoxic cytotoxins.

iii) Platinum-Nitrothiazoles

The rationale of targeting via metal complexes is applicable to other nitro-containing compounds with potential donor atoms besides the nitroimidazoles. An interesting example is that of thiazoles.



2-Amino-5-Nitro-Thiazole (ANT) 2-Nitrothiazole (2-NT)

Table 2. Chemical and biological data for some targeted metal radiosensitizer complexes

Complex	Enhancement ratio (Conc, uM)	Free ligand (at equivalent conc.)	Refs.
<i>cis</i> -[PtCl ₂ (NH ₃)(Miso)]	1.25 (100)	1.3	51)
<i>trans</i> -[PtCl ₂ (NH ₃)(Miso)]	1.25 (100)	1.3	
<i>cis</i> -[PtCl ₂ (NH ₃)(4-NO ₂ Im)]	1.08 (100)	1.1	44)
<i>cis</i> -[PtCl ₂ (NH ₃)(5-NO ₂ Im)]	1.16	1.1	
[RuCl ₂ (DMSO) ₂ (4-NO ₂ Im) ₂]	1.6 (200)	1.2	55)
[RuCl ₂ (DMSO) ₂ (N-Me-4-NO ₂ Im)]	1.3 (200)	1.2	56)
[RuCl ₂ (TMSO) ₂ (4-NO ₂ Im) ₂]	1.6 (200)	1.2	56)
[RuCl ₂ (TMSO) ₂ (Etanidazole)]	1.5 (200)	1.3	57)
<i>trans</i> -[PtCl ₂ (ANT-R) ₂]	1.6 (100)	1.4	61)
<i>trans</i> -[PtCl ₂ (ANT-A) ₂]	1.17 (100)	1.4	61)
<i>trans</i> -[PtCl ₂ (2-NT) ₂]	1.45 (25)	—	

ANT was originally chosen because it has radiosensitizing properties equivalent to misonidazole⁵⁸⁾ and, in addition, there are two donor sites — the ring nitrogen (ANT-R) and amine nitrogen (ANT-A). The sulfur atom is *not* a good donor atom in thiazoles⁵⁹⁾. Studies with palladium showed that linkage isomerism occurs — in MeOH the complex formed is *trans*-[PdCl₂(ANT-R)₂] whereas in aqueous solution the chelate produced by bidentate binding of both nitrogens [Pt(ANT)₂]Cl₂ is isolated⁶⁰⁾. Linkage isomers giving the *cis* and *trans* isomers of both [PtCl₂(ANT-R)₂] and [PtCl₂(ANT-A)₂] have been identified in the case of platinum⁶¹⁾. The different linkage isomers of *trans*-[PtCl₂(ANT)₂] (ring and amine-bound) show the interesting feature of different DNA-binding and radiosensitizing properties. The ring-bound form is the better DNA-binding form and also the better sensitizer. The R-form gives 10% inhibition of Bam HI at 300 uM compared to no inhibition by the A-form, under the same conditions as previously employed. In an extension of these studies we have found an E.R. of 1.45 at 25 μM for the complex *trans*-[PtCl₂(2-Nitrothiazole)₂], where the binding site is unequivocally the ring nitrogen⁶²⁾. The free 2-nitrothiazole ligand shows no radiosensitization and these results indicate that thiazoles are worthy of further investigation.

Comparison of Efficiency of Targeted Radiosensitizers

The original rationale for use of metal complexes of this type was that they may target the nitroimidazole to DNA. Of the complexes presented in Table 2, those of Ru and the Pt-nitrothiazole complexes show clear increase over the free ligands and give ER values comparable with many other purely organic compounds at these concentrations. Note that comparison with free ligand refers to administered dose rather than intracellular concentration. The Pt-nitroimidazole complexes do not show any greatly improved radiosensitization. There is no correlation between complexes of different structural types with respect to either DNA-binding or reduction potential of the nitro group (these data not included) but all are selective in hypoxia. The hypoxic toxicity of the platinum-nitroimidazole complexes renders them of interest as hypoxic toxins.

Some of the structural features referred to earlier may be quite important in dictating overall radiosensitizing efficiency. Because of the necessarily "fixed" nature of the nitro group in the complexes (nitro group bound to planar ligand, some rotation around Pt square-plane) the electron transfer may in fact be sterically hindered and inefficient, especially if the nitro group is not conjugated. The Pt complexes have lower reduction potentials than their corresponding Ru complexes (for example $E_{1/2}$ (pH 7 vs. S.C.E.) for *cis*-[PtCl₂(NH₃)(Etanidazole)] is -0.204 V and for [RuCl₂(TMSO)₂(Etanidazole)] is -0.345 V compared to the free ligand at -0.348 V. Until the structural features of Ru complexes are elucidated we cannot speculate on reasons for the differences. It is possible that a reductive group on the *periphery* of a molecule may be more efficient a sensitizer. A set of complexes has been reported where the metallation is through a secondary amine on the aliphatic side-chain, rather than the imidazole ring nitrogens, of the substituted nitroimidazole⁶³). This strategy to avoid the instability of the nitro-substituted ring gives active complexes but since the platinum is now some distance away from the nitro group it is not clear what, if any, electronic effects are involved.

3.3.2 Metal Complexes as Redox Centres

Radiosensitization by Metal Salts

The example of targeted radiosensitizers, by nature, contain a ligand with a nitro group, which is the electron-accepting group responsible for the biological activity. A funda-

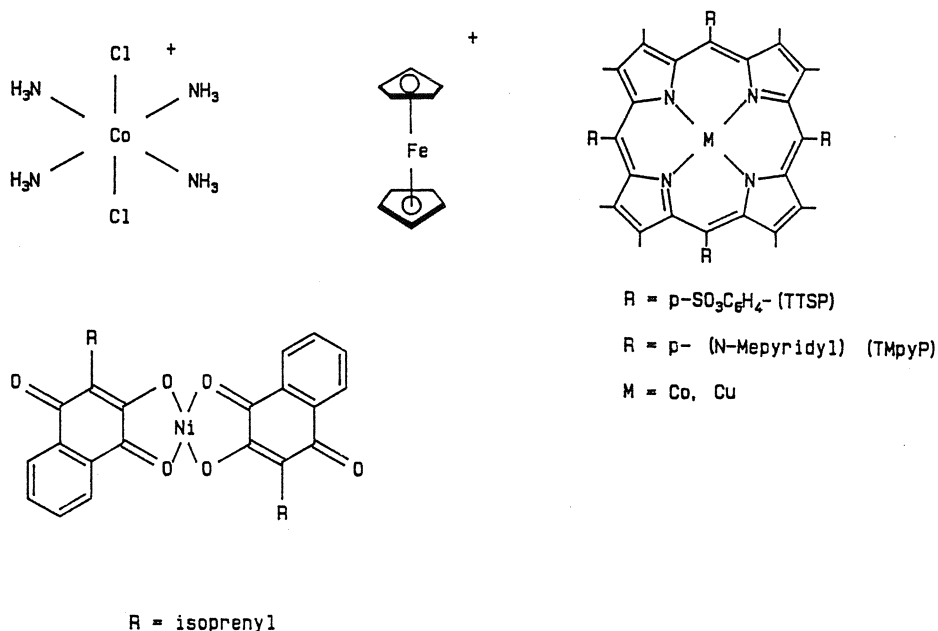


Fig. 6. Structures of some radiosensitizing metal complexes

mental aspect of metal complexes as hypoxia-selective agents is that complexes by themselves or associated with redox-active ligands other than nitroaromatics are capable of acting in biological redox reactions in the same manner as free nitroimidazoles, for example. A very wide variety of structural types is available for systematic mechanistic studies and the capacity for extension of the classic radiosensitizing mechanisms to bioinorganic chemistry would appear to be rich. An initial differentiation may be made between metal-centered and ligand-centered redox chemistry as well as between DNA-binding and compounds which do not bind to DNA. We may consider, in view of the nitroimidazole structure, that ligand-centered reductions on planar ligands would have good overlap with any damaged DNA site. This section discusses some selected examples and is intended to complement the earlier tabulations. Note that no strict comparisons between different complex types is allowable because of the differing conditions and concentrations, cell lines and parameters of activation employed by different workers. Figure 6 shows some of the complexes discussed and the variety of structures.

i) Cobalt-Amine and Porphyrin Complexes

The bacterial radiosensitization of the hexamminecobalt ion, $[\text{Co}(\text{NH}_3)_6]^{3+}$ and the pentammine complex has been reported⁶⁴⁾. These complexes are essentially inactive in the mammalian EMT6 cell line, again pointing out the difference in bacterial and mammalian systems. No selectivity is apparent for these complexes in hypoxic cells and some structure-activity relationships have been attempted for a wider series of cobalt complexes but the reproducibility and efficacy is in doubt. Abrams et al. have observed that all active complexes show a reduction potential of < 260 mV, which represents a cut-off point, there being no strict correspondence between reduction potential and OER⁶⁵⁾. The known binding to DNA of cobalt-amine complexes would certainly imply a DNA-binding role along with reduction. A clearer example at present is that of the metalloporphyrins, especially those of Co(III) which have been shown to sensitize⁶⁶⁾. Extensive studies on the binding of porphyrins and metalloporphyrins based on tetrakis-4-methylpyridylporphyrin have been made in recent years to DNA⁶⁷⁾. Copper and cobalt complexes of this and tetrakis-4-sulfonatophenylporphyrin radiosensitize *in vitro* and *in vivo*⁶⁸⁾. Investigation of the mechanism of action of this set of complexes should assess the contributions of reduction potential (electron transfer), peroxide activation, DNA-binding and correlation with Enhancement Ratio and strand breaks. Conceptually, a possible mechanism for metalloporphyrins is one identical to that of the targeted nitroimidazoles-DNA binding, followed by electron transfer from radiation-damaged DNA. As yet, the redox properties of DNA-bound metalloporphyrins have not been examined. A further possibility is that peroxide activation with hydroxyl radical production by a DNA-bound metalloporphyrin would very likely result in damage to the biomolecule. This concept is in essence similar to the proposed mechanism of action of the antitumor antibiotic bleomycin⁶⁹⁾, and further emphasizes the contention that a logical starting point for mechanistic studies of metal complexes as radiation sensitizers is extension and application of antitumor mechanisms.

ii) Ferricenium and Other Iron Complexes

The fact that the ferricenium ion (FeCp_2^+) is an effective radiosensitizer, $\text{DMF} = 2.0$ at $100 \mu\text{M}$, is of interest because of its good oxidizing power and stability ⁷⁰. The analogous Co complex is inactive. The metal-cyclopentadienyl system is relevant because of the antitumor activity of this series and recently the sensitization of $[\text{TiCl}_2\text{Cp}_2]$ has been studied ⁷¹. Another oxidizing iron complex is the nitroprusside salt, an effective sensitizer in V-79 cells ⁷². This effect was attributed to toxic ligand (CN^-) release but other factors such as oxidizing power, and possible chemistry of the NO group, should be considered.

iii) Copper Complexes

The possible radiosensitization by copper is of particular relevance because it is an essential trace element capable of functioning in many intracellular reactions. The radiosensitizing effects of copper salts in both bacterial ⁷³) and mammalian ⁷⁴) cells have been demonstrated. Hypoxic reduction to Cu(I), or the introduction directly of cuprous solutions in the oxygen-free medium resulted in enhanced sensitivity to radiation, a Dose Modifying Factor of 1.54 being obtained in the mammalian system. The interaction of the hydroxyl radical with Cu(II) to produce Cu(III) has also been suggested as a mechanism of sensitization ⁷⁵).

iv) 2-Hydroxy-1,4-naphthoquinone Chelates

The biological properties of $[\text{Ni}(\text{Lap})_2]$ (Lap = Lapachol, 2-hydroxy-3-isoprenyl-1,4-naphthoquinone, include both radiosensitization and chemosensitization. The reasons for choosing this complex to study was because independent results had indicated the complex could activate H_2O_2 — the complex, like many chelates including hemes, was found to be an active catalyst of luminol chemiluminescence in the presence of peroxide. The reaction between H_2O_2 and metal ions produces free radicals identical to those produced by ionizing radiation (See below). In view of the large body of data on activation of peroxide by metal complexes, a fascinating challenge is to adapt this chemistry to radiation sensitization. The nickel complex is a first step toward studying the feasibility of this proposition.

The biological properties of the complex are of considerable interest and may be summarized ⁷⁶).

- i) The complex is a moderately good radiosensitizer (ER 1.5 at $100 \mu\text{M}$), whereas the Cu and Zn analogs are not.
- ii) The Ni complex enhances DNA strand breaks in hypoxia, but does not appear to bind directly to the macromolecule. This property is similar to that of the electron-affinic compounds.
- iii) The complex is more toxic in hypoxic than in oxygenated cells and the complex produces breaks in hypoxia even in the absence of radiation.
- iv) Chemically, the $E_{1/2}$ of the Ni complex is -360 mV (pH 7.0, vs Ag/AgCl, pH 7.0), remarkably similar to the -385 mV of misonidazole, enhancing the similarities noted in the biological properties.

- v) Because of these similarities and the fact that, not only do electron-affinic compounds chemosensitize ⁷⁷⁾, but particularly that misonidazole enhances (chemosensitizes) the toxicity of cisplatin in hypoxia ⁷⁸⁾ the chemosensitization of the Ni complex and cisplatin was studied. There is a marked increase in the hypoxic toxicity of cisplatin in the presence of [Ni(Lapachol)₂] ⁷⁶⁾. The chemosensitization of cisplatin is a unique combinative effect of two metal species. The Ni complex may be considered as acting as an electron-affinic sensitizer; in comparison to misonidazole their biological properties are remarkably similar (if quantitatively different).

4 Metal Chemistry Relevant to Radiosensitization

This review has surveyed results on radiosensitization mostly obtained in tissue culture (in vitro). The bioinorganic chemistry of radiosensitization can be developed by extrapolation of known and relevant chemistry to an intracellular situation. This, of course, is easier to do in vitro, because efficacy in vivo will be dictated by a larger array of pharmacokinetic parameters. In this section brief examples of chemistry relevant to our mechanistic understanding of metal complexes as radiosensitizers is summarized. A further general point to make is that radiosensitization may be considered an oxidising process whereas radioprotection is reductive. The two processes are closely related and some small molecules which mimic SOD are also somewhat radioprotective in vivo ⁷⁹⁾. A further copper complex reported to have protecting properties is the complex with the 3-mercapto-2-hydroxypropyl ether of the polysaccharide dextran ⁸⁰⁾. This duality (complexes may either protect or sensitize depending on structure) makes metal systems particularly attractive for study.

The rationale of radiation sensitization by electron-affinic compounds involves the interaction of a compound on radical-damaged DNA. An alternative statement is that sequestering of e_{aq}^- can increase concentrations of the damaging $\cdot OH$ ⁸¹⁾. Suffice it to say that the reactions of metal cations with the hydrated electron are well characterised and, indeed, cover a wide range of rate constants depending on the electronic structure of the complex ⁸²⁾. Similarly, reactions with superoxide and peroxide are particularly well categorized. Metal ions and hydrogen peroxide produce free radicals similar to those from radiation and since H_2O_2 is a primary product of the radiolysis of water, (as well as being produced by secondary reactions in oxygenated water), metal complexes might activate the species thus essentially prolonging the lifetime of oxidizing radicals, in a manner analogous to the early suggestions of Adams that delocalized organics could prolong the lifetime of the aquated electron. The production of hydroxyl radical from H_2O_2 was shown not to result in sensitization ⁸³⁾, however, if peroxide or hydroxyl radical is produced randomly, the radicals will react in a non-specific manner, whereas localization near the target e.g., by metal complex binding, could enhance damage. Relevant to these observations is the well-documented strand cleavage of DNA by bleomycin ⁸⁴⁾ and the Cu-phenanthroline system ⁸⁵⁾. Note that both the porphyrin and naphthoquinone chelates discussed above may react with peroxide. The factors relating to the

chemistry of metal complexes with oxygen substrates which may induce a biological event (sensitization or protection) need to be investigated thoroughly.

Possibly the most direct example of relevance is the enhancement in strand breaks observed upon irradiation of frozen Cu^{2+} /DNA mixtures, a clear demonstration that activation chemistry can indeed occur⁸⁶⁾. The need for systematic study of metal complexes under identical conditions is emphasized by the fact that while ferricyanide, $[\text{Fe}(\text{CN})_6]^{3-}$, is a sensitizer of bacterial cells and a weak sensitizer in mammalian cells, (See Sect. 2.2) physico-chemical studies of hydroxyl damage on DNA showed that the reduced ferrocyanide salt, $[\text{Fe}(\text{CN})_6]^{4-}$, protected against strand breaks⁸⁷⁾. These examples further emphasize the duality of metal complexes—depending on structure complexes they may sensitize or protect.

The many modes of binding of metal complexes to DNA are now well understood—well defined examples of base binding, outer-sphere, and intercalation being well known. The more recent results on the reactions of complexes with DNA, especially the photo-sensitized cleavage of DNA by simple Co(III) complexes⁸⁸⁾, and also Cobalt-bleomycin⁸⁹⁾ may well be relevant to the actions of cobalt chelates as sensitizers. A point to note is that the DNA-binding ability needed to achieve a biological response is much higher than that needed to demonstrate reactivity in a purely chemical reaction. Although no “cut-off” point or correlation between DNA-binding in the test tube and biological activity is readily identified the constraints of cellular uptake, membrane transport and even interaction (deactivation) by other cellular components are factors which must be taken into account *in vivo*.

5 Summary

This review has intended to demonstrate the differing mechanistic pathways by which metal complexes may radiosensitize hypoxic cells. No exhaustive tabulation of data or survival curves has been attempted and, indeed, is almost impossible at the present time due to lack of uniformity in experimental conditions. The survey should hopefully convince that the area is a fruitful one for further systematic mechanistic studies as well as expanding on the range of complexes of possible clinical use in the treatment of cancer.

6 Acknowledgements

I wish to especially thank Dr. K. A. Skov, much of whose collaborative work is summarized here, for many helpful discussions. The collaboration of Dr. R. C. Richmond is also acknowledged. The work is supported through operating grants from MRC (Canada) and NIH.

7 References

1. Kennedy KA, Teicher BA, Rockwell SA, Sartorelli, AC (1980) *Biochem. Pharmacol.* 29: 1
2. Gray LH, Conger AD, Ebert M, Hornsey S, Scott OCA (1953) *Brit. J. Radiology* 26: 638
3. Thomlinson RH, Gray LH (1953) *Br. J. Cancer* 9: 539

4. Adams GE (1977) In: Becker F (ed) *Cancer, a comprehensive treatise* vol. 6 Plenum, New York
5. Farrell N (1989) In: James BR, Ugo R (eds) Chapter 8 *Transition metal complexes as drugs and chemotherapeutic agents (in Catalysis by metal complexes)* Reidel (In Press)
6. Skov KA (1987) *Radiat. Res.* 112: 217
7. von Sonntag C (1987) *The chemical basis of radiation biology.* Taylor and Francis, London
8. Kleinzeller A, Springer GF, Wittman HG (eds) (1978) *Effects of ionizing radiation on DNA physical, chemical and biological aspects (Molecular Biology Biochemistry and Biophysics vol. 27)* Springer-Verlag, Berlin Heidelberg New York
9. Chapman JD, Reuvers AP, Borsa J, Greenstock CL (1973) *Radiat. Res.* 56: 291
10. Elkind MM, Redpath JL In: Becker F (ed) *Cancer, a comprehensive treatise* vol. 6 Plenum, New York p 51
11. Leenhouts HP, Chadwick KH (1978) *Adv. Radiat. Biol.* 7: 56
12. von Sonntag C (1981) *Adv. Radiat. Biol.* 9: 109
13. Hall EJ (1978) *Radiobiology for the radiologist.* Harper and Row New York
14. Palcic B, Brosing JW, Lam GYK, Skasgard LD (1985) In: Le Cam LM, Olshen RA (eds) *Proceedings of the Berkeley conference in honor of Jerzy Neyman and Jack Kiefer Wadsworth*, p 331
15. Palcic B, Brosing JW, Skasgard LD (1982) *Br. J. Cancer* 46: 980
16. Sparrow AH, Underbrink AG, Sparrow RC (1967) *Radiat. Res.* 32: 915
17. Greenstock CL (1981) *J. Chem. Ed.* 58: 157
18. Nori D, Kim JH, Hilaris BS, Chu F (1984) *Cancer Investigation* 2(4): 321
19. Adams GE, Dewey DL (1963) *Biochem. Biophys. Res. Comm.* 12: 473
20. Adams GE (1970) In: Moroson H, Quintiliani ML (eds) *Radiation protection and sensitization*, Taylor and Francis, p 14
21. Moore A, Palcic B, Skasgard LD (1976) *Radiat. Res.* 67: 459
22. DeWit L (1987) *Int. J. Radiat. Oncol. Biol. Phys.*, 13: 403
23. Nias AHW (1985) *Int. J. Radiat. Biol.* 48: 297
24. Duple EB, Richmond RC (1980) In: Prestayko AW, Crooke ST, Carter SK (eds) *Cisplatin, Current Status and Clinical Developments* Academic, London, p 125
25. Duple EB, Richmond RC, O'Hara JA, Coughlin CT (1985) *Cancer Treat. Rev.* 12 (Supp. A)
25. Richmond RC, Simic MG (1978) *Br. J. Cancer* 37 (Supp. III): 20
27. Butler J, Hoey BM, Swallow AJ (1985) *Radiat. Res.* 102: 1
28. Duple EB, Richmond RC (1978) *Br. J. Cancer* 37 (Supp. III): 98
29. Skov KA, Korbelik M, Placic B (1988) *Int. J. Radiat. Biol.* In Press
30. Skov KA Personal Communication
31. Bridges BA (1960) *Nature (London)* 188: 415
32. Biaglow JE, Varnes ME, Clark EP, Epp ER (1983) *Radiat. Res.* 95: 437
33. Bridges BA (1974) *Adv. Radiat. Biol.* 3: 159
34. Moroson H, Tenney D (1968) *Experientia* 24: 1041
35. Chibber R, Stratford IJ, O'Neill P, Sheldon PW, Ahmed I, Lee B (1985) *Int. J. Radiat. Biol.* 48: 513
36. Howard RA, Spring TG, Bear JL (1976) *Cancer Res.* 36: 4402
37. Richmond RC, Farrell NP (1988) *Radiat. Res.* (Submitted)
38. Farrell N, Skov KA (Unpublished Results)
39. Farrell N, Gomes Carneiro TM, Einstein FWB, Jones TR, Skov KA (1984) *Inorg. Chim. Acta* 92: 61
40. Farrell N, Skov KA (1987) *J. Chem. Soc. Chem. Commun.* 1043
41. Bales JR, Coulson CJ, Gilmour DW, Mazid MA, Neidle S, Kuroda R, Peart BJ, Ramsden CA, Sadler PJ (1983) *J. Chem. Soc. Chem. Comm.* 432
42. Bales JR, Mazid MA, Sadler PJ, Aggarwal A, Kuroda R, Neidle S, Gilmour DW, Peart BJ, Ramsden CA (1985) *J. Chem. Soc. Dalton Trans.* 795
43. Reedijk J, van Kralingen CG (1978) *Inorg. Chim. Acta* 30: 171
44. Farrell N, Skov KA (1988) Manuscript in preparation
45. Farrell N, Rochon FD, Kong P-C, Skov KA *Inorg. Chem.* (Submitted)
46. Elguero J, Marzin C, Katritzky AR, Linda P (1976) *Adv. Heterocyclic Chem. Supp.* 1; Academic, New York, p 266
47. Farrell N, Fonseca E *Inorg. Chem.* (Submitted)

48. Adams GE, Flockhart IR, Smithen CE, Stratford IJ, Wardman P, Watts ME (1976) *Radiat. Res.* 67: 9
49. Greenstock CL, Ruddock GW, Neta P (1976) *Radiat. Res.* 66: 472
50. Skov KA, Adomat H, Konway DC, Farrell NP (1987) *Chem.-Biol. Interact.* 62: 117
51. Skov KA, Farrell NP, Adomat H (1987) *Radiat. Res.* 112: 273
52. Chaplin DJ, Acker B (1987) *Int. J. Radiat. Oncol. Biol. Phys.*
53. Adams GE, Ahmed I, Sheldon PW, Stratford IJ (1984) *Br. J. Cancer*, 49: 571
54. Mestroni G et al. (See Chapter This Symposium)
55. Chan PKL, Skov KA, James BR, Farrell NP (1986) *Int. J. Radiat. Biol.* 12: 1059
56. Chan PKL, Chan PKL, Frost DC, James BR, Skov KA (1988) *Can. J. Chem.* 66: 117
57. Clarke MJ (1980) *Metal Ions in Biol. Syst.* 11: 231
58. Rockwell S, Mroczkowski Z, Rupp D (1982) *Radiat. Res.* 90: 575
59. Matsui T, Nagano M (1974) *Chem. Pharm. Bull.* 22: 2123
60. Farrell N, Gomes-Carneiro TM (1987) *Inorg. Chim. Acta* 126: 137
61. Skov KA, Farrell NP (1987) *Inter. J. Radiat. Biol.* 52: 289
62. Farrell NP, Skov KA (Unpublished results)
63. Chibber R, Stratford IJ, Ahmed I, Robbins AB, Goodgame DML, Lee B (1984) *Int. J. Radiat. Oncol. Biol. Phys.* 10: 1213
64. Richmond RC, Simic M, Powers EL (1975) *Radiat. Res.* 63: 140
65. Teicher BA, Jacobs JL, Cathcart KNS, Abrams MJ, Vollano JF, Picker DH *Radiat. Res.* (In press)
66. O'Hara JA, Douple EB, Abrams MJ, Picker DH, Giandomenico CM, Vollano F (1988) *Int. J. Radiat. Oncol. Biol. Phys.* (In press)
67. Pasternak RE, Gibbs EJ, Villafrance JJ (1983) *Biochemistry* 22: 5409
68. Skov KA: Personal Communication
69. Stubbe J (1987) *Chem. Rev.* 87: 150
70. Joy AM, Goodgame DML, Stratford IJ (1988) *Int. J. Radiat. Oncol. Biol. Phys.* (Submitted)
71. Kopf-Maier P This Symposium
72. Douple EB, Green CJ, Simic MG (1980) *Int. J. Radiat. Oncol. Biol. Phys.* 6: 1545
73. Cramp WA (1965) *Nature (Lond.)*. 206: 636
74. Hesselwood IP, Cramp WA, McBrien DCH, Williamson P, Lott KAK (1978) *Br. J. Cancer* 37 (Supp. III): 95
75. Kirschner I, Citri N, Levitzki A, Anbar M (1970) *Int. J. Radiat. Biol.* 17: 81
76. Skov KA, Adomat H, Farrell NP (1987) In: Nicolini M (ed) *Platinum coordination compounds in cancer chemotherapy* Martinus-Nijhoff, p 733
77. Siemann DW (1984) *Int. J. Radiat. Oncol. Biol. Phys.* 10: 1585
78. Stratford IJ, Williamson C, Adams GE (1980) *Brit. J. Cancer* 41: 517
79. Sorensen JRJ (1984) *J. Med. Chem.* 27: 1749
80. Wieczorek Z et al. (1983) *Arch. Immunol. Ther. Exp.* 31: 715
81. Powers EL (1972) *Israel. J. Chem.* 10: 1199
82. Hart EJ, Abner M (1970) *The hydrated electron*, Wiley, New York p 170
83. Ward JF, Blakeley JW, Joner EI (1985) *Radiat. Res.* 103: 383
84. Sugiura Y, Takita T, Umezawa H (1986) *Metal Ions in Biol. Systems* 19: 81
85. Marshall LE, Graham DR, Reich KA, Sigman DS (1981) *Biochemistry* 20: 244
86. Cullis PM, McClymont JD, Bartlett MNO, Symons MRC (1987) *J. Chem. Soc. Chem. Comm.* 1859
87. Achey P, Duryea H (1974) *Int. J. Radiat. Biol.* 25: 595
88. Barton JK, Raphael A (1984) *J. Am. Chem. Soc.* 106: 2466
89. Chang CH, Meares CF (1984) *Biochemistry* 23: 2268

Radioruthenium-Labeled Compounds for Diagnostic Tumor Imaging

Suresh C. Srivastava¹, Leonard F. Mausner¹, and Michael J. Clarke²

¹ Medical Department Brookhaven National Laboratory Upton, NY 11973/USA

² Department of Chemistry Boston College Chestnut Hill, MA 02167/USA

Among the various radionuclides of ruthenium, ⁹⁷Ru and ¹⁰³Ru have proven to be quite attractive for *in vitro* and *in vivo* research investigations. Ruthenium-97, in particular, has excellent nuclear decay characteristics ($t_{1/2}$ 69.6 h; decay mode by electron capture; 216 keV gamma, 86%; no betas) and thus is a promising radionuclide for diagnostic imaging applications. Compared to other commonly used intermediate half-life nuclides (e.g., ⁶⁷Ga, ¹¹¹In), ⁹⁷Ru provides marked improvement in image quality and imparts significantly less radiation dose to the patient. No-carrier-added ⁹⁷Ru is routinely prepared at the Brookhaven Linac Isotope Producer (BLIP) from proton spallation of high-purity rhodium, using the ¹⁰³Rh (p, 2p5n) ⁹⁷Ru reaction. Ruthenium-103 (available commercially as a fission product), although not particularly appropriate for imaging, has nonetheless proven useful for chemical, *in vitro*, and preclinical studies.

Extensive chemical and *in vivo* investigations of a number of radioruthenium-labeled compounds, for example, DTPA (diethylenetriamine pentaacetic acid), EDTMP (ethylenediamine tetramethylene phosphonate), DMSA (dimercaptosuccinic acid), transferrin, bleomycin, monoclonal antibodies, and DISIDA (diisopropyl phenylcarbamoylmethyl iminodiacetic acid) have given promising results that warrant clinical evaluation. For many applications requiring imaging over an extended period, ⁹⁷Ru agents are superior or unique (e.g., DTPA for cisternography, phosphonates for bone imaging, DMSA for kidney studies, and DISIDA for hepatobiliary function studies). Preliminary clinical trials with ⁹⁷Ru DISIDA for the diagnosis of hepatobiliary disorders (biliary atresia, acute cholecystitis, etc.) have been carried out. For tumor imaging, ⁹⁷Ru-transferrin appears quite promising and in animals has produced results that are superior to those obtained with the commonly used ⁶⁷Ga citrate. Antitumor monoclonal antibodies labeled with ⁹⁷Ru may provide additional effective agents for the radioimmunoscinographic detection of tumors.

1 Introduction	113
2 Radionuclides of Ruthenium	113
2.1 General Features	113
2.2 Production of ⁹⁷ Ru: Methods and Radiochemical Separation	114
2.3 Radiation Dosimetry	118
3 Radiochemistry of Ruthenium	118
4 Biological Studies for Health Effects	119
5 Chemistry Relevant to Radiopharmaceutical Design	121

6 Labeled Compounds and Radiopharmaceuticals	124
6.1 General Features	124
6.2 Simple Salts and Inorganic Compounds	126
6.2.1 Ruthenium Chloride	126
6.2.2 Ruthenium Red and Other Ruthenium Ammine Complexes	128
6.3 Phosphonate Complexes	130
6.4 Chelates with Organic Ligands	131
6.4.1 Hydrophilic Chelates	132
6.4.2 Lipophilic Chelates	134
6.5 Colloidal Preparations	138
6.6 Organometallic Derivatives	139
6.7 Tumor-Localizing Agents	140
7 Conclusion	145
8 Acknowledgements	146
9 References	146

1 Introduction

Diagnostic imaging procedures in nuclear medicine are based primarily on the radio-tracer principle. Radiolabeled compounds (radiopharmaceuticals) try to trace a particular physiological process by behaving in a way that is indistinguishable from a natural physiological substance in the body, and provide functional information in an anatomical framework. One can trace quantity (for example, thyroid uptake), volume (as in blood volume), rate (as in a renogram), or the nature of a biological process (as in measurements of physiology). The versatility of nuclear medicine is actually enhanced by the fact that it is possible to develop a variety of radiolabeled compounds for particular applications. Imaging can provide information on the active biological transport of a radiopharmaceutical and its selective localization in an organ system with reference to time. However, to visualize a small region of interest within a short time interval, administration of rather large amounts of radioactivity is required in order to generate statistically significant images. Short-lived gamma emitters whose physical and biological half-lives are matched with the time of the study are best suited for use with current imaging instrumentation.

Because of its 6-h half-life, optimum imaging properties, and easy availability from a generator, technetium-99m is at present the most widely used radionuclide for clinical imaging studies^{1,2}. Many applications, however, require longer half-life isotopes to allow for delayed imaging (1–7 days after injection), and to allow for slow *in vivo* pharmacokinetics (uptake and/or clearance) of the administered radiopharmaceutical. In addition, it is often necessary to use exploitable chemical differences among the isotopes for particular radiopharmaceutical syntheses. Ruthenium radionuclides (in particular, ⁹⁷Ru) offer many of the above advantages; and, indeed, a number of experimental radiopharmaceuticals based on ⁹⁷Ru have been prepared and studied over the last 10 years. This review attempts to summarize and highlight the various developments and to address the synthesis and applications of radioruthenium-labeled compounds for a number of diagnostic imaging procedures.

2 Radionuclides of Ruthenium

2.1 General Features

The radionuclides of ruthenium which are potentially useful as tracers are listed in Table 1. This list does not include radionuclides with half-lives less than 5 minutes. The most important properties for nuclear medicine imaging are the half-life, and the energy and abundance of emitted gamma rays. Gamma ray energies of 100–300 keV are detected with high efficiency using instrumentation available to most nuclear medicine departments. From the decay properties summarized in Table 1³) it is clear that ⁹⁷Ru is the most suitable radionuclide for *in vivo* scanning. This was first suggested by Subramanian and McAfee⁴) in 1970. The complete list of emissions from ⁹⁷Ru is given in Table 2⁵). Although ⁹⁷Ru is the radionuclide of choice for nuclear medicine imaging, chemical and *in vitro* studies can often be more conveniently carried out using the longer-lived ¹⁰³Ru. Ruthenium-103 is commercially

Table 1. Decay data for ruthenium radionuclides^a

Radionuclide	Half-Life	Principal Decay Mode (% Branching)	Main γ -Rays		Suitability for in vivo Abundance Imaging
			Ev (keV)	Abundance (%)	
⁹⁴ Ru	51.8 min	EC (100) ^b	367 892	79.2 21.0	Poor
⁹⁵ Ru	1.65 h	EC (85) β^+ (15)	336 627	71.1 18.1	Poor May be useful for PET
⁹⁷ Ru	2.88 d	EC (100)	216 324	86.1 10.3	Excellent
¹⁰³ Ru	39.35 d	β^- (100)	497 610	86.4 5.4	Fair
¹⁰⁶ Ru	368 d	β^- (100)	No gammas		None

^a Data from Ref. [3]^b EC = electron capture**Table 2.** Emissions of ⁹⁷Ru^a

Radiation Type	Energy (keV)	Intensity %
Auger-L	2.17	97
Auger-K	15.5	20
Int. conv. electron-K	194.6	2.83
Int. conv. electron-L	212.6	0.340
Int. conv. electron-K	303.4	0.185
L x-ray	2.42	4.6
K _{α2} x-ray	18.25	20.0
K _{α1} x-ray	18.37	38.3
K _β x-ray	20.6	11.5
γ	108.80	0.108
γ	215.68	85.50
γ	324.48	10.86
γ	460.55	0.117
γ	569.27	0.872
14 γ 's	108–855	<0.1

^a Data from Ref. [5]

available from Oak Ridge National Laboratory and from other sources. It is produced by fission of uranium and separated from the fission product mixture by distillation.

2.2 Production of ⁹⁷Ru: Methods and Radiochemical Separation

Different nuclear reactions have been studied for the preparation of ⁹⁷Ru. These methods are summarized in Table 3. The earliest study⁴⁾ used the ⁹⁶Ru(n, γ)⁹⁷Ru reaction at a reactor. This route is simple in that no chemical separation is necessary, but it requires a target of enriched ⁹⁶Ru (natural abundance is only 5.5%) and

Table 3. Nuclear reactions for ^{97}Ru production

Reaction	Incident Particle Energy (MeV)	Ref.
$^{96}\text{Ru} (n, \gamma)$	thermal	4
$^{99}\text{Tc} (p, 3n)$	37	6
$^{\text{nat}}\text{Mo} (^3\text{He}, xn)$	30	8
	36	9
$^{\text{nat}}\text{Mo} (\alpha, xn)$	22.1	8
	28	9
	30	10
	29	11
$^{103}\text{Rh} (p, 2p5n)$	193	13
(p, α 3n)	67.5	16
(p, pd 4n) etc.		

provides only low specific activity. This means that radioactive atoms of ^{97}Ru are diluted with the stable atoms of the target material. This in turn requires large amounts of ligand to fully bind ruthenium during radiopharmaceutical preparation. Thus charged particle irradiations of different elements have been utilized to produce "no carrier added" ruthenium-97.

The first such reaction studied was $^{99}\text{Tc}(p, 3n)^{97}\text{Ru}$, reported by Lebowitz et al. ⁶⁾ in 1974. Unpublished data from this group at Brookhaven National Laboratory provide more detail on this process. The target was 983 mg/cm² of ^{99}Tc metal powder ($t_{1/2} = 2 \cdot 14 \times 10^5$ years) poured into an aluminium well and covered with a 0.025 cm aluminium window. The incident beam energy was 37 MeV and a thick target yield of 5.3 mCi/ μ Ah was determined. The cross section was measured to be 527 ± 16 mb. Technetium-95 and ^{96}Tc were found in the target solution and a cross section of $0.39 \pm .04$ mb was measured for ^{96}Tc production at 37 MeV. No ^{95}Ru or ^{96}Ru were detected. The chemical separation involved dissolution of the Tc powder target in 5% NaOCl followed by coprecipitation of ^{97}Ru with $\text{Fe}(\text{OH})_3$. The TcO_4^- species does not coprecipitate under these conditions. The precipitate was dissolved in HNO_3 and reprecipitated with NaOH. Ruthenium was leached from the $\text{Fe}(\text{OH})_3$ with 5% NaOCl and extracted from a pH 4 solution of HCl into CCl_4 . Overall ruthenium recovery was about 70%. The advantages of this route are high yield and high radiopurity. However, the difficulty and expense of preparing a large radioactive target has prevented the widespread use of this reaction.

The cyclotron production with ^3He or α particle irradiation of natural molybdenum targets, via the $\text{Mo}(^3\text{He}, xn)$ and the $\text{Mo}(\alpha, xn)$ reactions, has been reported by several authors ⁷⁻¹²⁾. Various approaches to the radiochemical separation of pure ruthenium from irradiated Mo have been studied. These have included solvent extraction of RuO_4 into CCl_4 ^{8,9)} or into pyridine ¹⁰⁾, dry distillation of RuO_4 ¹⁰⁾, wet distillation of RuO_4 ^{9,11)}, and ion exchange in nitric acid with a tin dioxide column followed by an anion exchange column ¹²⁾. All the methods gave good radiochemical yields (>80%) and high decontamination factors from Tc and Mo radioactivity present in the irradiated targets. For routine, remote production, however, the wet distillation was recommended by Comparetto et al. ⁹⁾, while ion exchange was preferred by Pao et al. ¹²⁾.

For both ^3He and α reactions, ^{94}Ru and ^{95}Ru are produced at all bombarding energies studied, necessitating a decay period (typically 24 h) before chemical processing begins. The cumulative thick target yields for $^{94,95,97}\text{Ru}$, calculated from measured cross sections, are nearly identical from the ^3He and α -induced reactions. However, longer-lived ^{103}Ru is unfortunately produced in the α bombardments from the $^{100}\text{Mo}(\alpha, n)$ reaction. The level of ^{103}Ru impurity was found to be 0.2% of ^{97}Ru at end of bombardment⁹⁾. The highest reported ^{97}Ru yield was 80 $\mu\text{Ci}/\mu\text{Ah}$ with 36 MeV ^3He particles on a 0.5 mm-thick Mo foil⁹⁾. This is comparatively low.

In 1978, Ku et al.¹³⁾ reported a high yield ^{97}Ru production method using proton spallation at 200 MeV on metallic Rh targets. A subsequent paper by Srivastava et al.¹⁴⁾ provides more detail on the chemical separation involved. To date this method constitutes the most useful procedure for the production of high specific activity ^{97}Ru . Indeed, most of the radiopharmaceutical syntheses described later in this chapter have utilized this source.

The method involves bombarding high purity rhodium foil with 193 MeV protons at the Brookhaven Linac Isotope Producer (BLIP). The foil, 0.025 cm-thick and measuring 2.5×2.5 cm in area, is clipped onto a stainless steel backing plate for insertion into a BLIP target holder. Production irradiations generally occur over a weekend. After bombardment, the target is transferred to a processing hot cell and dissolved by a.c. electrolysis in a small dissolving cell made of teflon with graphite electrical contacts. Current densities of 0.3 A/cm² for about 15 h are used with 6 N HCl as the electrolyte. This target solution contains $^{102,101m,101}\text{Rh}$, $^{101,100}\text{Pd}$, $^{95,96}\text{Tc}$ as well as ^{97}Ru . This solution is sucked by vacuum into a flask where it is evaporated to near dryness to remove the HCl. After adding 3 ml of water, the solution is transferred by pressure to a distillation flask. To this flask is added 3 ml of 12 N H₂SO₄ and 3 ml of KMnO₄ as the oxidizing mixture. Ruthenium-97 is then distilled as RuO₄ and the distillate is collected in a vessel containing 5 ml 1:1 HCl:EtOH to give a solution of ruthenium(III) chloride. The ^{97}Ru chemical yield averages 91% with added carrier ruthenium (>1 μg) and about 83% without carrier added. Since even high purity Rh foil contains some Ru impurity (we have measured by atomic absorption up to 20 ppm in some cases), addition of carrier may not be necessary. Technetium-96, a side product, is potentially useful as a longer-lived ($t_{1/2} = 4.35$ d) stand-in for ^{99m}Tc ($t_{1/2} = 6$ h) and can also be recovered. To do this, the rhodium sulfate residue is transferred to a separatory funnel and 11 N NaOH added to make the solution basic. Methyl ethyl ketone is added and the phases mixed by bubbling air. Technetium (present as pertechnetate) extracts nearly quantitatively (97%) into the organic phase which is then evaporated to dryness and the radioactivity recovered in saline. The apparatus to remotely perform these separations is shown schematically in Fig. 1.

The typical production rate (radioactivity/integrated current) with a $2.54 \times 2.54 \times 0.25$ cm rhodium foil is 33 $\mu\text{Ci}/\mu\text{Ah}$. This is not the true nuclear yield achievable because the beam strike area is considerably larger than the target area. This is necessary at BLIP to reduce the power density deposited in downstream salt targets and prevent their melting. The small area Rh target is, however, sufficient to produce clinically useful quantities. After correcting for the fraction of the beam hitting the Rh target, a production rate of 278 $\mu\text{Ci}/\mu\text{Ah}$ is obtained. This yield is achieved with a relatively thin target which degrades the proton energy only

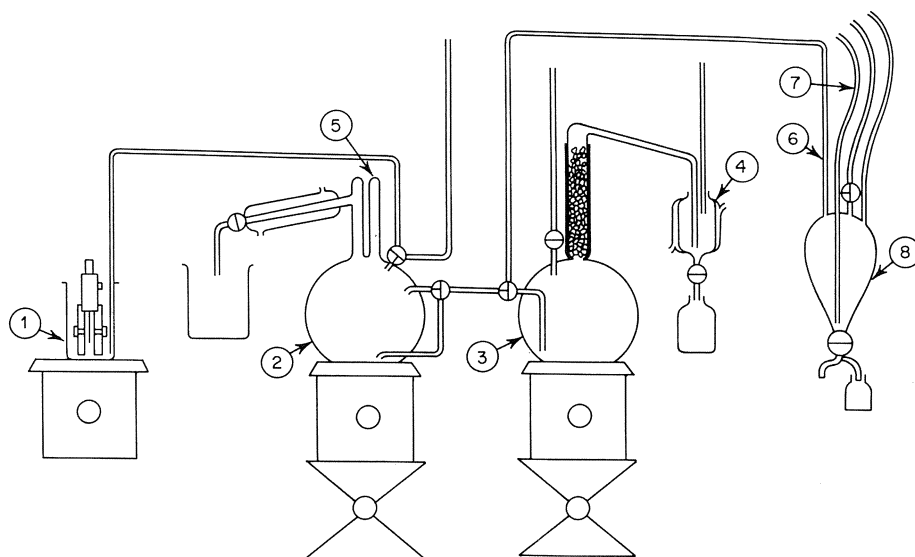


Fig. 1. Processing apparatus for ^{97}Ru and ^{96}Tc from a rhodium target. (1) AC electrolysis cell; (2) HCl distillation flask; (3) Ru distillation flask; (4) ice water cooled Ru collection vessel; (5) Thermocouple well; (6) ^{96}Tc transfer line; (7) air bubbler; (8) ^{96}Tc extraction vessel

0.86 MeV et 193 MeV incident. In contrast, the 0.05 cm Mo foil target used by Comparotto⁹⁾ is thick enough to stop the 36 MeV ^3He beam used in that work. Cross section calculations performed with the ALICE code¹⁵⁾ predict a slow increase in cross section with decreasing energy at 200 MeV. Thus, a thicker target could make proportionally more ^{97}Ru , several curies per run, if necessary.

In 1983, Lagunas-Solar et al.¹⁶⁾ realized that there are eleven proton-induced reactions on ^{103}Rh that lead to ^{97}Ru in addition to the $^{103}\text{Rh}(p, 2p5n)^{97}\text{Ru}$ reaction which is likely to predominate at 200 MeV. These have energetic thresholds ranging from 20.6 MeV to 60.1 MeV. This group measured thick target yields, and total cross sections for ^{97}Ru in the 67 to 37 MeV proton energy range. The cross section peaked at 52 MeV with a value of 56 mb. A 0.305 cm-thick Rh foil, sufficiently thick to degrade the incident 67.5 MeV protons to 43 MeV, gave a yield of 1.3 mCi/ μAh at EOB. Indeed, calculations with ALICE covering the entire energy range of 40–200 MeV show a double-humped excitation function¹⁷⁾, with the maxima occurring at 100 MeV. Although the theoretical cross sections are significantly higher than measured ($\sigma = 99$ mb at 50 MeV), the shape of the excitation function is compatible with both the BNL and Lagunas-Solar data. This work shows that good yield of ^{97}Ru can be obtained at low proton energy.

One to two hundred mCi batches of ^{97}Ru have routinely been produced and processed using the BLIP facility. Charged particle accelerators for radionuclide production are presently available in many other places and thus sufficient quantities of ^{97}Ru can in principle be made available for future clinical use.

2.3 Radiation Dosimetry

Studies on radiation dosimetry from administered rutheruim have not been carried out in a systematic fashion. Since ^{97}Ru is the optimum ruthenium nuclide for diagnostic imaging, a careful assessment of its in vivo dosimetry is essential for human applications.

In general, the radiation dose from ^{97}Ru is quite favorable compared to other routinely used intermediate half-life radionuclides. On a per millicurie basis, for example, ^{97}Ru delivers approximately half the absorbed dose to tissues than indium-111. Ruthenium-97 emits primarily one 216 keV photon (86%) whereas ^{111}In emits two gamma rays of 173 and 247 keV with a respective abundance of 89.6 and 94%. Indium-111 also emits more internal conversion electrons that are associated with the higher gamma emissions. When both ^{111}In photons are included for imaging, the dose advantage from ^{97}Ru (per imaging photon) is lost. However, the image quality of ^{111}In in this case is poor since scattering of the 247-keV photon into the 173-keV photopeak considerably degrades the resolution. When imaging with a single energy photon, ^{97}Ru has a clear advantage over indium-111.

In terms of the cellular dose (or microdose), ^{111}In and ^{97}Ru produce comparable effects¹⁸⁾ based again on usable imaging photons. On a purely nominal radioactivity scale, however, the dose from ^{97}Ru is about half that from indium-111. This is due to differences in the high-LET (linear energy transfer) low-energy emissions that are responsible for greater localized doses. Table 4 shows theoretical absorbed radiation dose estimates from these emissions (Auger and conversion electrons, and x rays) for ^{97}Ru , ^{111}In , and iodine-125.

Estimation of radiation dose has been attempted for a number of experimental ^{97}Ru radiopharmaceuticals. These studies will be discussed in a later section along with the description of the individual radiolabeled compounds.

3 Radiochemistry of Ruthenium

The radiochemistry of ruthenium is quite complicated and not totally understood. Many ruthenium radionuclides are byproducts of uranium fission, constituting about 6 per cent of the total activity. Their isolation from solutions left after the treatment of nuclear fuel elements has been an important problem. Considerable difficulties arise because of the variable oxidation states of ruthenium that result in the production of many different compounds with undefined structure and composition.

Table 4. Absorbed radiation dose, rad/ $\mu\text{Ci-h}$

Nuclide	Auger, conversion electrons & x-rays	Auger and conversion electrons
Indium-111	0.1102	0.0682
Ruthenium-97	0.0539	0.0259
Iodine-125	0.1140	0.0294

The dissolution of uranium rods in nitric acid produces the volatile RuO_4 which is partly carried away with gaseous reaction products. However, the majority of the RuO_4 gets reduced by the nitrogen oxides to produce Ru(II) and Ru(III) nitrosyl compounds, predominantly nitrosylruthenium trinitrate, and the sodium and potassium salts of the $[\text{RuNO}(\text{NO}_2)_4\text{OH}]^{2-}$ anion¹⁹⁾. Development of primary processes for separating ruthenium from uranium and plutonium has encountered many difficulties not just because of the chemical similarities of the three elements, but because the behavior of fission product ruthenium varies considerably due to slow changes between a variety of chemical structures. The chemistry is nonetheless dominated by compounds of the trivalent nitrosylruthenium, (RuNO) (III), whose derivatives display the characteristics of six-coordinate octahedral complexes with d_2sp^3 orbitals (similar to, for example, Co(III) or Pt(IV)). Binuclear oxygen-bridged compounds frequently predominate owing to the hydrolysis of the weak nitrate complexes. When the mixtures are heated with strong oxidizing agents in acid solution (KIO_4 , Ce(IV), KMnO_4 , osmate, bismuthate, etc.), the nitrosyl and other compounds of ruthenium are slowly oxidized to RuO_4 which can then be separated by dry or wet distillation. Collection of RuO_4 in ethanol/HCl produces Ru(III) chloro complexes¹⁴⁾. In this state, it reacts with a number of complexing agents although the kinetics of these reactions are slow due to the inertness of the d^5 Ru(III) ion. Small quantities of Ru(IV) when present can be readily reduced to Ru(III) using refluxing ethanol solutions²⁰⁾. Ruthenium(III) can be reduced to the more kinetically labile Ru(II) using stannous salts and other reducing agents although a careful control of reaction conditions is required to minimize the production of elemental ruthenium. Many Ru(II) coordination compounds get reoxidized to the more stable Ru(III) species, except in the case of ligands that preferentially stabilize the lower oxidation state itself⁵⁷⁾.

4 Biological Studies for Health Effects

A number of ruthenium compounds including the chloro complexes are biologically relevant since trace quantities of fission product ruthenium (whose complete removal from effluents using conventional methods such as precipitation, ion exchange, microbiological treatment, etc. is impossible) find their way into sea water and in the digestive system of mammalian species. Numerous investigations have been undertaken in order to understand and define the behavior of ruthenium in mammals, fish, plants, and algae²¹⁻⁴⁷⁾. The ruthenium compounds used in many of these studies have, however, not been properly characterized and often a mixture of the various species was administered into the animals. In general, ruthenium was found to be absorbed within a few hours following ingestion predominantly through the small intestine^{26, 28, 31-33)}. It is also reported that prior mixing of ruthenium with food led to a non-adsorbable form and resulted in prompt excretion of a major fraction of the administered material³⁸⁾. Absorption of the nitrosylruthenium species was higher (13% of ingested amount) compared to that of the trichloro compound ($\approx 3\%$)²⁸⁾. When ruthenium is administered intravenously or following its absorption into the blood, it distributes throughout the body and is only very slowly excreted^{23, 35)}. A substantial fraction ($\approx 80\%$) is excreted into the urine within 6-10 days; the remainder,

however, remains in the body for a much longer period ($t_{1/2} = 4-8$ weeks)^{26,32}. The excretion of ruthenium takes place both through the kidneys and the liver and these organs thus accumulate significantly higher concentrations^{23,31-34}.

Ruthenium in blood has been shown to predominantly bind to plasma proteins^{23,32} in particular to transferrin⁴⁸. Use of chelating agents during the initial few days helps in the removal and excretion of the metal; however, this treatment is not effective once the ruthenium is allowed to remain in the blood for longer periods since it becomes more firmly bound²³. Depending upon the dose administered, bony structures and muscle also accumulate substantial amounts^{14,32,34}. When the ruthenium is hydrolyzed before injection or when colloidal forms are introduced, its uptake is primarily into the reticuloendothelial system (liver, spleen, bone marrow)³⁴.

Significant toxic effects were reported in rats when higher doses of ruthenium chloride were injected. Most notable was the toxicity to the liver, which was explained by the inhibition of mitochondrial respiration resulting from the loss of electron transport and many other energy-linked functions^{36,37}. The concentration of ruthenium builds up slowly in the liver cell nuclei but eventually reaches higher values than in the cytosol. Binding to macromolecules within the nucleus results in a considerable slowing down of the outward diffusion across the membrane²². Toxic effects were minimal when only trace concentrations of ruthenium were administered³⁷.

Studies have also been reported on the biological effects of ruthenium red $[(\text{NH}_3)_5\text{Ru}-\text{O}-(\text{NH}_3)_4\text{Ru}-\text{O}-\text{Ru}(\text{NH}_3)_5]^{6+}$ ³⁸ which has long been used as a cytological stain for microscopic investigations^{39,57}. It binds selectively to mucopolysaccharides in tissue^{39,46} and produces a precipitate by forming ion pairs with sulfate or carboxylate groups and hydrogen bonding to sugar hydroxyl groups via the ammine portions. The dye selectively stains tissue mitochondria and this binding results in the inhibition of the mitochondrial calcium uptake⁴⁰⁻⁴¹. Higher concentrations (10-50 nanomol per mg mitochondria) produce inhibition of mitochondrial respiration as well as the blockage of calcium binding and transport³⁷. However, since commercial ruthenium red is frequently no more than 70% pure, it is likely that the ammine portions. The dye selectively stains tissue mitochondria and this binding lower molecular weight ruthenium contaminant⁴². Following in vivo administration, appreciable concentration of ruthenium red has been reported in tissues rich in mucopolysaccharides and mucoproteins, e.g., bone, stomach, and ovary^{43,44}. Since mucopolysaccharides are found in abundance around certain tumors, ruthenium red was also investigated for its ability to accumulate into tumors⁴⁴⁻⁴⁶. In another study, no specific affinity for tumor was observed, perhaps because of the tumor model employed⁴³.

The potential hazards to humans from the ingestion of ¹⁰³Ru and ¹⁰⁶Ru products in nuclear waste have prompted many of these earlier biological investigations. Even though these studies are not directly applicable to nuclear medicine, they have nonetheless provided a basis for further biodistribution studies using ruthenium-based radiopharmaceuticals.

5 Chemistry Relevant to Radiopharmaceutical Design

Excellent monographs^{20, 49)} and reviews^{18, 50–59)} have appeared that deal with various aspects of the chemistry of ruthenium, particularly those that are useful and relevant to the design and development of ruthenium-labeled compounds for imaging applications. Particularly useful are prior reviews^{57–59)} which include a thorough discussion of the chemistry and biochemistry of ruthenium with special emphasis on the relevance to the design of anticancer agents and other biologically active compounds for various applications.

Ruthenium displays up to ten different oxidation states (–2 to +8) in its compounds, although the ones that predominate in aqueous solution are Ru(II), Ru(III), Ru(IV), and Ru(VIII). The most common compounds are those of Ru(III), and in general most chemical syntheses start with $\text{RuCl}_3 \cdot 3 \text{H}_2\text{O}$. Although in solution this consists of a mixture of Ru(III) and Ru(IV) chlorides, essentially complete conversion to Ru(III) can be effected by refluxing in ethanol²⁰⁾. The many possible reactions of $\text{RuCl}_3 \cdot x\text{H}_2\text{O}$ are shown in Fig. 2²⁰⁾. It is readily obvious that a variety of syntheses can be achieved starting with this compound. Of particular note are the ammine compounds of both Ru(II) and Ru(III). These compounds are easily prepared in a well-defined chemical form and indeed complexes such as $[(\text{NH}_3)_6\text{Ru}]\text{Cl}_3$ have been utilized as starting materials. A number of pathways for the preparation of ruthenium ammine compounds are shown in Fig. 3⁶⁰⁾.

The complexes of Ru(II) and Ru(III) are almost always six coordinate low-spin are fully populated in Ru(II) complexes but are deficient by one electron in Ru(III) complexes with an octahedral geometry. The three (t_{2g}) d-orbitals facing the octahedron complexes⁵⁶⁾. Because of this difference of one electron, the chemistry of Ru(II) and Ru(III) displays certain characteristic differences. Thus, Ru(III) can behave as a “hard” metal ion functioning as a *pi*-acceptor, whereas Ru(II) species are relatively “soft” *pi*-donors^{57, 61)}. As mentioned earlier, stable species of ruthenium in aqueous solution are dominated by its compounds with nitrogen containing ligands, in particular nitrosyl⁵⁵⁾, ammonia, organic amines and imines^{51, 52, 62)}, and various chelating agents containing nitrogen donor groups⁶³⁾. A number of ruthenocene derivatives are also reported to exist in aqueous solution, and their radiosynthesis and biological properties have been the subject of numerous investigations by Wenzel and coworkers^{35, 64–75)}.

The extended size of Ru(II) allows it to enter into strong backbonding interactions with many *pi*-acceptor ligands, particularly the nitrogen heterocycles. These complexes often exhibit intense metal-to-ligand charge transfer spectral bands that can be used for the characterization and quantification of these species. Smaller size and the higher charge of Ru(III) result in a higher affinity of this ion for anionic ligands such as chloride and oxygen. Due to the presence of a partially empty *d*-orbital, Ru(III) also functions as a *pi*-acceptor and readily forms complexes with *pi*-donor ligands. In such compounds, a strong ligand-to-metal charge transfer spectral band appears which can be employed for quantitative measurements⁵⁷⁾.

There are significant differences in the kinetic stability among Ru(II) and Ru(III) complexes. In general, Ru(II) complexes form more readily but are quite prone to ligand exchange reactions. Conversely, Ru(III) is substitutionally more inert and once complexed is slower to dissociate. Heating improves the kinetics of complex formation

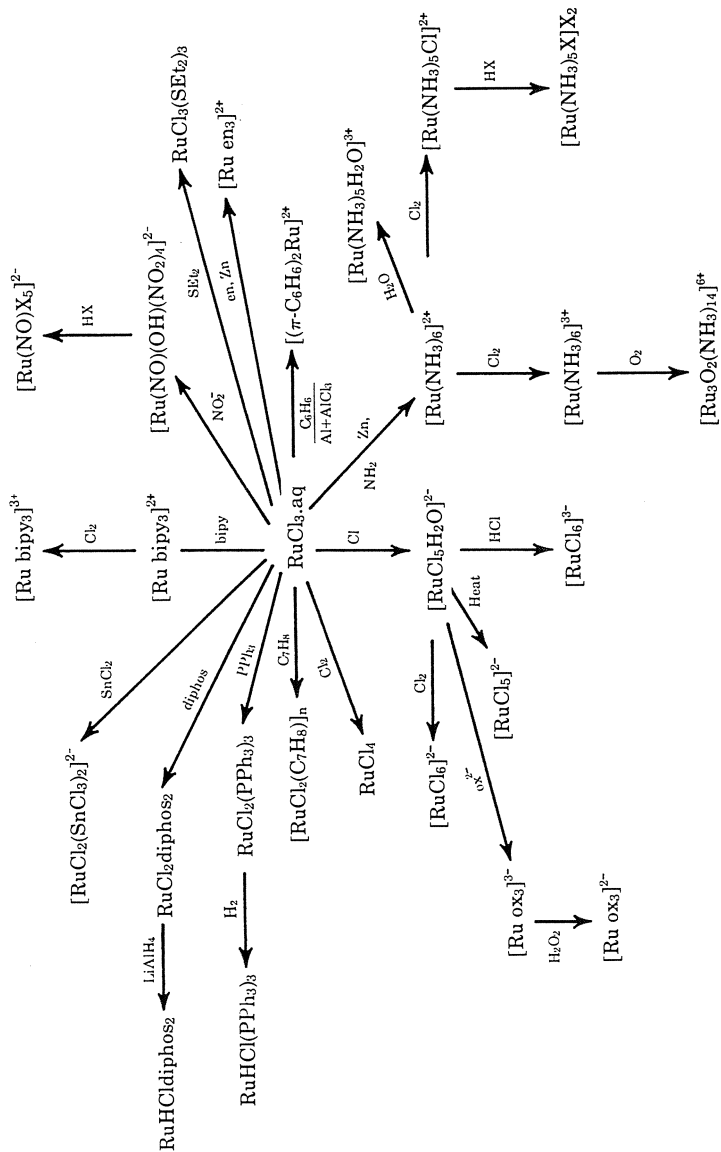
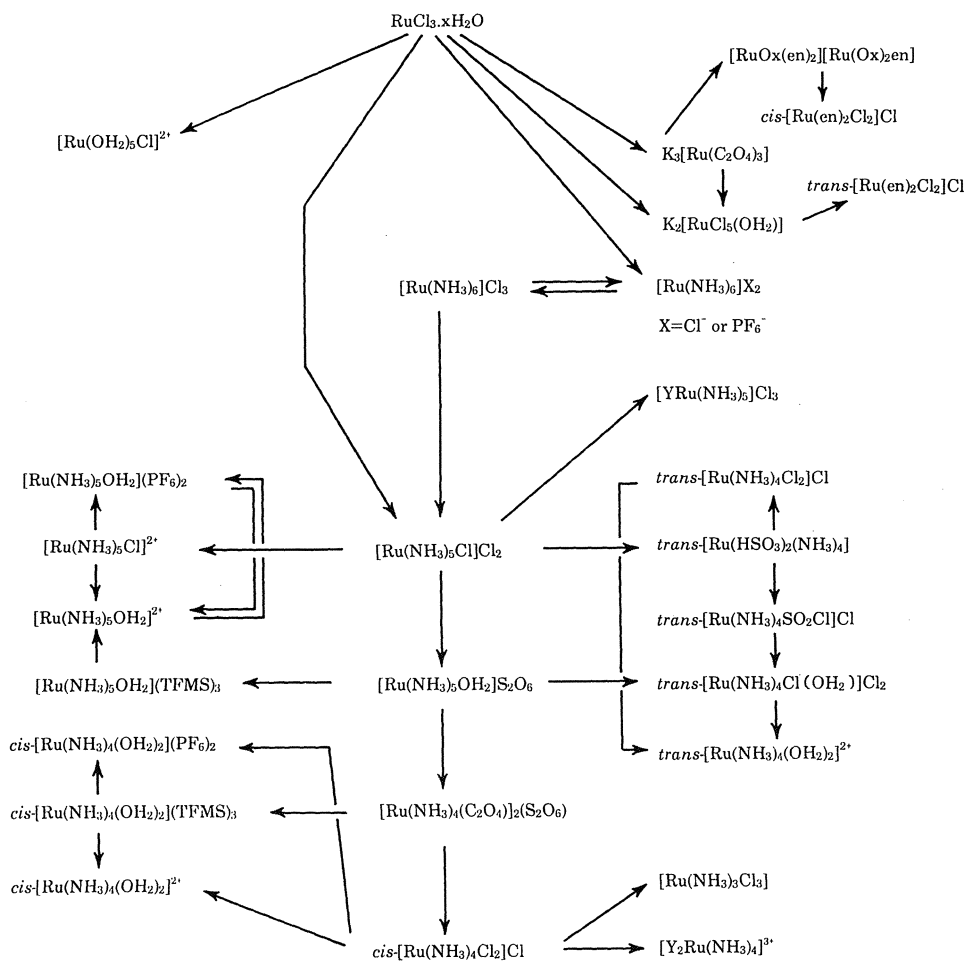


Fig. 2. Chemical reactions of ruthenium trichloride (adapted from Griffith, Ref. 20)



Abbreviations: Ox, oxalate; en, ethylenediamine; Y, purine, pyrimidine, nucleoside or nucleotide; TFMS, trifluoromethane sulfonate.

Fig. 3. Synthetic pathways for the preparation of various ruthenium ammine compounds. (Clarke and Dowling, unpublished data)

and helps to insure complete reaction, particularly when radiotracer concentrations are employed. The kinetic stability is not only a function of the oxidation state, but also depends upon the nature of the ligands used. *Trans*-labilizing ligands, for example, will promote the rate of ligand substitution on Ru(III) compounds⁵⁷.

In terms of chemical stability, the chloro complexes are intermediate between the weak nitrate and strong nitrosyl complexes. A large number of ^{103}Ru -labeled chlororuthenium complexes have been prepared at both "carrier-free" and carrier-added

levels^{14, 76}). Although the studies strongly support a correspondence in structure, the evidence for many compounds is not entirely conclusive.

The effect of back-donation of electron density helps stabilize the lower oxidation states of ruthenium. Coordination with *pi*-acceptor ligands thus increases the reduction potential of ruthenium whereas with electron donor ligands, it is generally decreased. The electron transfer rates of Ru(II) complexes with anionic ligands, for example, are rapid and thus oxidation to Ru(III) with ligand retention is favored in this any many similar situations. Small quantities of Ru(II) also serve as a redox catalyst and allow the facile substitution of a variety of ligands on Ru(III) complexes⁵⁷⁻⁷⁷).

6 Labeled Compounds and Radiopharmaceuticals

6.1 General Features

A variety of useful and potentially useful rutheruthenium-labeled compounds have been synthesized and evaluated for in vivo imaging applications. A number of these appear to have shown sufficient promise to warrant clinical investigation. In a 1983 review¹⁸), Waters provided a summary of the work on medical applications of ruthenium isotopes, which also included a description of many radiolabeled compounds.

Even though simple metal salts have been used and/or evaluated, the emphasis primarily has been on metal complexes and chelates containing a variety of organic ligands and biologically active molecules. Since diagnostic usefulness is determined both by the selectivity as well as the absolute concentration of the radiolabeled agent in the desired tissue relative to other normal tissues, the use of coordination complexes often leads to better results than simple salts and inorganic compounds. In actual practice, preferential localization is at best what can be achieved under most circumstances. Following the administration of labeled ruthenium compounds, rapid distribution of the activity takes place in several body compartments prior to excretion, and only in a few cases is the selective concentration high enough for the agent to be useful for nuclear medicine imaging.

The distribution and the excretion mechanisms of soluble ruthenium chelates (like other metal chelates) are dictated mainly by the structure and the lipophilicity of the chelate. Intravenously administered chelates rapidly equilibrate in the extracellular (intravascular and interstitial) fluid spaces. Depending upon the structure, they may also distribute intracellularly either by passive diffusion or through a specific transport and uptake process. The excretion pathway is determined also by the structure of the chelate. Small-molecular-weight hydrophilic chelates do not bind to plasma proteins and are rapidly excreted intact by glomerular filtration through the kidneys into urine. If the compound incorporates an aromatic structure or is more lipophilic due to other structural attributes, it is rapidly extracted from the blood into the liver (hepatocytes, polygonal cells) and then excreted into the bile. This hepatobiliary excretion mechanism also depends upon many factors other than the hydrophilic/lipophilic balance in the structure of the metal complex. The renal and hepatic

Table 5. Radiolabeled ruthenium compounds and their potential applications in nuclear medicine

Compounds	Application
<i>Simple salts (ionic)</i>	
Ruthenium chloride	
Potassium <i>tris</i> -oxalatoruthenium (III)	Tumor localization;
Potassium pentachloro-aquo-ruthenate (III)	myocardial agents
<i>Hydrophilic chelates</i>	
Tartrate	Kidney agents;
Citrate	tumor localization;
Diethylenetriamine pentaacetic acid (DTPA)	cisternography
Glucosheptonate	
Dimercaptosuccinate	
<i>Lipophilic chelates</i>	
8-hydroxyquinoline (oxine)	Hepatobiliary
Oxine 7-carboxylic acid	agents; labeling blood
1,10-phenanthroline derivatives	cells; study of
Lidocaine iminodiacetic acid (HIDA)	cellular transport
Dimethylsulfoxide	mechanisms; brain
	perfusion; tumor
	localization
<i>Phosphate compounds</i>	
Pyrophosphate	Bone agents (for normal
Ethylidene hydroxydisodium phosphonate (EHDP)	uptake and for physiological
Ethylenediamine tetramethylene phosphonate (EDTMP)	studies); agents for myocardial
Methylene diphosphonate (MDP)	infarct localization
<i>Ammine compounds</i>	
Chloropentaammineruthenium (III) chloride	Tumor localization
<i>cis</i> -dichlorotetraammineruthenium (III) chloride	
<i>cis</i> -dichlorobis(ethylenediamine)ruthenium (III) chloride	
Trichlorotriammineruthenium (III)	
<i>Ammineruthenium (III) complexes</i>	
Purines, pyrimidines, nucleosides, nucleotides	Tumor localization
<i>Colloidal preparation</i>	
Ruthenium-sulfur colloid	Lymphoscintigraphy
<i>Labeled proteins</i>	
Human serum albumin	Blood volume studies;
Transferrin	tumor localization
Monoclonal antibodies	

excretion pathways are often competitive unless the structural attributes of the complex exclusively dictate one pathway or the other.

Ruthenium compounds displaying diverse *in vivo* characteristics have been prepared and reported in the literature^{14, 18)}. The various promising or potentially promising compounds are listed in Table 5⁷⁶⁾. The classification is based arbitrarily on chemical structure, lipophilicity, or the nature of the ligand used. Imaging applications of the various derivatives are described in the right-hand column. Based on

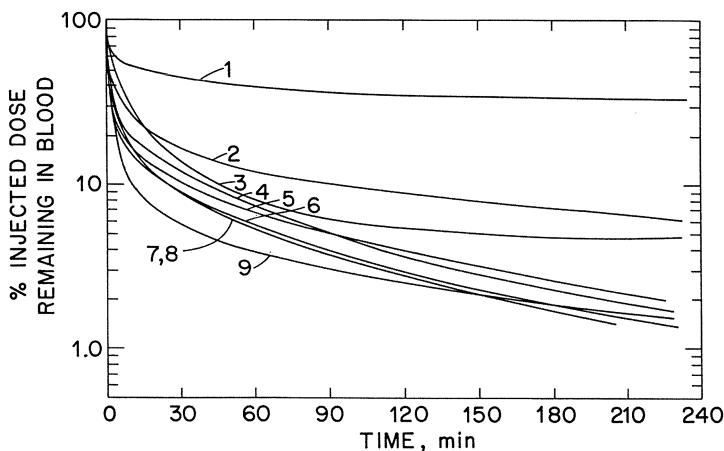


Fig. 4. Blood clearance of several radioruthenium-labeled complexes in dogs. ^{99m}Tc -DTPA and ^{99m}Tc -MDP are included for comparison. 1, ruthenium chloride, pH 2; 2, Ru-EHDP; 3, Ru(II)tris-((3,4,7,8-tetramethyl 1,10-phenanthroline) dichloride); 4, ^{99m}Tc -DTPA; 5, Ru-citrate; 6, Ru-EDTMP; 7, Ru-MDP; 8, ^{99m}Tc -MDP; 9, Ru-DTPA

promising animal results, clinical evaluation of many of these compounds appears worthwhile.

Blood clearance data following intravenous administration of a number of ^{103}Ru compounds in dogs¹⁴⁾ are shown in Fig. 4. Ruthenium chloride (pH 2) clears slowly and at 30 min after injection, $\approx 40\%$ of the activity remains in circulation. At later time periods, the radioactivity remains widely distributed throughout the body, with muscle uptake being quite high ($\approx 10\%$ in mice, Table 6). Blood clearance of ^{103}Ru citrate and ^{103}Ru DTPA is very rapid and within 10 min after injection, a major fraction of the radioactivity leaves the circulation via the kidneys into the bladder. Clearance of ^{103}Ru phosphate compounds is also fast with prompt localization of the radioactivity in bone. Greater than 50% of the activity is excreted into the urine. As also seen from Fig. 4, the blood disappearance curves of many ^{103}Ru -labeled compounds are comparable to those of routinely used analogous ^{99m}Tc -labeled derivatives.

In the discussion that follows, ruthenium-labeled compounds have been grouped primarily according to the classification used in Table 5. For convenience, in a few cases certain compounds have been grouped (separately or in addition) on the basis of their projected application, e.g., bone agents (phosphonate compounds), and tumor agents, etc.

6.2 Simple Salts and Inorganic Compounds

6.2.1 Ruthenium Chloride

Biological distribution of ruthenium chloride was addressed in the earlier section on health effects. As mentioned, ruthenium in the ionic form, particularly as Ru(III), binds strongly to plasma proteins, predominantly with transferrin^{23, 32, 48)}.

Table 6. Tissue uptake of ruthenium-103 chloride^a in EMT-6 sarcoma-bearing mice (percent injected dose per g; n = 6)

Tissue	Time after injection, h					
	1	6	24	48	72	96
Blood	12.4 ± 0.9	8.0 ± 0.4	3.6 ± 0.3	1.8 ± 0.1	1.3 ± 0.1	0.9 ± 0.1
Tumor	4.2 ± 0.2	4.7 ± 0.2	5.4 ± 0.2	6.1 ± 0.4	4.7 ± 0.3	3.6 ± 0.3
Liver	10.1 ± 1.3	10.7 ± 0.9	6.1 ± 0.5	9.2 ± 0.3	5.6 ± 0.5	4.3 ± 0.5
Kidney	19.1 ± 1.2	17.2 ± 0.7	10.2 ± 0.5	8.6 ± 0.5	7.2 ± 0.3	6.2 ± 0.5
Muscle	2.3 ± 0.2	2.0 ± 0.3	1.2 ± 0.1	1.3 ± 0.2	1.2 ± 0.1	1.1 ± 0.1
Heart	4.4 ± 0.2	4.3 ± 0.2	3.6 ± 0.1	3.2 ± 0.2	2.6 ± 0.2	2.5 ± 0.3
Spleen	4.7 ± 0.5	5.6 ± 0.5	3.9 ± 0.4	3.3 ± 0.2	3.5 ± 0.4	3.3 ± 0.7
Bone	4.6 ± 0.4	4.2 ± 0.3	3.5 ± 0.3	2.7 ± 0.3	2.7 ± 0.2	2.3 ± 0.4
%Dose remaining in whole body	—	—	59.3 ± 0.9	45.4 ± 1.9	47.4 ± 0.8	40.7 ± 2.7

^a The injection solution was a mixture of Ru(III) and Ru(IV) chlorides. Results were identical when either of the separated species was injected. The pH was adjusted to 2.0 with a NaCl/HCl buffer ($\mu = 0.154$).

Ruthenium(III) chloride labeled with ¹⁰³Ru has been evaluated as a radiopharmaceutical by many investigators. Following intravenous administration into mice, it distributes throughout the various tissues with somewhat higher concentrations achieved in blood, kidneys, liver, muscle, and bone. Initially, the ruthenium trichloride behaves as a blood pool agent and clears only slowly with time (Fig. 4). Again, this is most likely due to its strong binding with plasma proteins. Due perhaps to this same reason, and in a manner analogous to gallium citrate^{82, 83}, Ru(III) chloride concentrates more into various types of tumors especially those that either express transferrin receptors or possess high concentrations of lactoferrin, ferritin, or various glycopeptides^{84, 85}. The usefulness of ruthenium(III) chloride as a tumor-imaging agent has been evaluated and described in several publications^{14, 47, 76, 78, 80, 81}. Sufficient localization was noted in animal models of subcutaneous Ehrlich's or AH-130 ascites tumors to enable scintigraphic imaging⁷⁸. In AH-130 tumors in rats, the uptake was five-fold higher than in the muscle, and the tumors could be delineated by gamma ray imaging⁷⁸. Tissue distribution in mice implanted with EMT-6 sarcoma (Table 6) shows that high concentrations persisting in blood and soft tissue including the liver and spleen make ruthenium chloride a less than satisfactory tumor-imaging agent particularly for the abdominal area⁷⁶. Nonetheless, based on the tumor-to-tissue ratios and tumor-localization indices (Table 7), ruthenium chloride particularly when labeled with ⁹⁷Ru appears to show some promise as a tumor-imaging agent.

Clinical trials in patients were reported in a study in 1976⁷⁹. In 37 patients, tumors were strongly positive in 54% and slightly positive in 27% of the cases. Head and neck tumors were clearly identified in 10 out of 13 cases (77%) and primary lung cancer was delineated in 6 out of 8 patients. In lung cancer patients, the

Table 7. Tumor to tissue ratios and tumor concentration index (TCI) of ruthenium-103 chloride in EMT-6 sarcoma bearing mice (n = 6)

Time after injection, h	Ratio, Tumor to					TCI ^a
	Blood	Muscle	Liver	Kidney	Spleen	
1	0.34	1.83	0.42	0.22	0.89	—
6	0.59	2.39	0.44	0.27	0.84	—
24	1.50	4.50	0.89	0.53	1.38	1.56
48	3.39	4.69	0.66	0.71	1.85	1.69
72	3.62	3.92	0.84	0.65	1.34	—
96	4.00	3.27	0.84	0.58	1.09	1.61

^a Tumor concentration index (TCI) is defined as the ratio of percent injected dose per g in the tumor to percent injected dose per g remaining in the whole body at any given time period. For interspecies comparisons, and for normalizing for different animal body weights, TCI could be expressed as per kg body weight.

ratio of tumor versus normal tissue uptake remained 1.35 to 2.45 for up to 4 weeks following the administration of ¹⁰³Ru chloride. All cases of hepatoma gave negative scans due to the high concentration of ruthenium chloride in the liver. In all cases, because of the slow blood clearance, late imaging (3–6 days or more) was required to acquire images with sufficient contrast ⁷⁹). Positive scans were also obtained in cases of inflammatory disease thus pointing to the non-specificity of tumor uptake or at least to a common mechanism of uptake in various disease states.

The mechanism for the subcellular accumulation and binding of ruthenium chloride in the liver and in tumor was the subject of a recent study ⁸¹). It was shown that with time, there was an increase in the concentration of ruthenium in the lysosomal fraction of mitochondria, similar to what is observed with ⁶⁷Ga citrate. The concentration of ruthenium was higher in connective tissue than in viable tumor or in necrotic tissue. A large fraction of ruthenium in the liver and tumor was bound to acid mucopolysaccharides of molecular weights greater than 40,000 ⁸¹).

6.2.2 Ruthenium Red and Other Ruthenium Ammine Complexes

In terms of radiopharmaceutical development, various ruthenium ammine compounds including the cytological dye ruthenium red have been investigated in animal systems. As mentioned earlier, ruthenium red was shown to selectively localize (or at least in higher concentrations compared to normal tissue) in certain tumors that are rich in mucopolysaccharides ^{44–46}). Concentrations higher than background were also noted in organs such as bone, stomach, and ovary ^{43, 44}). The argument again is that these tissues express higher concentrations of mucoproteins and mucopolysaccharides thus leading to greater uptake of ruthenium red. These findings were confirmed in another study ⁴³); however, the ascites tumor-bearing mice utilized in this investigation did not show preferential ruthenium red uptake in the tumor. At 24 h, specific binding sites were noted only in the liver ⁴³). These results suggest that while radiolabeled ruthenium red may have some promise as a tumor-localizing agent, its application in humans may be limited to certain types of tumors only. Data in humans will have to be obtained in order to assess its usefulness, if any.

Table 8. Tissue uptake of various ruthenium ammine compounds in tumor (EMT-6 sarcoma) bearing mice (percent injected dose per g; n = 6)^a

Compound	Time (h)	Tumor	Blood	Muscle	Liver	Kidney	Whole body retention (% dose)
K ₂ [RuCl ₅ (H ₂ O)] ^b	24	6.76	5.46	2.06	10.89	11.76	61.86
K ₃ [Ru(Ox) ₃].XH ₂ O ^c	24	5.97	3.81	2.03	5.22	6.32	57.77
[Ru(NH ₃) ₅ Cl]Cl ₂ ^d	24	3.29	1.97	0.79	2.37	5.89	48.39
	96	2.30	0.67	0.80	1.63	3.81	38.59
<i>cis</i> -[Ru(NH ₃) ₄ Cl ₂]Cl ^e	24	5.38	5.18	1.54	5.12	9.23	49.61
	72	5.93	2.10	1.32	4.14	7.21	43.80
	96	4.92	1.15	1.20	3.23	5.35	37.06
<i>cis</i> -[Ru(en) ₂ Cl ₂]Cl ^f	24	5.97	5.62	1.69	5.76	11.15	52.80
Gallium-67 citrate	24	7.09	1.81	0.53	9.30	9.21	59.58
	48	5.05	0.51	0.47	9.49	8.03	50.68
	96	3.54	0.36	0.37	8.19	7.14	38.29

^a All compounds were synthesized using stable ruthenium carrier; ruthenium dose 2–6 mg/kg body weight. Gallium-67 citrate is included here for comparison.

^b Potassium pentachloroaquoruthenate(III).

^c Potassium *tris*-(oxalato)ruthenium(III).

^d Chloropentaammineruthenium(III)chloride.

^e *cis*-Dichlorotetraammineruthenium(III)chloride.

^f *cis*-Dichlorobisethylenediammineruthenium(III)chloride.

A number of other ruthenium amines have been prepared and labeled with ruthenium-103^{48, 76, 86, 87}. The compounds were also synthesized at the carrier-added level and their purity and structure ascertained by elemental analysis and spectroscopic methods^{48, 76}. The ability of the ruthenium ammine compounds to serve as tumor-localizing agents was tested using EMT-6 sarcoma-bearing mice⁷⁶. Representative data are summarized in Table 8. Also included are data on ⁶⁷Ga citrate, for comparison. The biodistribution is not significantly different from that of plain ruthenium chloride (cf. Tables 6 and 7), suggesting that the ammine compounds also bind to plasma proteins and thus linger in blood for a prolonged period. Other tissues with high concentration of ruthenium were muscle, liver, kidney, and bone. Uptake by the tumor at 24 h, expressed as percent dose per gram, ranges between 3.3 and 6.8 and compares favorably with the corresponding value for gallium citrate (7.1). The soft tissue uptake of chloropentaammine ruthenium chloride and *cis*-dichlorotetraammine-ruthenium chloride is much lower than that of gallium citrate, particularly at late time periods. Most of the compounds are comparable to gallium with regard to whole body retention of activity. The tumor-to-blood (T/B) and tumor-to-muscle (T/M) ratios with several compounds (Table 9) may be high enough for delineating tumors by imaging. The uptake of gallium by the tumor reaches a plateau at about 24 h; thereafter, significant loss of activity is seen without comparable excretion from the body. This actually results in a decrease in the value of the tumor concentration index (Table 9). This index reaches a maximum value at different time periods with different ruthenium compounds. The TCI at 24–96 h ranges between 1.49 and 2.00 and is comparable to that of gallium citrate (1.45–1.81). *Cis*-dichlorotetraammineruthenium (III) chloride looks particularly promising when

Table 9. Tumor-to-tissue ratios and tumor concentration index (TCI) of various ruthenium ammine compounds in tumor (EMT-6 sarcoma) bearing mice (n = 6)^a

Compound	Time (h)	Ratio, Tumor-to-					TCI ^b
		Blood	Muscle	Liver	Kidney		
K ₂ [RuCl ₅ (H ₂ O)]	24	1.3	3.3	0.6	0.6		1.65
K ₃ [Ru(Ox) ₃].XH ₂ O	24	1.6	3.0	1.1	0.9		1.64
[Ru(NH ₃) ₅ Cl]Cl ₂	24	1.7		1.4	0.6		
	96	3.4	4.1	1.4	0.6		1.49
<i>cis</i> -[Ru(NH ₃) ₄ Cl ₂]Cl	24	1.1	3.5	1.1	0.6		1.56
	96	4.4	4.2	1.5	0.9		2.00
<i>cis</i> -[Ru(en) ₂ Cl ₂]Cl	24	1.1	3.6	1.1	0.5		1.70
Gallium-67 citrate	24	4.2	13.4	0.8	0.8		1.81
	96	10.3	10.6	0.4	0.5		1.45

^a For abbreviations and other explanations, see Tables 7 and 8; ⁶⁷Ga included for comparison.

^b For the definition of TCI, refer to Table 7.

compared to gallium citrate and may be a promising candidate for further evaluation.

Various ruthenium ammine complexes, including some of those in Tables 8 and 9, have shown antitumor activity in rats⁵⁷⁻⁵⁹, which is consistent with the hypothesis that some Ru(III) complexes can be activated toward binding to nucleic acids and proteins by *in vivo* reduction to Ru(II). However, the significant quantities of radio-labeled amines that were observed to bind to other, well aerated tissues, where the Ru(III) oxidation state should prevail, indicate that other binding mechanisms are also operating. One possibility is that electron transfer facilitates the binding of ruthenium to some protein binding sites (such as transferrin) through a process known as redox catalysis, which is occasionally employed in the synthesis of ruthenium(III) compounds⁷⁷. Further improvement in tumor localization may be possible through ligand modifications that would optimize the reduction potential and ligand exchange rate of the metal to take advantage of the generally lower pH and oxygen content of tumors, so as to increase binding in the tumor relative to normal tissue.

6.3 Phosphonate Complexes

Ruthenium(III) forms stable complexes with a variety of phosphonate ligands such as pyrophosphate [(O₃P—O—PO₃)⁴⁻], methylene diphosphonate [(O₃P—CH₂—PO₃)⁴⁻], ethylidene hydroxy-1,1-diphosphonate [(O₃P—C(OH)(CH₃)—PO₃)⁴⁻], and ethylenediamine tetramethylene phosphonate (EDTMP)^{14,88}. When starting the syntheses with ruthenium trichloride, the reactions are kinetically slow (particularly at radiotracer concentrations), and often a step such as heating at 90 °C (boiling water bath) is required to ensure complete reaction.

Following intravenous administration, the phosphonate complexes of ruthenium localize predominantly in bone¹⁴. The efficacy of the materials as bone imaging agents is, however, quite dependent upon the methods and conditions of preparation. In addition, the pyrophosphate and MDP complexes of radioruthenium are not

Table 10. Bone-to-organ ratios of ruthenium-103 phosphonates in mice at various time intervals after injection (n = 5)^{a, b}

Organ	¹⁰³ Ru-EDTMP ¹			¹⁰³ Ru-EHDP ²			^{99m} Tc-MDP ³		
	1 h	5 h	24 h	2 h	5 h	24 h	0.5 h	4 h	24 h
Blood	37.9	39.7	72.3	16.4	19.8	34.6	12.2	38.4	88.9
Muscle	77.8	80.4	85.0	53.1	60.8	91.9	27.6	91.3	115.7
Liver	42.4	37.0	35.6	35.7	31.6	39.0	1.2	3.2	7.0
Kidney	8.8	8.9	8.5	2.6	4.9	7.9	2.9	5.2	9.3
Lungs	19.5	19.4	20.4	10.4	10.8	13.9	6.1	9.8	16.9
Spleen	160.9	105.2	81.7	29.7	47.3	46.0	12.9	4.0	3.1

^a Technetium-99m-MDP is included for comparison.

^b Abbreviations: ¹ Ethylenediamine tetramethylene phosphonate; ² Ethylidene hydroxy-diphosphonate; ³ Methylene diphosphonate.

particularly stable in vivo; to some degree, they hydrolyze, bind to proteins and enter into ligand exchange reactions¹⁴). Complexes with ethylidene hydroxy diphosphonate (EHDP) and EDTMP were found to be more stable, and in mice produced preferential bone localization¹⁴). The biodistribution results (bone to organ ratios) are summarized in Table 10. The specificity of bone localization of the ruthenium agents is as good or superior to that obtained with the routinely used ^{99m}Tc-MDP (data shown in Table 10 for comparison). Absolute bone concentrations of ¹⁰³RuEHDP and ¹⁰³RuEDTMP are nearly identical to ^{99m}Tc-MDP; however, uptake in soft tissues and other non-osseous structures is much lower than ^{99m}Tc-MDP. This implies that ⁹⁷Ru-labeled EHDP and EDTMP could be superior bone imaging agents, particularly in situations where frequent imaging over a long period is required either to study long term bone physiology or to monitor the effects of intervention in pathophysiological conditions. Imaging in rabbits produced clear bone images at 3 h and up to 2 weeks following injection¹⁴). The clinical effectiveness of these compounds is yet to be determined.

Based on the analogy with ^{99m}Tc phosphonate complexes (particularly pyrophosphate), ¹⁰³Ru- and ⁹⁷Ru-labeled phosphonates have been evaluated as agents for localizing myocardial infarcts or areas of diffuse myocardial injury¹⁴). While some uptake resulted in experimental myocardial injury in rats, the target to non-target ratios were not favorable for imaging until late time periods after injection. There appears to be no distinct advantage to using ruthenium phosphonates over ^{99m}Tc phosphonates for such applications.

6.4 Chelates with Organic Ligands

A variety of ruthenium chelates, including those that are analogous to the widely used ^{99m}Tc-labeled chelates, have been prepared and studied. These can be broadly classified into two categories: hydrophilic chelates that are primarily excreted into the urine via glomerular filtration by the kidneys, and lipophilic chelates whose main excretion pathway is through the liver into the bile. There are many borderline cases where the two routes of excretion act in a mutually competitive manner.

Other than the lipophilic/hydrophilic balance in the chelate, there are many other chemical and structural factors that also control the in-vivo biodistribution and excretion of the injected material.

6.4.1 *Hydrophilic Chelates*

Agents in this class that have been labeled with ^{103}Ru and/or ^{97}Ru , and evaluated in appropriate animal systems, include various hydroxy and thio carboxylic acids and polyaminocarboxylate compounds ^{14,88,95-98}. These relatively small to medium size (M. W. ≈ 500) ionic chelates are rapidly eliminated from the blood and generally distribute homogeneously throughout the kidney before being excreted into the urine. The renal clearance mechanism involves predominantly glomerular filtration and there may be varying degrees of secretion or absorption of the chelate by the renal tubules depending upon its chemical structure and other characteristics. Freely filterable chelates that do not engage in tubular secretion or reabsorption are best suited for the quantitative measurement of the glomerular filtration rate (GFR) of the kidneys. Assessment of other renal functions is made possible by obtaining plots of localized activity in the kidneys with time through sequential imaging, and by determining effective renal plasma flow which is a product of the renal plasma flow and the extraction efficiency of the kidneys. The half times of maximum kidney uptake and urinary excretion vary from agent to agent and in order to obtain quantifiable data, normal baseline values must be determined.

Hydroxy carboxylic acids such as tartrate and citrate ¹⁴) form stable chelates with ruthenium at slightly acid to neutral pH, and can be prepared by simply mixing a pH 2 solution of ^{103}Ru or ^{97}Ru chloride with an excess of the ligand and then adjusting the pH to between 5 and 7.5 with an appropriate inert buffer. A final heating step (for example, immersion of the mixture in a boiling water bath for 10-30 min) is necessary in order to ensure complete reaction, particularly at radiotracer concentrations when no added ruthenium carrier is present. The blood clearance of the citrate chelate in dogs is shown in Fig. 4. Within 10 min following injection, most of the compound is extracted by the kidneys and excreted into the urine. Soft tissue uptake was not evident in the images ¹⁴).

The chelate with 2,3-dimercaptosuccinic acid (DMSA) was prepared and studied for delayed renal imaging applications ^{97,98}). Anghileri et al. ⁹⁸) labeled DMSA with ^{103}Ru and studied its biodistribution in rats and rabbits. The probable mechanism for renal accumulation of this complex was explained on the basis of binding of ^{103}Ru -DMSA to metallothionein. Oster and coworkers used two preparations, one with and the other without the addition of $\text{SnCl}_2 \cdot 2\text{H}_2\text{O}$ ⁹⁷). For optimum kidney concentration, the most suitable procedure was as follows. Sixty mg DMSA was dissolved in 10 ml of 1 *N* sodium hydroxide. For tin containing preparations, 30 mg $\text{SnCl}_2 \cdot 2\text{H}_2\text{O}$ was dissolved in 1 ml conc HCl, diluted to 10 ml with water, and added to the DMSA solution. The pH was adjusted to between 8 and 9 and the solution was millipore filtered (0.22 μm). Ruthenium-97 chloride in 6 *N* HCl (~ 0.5 ml volume, ~ 2 mCi) was evaporated to dryness and then the DMSA solution (with or without tin) added to it. The same procedure was followed for labeling with ruthenium-103. Quality control included polyamide thin-layer chromatography in 99.5% methanol, and cellulose acetate electrophoresis in borate buffer. Labeling

yields were found to be consistently greater than 95 percent. The tin containing preparations in mice showed higher kidney uptake with time and a corresponding decrease in blood and liver activity. Approximately 58% of the injected activity was excreted into the urine within the first 30 min, and an additional 12% in the next three hours. The optimum DMSA/Sn²⁺ molar ratio was determined to be 2.47. The kidney to blood ratio with this preparation in mice increased from 5.3 at 30 min to 55.1 at 4 hours⁹⁷). In normal dogs at 40 h, concentration ratios were: kidney to blood, 70; kidney to muscle, 367; and kidney to liver, 8. In normal dogs, the mean blood clearance half time was 25 min whereas in dogs with renal insufficiency (ligated renal artery) it was approximately 45 minutes and the rapid component seen in normal dogs was missing as well. The images of the kidney were excellent. Urinary excretion (less residence time in kidneys) was three times higher when tin free preparations were used. The absorbed dose to various organs has been estimated^{96,97}).

The exact role of tin (which is an essential component for ^{99m}Tc-DMSA preparation) in the preparation of ruthenium-DMSA is not understood. The ^{99m}Tc-DMSA complex supposedly does not contain tin in its structure⁹⁹) but whether this is also the case with ruthenium remains to be elucidated. Binding of ruthenium to DMSA does not require Sn²⁺ but in its presence, the renal parenchymal uptake increases considerably. Further studies will be necessary in order to determine whether or not the cortical imaging agent is a mixed Ru—Sn—DMSA chelate.

The ruthenium chelate with DTPA was prepared and reported to rapidly clear from the blood in dogs following intravenous injection¹⁴). The activity decreased to about 10% in 10 min and then slowly to about 4% in 60 min (Fig. 4). There was a correspondingly high uptake into the kidneys but excretion into the urine was rapid. The usefulness of ⁹⁷Ru-DTPA as a cerebrospinal fluid (CSF) imaging agent (cisternography) was evaluated in another study⁹⁵). It was pointed out that ⁹⁷Ru-DTPA may be a better agent for cisternography particularly in conditions such as the evaluation of hydrocephalus where delayed imaging is necessary. The superiority stems from the reasons that include longer half-life (compared to ^{99m}Tc-DTPA), reduced radiation dose (compared to ¹⁶⁹Yb-DTPA, and possibly ¹¹¹In-DTPA), and better imaging properties.

Radioruthenium labeled DTPA was prepared using acid solutions of ¹⁰³Ru or ⁹⁷Ru to which 2 ml of a 4.5 mg/ml solution of CaNa₂DTPA in 0.2 N NaOH was added and the pH adjusted to 3.5. The mixture was heated at 90 °C for 30 min, cooled, adjusted to pH 6.5, and finally passed through a 0.22 μm millipore filter. In a comparative study in dogs⁹⁵), identical doses (0.4 mCi) of ¹¹¹In-DTPA and ⁹⁷Ru-DTPA were injected into the cisterna magna. Activity over the head, in the blood, and in urine was monitored over time by imaging or sample collection and counting. The fast component of CSF disappearance of ⁹⁷Ru-DTPA was slightly steeper than that of ¹¹¹In-DTPA. The slow components however, gave similar slopes. Ruthenium-97-DTPA persisted in the blood a little longer and its excretion was slightly slower. Tissue distribution results (within statistical error) were similar for both tracers. Radiation dose estimates^{95,96}) showed that if both ¹¹¹In photons were used for imaging (in which case the images are of poorer quality), the doses to CSF and to various organs were comparable to those from ⁹⁷Ru-DTPA. On a per millicurie basis, ⁹⁷Ru delivers approximately half the absorbed dose to tissues compar-

ed to indium-111. These results demonstrate that ^{97}Ru -DTPA may be a better CSF imaging agent than ^{111}In -DTPA. Human studies have not yet been attempted.

6.4.2 Lipophilic Chelates

The definition for lipophilic chelates is used in this section loosely since the compounds included display varying degrees of polar/non-polar balance in their structures. More applicable criteria are that the major excretion pathway is via the hepatobiliary system and/or that the chelates are lipophilic enough to be transported across the cell membrane and thus be useful for labeling cellular blood elements.

Hepatobiliary agents that are useful for the assessment of the function and disorders of the liver and gallbladder generally are lipophilic compounds with sufficient polar character to be water soluble. The most widely used radio-pharmaceuticals for hepatobiliary imaging are $^{99\text{m}}\text{Tc}$ chelates with iminodiacetate derivatives of lidocaine analogs ^{1, 2, 100, 101}. These include HIDA (2,6-dimethylphenyl carbamoylmethyl iminodiacetic acid), *p*-isopropyl HIDA (PIPIDA), diisopropyl HIDA (DISIDA), *p*-butyl HIDA (BIDA), and others.

The above compounds have also successfully been labeled with ruthenium and found to behave *in vivo* as hepatobiliary agents ¹⁰²⁻¹⁰⁴. Their advantage over $^{99\text{m}}\text{Tc}$ -labeled analogs is that they make delayed imaging of the hepatobiliary tract possible and thus yield diagnostic information which cannot be obtained with $^{99\text{m}}\text{Tc}$. Examples are biliary atresia, choledocal cyst, neonatal hepatitis, and severe hepatitis, etc., where extended observation periods are required in order to make the correct diagnosis ¹⁰².

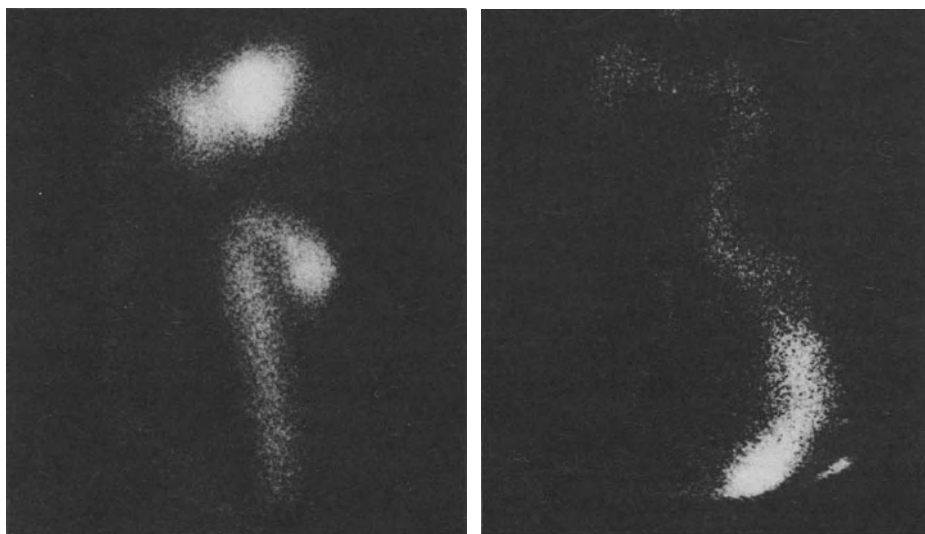


Fig. 5. Scintiphotos of normal dog at 150 min (*left*) and 72 h (*right*) following the administration of ^{97}Ru -PIPIDA. The gallbladder was visualized early (<20 min). The intestines appeared after 150 min and were seen up to 72 h. Notice the excellent imaging properties of ^{97}Ru

The radoruthenium labeled HIDA analogs fulfill the criteria of a good hepatobiliary agent, namely, high initial uptake by the liver and rapid excretion into the bile. The kinetics of the transit of these compounds into the gallbladder and intestines are, however, slightly variable and depend upon the substituents on the aromatic ring. Movement of the activity into the gallbladder and beyond roughly follows the following order: DISIDA > BrMe₃HIDA > PIPIDA > HIDA > BIDA_{103, 104}).

In dogs, ⁹⁷Ru-PIPIDA and ^{99m}Tc-PIPIDA showed similar blood clearance rates¹⁰²). The fast blood clearing component (~90%) had a t 1/2 of 67 min for ^{99m}Tc-PIPIDA and a t 1/2 of 62 min for ⁹⁷Ru-PIPIDA. Scans with ⁹⁷Ru-DISIDA showed the liver clearly at 7 min, and at 20 min, the gallbladder was visualized. The intestines appeared after 150 min and could be seen up to 72 h. A typical scan is shown in Fig. 5. Biodistribution studies in normal rats also exhibited similar organ distribution for ¹⁰³Ru and ^{99m}Tc labels except that with ¹⁰³Ru-PIPIDA, the blood activity was slightly higher and the kidney concentration was lower¹⁰²). Compared to ¹³¹I-Rose Bengal which has been utilized for long-term imaging of the hepatobiliary system, the radiation dose from ⁹⁷Ru-PIPIDA was found to be between a half and one-tenth for various organs.

Table 11. Tissue distribution of radoruthenium-labeled HIDA derivatives in mice^a

Compound	Time, min	Percent dose per organ						
		Blood	Liver	Gut	Kidneys	Spleen	Muscle	Bone
Ruthenium acetate	5	13.20	10.20	7.32	3.77	0.27	16.60	6.85
	30	8.46	8.91	7.76	2.13	0.27	10.60	6.93
	120	5.94	7.96	11.60	1.81	0.24	9.17	6.27
Diisopropyl HIDA	5	2.14	19.42	68.30	0.67	0.03	2.71	0.76
	30	0.98	6.69	86.92	0.17	0.01	1.44	0.46
	120	0.67	3.80	91.97	0.14	0.01	0.94	0.37
Diisopropyl HIDA with tin	5	1.85	23.67	60.60	1.05	0.04	2.81	1.00
	30	0.28	2.60	92.81	0.19	0.01	0.48	0.14
	120	0.13	2.82	95.43	0.05	0.01	0.20	0.09
Bromotrimethyl HIDA	5	4.62	24.78	52.57	0.81	0.08	5.04	6.84
	30	1.55	4.06	87.35	0.32	0.03	1.80	0.53
	120	1.13	3.38	90.65	0.18	0.03	1.14	0.50
Bromotrimethyl HIDA with tin	5	7.33	40.96	30.15	1.13	0.16	4.95	2.62
	30	3.02	14.32	74.14	0.70	0.14	2.76	1.17
	120	1.80	5.01	89.07	0.35	0.22	1.27	0.68

^a HIDA is the abbreviation used for 2,6-dimethyl phenylcarbonylmethyl iminodiacetate. Results shown are the average from three mice. Blood, bone, muscle were assumed to constitute 7, 10, and 43 % of body weight, respectively. Ruthenium-103 acetate is included for comparison. The average whole body recovery of radioactivity was $96.7 \pm 3.4\%$ for all compounds (at 5–120 min), except for acetate (80 % at 5 min, 59 % at 30 min, and 54 % at 120 min).

Since these hepatobiliary agents are taken up into the liver by active transport into the hepatocytes, their concentration reaches an upper limit and often exhibits nonlinear Michaelis-Menten type of profiles. Presence of competing materials such as bilirubin which are transported by the same anion transport mechanism, also interferes with an accurate quantification of hepatocyte function. In neonatal jaundice, for example, much higher blood bilirubin levels are encountered and in such cases use of ^{97}Ru -BIDA was claimed to provide much better information¹⁰³. This could be attributed to the higher lipophilicity of this material (as also with $^{99\text{m}}\text{Tc}$ -BIDA) that causes less renal excretion and also allows visualization of the biliary passage despite higher blood bilirubin levels¹⁰³.

Complexes of ruthenium with DISIDA and bromotrimethyl HIDA (BrMe_3HIDA) were prepared using ^{103}Ru and evaluated in mice¹⁰⁴. The biodistribution was essentially identical with that of the corresponding $^{99\text{m}}\text{Tc}$ analogs. High hepatic uptake and negligible renal excretion resulted with both DISIDA and BrMe_3HIDA ; however, uptake kinetics and hepatic transit times were slightly different. Representative results are shown in Table 11. The chelates were also prepared using commercial $^{99\text{m}}\text{Tc}$ -labeling kits that contain stannous tin as a reducing agent. In such cases (for both DISIDA and BrMe_3HIDA), blood clearance as well as the clearance from other tissues of ^{103}Ru activity was more rapid compared to preparations without tin, but the rest of the biodistribution was essentially similar. The role of tin, if any, in these preparations is not understood. Structural characterization of the various complex species (perhaps at the carrier-added level) may be necessary in order to obtain such information.

Imaging studies with ^{97}Ru -DISIDA in about 20 patients were reported recently^{105, 106}. The patients presented with a variety of hepatobiliary clinical problems as well as problems of duodenogastric reflux (DGR) and gastric emptying. A commercially available DISIDA kit (containing stannous ion) was utilized with 10% ethanol in the final preparation. Sequential images of the superior abdomen were obtained during 1 h following injection. A typical patient scan is shown in Fig. 6. Delayed images also were of excellent quality (not shown) and were consistent with the biodistribution data obtained in experimental animals. The scintiscans correlated well with other imaging procedures (ultrasound, CT) and clinical findings. Biliary atresia was ruled out in an infant in whom the gallbladder was not visualized. Surgical exploration revealed the presence of chronic and subacute cholecystitis and a patent common bile duct.

Intravenous administration of ^{97}Ru -DISIDA and of solid test meal labeled with $^{99\text{m}}\text{Tc}$ -sulfur colloid also allowed the simultaneous detection and quantification of DGR and determination of the gastric emptying rate in patients with duodenogastric disorders¹⁰⁷. This method represents a distinct advantage over the current techniques which require two separate studies if a solid meal is used, or mandate a liquid meal for a simultaneous study.

Chelates of ruthenium(II) with 1,10-phenanthroline and with 3,4,7,8-tetramethyl 1,10-phenanthroline have also been synthesized and evaluated in animals. The complexes were prepared by reducing the ruthenium solution (^{97}Ru or ^{103}Ru ; both carrier-free and with added carrier) with hydroxylammonium chloride in the presence of the ligand, and subsequent heating for 30 min following pH adjustment (to between 7 and 8). The blood clearance of $\text{Ru(II)tris-(3,4,7,8-tetramethyl 1,10-$

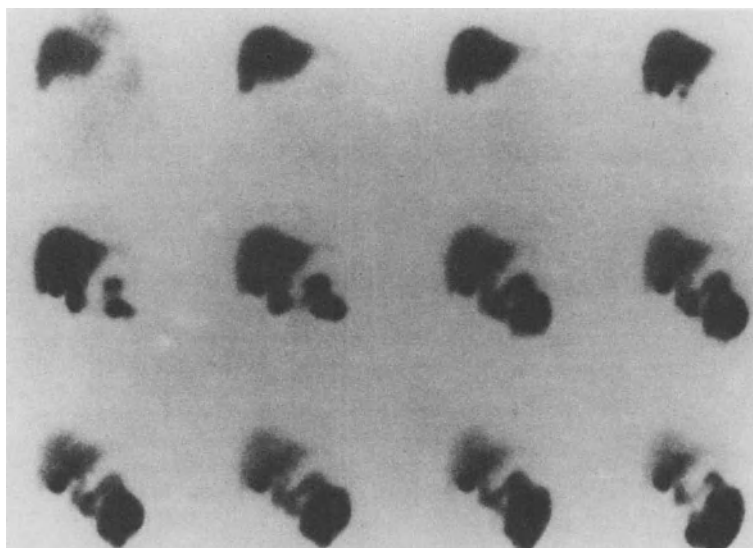


Fig. 6. Sequential composite images, 0–60 min following injection of 1.1 mCi of ^{97}Ru -DISIDA in a patient. Prompt filling of the gallbladder and passage of tracer into the intestine are clearly seen. (Zanzi and Srivastava, 1987, unpublished data)

phenanthroline)dichloride in dogs is shown in Fig. 4. Blood levels initially drop quite rapidly but thereafter (beyond ~ 30 min) a small fraction lingers on for several hours due to protein binding. Biodistribution of Ru(II)tris-(1,10 phenanthroline)dichloride in mice showed slow whole body excretion, with relatively high levels of radioactivity retained in the liver and the kidneys ^{14, 88}. The radioactivity peaked in these organs between 1 and 6 h, and then slowly dropped to lower values at 24 h (liver 15 and 9% and kidneys 51 and 30% injected dose per g at 1 and 24 h, respectively). Blood levels were quite low (0.4% and 0.2% dose per g at 1 and 24 h). As expected, the more lipophilic Ru(II)tris(3,4,7,8-tetramethyl 1,10-phenanthroline)dichloride behaved as a hepatobiliary agent and retention by the kidneys and excretion into the urine were reduced considerably ⁸⁸. The liver concentration at 1, 6, and 24 h respectively was 62, 67, and 64% dose per g and the corresponding values for the kidneys were 11, 9, and 8. This compound appears to be a promising candidate for evaluation in humans, particularly when a slower transit of the tracer from the liver into the intestines is considered advantageous for a particular study.

A lipophilic chelate of ruthenium with 8-hydroxyquinoline (oxine)7-carboxylic acid acetate (Ru-oxine-7 CA acetate) was prepared and investigated ^{14, 88}. The compound was rapidly extracted from the blood into the liver and then excreted through the biliary tract into the intestines. Urinary excretion in dogs and rabbits was insignificant ¹⁴. Greater than 70% of the radioactivity had cleared the body, however, at 24 h. In mice, the behavior was somewhat different: blood, liver, and kidneys respectively accounted for 2.3, 3.0, and 2.9% injected dose per g at 24 h, and the whole body retention was only 19.0% ⁴⁸. It appears that there is a variation in the handling of this compound by different animal species.

A more promising application of Ru-oxine 7-CA acetate appears to be for blood cell labeling. Indium-111 chelates (oxine¹⁰⁸), tropolone¹⁰⁹, mercaptoquinoline N-oxide¹¹⁰) are at present the most widely utilized intermediate half-life agents for the labeling of leukocytes and platelets¹¹¹). These labeled preparations provide crucial diagnostic information in patients with abscesses, inflammations, thrombosis, vascular lesions, and many related disorders. However, with the currently used¹¹¹In-oxine technique, to achieve successful labeling, cells must be isolated free of plasma since indium strongly binds to transferrin in plasma. It was pointed out¹¹²) that the binding of ruthenium to transferrin is quite slow under cell labeling conditions and thus ruthenium-oxine could be a better label and may provide acceptable labeling in the presence of plasma. Physical and physiological cell damage associated with the removal of plasma and the trauma of separation can thus be minimized. Of the various Ru-oxine chelates tested, Ru(III)-oxine 7 CA acetate gave the best labeling of both leukocytes and platelets. Labeling yields in the presence of plasma were between 45 and 65%¹¹²). Less radiation damage to cells from⁹⁷Ru compared to¹¹¹In should provide an additional advantage although again if both indium photons are used for imaging this advantage is reduced. Even in this case, based on the fewer low energy emissions from⁹⁷Ru (Table 4) it would appear, however, that the radiation damage (microdose) to cells may be considerably smaller. Since the mechanisms for intracellular binding of ruthenium are not understood, the above inferences are at best semi-quantitative at this time. Further studies will be required to more precisely answer the questions on radiation dosimetry.

6.5 Colloidal Preparations

Radiocolloids depending upon their particle size, net electrical charge and other properties have found many routine uses in nuclear medicine. Imaging of the bone marrow, studies of the reticuloendothelial system of the liver and spleen, and lymphoscintigraphy are important applications.

Whereas the good imaging characteristics of⁹⁷Ru would allow long-term imaging and studies of the above-mentioned structures, investigations on colloidal ruthenium preparations have not received much emphasis. In one study¹⁴) a ruthenium-sulfur colloid was prepared and evaluated for imaging the lymphatic system in rabbits. A commercial antimony sulfide colloid kit was utilized for preparing the^{99m}Tc-labeled material which was used as a control for comparison. The ruthenium colloid was prepared as follows. To a neutralized solution of¹⁰³Ru-chloride, 40 mg of sodium carbonate and 30 mg of gelatin were added. Hydrogen sulfide was bubbled into the mixed solution for 5 min. The solution was degassed at 50 °C by bubbling nitrogen and the pH was then adjusted to 7 with hydrochloric acid. Intermittent degassing was also required during the pH adjustment step. The particle size of the resulting radiocolloid was determined to be < 30 nm using the polycarbonate membrane (Nucleopore) filtration technique. Paper and thin-layer chromatography were used for quality control to determine the amount of unbound ruthenium (consistently < 5%). The¹⁰³Ru-sulfur colloid was injected subcutaneously into the right foot pad of rabbits and images obtained for up to five days post injection. Typical scans are shown in Fig. 7. These images are claimed to be superior to those using the^{99m}Tc-antimony sulfide colloid. A significant portion of the latter does not

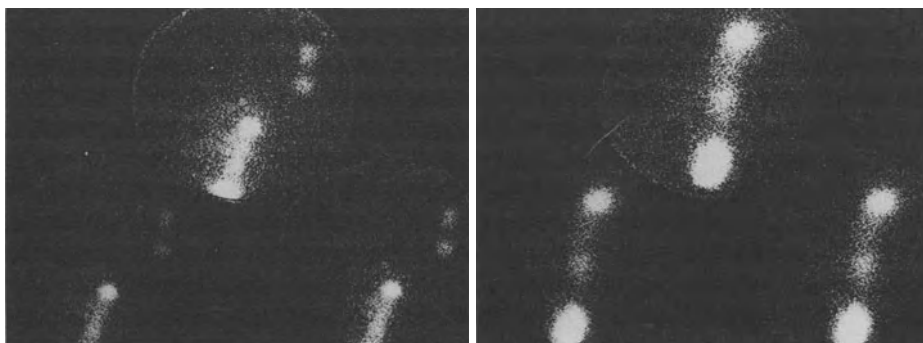


Fig. 7. Visualization of the lymphatics in rabbit using ^{103}Ru -sulfur colloid (<30 nm particles) subcutaneously injected into the right foot pad. *Left*: 15 min post injection; *right*: 2 days post injection

move from the injection site and movement to the pelvic area and beyond is quite slow. In contrast, the ^{103}Ru -sulfur colloid moves up the lymphatic system relatively rapidly and good images of the pelvic nodes are obtained at 15 min to 2 days after injection. Late imaging is obviously not possible with $^{99\text{m}}\text{Tc}$ and this is again where the major advantage of ^{97}Ru would lie in a practical sense.

6.6 Organometallic Derivatives

Within this class of compounds, the main emphasis has been on investigations with ruthenocene and its derivatives. As mentioned earlier, Wenzel and coworkers have undertaken extensive studies on the synthesis and biological evaluation of a member of ^{103}Ru -ruthenocene derivatives with a view to developing organ-specific imaging agents ^{35, 64–75, 89–92}). Despite the fact that stable organometallic bonds in ruthenocene prevent ruthenium from direct binding to other ligands, it has been suggested that variously derivatizing the aromatic ligand may induce ruthenium to localize in specific organs.

The synthesis of radiolabeled metallocenes using ferrocene as a precursor was first reported in 1975 ⁸⁹). Thin-layer chromatography was utilized for the separation of ^{59}Fe , ^{103}Ru , and ^{191}Os derivatives. The parent compound ruthenocene was shown to be more stable *in vivo* in mice and rats than ferrocene, and was eventually excreted through the bile as well as urine following hydroxylation and formation of a glucuronide conjugate in the liver ⁹⁰). Liver and the gastrointestinal system retained a small fraction of the compound for many weeks after injection perhaps due to the formation of ionic ruthenium ⁷⁰). Ruthenocene carboxylic acid was found in mice to be rapidly excreted via the kidneys ($t_{1/2} \sim 2$ h) and thus may be promising as a renal imaging agent ³⁵). The estradiol and cholesterol esters of ruthenocene carboxylic acid were also studied as possible imaging agents for the adrenals, uterus and ovary, and for other applications ⁶⁸). However, these agents displayed the highest concentration in the kidneys and liver. Acetyl ruthenocene derivatives ^{65–71}) on the other hand were shown to appreciably localize in the adrenals ⁶⁵) but high concentrations in surrounding structures including the liver, kidney as well as in the lung considerably

diminish its promise as an adrenal imaging agent. The cinnamoyl and 3-phenylpropenyl-1-one derivatives of ruthenocene were found to localize in thymocytes following intraperitoneal administration into mice and rats^{93,94}. The uptake appears to be due to the thymus specificity of a liver metabolite of these compounds. A number of ruthenocene derivatives were also studied for tumor localizing properties⁶⁶. Of these, two that showed favorable tumor to organ ratios comparable to those achieved with ⁶⁷Ga citrate were vinylbenzoyl- and di(methylcarboxylate)ruthenocene. The tumor concentration, however, was low and quite variable and dependent upon the tumor size.

A number of other ruthenocene derivatives were synthesized and studied recently. The aminosugar derivatives (glucosamine, galactosamine, mannosamine) were found to localize in the kidneys and liver in high concentration and eventually excreted intact into the urine⁶⁹. The derivatives with biogenic amines were also prepared and studied⁷². The ^{103m}Rh-rhodocene derivatives were separated from the parent ¹⁰³Ru-ruthenocene derivatives by solvent extraction, and their *in vivo* distribution was shown to differ from the parent compounds⁹¹. In a recent study⁹², the organ distribution of ¹⁰³Ru-acetyl ruthenocene was shown to be markedly affected by competing drugs in addition to being sex-dependent. The effect could be due to competition for steroid receptors or due to enzyme activation that may result into the production of different binding moieties. The synthesis of ¹⁰³Ru-labeled ruthenocene haloperidol using ferrocene haloperidol precursor was reported recently⁷⁵. Contrary to expectations of its localization into brain, the compound was found to show high concentration in the lungs.

Ruthenocene derivatives labeled with ⁹⁷Ru may eventually find useful human applications. However, evaluations to assess their clinical utility have not been undertaken.

6.7 Tumor Localizing Agents

A number of ruthenium compounds, investigated as agents suitable for tumor imaging, have already been covered in earlier sections under different categories. These include ruthenium chloride, various ammine complexes (including ruthenium red), and chelates and organometallic derivatives. This section focuses on some of the recent and more promising tumor localizing agents that constitute diverse chemical compositions and structures. Attempts have been made to radiolabel chemotherapeutic drugs, proteins and macromolecules, and miscellaneous ruthenium compounds that display antitumor action, and to investigate their tumor localizing properties in animal tumor models.

The anticancer drug bleomycin (BLM) tends to concentrate in a number of tumors¹¹³) and attempts have been made to label it, for tumor imaging applications, with a variety of radiometals including ⁵⁷Co¹¹⁴⁻¹¹⁷), ⁶⁴Cu and ⁶⁷Cu¹¹³⁻¹²⁰), ¹¹¹In¹²⁰⁻¹²²), ⁶²Zn¹²³) and ^{69m}Zn, ^{99m}Tc, ⁶⁷Ga etc.¹²⁰). Among these, only ¹¹¹In- and ⁵⁷Co-labeled preparations have shown sufficient promise for tumor delineation by radiosciintigraphy. Bleomycin has also been labeled with no carrier added ¹⁰³Ru with a 50% radiochemical yield¹²⁴) and the biodistribution results were claimed to be encouraging. In another study, labeling with both ¹⁰³Ru and ⁹⁷Ru was carried out in a more reproducible fashion and with consistently greater than 75% incorporation

of the radioactivity¹¹⁹). The method was as follows. To an aqueous solution (9 mg/ml) of BLM, under slow argon bubbling, was added an aliquot (1–5 µg tin) of a freshly prepared stannous chloride solution (1 mg/ml in 0.1 N HCl). Carrier-free ⁹⁷Ru or ¹⁰³Ru trichloride in 3 N HCl was added next, and the pH then adjusted to between 6 and 8 using dilute NaOH. The molar ratio of BLM to tin was kept between 27 and 135. The mixture following incubation at 37 °C for 3 h was chromatographically purified using an ammonium formate gradient (0.05–1.0 M). Three UV peaks were separated: BLM A₁, B₂, and A₂, all containing a proportionate amount of radoruthenium. In addition, TLC (silica gel) using 10% (w/v) ammonium acetate/methanol (1:1) gave fractions with R_f values of 0.73, 0.63, and 0.38 corresponding to BLM A₁, B₂, and A₂, respectively. An unknown radioactivity peak at R_f = 0.22 was also present. Biodistribution data in melanoma-bearing mice demonstrated the following relative effectiveness for various labeled. BLM preparations for tumor imaging: ⁵⁷Co > ⁶⁷Cu > ⁹⁷Ru¹¹⁹). The tumor to tissue ratios (at 24 h) for ⁶⁷Cu-BLM and ⁹⁷Ru-BLM were comparable (Blood, 1.7–3.4; muscle, 5.7–7.6; liver, 0.6–0.7; lung, 0.7–1.0); however, ⁵⁷Co-BLM provided much higher ratios (Blood, 37; muscle, 25; liver, 3; lung, 11) and the greatest total uptake in tumor (1–2% per g). In all cases, >90% of the injected activity was excreted at 24 h. Even though these results indicate Ru-BLM to be only modestly effective for imaging, other tumor models must be evaluated in order to more precisely determine the ultimate clinical potential of ⁹⁷Ru-BLM as a tumor imaging agent. In another recent study¹²⁵) the ¹⁰³Ru analog of a stable, previously characterized (nmr, differential pulse electrochemistry), Ru(NH₃)₅(pyrimidine)-BLM derivative was prepared. The method consisted of preparing chloropentaammineruthenium(III) from a ¹⁰³Ru chloride using standard techniques and then converting it in situ to aquopentaammineruthenium(II) by Zn/Hg reduction in trifluoroacetic acid under argon. To the resulting mixture, 15 mg synthetic BLM-A₂ (or commercial BLM mixture) was added and oxygen bubbled for 1 h. Sephadex CM-120 purification gave the labeled derivative in 50–80% yield. The product was stable indefinitely when stored frozen. Tissue distribution in normal and tumor bearing mice showed a behavior essentially unchanged from unlabeled bleomycin. In preliminary studies, the whole body activity at 24 h was 16 ± 4% of the injected dose and uptake by the tumor (melanoma) was 2.1 ± 0.4% per gram. Tumor to tissue ratios were: blood, 4.0; muscle, 7.1; kidney 0.44; and liver, 1.23. Results of this study suggest that ⁹⁷Ru-BLM using this procedure should be a more promising agent for tumor localization. It should also prove useful as a radio-tracer in investigations to study the distribution and the mechanism of action of bleomycin on human tumors.

The lipophilic chelates of Ru(II) with 1,10-phenanthroline (including the tetramethyl derivative), and of Ru(III) with 8-hydroxyquinoline 7-carboxylic acid acetate (oxine 7-CA acetate) have also been investigated for tumor localizing properties¹²⁶). These compounds, as described in an earlier section, behave primarily as hepatobiliary agents but differ in their biliary excretion kinetics and to some extent are also excreted into the urine. As expected, the tumor uptake in mice (EMT-6 sarcoma) of the 1,10-phenanthroline chelate was about twice as high compared to the more lipophilic 3,4,7,8-tetramethyl 1,10-phenanthroline chelate. Even though some tumor-to-tissue ratios of the former were adequate for imaging (Blood, 1.7; muscle, 7.7), high concentrations in the liver and the kidneys would preclude its usefulness for

scanning tumors in the abdominal region. The chelate of Ru(III) with oxine 7-CA acetate, on the other hand produced more interesting results⁴⁸. The excretion of this compound in mice was quite rapid with about 80% of the activity (¹⁰³Ru) leaving the body at 24 h. At 72 h, the retained dose was 9.6%. Even though the absolute tumor concentration in EMT-6 sarcoma mice was lower compared to ⁶⁷Ga citrate (2.4% vs 7.1% per g at 24 h), the tumor concentration index (TCI) was higher especially at late time periods (2.7 vs 1.6 at 72 h). This is due to the higher excretion of the ruthenium chelate and its more favorable tumor to tissue (particularly liver and gut) ratios. Further evaluation of this compound in other tumor models and in higher animals should be highly worthwhile. The mechanism of the tumor uptake also needs to be elucidated.

A complex of ruthenium with transferrin (TF) appears so far to be the most promising agent for tumor imaging applications^{48, 96, 127, 128}. Based on animal results, ⁹⁷Ru-TF indeed seems to fulfill the various requirements for a good tumor imaging agent. The criteria include rapid and high total tumor uptake, good tumor to normal tissue ratios, low whole body retention (high tumor concentration index), and suitable imaging photons. The typical radiolabeling procedure^{48, 96, 129} is as follows. Twenty mg purified iron-free human transferrin is dissolved in 2 ml of a 0.1 M pH 7 sodium acetate solution. The desired amount of ruthenium activity ¹⁰³Ru or ⁹⁷Ru as chlorides in ~3 N HCl) is added to a separate vial and the HCl blown off with nitrogen under gentle heating. A two-fold molar excess of nitrilotriacetic acid solution is added, the pH adjusted to 2.5–3, and the mixture heated at 90–100 °C for 30 minutes. The pH is then adjusted to 6–7. The dissolved TF in acetate buffer is next added to the cooled Ru vial followed by 0.1 ml of 0.1 M sodium bicarbonate

Table 12. A comparison of the in vivo distribution of ¹⁰³Ru-labeled transferrin (TF) and ⁶⁷Ga-citrate (Ga) in tumor (EMT-6 sarcoma) bearing mice (percent dose per g; n = 6)^a.

Tissue	Time after injection, h							
	6		24		48		72	
	TF	Ga	TF	Ga	TF	Ga	TF	Ga
Blood	23.73	11.17	12.89	1.81	4.56	0.51	2.49	0.44
Tumor	8.67	6.01	12.75	7.09	13.34	5.05	12.39	4.53
Liver	12.26	8.52	8.85	9.30	7.46	9.49	6.06	8.35
Kidney	8.92	7.44	8.42	9.21	7.16	8.03	6.14	7.50
Muscle	1.38	0.87	1.57	0.53	1.32	0.47	1.07	0.47
Heart	4.60	3.09	3.81	2.21	2.47	1.69	1.92	1.82
Spleen	9.12	5.78	8.74	8.37	7.30	6.60	5.77	6.52
Bone	4.26	16.16	3.56	17.75	2.61	17.55	2.50	15.38
% Dose remaining in whole body	80.0	65.2	66.6	59.6	55.9	50.7	44.2	43.9

^a The ¹⁰³Ru-transferrin was purified on a Sephadex G-150 (0.9 × 100 cm) column. Fraction used here consisted essentially of monomeric transferrin with ≈65% of the original ¹⁰³Ru activity associated with it. Dose of transferrin was ≈3.3 mg/kg body weight.

solution. The mixture, final volume ~ 3 ml, pH about 7.5–8, is heated at 40 °C for 2 h. The preparation is purified on a 0.9×100 cm G-150 Sephadex column with 0.154 M NaCl–0.005 M pH 7 sodium acetate as the eluent. Pure monomeric labeled TF separates in a 60–90% yield, based on radioactivity. The purity of this fraction based on polyacrylamide gel electrophoresis (tris-borate buffer, pH 8.6) should exceed 95%.

Representative tissue distribution results following the intravenous administration of ^{103}Ru -TF in mice with subcutaneous EMT-6 sarcoma are summarized in Tables 12 and 13 and shown in Fig. 8⁴⁸). Corresponding results obtained with ^{67}Ga citrate are included for comparison. The maximum tumor concentration and the time needed to reach this concentration were very similar in another study in adenocarcinoma transplanted mice¹²⁸). In this tumor system, ^{67}Ga citrate, ^{123}I -TF, ^{131}I -albumin, and ^{123}I -fibrinogen gave similar maximum tumor concentrations (5.1, 6.9, 5.8, 4.7% dose per g respectively). The time required to achieve these concentrations ranged from 2 h for ^{67}Ga to 6 h for ^{123}I -fibrinogen and ^{123}I -TF¹²⁸). The maximum tumor concentration of ^{97}Ru -TF was three times higher (16.8% dose per g) but it took longer (24 h) to achieve this concentration. Whole body autoradiographs in rats with ^{97}Ru -TF and ^{67}Ga citrate showed a uniform and homogeneous distribution of activity within the tumors pointing to a common localization mechanism and similar binding to cellular components for both radiotracers.

It is possible that when ruthenium chloride is administered intravenously, a major portion of it becomes bound to transferrin and is initially transported to various tissues as the ruthenium-transferrin complex. Apparently, the in-vivo kinetics of this binding are not very favorable; the result is nonspecific localization of a significant part of the ruthenium activity in other tissues (Tables 6–7). When in-vitro labeled ruthenium transferrin is injected, a more specific tumor uptake results with diminished background activity (Tables 12–13). These results can be explained on the basis of the hypothesis of the presence of transferrin receptor sites on the tumor cell surface. Considerable evidence has been accumulated recently in support of a transferrin

Table 13. Tumor-to-tissue ratios and tumor concentration index (TCI) of ^{103}Ru -labeled transferrin compared to ^{67}Ga citrate^a

Compound	Time (h)	Ratio, Tumor-to-				TCI ^b
		Blood	Muscle	Liver	Kidney	
Ruthenium-103-transferrin	6	0.4	6.6	0.7	1.0	—
	24	1.0	8.8	1.5	1.5	2.70
	48	3.0	10.6	1.8	1.9	3.60
	72	5.0	11.8	2.0	2.0	4.08
Gallium-67 citrate	6	0.5	7.3	0.7	0.8	—
	24	4.2	13.4	0.8	0.8	1.81
	48	10.7	11.0	0.6	0.6	1.48
	72	10.7	10.8	0.6	0.6	1.57

^a Biodistribution studies were performed in EMT-6 sarcoma-bearing mice. For representative data, see Table 12.

^b For the definition of TCI, refer to Table 7.

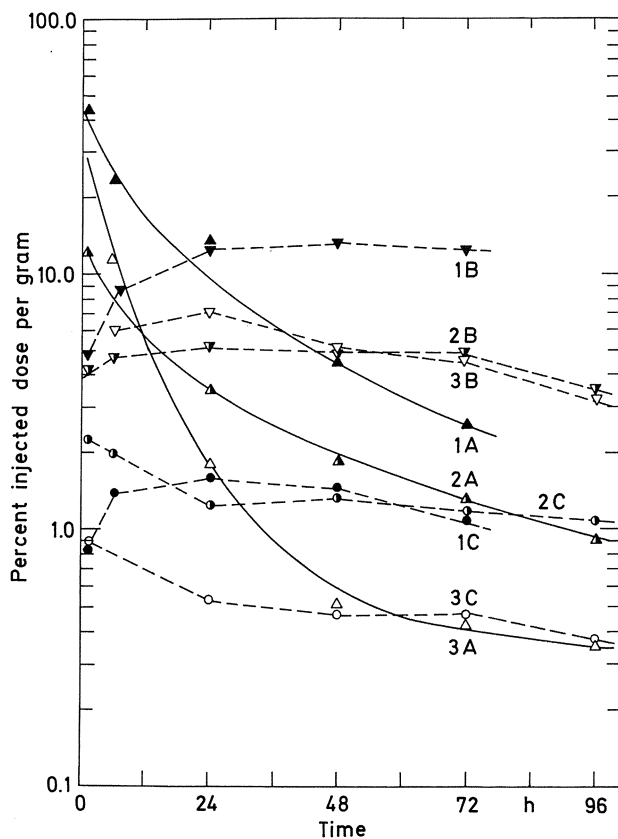


Fig. 8. Activity levels of ^{103}Ru -transferrin (1), ^{103}Ru -chloride (2), and ^{67}Ga -citrate (3) in blood (A), tumor (B), and muscle (C) at various time intervals in EMT-6 sarcoma (Balb/c) mice ($n = 5$ for each data point)

mediated uptake of gallium citrate by tumor tissue^{82-85, 130-132}) and it is likely that a similar mechanism is operative in the case of ruthenium-labeled transferrin.

The blood disappearance of various labeled transferrin preparations was different¹²⁸). Iodinated TF persisted in the circulation longer than ^{97}Ru -TF which in turn persisted longer than ^{67}Ga citrate. Higher tumor uptake of Ru-TF may indeed be the result of its longer blood persistence which allows a longer reperfusion time. The difference in biodistribution between the various TF radiotracers and in particular between ^{97}Ru -TF and ^{67}Ga citrate could nevertheless be due to not one single but perhaps several mechanisms. Differences in the extraction kinetics and thermodynamic and kinetic stability constants of the metal-TF complexes may produce variations in tissue distribution or again, these could be caused by the relative affinities that the TF complexes may have for the tumor cell membrane binding sites. It is obvious that detailed mechanistic studies will be necessary in order to clarify these issues.

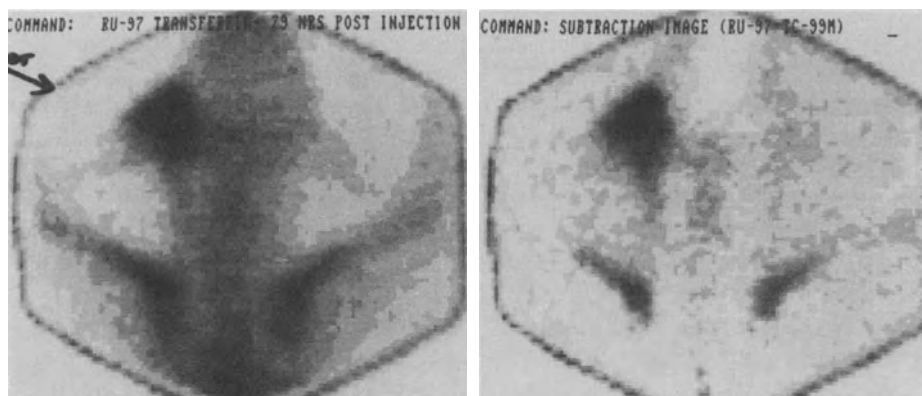


Fig. 9. ^{97}Ru -transferrin images in a dog with a fibrosarcoma of the left ear involving the lymph glands of the neck with metastases to the lung, in addition to a mammary tumor, 79 h after injection. *Left:* without background subtraction. *Right:* blood background subtracted using $^{99\text{m}}\text{Tc}$ -labeled human serum albumin. (Srivastava and Bigler, unpublished data)

The biological advantages of ^{97}Ru -TF over ^{67}Ga citrate are not significantly greater except for imaging in the abdominal area. However, the higher tumor uptake and higher tumor concentration indices that are achieved with ^{97}Ru -TF combined with better imaging properties of ^{97}Ru (Fig. 9) demonstrate the superiority of ^{97}Ru -TF as a tumor imaging agent. The figure of merit for ^{97}Ru -TF based on animal results is 3–5 times higher than that of ^{67}Ga citrate. Human evaluation of ^{97}Ru -TF is warranted and will be necessary to validate and confirm the favorable animal results.

7 Conclusion

Even though $^{99\text{m}}\text{Tc}$ -labeled compounds have dominated the scene in radiopharmaceutical development for over twenty years and their clinical advantage is clearly well established, considerable effort from time to time has been focused on investigations involving intermediate half-life isotopes for a number of specific applications. In terms of nuclear and chemical characteristics, ^{97}Ru appears to be an ideal radionuclide for applications that require periodic or delayed imaging for up to several days following a single administration into the patient. Work summarized in this chapter demonstrates that a number of ^{97}Ru -labeled compounds exhibit sufficient promise to fulfill this important need in nuclear medicine. Based on data in laboratory animals, many ^{97}Ru compounds warrant a systematic and widespread clinical evaluation. One of the compounds (^{97}Ru -DISIDA) has already been investigated in patients and exhibits superior characteristics for the delayed imaging of various hepatobiliary disorders. Ruthenium-97-labeled transferrin shows particular promise as a tumor imaging agent.

A major reason for the lack of progress to the stage of human studies has been the limited and unreliable supply of ruthenium-97. Economical production

requires use of a charged particle accelerator and these are not routinely available except in specialized institutions. Recently developed production methods particularly in the U.S. are expected to resolve this problem, and make adequate quantities of ^{97}Ru available for clinical investigations. In addition, continuing interest in clinical and biological research on ruthenium compounds, as exemplified by the material presented in this volume, bodes well for the future of ^{97}Ru in clinical radioimaging.

8 Acknowledgements

The authors are grateful to many colleagues and collaborators whose contributions have been included and cited in this chapter. Excellent secretarial assistance of Mrs. A. Ruggiero is thankfully acknowledged. Work at Brookhaven National Laboratory was carried out under the auspices of the U.S. Department of Energy, Office of Health and Environmental Research, under Contract No. DE-AC2-76CH00016.

9 References

1. Srivastava SC, Richards P (1983) Technetium labeled compounds, in: Rayudu GVS (ed), *Radiotracers in Biology and Medicine*, CRC Press, Boca Raton, Florida, pp 107–185
2. Clarke MJ, Podbielski L (1987) *Medical Diagnostic Imaging with Complexes of ^{99m}Tc* , *Coord Chem Rev* 78: 253–331
3. Lederer CM, Shirley VS (eds) (1978) *Table of Isotopes 7th edn*, Wiley, New York
4. Subramanian G, McAfee JG (1970) *J Nucl Med* 11: 365
5. Koehler DC (1981) *Radioactive Decay Data Tables* available from NTIS, Springfield VA: USDOE/TIC-11026
6. Lebowitz E, Kinsley M, Klotz P, Bachsmith C, Ansari A, Richards P, Atkins HL (1974) *J Nucl Med* 15: 511
7. Graf HP, Munzel HJ (1974) *J Inorg Nucl Chem* 36: 3647
8. Comar D, Crouzel C (1976) *Radiochem Radioanal Lett* 27: 307
9. Comparetto G, Qaim SM (1980) *Radiochim Acta* 27: 177
10. Silvester DJ, Helus F, Maier-Borst W (1979) *J Labelled Compds Lett* 27: 307
11. Gessener M, Music S, Babarovic B, Vlatkovic (1979) *Int J. Appl Radiat Isot* 30: 578
12. Pao PJ, Zhou JL, Silvester DJ, Waters SL (1981) *Radiochem Radioanal Lett* 46: 21
13. Ku T, Richards P, Srivastava SC, Prach T, Stang LG (1978), *Proc 2nd Congr World Fed Nucl Med Biol*, WFNMB, Washington, p 17
14. Srivastava SC, Richards P, Som P, Meinken G, Atkins HL, Sewatkar A, Ku TH (1980) in: *Frontiers in nuclear medicine*, Springer, Berlin Heidelberg New York, pp 123–133
15. Blann M (1984) *Lawrence Livermore National Laboratory Report UCID-20169*
16. Lagunas-Solar M, Avila MJ, Navarro NJ, Johnson PC (1983) *Int J Appl Radiat Isot* 34: 915
17. Ward, T, Brookhaven National Laboratory, private communication
18. Waters SL (1983) *Coord Chem Rev.* 52: 171
19. Fletcher JM, Martin FS (1957) in: *Peaceful uses of atomic energy*, vol 7, IAEA, Vienna, pp 141–144
20. Griffith WP (1967) in: *The chemistry of the rarer platinum metals*. Interscience, London
21. Thompson RC, Weeks MH, Holles OL, Ballou GE, Oakley WD (1958) *Am J Roentgenol* 79: 1026
22. Gilbert IG (1964) *Biochim Biophys Acta* 79: 568
23. Seidel D, Catsch A, Schweer KH (1963) *Strahlentherapie* 122: 595
24. Sastry BV (1966) *Toxic Appl Pharmacol* 9: 419
25. Pusch WH (1968) *Health Phys* 15: 515
26. Yamagata I, Iwashima K, Knuma T, Watari K, Nagai T (1969) *Health Phys* 16: 159

27. Furchner JE, Richmond CR, Drake GA (1971) *Health Phys* 21: 355
28. Enomoto Y, Watari K, Ichikawa R (1972) *J Radiat Res* 13: 193
29. Berg CG, Ginsberg E (1976) *Health Phys* 30: 329
30. Webber CE, Harvey JW (1976) *Health Phys* 30: 352
31. Bruce RS, Carr TEF (1961) *Reactor Sci Technol, J Nucl Energy* 14: 9
32. Bruce RS, Carr TEF (1961) *Reactor Sci Technol, J Nucl Energy* 14: 145
33. Bruce RS, Carr TEF, Collins ME (1962) *Health Phys* 8: 397
34. Buldakov LA (1961) in: *Raspredelenie, Biol Deistvie i Migratsiya Radiat Izotopov*, Gos Izd Met Lit Sb, Moscow, p 164
35. Wenzel M, Nipper E, Klose W (1977) *J. Nucl Med* 18: 367
36. Vasington FD, Gazzotti P, Tiozzo R, Carofoli E (1972) *Biochim Biophys Acta* 256: 43
37. Moore CL (1971) *Biochem Biophys Res Comm* 42: 298
38. Smith PM, Fealey T, Early JE, Silverton JV (1971) *Inorg Chem* 10: 1943
39. Luft JH (1965) *J Cell Biol* 27: 61A
40. Rieder K, Taube H (1977) *J Amer Chem Soc* 99: 7891
41. Fischer H, Tom GM, Taube H (1976) *J Amer Chem Soc* 98: 5512
42. Reed KC, Bygrave FL (1974) *FEBS Letters* 46: 109
43. Petitjean F, Loch C, Somar D (1981) *J Labelled Compds Radiopharm* 18: 170A
44. Anghileri LJ (1974) *J Nucl Med Biol* 18: 155
45. Anghileri LJ (1975) *Strahlentherapie* 149: 173
46. Anghileri LJ (1975) *J Nucl Med* 16: 795
47. Gustafson GT, Pihl E (1967) *Acta Pathol Microbiol Scand* 68: 393
48. Srivastava SC, Richards P, Meinken GE, Larson SM, Grunbaum Z (1981) in: *Radiopharmaceuticals-structure-activity relationships*, Grune and Stratton, New York, pp 207-223
49. Livingstone SE (1975) in: *The chemistry of ruthenium, rhodium, palladium, osmium, iridium, and platinum*, Pergamon, New York
50. Kaplan PD (1976) in: *The platinum metals. Part I: Ruthenium, osmium, rhodium, and iridium*, Ann Rep Inorg Gen Synth Academic Press, New York, pp 222-247
51. Ford PC (1970) *Coord Chem Rev* 5: 75
52. Taube H (1973) *Survey of Progr Chem* 6: 1
53. Durig JR, Danneman J, Behnke WD, Mercer EE (1976) *Chem Biol Interact* 13: 287
54. Giraldi T, Sava G, Bertoli G, Mestroni G, Zassinovich G (1977) *Cancer Res* 37: 2662
55. Bottomley F (1978) *Coord Chem Rev* 26: 7
56. Taube H (1978) *Coord Chem Rev* 26: 33
57. Clarke MJ (1980), *Oncological Implications of the chemistry of ruthenium* in: Sigel H (ed) *Metal ions in biological systems*, Vol 11, Dekker, New York, pp 231-283
58. Clarke MJ (1983), *Ruthenium anticancer agents and the relevant reactions of ruthenium purine complexes*, in: Lippard S (ed), *Chemistry and biochemistry of platinum, gold and other therapeutic agents*, ACS Symposium Series #209, pp 335-354
59. Clarke MJ (1989), *Ruthenium chemistry pertaining to the design of anticancer agents*, This volume, pp 25
60. Clarke MJ, Dowling M, Unpublished data
61. Kuehn CG, Taube H (1976) *J Amer Chem Soc* 98: 689
62. Diamond SE, Taube H (1975) *J Amer Chem Soc* 97: 5921
63. Matsubata T, Creutz C (1978) *J Amer Chem Soc* 100: 6255
64. Stadlbauer D, Nipper E, Wenzel M (1977) *J Labelled Compds Radiopharm* 13: 491
65. Taylor A, Wenzel M (1978) *Biochem J* 172: 77
66. Wenzel M (1978) *Strahlentherapie* 154: 506
67. Schneider M, Wenzel M (1980) *J Labelled Compds Radiopharm* 17: 1
68. Hoffmann K, Riesselmann B, Wenzel M (1980) *J Labelled Compds Radiopharm* 17: 421
69. Schneider M, Wenzel M (1981) *J Labelled Compds Radiopharm* 18: 293
70. Wenzel M, Schneider M, Macha J (1981) *Int J Appl Radiat Isot* 32: 797
71. Schneider M, Wenzel M (1981) *J Labelled Compds Radiopharm* 19: 625
72. Wenzel M, Asindraza P, Schachschneider G (1983) *J Labelled Compds Radiopharm* 20: 1061
73. Wenzel M, Meinhold H, Schachschneider G (1985) *Eur J Nucl Med* 10: 138
74. Wenzel M, Preiss D (1986) *Naturwiss* 73: 509
75. Wenzel M, Wu Y (1988) *Appl Radiat Isot* 39: 1237

76. Srivastava SC, Richards P, Meinken GE, Som P, Atkins HL, Larson SM, Grunbaum Z, Rasey JS, Dowling M, Clarke MJ (1979) in: *Radiopharmaceuticals II*; Proc 2nd Int Symp Radiopharm, Soc Nucl Med, New York, pp 265–274
77. Stritar JA, Taube H (1969) *Inorg Chem* 8: 2281
78. Tanabe M, Yamamoto G (1975) *Acta Med Okayama* 29: 431
79. Tanabe M (1976) *Radioisotopes* 25: 44
80. Mizukawa K, Yamamoto G, Tamai T, Tanabe M, Yamato M (1978) *Radioisotopes* 27: 19
81. Ando A, Ando I, Hiraki T, Hisada K (1988) *Nucl Med Biol* 15: 133
82. Larson SM, Rasey JS, Allen DR, Grundbaum Z (1979) *J Nucl Med* 20: 843
83. Nouvaim AA, Lentle BC, Hill JR (1979) *Int J Nucl Med Biol* 6: 193
84. Hoffer PB (1980) *J Nucl Med* 21: 282
85. Weiner RE, Schreiber GJ, Hoffer PB (1983) *J. Nucl Med* 24: 608
86. Meyer CD, Davis MA (1980) *J. Nucl Med* 21: 79A (Abstr)
87. Subramanyan V, Pratt FF, Mysliwy T, Liteplo M, Camin LL, Liberatore FA, Bilafer FAC, Nigam S, Sivakoff S (1981) *J Labelled Compds Radiopharm* 18: 161A (Abstr)
88. Srivastava SC, Som P, Meinken GE, Sewatkar A, Ku TH (1978) in: *Proc 2nd Int Congr World Fed Nucl Biol*, Washington DC, p 19
89. Langheim D, Wenzel M, Nipper E (1975) *Chem Ber* 198: 146
90. Taylor A, Wenzel M (1978) *Xenobiotica* 8: 107
91. Wenzel M, Wu Y (1987) *Appl Radiat Isot* 38: 67
92. Shani J, Livschitz T, Wenzel M (1985) *Int J Nucl Med Biol* 12: 13
93. Wenzel M, Herken R, Klose W (1977) *Z Naturforsch* 38a: 473
94. Wenzel M, Klose W (1977) *Klin Wochenschrift* 55: 559
95. Oster ZH, Som P, Gil MC, Fairchild RG, Goldman AG, Schachner ER, Sacker DF, Atkins HL, Meinken GE, Srivastava SC, Richards P, Brill AB (1981) *J Nucl Med* 22: 269
96. Som P, Oster ZH, Fairchild RG, Atkins HL, Brill AB, Gil MC, Srivastava SC, Meinken GE, Goldman AG, Richards P (1981) in: *Proc 3rd Intl Radipharm Dosimetry Symp*, Oak Ridge, 1980, HHS Publ FDA 81-8166, pp 346–363
97. Oster ZH, Som P, Gil MC, Goldman AG, Meinken GE, Srivastava SC, Atkins HL, Richards P, Brill AB (1981) *Radiology* 141: 185
98. Anglieri LJ, Ottaviani M, Ricard S, Raynaud C (1981) *Eur J Nucl Med* 6: 403
99. Ikeda I, Inoue O, Kurata K (1977) *J Nucl Med* 18: 1222
100. Loberg MD, Cooper M, Harvey E, Callery P, Faitch W (1976) *J Nucl Med* 17: 633
101. Klingensmith WC, Fritzberg AR, Kuni CC, Lilly JR (1980) *J. Nucl Med* 21: P19
102. Schachner ER, Gil MC, Atkins HL, Som P, Srivastava SC, Badia J, Sacker DF, Fairchild RG, Richards P (1981) *J Nucl Med* 22: 352
103. Schachner ER, Gil MC, Som P, Oster ZH, Atkins HL, Subramanian G, Badia J, Srivastava SC, Richards P, Treves S (1983) *Nucl Med Commun* 4: 94
104. Srivastava SC, Meinken GE (1984) *J Labelled Compds Radiopharm* 21: 1048
105. Zanzi I, Srivastava SC, Meinken GE, Robeson W, Mausner LF, Fairchild RG, Margouloff D (1986) *J. Nucl Med* 27: 1072
106. Zanzi I, Srivastava SC, Meinken GE, Robeson W, Mausner LF, Fairchild RG, Margouloff D (1989) *Nucl Med Biol* (in press)
107. Zanzi I, Markowitz J, Srivastava SC, Robeson W, Mausner LF, Meinken GE, Margouloff D (1987) *J Nucl Med* 28: 596
108. Thakur ML, Welch MJ, Joist JH, Coleman RE (1976) *Thromb Res* 9: 345
109. Danpure HJ, Osman S, Brady F (1982) *Br J Radiol* 55: 247
110. Thakur ML, Barry MJ (1982) *J Labelled Compds Radiopharm* 19: 1410
111. Desai AG, Thakur ML (1986) *CRC Critical Rev Clin Lab Sci* 24: 95
112. Zoghbi SS, Thakur ML, Gottschalk A, Pande S, Srivastava SC, Richards P (1981) *J Labelled Compds Radiopharm* 18: 280
113. Hecht SM (ed) (1979) *Bleomycin: chemical, biochemical, and biological aspects*, Springer Berlin Heidelberg New York
114. Nouel JP, Renault H, Robert CJ, Wicart L (1972) *Nouv Presse Med* 1: 95
115. Maeda T, Kono A, Kohima M (1973) *Jpn J Nucl Med* 10: 109
116. Eckelman WC, Rzeszutarski WJ, Siegel BA, Kubota H, Chelliah M, Stevenson T, Reba RC (1975) *J Nucl Med* 16: 1033

117. Nieweg OE, Beekhuis H, Piers DA, Sluiter HJ, Van der Wal AM, Woldring MG (1984) *Cancer* 53: 1675
118. Van de Poll MAPC, Versluis A, Rasker JJ, Jurjens H, Woldring MG (1976) *Nucl-Med* 15: 86
119. Shao HS, Meinken GE, Srivastava SC, Slosman D, Sacker DF, Som P, Brill AB (1986) *J Nucl Med* 27: 1044
120. Reba RC, Eckelman WC, Poulouse KP, Grove RB, Stevenson JS, Rzeszotarski WJ, Primack A (1975) in: *Radiopharmaceuticals*, Subramanian G, Rhodes BA, Cooper JF, Sodd VJ (eds), Soc Nucl Med, New York, pp 464–473
121. Thakur ML, Merrick MV, Gunasekera SW (1973) in: *Radiopharmaceuticals and labeled compounds*, IAEA Vienna, pp 183–193
122. Graham LS, Verma RC, Touya JJ, Siverstein MJ, Bennett LR (1975) in: *Radiopharmaceuticals*, Subramanian G, Rhodes BA, Cooper JF, Sodd VJ (eds), Soc Nucl Med, New York, pp 452–457
123. Taylor DM, Cottral MF (1975) in: *Radiopharmaceuticals*, Subramanian G, Rhodes BA, Cooper JF, Sodd VJ (eds), Soc Nucl Med, New York, pp 458–463
124. Stern PH, Halpern SE, Hagan PL, Howell SB, Dabbs JE, Gordon RM (1981) *J Natl Cancer Inst* 66: 807
125. Margalit R, Gray HB, Youngquist S, Clarke MJ, Srivastava SC, Meinken GM (1985) Unpublished data
126. Srivastava SC, Richards P, Meinken G, Som P, Atkins HL, Larson SM, Grunbaum Z, Rasey JS (1978) Brookhaven National Laboratory Report #24894
127. Srivastava SC, Meinken GE, Richards P, Larson SM, Grunbaum Z, Rasey JS (1980) *J Nucl Med* 21: P79
128. Som P, Oster ZH, Matsui K, Guglielmi G, Persson BRR, Pellettieri ML, Srivastava SC, Richards P, Atkins HL, Brill AB (1983) *Eur J Nucl Med* 8: 491
129. Richards P, Srivastava SC, Meinken GE (1984) U.S. Patent #4,448,762
130. Larson SM (1978) *Sem Nucl Med* 8: 193
131. Wong H, Turner UK, English D (1980) *Int J Nucl Med Biol* 7: 9
132. Tzen K, Oster ZH, Wagner HN (1990) *J Nucl Med* 21: 31

The Antitumor Activity of Transition and Main-Group Metal Cyclopentadienyl Complexes

Petra Köpf-Maier

Institut für Anatomie, Freie Universität Berlin, Königin-Luise-Straße 15, D-1000 Berlin 33, FRG

Cyclopentadienyl metal complexes are organometallic compounds which exhibit antiproliferative properties *in vivo* and *in vitro*. They contain a non-platinum-group metal as central atom and are represented by compounds of different structural type:

- i) neutral bis(η^5 -cyclopentadienyl)metal ("metallocene") diacido complexes $(C_5H_5)_2MX_2$ including an early transition metal such as titanium(IV) or vanadium(IV) as central metal atom;
- ii) ionic metallocenium salts $[(C_5H_5)_2M]^+X^-$ containing a medium transition metal, e.g., iron(III), as central metal;
- iii) uncharged decasubstituted metallocenes $(C_5R_5)_2M$ ($R = C_6H_5, C_6H_5CH_2$) with a main-group element, e.g., tin(II) or germanium(II), as central metal.

Numerous representatives of these diverse types of cyclopentadienyl metal complexes were shown to exhibit antiproliferative and antitumor properties *in vitro* and *in vivo*, whereby most available data concern titanocene complexes. The latter revealed to be effective against fluid experimental tumors (e.g., Ehrlich ascites tumor, sarcoma 180) as well as against solid animal tumors (e.g., sarcoma 180, B16 melanoma, colon 38 carcinoma, Lewis lung carcinoma) and heterotransplanted human lung and colon carcinomas. In most cases, the activity was demonstrated by pronounced growth inhibition of the tumors following substance application and confirmed by cytokinetic phenomena as well as by severe cytologic and histologic changes occurring in treated tumors.

The observed cytobiological events gave interesting insights into the molecular mechanism of action of antitumor cyclopentadienyl metal complexes and showed that mainly nucleic acid metabolism is influenced by treatment with metallocene complexes. Model complexes have been synthesized by several authors, illustrating the possibilities of metal (Ti, Mo) nucleobase linkage as well as metal (Mo, V) phosphate interaction.

All these results qualify organometallic metal complexes to be a new and independent group of non-platinum-group metal antitumor agents which clearly differ from known organic and inorganic cytostatics and are distinguished by unusual biological properties. They represent interesting candidates for future biological and clinical investigations.

Pharmacokinetic and toxicological studies showed a main accumulation of titanium in the liver and the intestine and revealed hepatotoxicity to be obviously the dose-limiting toxicity, whereas nephrotoxicity and the depression of bone marrow function seemed to be negligible.

1 Introduction	153
2 Antiproliferative Properties of Cyclopentadienyl Metal Complexes	154
2.1 Results with Cells Cultured <i>in Vitro</i>	154
2.2 Results with Ascitic Animal Tumors	156
2.3 Results with Solid Animal Tumors	161
2.4 Results with Heterotransplanted Human Tumors	164

3	Other Biological Properties	170
3.1	Radiosensitizing Properties	170
3.2	Antiviral Properties	170
3.3	Antiinflammatory Properties	172
4	Toxicologic and Pharmacokinetic Properties	172
4.1	Organ Toxicity	172
4.2	Organ Distribution and Pharmacokinetics	174
5	Cellular Mode of Action.	176
5.1	Precursor Incorporation Studies	176
5.2	Cytokinetic Studies	176
5.3	Studies into Subcellular Distribution of Central Metal Atoms	177
6	Model Complexes	180
7	Conclusions and Outlook	182
8	Acknowledgements	183
9	References	183

1 Introduction

By the detection of antitumor properties for the inorganic complex *cis*-diammine-dichloroplatinum(II) *cis*-(NH₃)₂PtCl₂, the so-called cisplatin^{1,2}, a new era of cancer chemotherapy was opened. This event markedly improved the therapeutic situation in the case of urogenital tumors, carcinomas of the head and neck, and to a less extent, in the case of lung tumors²⁻⁵. Moreover, a broad search for other antitumor inorganic and organometallic complexes was stimulated, with the hope that

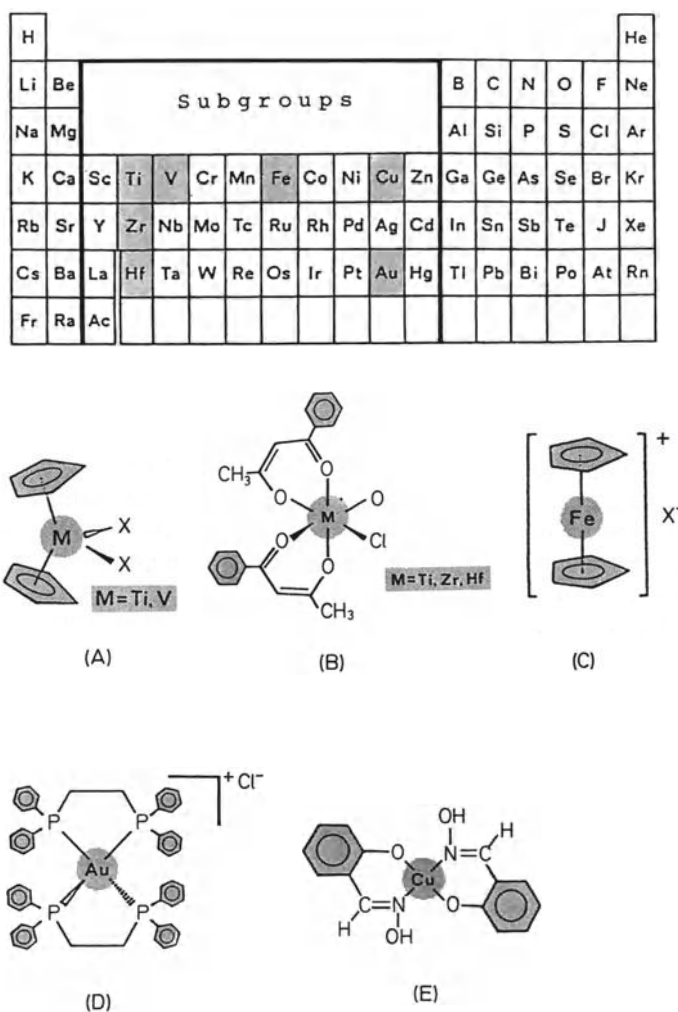


Fig. 1. Examples of transition metal antitumor complexes and position of their central metal atoms in the Periodic Table of Elements. (A) Bis(η^5 -cyclopentadienyl)metal(IV) dihalides; (B) bis(benzoyl-acetonato)titanium(IV) dihalides; (C) bis(η^5 -cyclopentadienyl)iron(III) complex salts; (D) *trans* bis(salicylaldoximato)copper(II); (E) bis[1,2-bis(diphenylphosphino)ethane]gold(I) chloride

new compounds might widen the field of indication and further improve the therapeutic situation for patients suffering from neoplastic diseases.

For numerous platinum³⁻⁵, rhodium⁶, and ruthenium^{7,8} complexes, anti-tumor properties have been described during the past years. With regard to non-platinum-group metal cytostatics, main-group metal compounds can be distinguished from transition metal complexes. Within the first group, gallium salts of the type of gallium(III) nitrate⁹ and organometallic germanium complexes such as the monomeric 8,8-diethyl-2-[3-(N-dimethylamino)propyl]-2-aza-8-germaspiro[4,5]decane (spirogermanium)¹⁰ and the polymeric bis[(carboxyethyl)germanium] trioxide (germanium sesquioxide, Ge-132)¹¹ are the main representatives that have been investigated in clinical trials since several years. In the case of non-platinum-group transition metal compounds, numerous complexes of quite different kind were found to exhibit strong antitumor properties (Fig. 1):

- Early transition metal complexes containing, e.g., titanium or vanadium as central metal atom. These compounds are represented by bis(η^5 -cyclopentadienyl)diacydo-metal(IV) complexes such as titanocene or vanadocene dihalides¹²⁻¹⁴ and bis(benzoylacetato)titanium(IV) dihalides and bis(alkoxides)^{15, 16}.
- Medium transition metal complexes of the type of bis(η^5 -cyclopentadienyl)iron(III) (ferricenium) complex salts showed antiproliferative effectivity against experimental and human tumors¹⁷.
- In the case of late transition metal compounds, growth-inhibiting efficacy was found for copper^{18, 19} and gold²⁰⁻²² complexes, e.g., for *trans*-bis(salicylaldoximate)copper(II)¹⁹, for 2,3,4,6-tetra-0-acetyl-1-thio- β -D-glucopyranosato-S(triethylphosphine)gold(I)¹⁹, for 2,3,4,6-tetra-0-acetyl-1-thio- β -D-glucopyranosato-S(triethylphosphine)gold(I) (auranofin)²¹ and for bis[1,2-bis(diphenylphosphino)ethane]gold(I) chloride²². It is worth mentioning that gold(I) complexes like auranofin represent established drugs which have been clinically approved for a long time against autoimmune disease rheumatoid arthritis.

The present study deals with the antitumor properties of cyclopentadienyl complexes as representatives of organometallic non-platinum-group metal compounds. Examples are given of compounds of various structural types which either contain early transition metals, medium transition metals, or even main-group metals as central atoms.

2 Antiproliferative Properties of Cyclopentadienyl Metal Complexes

2.1 Results with Cells Cultured in Vitro

In vitro, the antiproliferative activity of various metallocene dichloro complexes $(C_5H_5)_2MCl_2$ containing titanium, vanadium, molybdenum, hafnium, or zirconium as central metal atom M, and of some ferricenium salts $[(C_5H_5)_2Fe]^+X^-$ (X^- = diverse anions) (Fig. 2) was investigated against various strains of cultured tumor and normal cells^{23, 24}. The results obtained with Ehrlich ascites tumor cells are summarized in Figs. 3 and 4.

- Vanadocene dichloride effected the most pronounced cytostatic activity in vitro, reducing cell proliferation by more than 50% at a concentration level as low as 5×10^{-6} mol/l (Fig. 3).

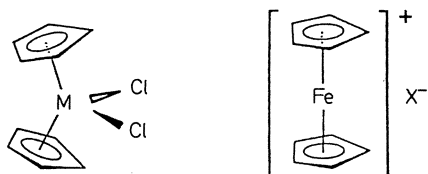


Fig. 2. Structures of metallocene dichloro and ferrocenium complexes

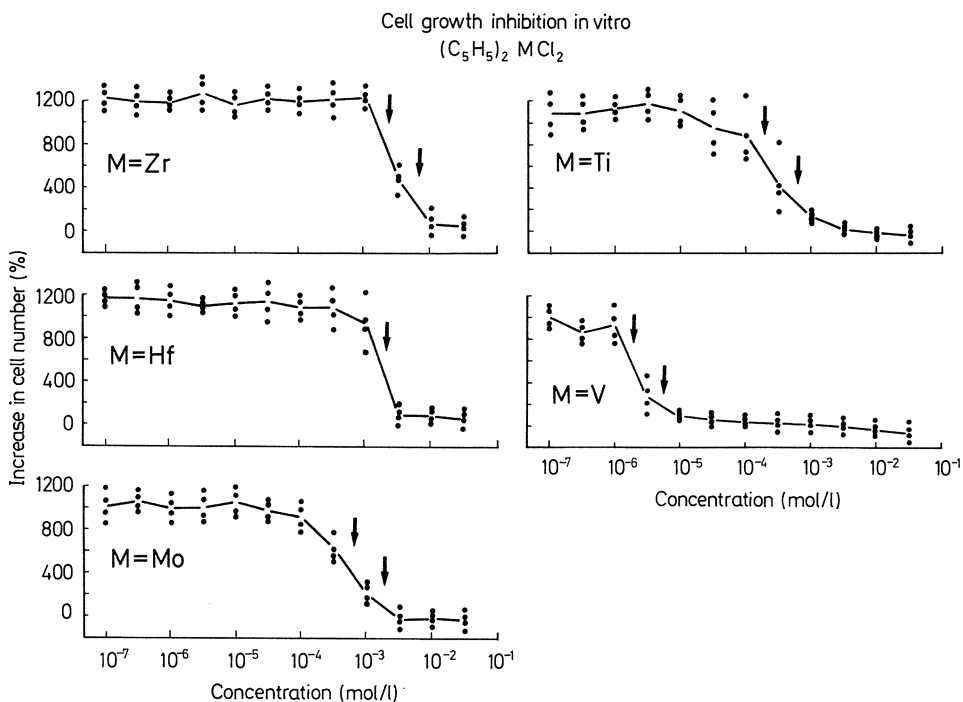


Fig. 3. Effect of a 90-min treatment of in-vitro-cultured Ehrlich ascites tumor cells with various concentrations of metallocene dichlorides on the increase in cell number, determined 72 h after removal of the agents. Arrows indicate highly significant differences ($\alpha < 0.1\%$) between proliferation rates of neighboring groups

- In the case of ferricenium salts, tenfold higher concentrations between 10^{-5} and 10^{-4} mol/l were needed to cause a 50% reduction of proliferation (Fig. 4).
- For titanocene and molybdenocene dichloride, even higher concentrations of 5×10^{-4} and 10^{-3} mol/l were required to induce equivalent effects in vitro (Fig. 3).
- Zirconocene and hafnocene dichlorides, finally, inhibited cellular growth only at concentrations of 5×10^{-3} mol/l and higher (Fig. 3).

Using other cell lines cultured in vitro, e.g., human KB²⁵⁾, HeLa²⁵⁾, epidermoid tumor cells²⁶⁾, or human embryonic fibroblasts²⁷⁾, it was shown that there is apparently no cell specificity for the antiproliferative action of metallocene com-

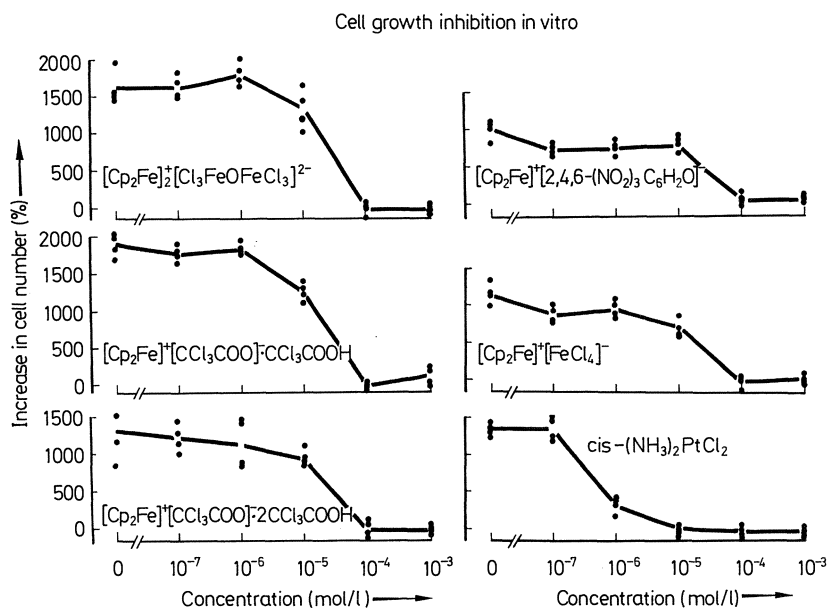


Fig. 4. Effect of continuous exposure of in-vitro-cultured Ehrlich ascites tumor cells at various concentrations of ferricenium salts on the increase in cell number determined 72 h after drug addition

pounds. The growth of animal and human tumor cells as well as of normal, non-transformed cells was suppressed by the same concentrations of titanocene or vanadocene complexes as mentioned above.

2.2 Results with Ascitic Animal Tumors

Numerous types of cyclopentadienyl metal complexes were investigated against *Ehrlich ascites tumor* growing in the peritoneal cavity of mice. Antitumor properties were shown for the following compounds:

- Neutral bis(η^5 -cyclopentadienyl)metal (“metallocene”) diacido complexes $(\text{C}_5\text{H}_5)_2\text{MX}_2$ containing early transition metal central atoms in oxidation state +4 such as titanium(IV), vanadium(IV), and molybdenum(IV) induce optimum cure rates of 100%. They are mainly represented by diverse metallocene dihalides^{28, 29)}, titanocene carboxylates³⁰⁾ and titanocene phenolates, thiophenolates, selenophenolates, and dithiolene chelates³¹⁾ (Fig. 5). The pharmacological and toxicological properties of some of these compounds are summarized in Fig. 6.
- Ionic cyclopentadienyl titanium complexes³²⁾, corresponding to the general formula $[(\text{C}_5\text{H}_5)_2\text{TiXL}]^+\text{X}^-$ or $[(\text{C}_5\text{H}_5)_2\text{TiL}_2]^{2+}(\text{Y}^-)_2$, where X is an anion or ligand anionic donor site and L is a donor molecule or ligand neutral donor site, are mainly represented by the compounds given in Fig. 7. They are characterized by similarly pronounced antitumor properties as titanocene diacido complexes, effecting optimum cure rates between 67 and 100% (Fig. 8). As these

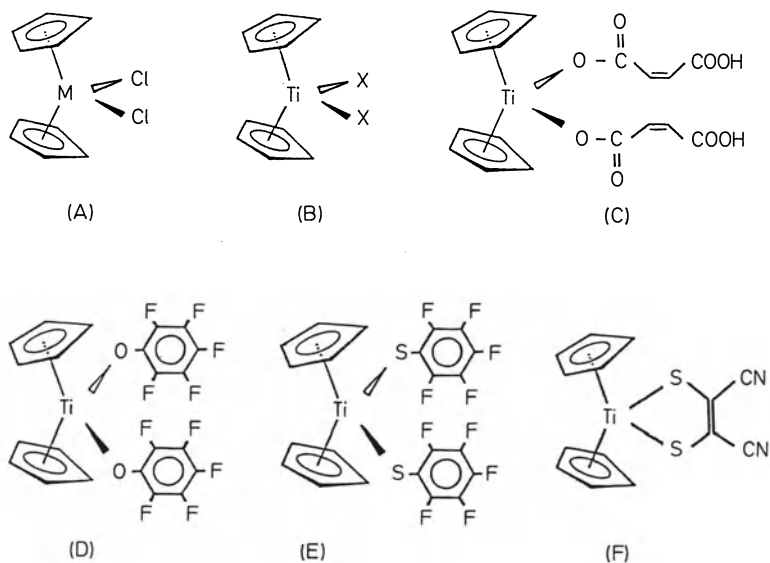


Fig. 5. Structures of some antitumor metalocene diacido complexes. (A) Metalocene dichlorides (M = Ti, V, Nb, Ta, Mo, W); (B) titanocene dihalides (X = F, Cl, Br, I); (C) titanocene bis(hydrogenmaleinate); (D) titanocene bis(pentafluorophenolate); (E) titanocene bis(pentafluorothiophenolate); (F) titanocene dithiolenyl chelate

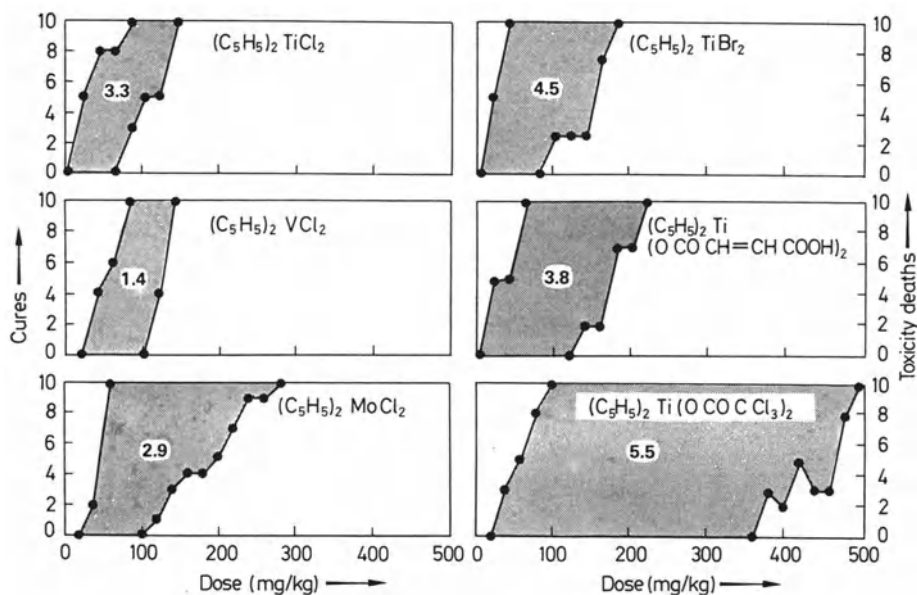


Fig. 6. Dose-activity and dose-lethality relationships of some metalocene complexes against Ehrlich ascites tumor in mice. Surviving animals

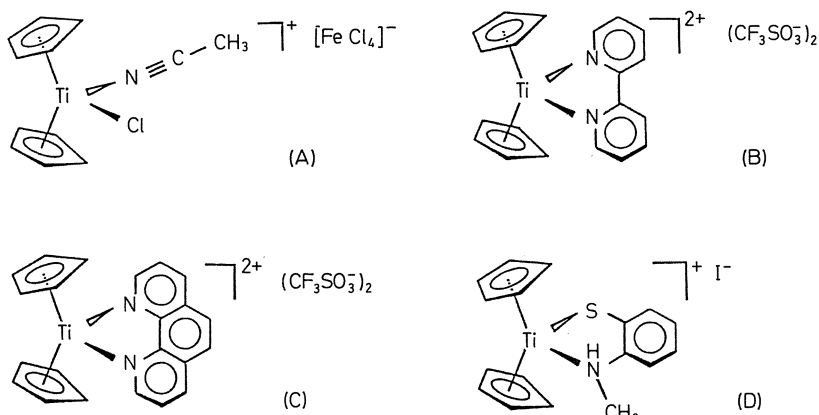


Fig. 7. Structures of some ionic titanocene complexes. (A) Bis(cyclopentadienyl)acetoneitrile(chloro)titanium(IV) tetrachloroferrate(III); (B) bis(cyclopentadienyl)-2,2'-bipyridyltitanium(IV) bis(trifluoromethanesulfonate); (C) bis(cyclopentadienyl)-*o*-phenanthroline-titanium(IV) bis(trifluoromethanesulfonate); (D) bis(cyclopentadienyl)-*N*-methyl-*o*-aminothiophenolate titanium(IV) iodide

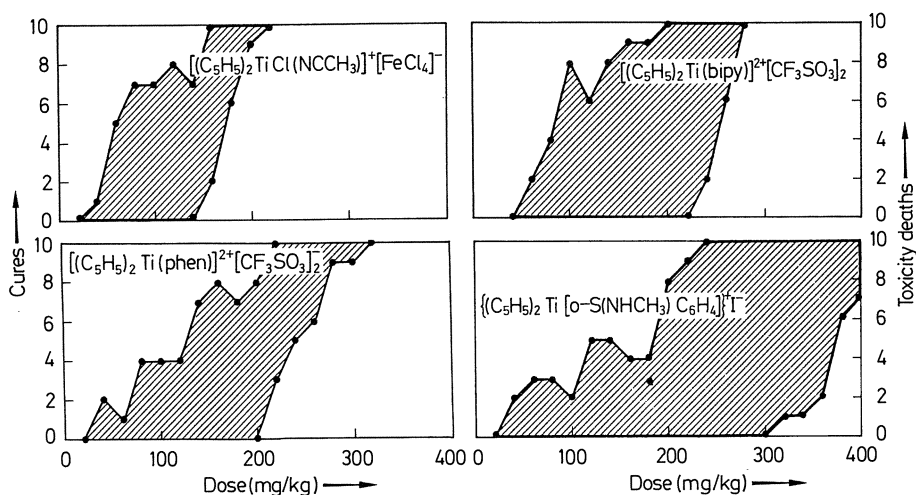


Fig. 8. Dose-activity and dose-lethality relationships of some ionic titanocene complexes against Ehrlich ascites tumor in mice. Surviving animals

compounds are distinguished by improved solubility in water in comparison to titanocene diacido complexes, they are interesting candidates for further experimental investigations.

— Ferricenium complexes $[(C_5H_5)_2Fe]^+ X^-$ (Fig. 2) represent another group of anti-tumor salt-like cyclopentadienyl metal compounds¹⁷⁾. They contain a mid-transition metal as the central metal ion, lack acido ligands bound covalently to the central metal atom and are characterized by improved water solubility. The

anions X^- within $[(C_5H_5)_2Fe]^+X^-$ can be represented by diverse groups, e.g., $FeCl_4^-$, picrate, trichloroacetate, all complexes inducing optimum cure rates between 70 and 100% (Fig. 9).

- Another group of antitumor metallocene compounds is given by neutral stannocene and germanocene complexes, decasubstituted at the cyclopentadienyl rings by phenyl or benzyl groups ^{33,34} (Fig. 10). These complexes contain elements of main-

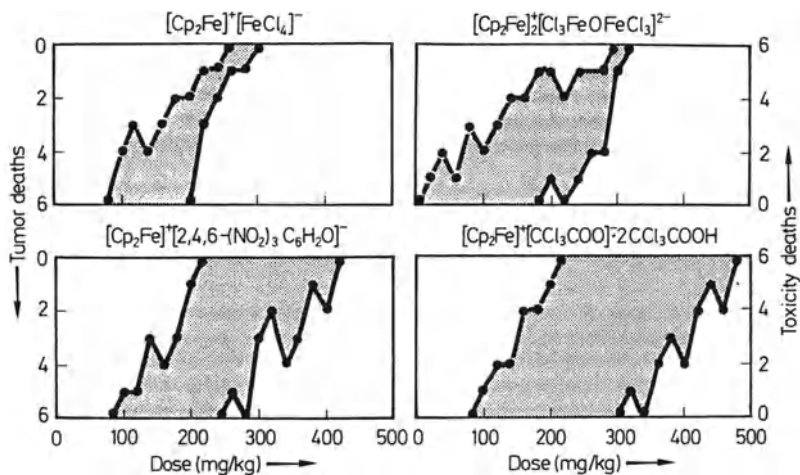


Fig. 9. Dose-activity and dose-lethality relationships of some ferricenium complexes against Ehrlich ascites tumor in mice. Surviving animals

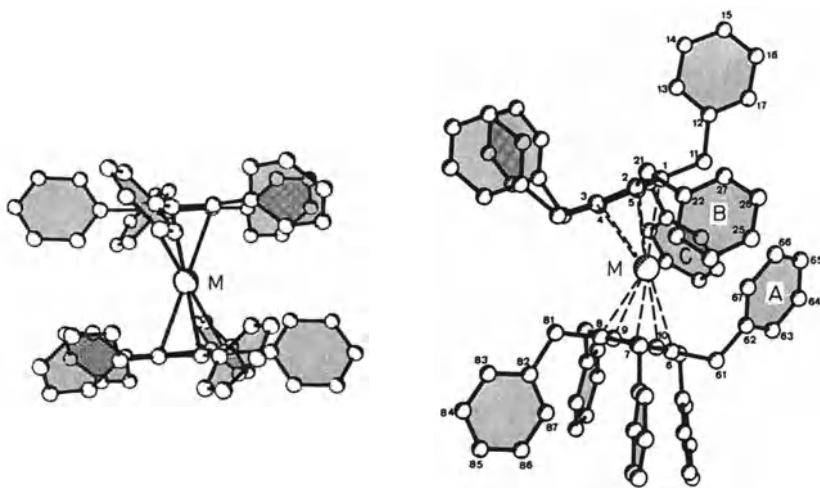


Fig. 10. Molecular structures of main-group metallocene complexes (M = Sn, Ge), decasubstituted by phenyl (on the left) or benzyl (on the right) groups. Modified according to Refs. ^{77, 78}

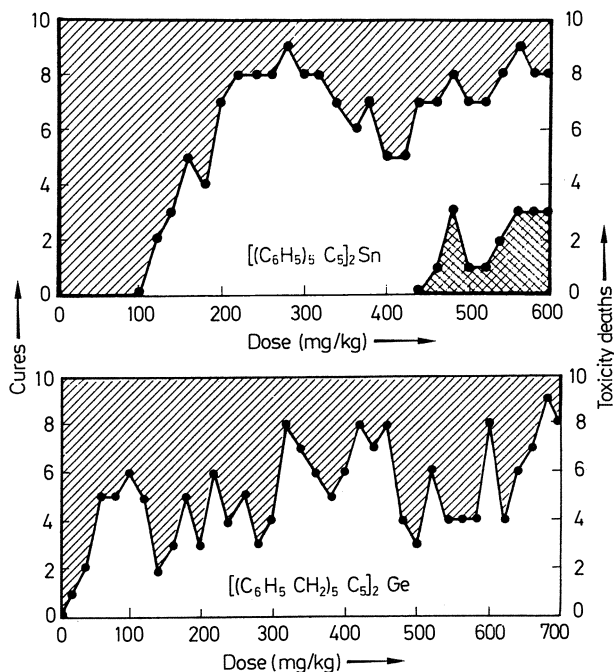


Fig. 11. Dose-activity and dose-lethality relationships of decaphenylstannocene and decabenzylgermanocene against Ehrlich ascites tumor in mice. Surviving animals

group IV as central metal atom and effect optimum cure rates of 60 to 100% against Ehrlich ascites tumor (Fig. 11).

The described results underline that quite different kinds of bis(η^5 -cyclopentadienyl)-metal complexes, comprising compounds of early or mid-transition metals or main-group elements, are characterized by similar antitumor properties against Ehrlich ascites tumor. The complexes are represented by compounds of various structural type and include neutral as well as salt-like complexes.

Another fluid tumor which is sensitive to titanocene and vanadocene diacid complexes is *sarcoma 180*. Best results were achieved with titanocene dichloride, which prolonged the mean survival period of mice by 160–185% and caused cures of 40–50% of the treated animals³⁵⁾ (Fig. 11).

In spite of the pronounced antitumor efficacy of titanocene complexes against Ehrlich ascites tumor and *sarcoma 180*, the titanocene and vanadocene dichlorides showed only marginal activity against the lymphoid leukemia L1210 and the lymphocytic leukemia P388 in vivo³⁶⁾. After application of single doses, the survival of animals bearing these tumors was prolonged by only 20–30%. No further increases in life span were inducible, e.g., by multiple substance administration.

At this point it is worth mentioning that a comparable discrepancy in the antitumor activity against the leukemias L1210 and P388, on the one hand, and against Ehrlich ascites tumor and numerous solid tumors, on the other hand, is not confined to metallocene and ferrocenium complexes. Similar discrepancies were also found in

the case of other inorganic and organometallic metal complexes, such as those of titanium¹⁶⁾, copper¹⁹⁾, gold²²⁾, or germanium³⁷⁾. Therefore, it may be suggested that neither the L1210 nor the P388 system, which belong to the standard test systems of the National Cancer Institute, are appropriate tumor systems for initial screening trials in the course of antitumor testing of metal complexes.

2.3 Results with Solid Animal Tumors

Investigations with solid experimental tumors were undertaken to study the systemic activity of metallocene and ferricenium compounds.

When animals bearing *Ehrlich ascites tumor*, which grew subcutaneously in the nuchal region, were treated with intraperitoneal injections of titanocene dichloride, vanadocene dichloride, or diverse ferricenium complexes, the growth of the tumors was inhibited in a clearly dose-dependent manner by 40–86%, i.e., tumor masses in treated animals ranging between 60 and 14% of those in the control group. Best results, i.e., tumor masses of only 14–20%, were obtained by administration of twofold doses of titanocene dichloride³⁶⁾ (Fig. 12).

For the case of *solid sacroma 180* growing subcutaneously in the flanks of mice, the therapeutic effects of the titanocene and ferricenium complexes listed in Tables 1 and 2 were analyzed after intraperitoneal substance administration. Ferricenium complexes reduced tumor weights by 35–50% to tumor masses of 50–65%, whereas the titanocene compounds suppressed tumor development in a more pronounced, clearly dose-dependent and significant manner. Best values of growth reduction by 50–80% (corresponding to tumor weights of treated tumors amounting to 50–20%

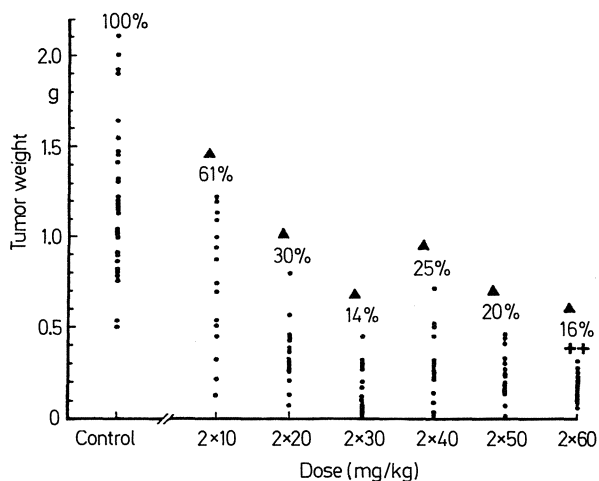


Fig. 12. Ranged weights of solid Ehrlich ascites tumors on day 8 after tumor transplantation following treatment with titanocene dichloride. The numbers on the top represent T/C values. Significant ($\alpha < 0.05$), highly significant ($\alpha < 0.01$) difference of the tumor weights compared to the controls. + Toxic deaths before key-date

Table 1. Growth inhibitions effected by some titanocene complexes in diverse solid experimental animal tumors

Compound	Applied dose (mg/kg)	Solid animal tumor systems			
		Sarcoma 180	Colon 38 adeno-carcinoma	B16 melanoma	Lewis lung carcinoma
$(C_5H_5)_2TiCl$	1 × 50	34	59	59	31
	1 × 60	—	61	61	65
	3 × 30	—	63	15	53
	3 × 40	42	72	31	71
	3 × 50	77	—	63	—
	5 × 20	—	72	31	34
	5 × 30	—	81	80	66
	5 × 40	—	81	80	66
$(C_5H_5)_2TiBr_2$	1 × 50	6	52	51	13
	1 × 60	—	64	58	25
	1 × 70	—	61	55	52
	3 × 40	—	45	28	45
	3 × 50	47	63	52	56
	3 × 60	63	—	56	—
	5 × 30	—	51	68	40
	5 × 40	—	58	74	50
$(C_5H_5)_2Ti-(cis-O_2CCH=CHCOOH)_2$	1 × 80	5	18	0	16
	1 × 100	—	—	—	34
	1 × 120	27	28	11	—
	3 × 40	—	35	6	56
	3 × 60	24	43	37	—
	3 × 80	—	69	—	—
	3 × 100	47	—	50	—
	5 × 40	—	63	12	43
$[(C_5H_5)_2TiCl-(NCCH_3)]^+[FeCl_4]^-$	1 × 70	—	2	—	31
	1 × 80	—	10	10	55
	3 × 40	—	70	—	46
	3 × 50	—	66	—	66
	3 × 60	—	—	54	—
	5 × 30	—	62	47	41
	5 × 40	—	76	56	75

^a Given are values of tumor growth inhibition in % of control tumor size, calculated by $100\% - T/C$ ($T/C = \text{mean tumor weight of a dose group} \times 100 / \text{mean tumor weight of the control group}$)

in relation to those of control tumors) were observed after application of three- and fivefold injections ³⁵⁾.

Treatment of animals bearing subcutaneously growing *solid B16 melanoma* with diverse bis(cyclopentadienyl)titanium ³⁸⁾ or bis(cyclopentadienyl)iron ³⁹⁾ compounds significantly influenced tumor development and diminished the growth of the tumors by 50–80% (Tables 1, 2). Best results were observed for titanocene dichloride among all titanocene and ferrocenium complexes administered.

Table 2. Growth inhibitions^a effected by some ferricenium salts in diverse solid experimental animal tumors

Compound	Applied dose (mg/kg)	Solid animal tumor systems				
		Ehrlich ascites tumor	Sarcoma 180	Colon 38 adenocarcinoma	B16 melanoma	Lewis lung carcinoma
[(C ₅ H ₅) ₂ Fe] ₂ [Cl ₃ FeOFeCl ₃] ²⁻	1 × 120	—	—	18	0	20
	1 × 150	—	—	52	23	58
	1 × 170	—	—	—	—	57
	3 × 100	52	22	42	11	32
	3 × 120	56	34	63	55	56
	3 × 120	52	44	—	—	53
	5 × 80	—	—	37	43	48
	5 × 100	—	—	44	54	—
	5 × 120	—	—	64	56	59
	[(C ₅ H ₅) ₂ Fe] ⁺ [2,4,6-(NO ₂) ₃ C ₆ H ₂ O] ⁻	1 × 120	—	—	6	4
1 × 150		—	—	0	26	50
1 × 180		—	—	—	—	66
3 × 100		0	—	21	0	24
3 × 120		—	0	31	8	54
3 × 150		4	48	52	0	54
3 × 200		17	35	—	—	—
5 × 80		—	—	13	8	13
5 × 100		—	—	41	14	5
5 × 120		—	—	53	31	45
[(C ₅ H ₅) ₂ Fe] ⁺ [CCl ₃ COO] ⁻ 2 CCl ₃ COOH	1 × 220	—	—	0	0	39
	1 × 250	—	—	37	22	36
	3 × 100	44	—	—	—	—
	3 × 150	48	—	—	—	—
	3 × 180	—	25	43	0	46
	3 × 200	58	50	73	60	71
	5 × 150	—	—	23	27	60
	5 × 180	—	—	53	29	67

^a See explanation to Table 1

Another solid tumor, the growth of which is suppressed by metallocene complexes, but which is inhibited only by a few other cytostatic drugs such as 5-fluorouracil or cyclophosphamide⁴⁰⁾, is the murine *colon 38 adenocarcinoma*. Maximum reductions of tumor growth by 50–70% were effected by titanocene dihalides³⁸⁾, especially by titanocene dichloride, and ferricenium complexes³⁹⁾ (Tables 1, 2).

Lewis lung carcinosarcoma represents another experimental tumor which is sensitive to cyclopentadienyl metal complexes²⁵⁾. When animals bearing this tumor were treated with titanocene (Table 1) or ferricenium (Table 2) complexes, again significant and dose-dependent suppressions of tumor growth were induced by administration of

sublethal doses. The values of growth inhibition ranged between 50 and 75 %, whereby superior activity was detected for the neutral complex $(C_5H_5)_2TiCl_2$ and the ionic titanocene complex salt $[(C_5H_5)_2TiCl(NCCH_3)]^+[FeCl_4]^-$.

Summarizing the results effected by cyclopentadienyl metal complexes in solid experimental animal tumors, it becomes evident that:

- i) titanocene, vanadocene, and ferricenium complexes exhibit systemic activity against numerous experimental tumor systems and
- ii) titanocene and ferricenium compounds are obviously characterized by a similar spectrum of effectivity against experimental animal tumors.

2.4 Results with Heterotransplanted Human Tumors

Testing of human tumors heterotransplanted to athymic nude mice plays an increasingly important role in preclinical screening of cytostatic drugs^{41,42}). Human tumors preserve drug susceptibility and histologic reactivity after xenografting and transplanting them over many passages in nude mice^{43,44}). Thus, it seems to be possible to determine the activity of new cytostatic agents against human tumors and to outline the spectrum of antitumor activity already in the preclinical stage. Several comparative studies performed during the past years revealed a high correlation between positive responses obtained with individual tumors growing in nude mice and the clinical results with the same drugs^{41-43,45,46}).

Some representatives of titanocene and ferricenium complexes were tested during the past years against selected xenografted tumors of different types. Most experiments were done with titanocene dichloride.

In the case of a human *breast carcinoma* heterotransplanted to athymic mice and growing there in the 18th–21st passage, the rapid proliferation of the tumor was clearly suppressed by titanocene dichloride and dibromide by 70–80 % leading to tumor masses of 30–20 % in comparison to control tumors (100 %)⁴⁷).

When animals bearing a xenografted *cervix carcinoma*, which was also characterized by rapid growth velocity, were treated with titanocene dichloride, again the growth velocity of treated tumors was slowed down in a statistically significant manner⁴⁷), whereby minimum tumor masses amounted to 25–35 % corresponding to tumor inhibition by about 70 %.

Against *lung malignancies*, titanocene dichloride effected growth suppression in the case of several individual tumors. Against the lung adenocarcinoma L261⁴⁸), sublethal doses of the compound caused growth inhibitions by 60–75 % to tumor masses of 40–25 % of control tumors (Fig. 13). Similar decreases in tumor mass values were attained by treatment with other titanocenes such as titanocene dibromide (50 %) and titanocene bis(hydrogenmaleinate) (50–20 %) (Fig. 13). The growth suppressions induced were stable and clearly persisted beyond the end of treatment period. Cisplatin and cyclophosphamide were applied for comparison purposes. Both cytostatics induced growth suppression of similar strength resulting in tumor sizes 30 and 40 % of the controls, respectively.

Another lung tumor investigated was the small cell lung carcinoma L182⁴⁸) which proliferated more slowly than L261. Sublethal doses of titanocene dichloride, titanocene dibromide and titanocene bis(hydrogenmaleinate) reduced tumor pro-

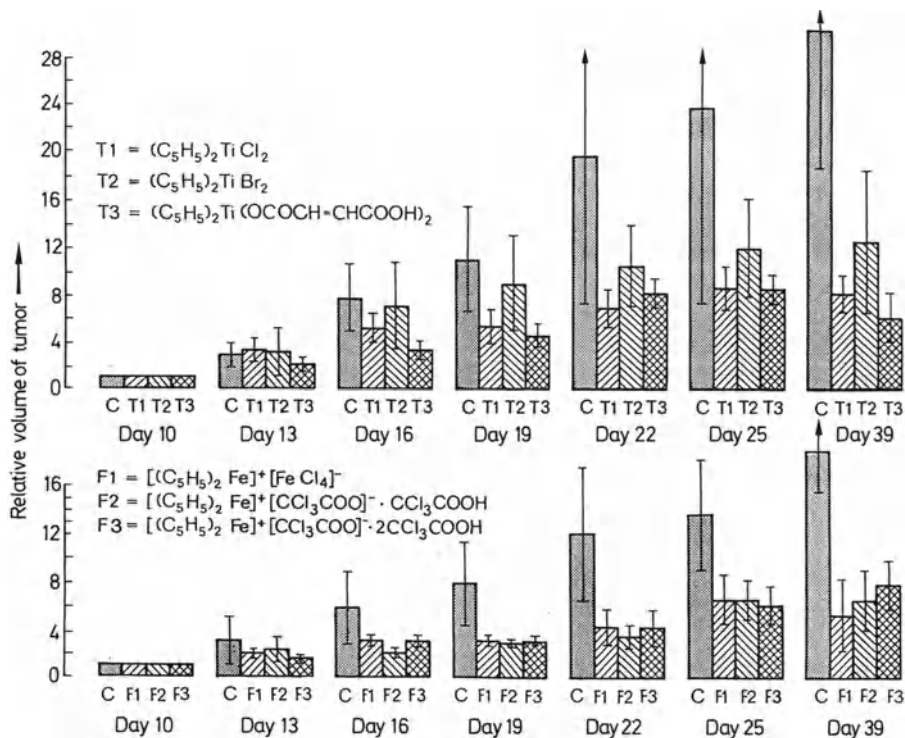


Fig. 13. Influence of three titanocene and three ferricenium complexes, applied according to sublethal Q3D \times 5 regimes (D = 15, 20, or 40 mg/kg for T1, T2, T3; D = 70, 50, 120 mg/kg for F1, F2, F3), upon the growth of a human lung adenocarcinoma (L261), heterotransplanted to athymic mice on day 0. Substance injections on days 10, 13, 16, 19, 22. The parameter evaluated is the relative increase of tumor volume in relation to the starting tumor size on day 10. Given are mean values of relative volume of tumor, determined in 4–5 animals, and standard deviations \pm s

liferation by about 50%, LD₁₀ doses by 69–83% (tumor masses 31–17% of controls). Cisplatin, which represents one of the more active drugs against small cell carcinomas of the lung, effected growth inhibition by about 70% to tumor masses of 31% of controls at the LD₁₀ dose level.

Data concerning the influence of ferricenium complexes upon lung malignancies are available with the adenocarcinoma L261 (Fig. 13) and the small cell carcinoma L182⁴⁷⁾. In both cases, the growth suppressions induced by diverse ferricenium complexes were less pronounced than by titanocene complexes or cisplatin and ranged between 30 and 70%. The greatest inhibition of tumor masses effected with sublethal doses of $[(C_5H_5)_2Fe]^+[CCl_3COO]^- \cdot 2CCl_3COOH$ were 50% (L261) (Fig. 13) and 25% (L182), i.e., the masses of treated tumors amounted to 50% and 75% of control tumor size.

Human adenocarcinomas derived from the gastrointestinal tract, especially from the colon including the colon rectum and the stomach, are generally rather insensitive

Table 3. Growth inhibitions effected by titanocene dichloride in fourteen heterotransplanted human colorectal carcinomas

Tumor	Optimum inhibition value (%)	Tumor	Optimum inhibition value (%)
<u>Colon carcinomas</u>		<u>Sigma carcinomas</u>	
CX 1	68	S 90	75
CX 2	74	S - Sb 1	58
C - Stg 2	91	S - Sb 2	52
C - Stg 3	71	S - Stg 4	71
C - Stg 6	22	<u>Rectum carcinomas</u>	
C - Hbg 1	49	R - Sb 1	7
C - Hbg 2	27	R 85	55
		<u>Stomach carcinoma</u>	
		M - Stg 4	69

The parameter evaluated is optimum tumor growth inhibition in % (for definition cf. Table 1), determined 3 days after last substance injection. Shaded bars indicate growth inhibition exceeding 50%

to common cytostatic agents. The only drugs exhibiting limited clinical value against these malignancies are, e.g., 5-fluorouracil and mitomycin C.

The influence of titanocene and ferricinium complexes on the development of human gastrointestinal carcinomas was investigated in the case of two rectum carcinomas, four sigma carcinomas, seven tumors derived from the upper parts of the colon and one stomach adenocarcinoma^{47,49,50}). All tumors had been xenografted into athymic nude mice and the compounds were administered according to a Q2Dx5¹ or Q3Dx5² schedule. Antitumor activity, i.e., growth suppression by more than 50%, was observed in one out of two rectum tumors, in all sigma carcinomas, in four out of seven carcinomas of the upper colon and in the case of the stomach adenocarcinoma. Table 3 summarizes the optimum inhibition values observed with all gastrointestinal carcinomas investigated. These results unfold that obviously the growth of ten out of fourteen gastrointestinal tumors was suppressed significantly by titanocene dichloride by 50–94%, corresponding to T/C ratios ranging between 50 and 6%.

Regarding the CX1 tumor, one of the human standard tumors at the National Cancer Institute, growth suppressions by 50–70% were effected, which persisted

¹ Q2D × 5, fivefold injection of substance every two days;

² Q3D × 5, fivefold injection of substance every three days.

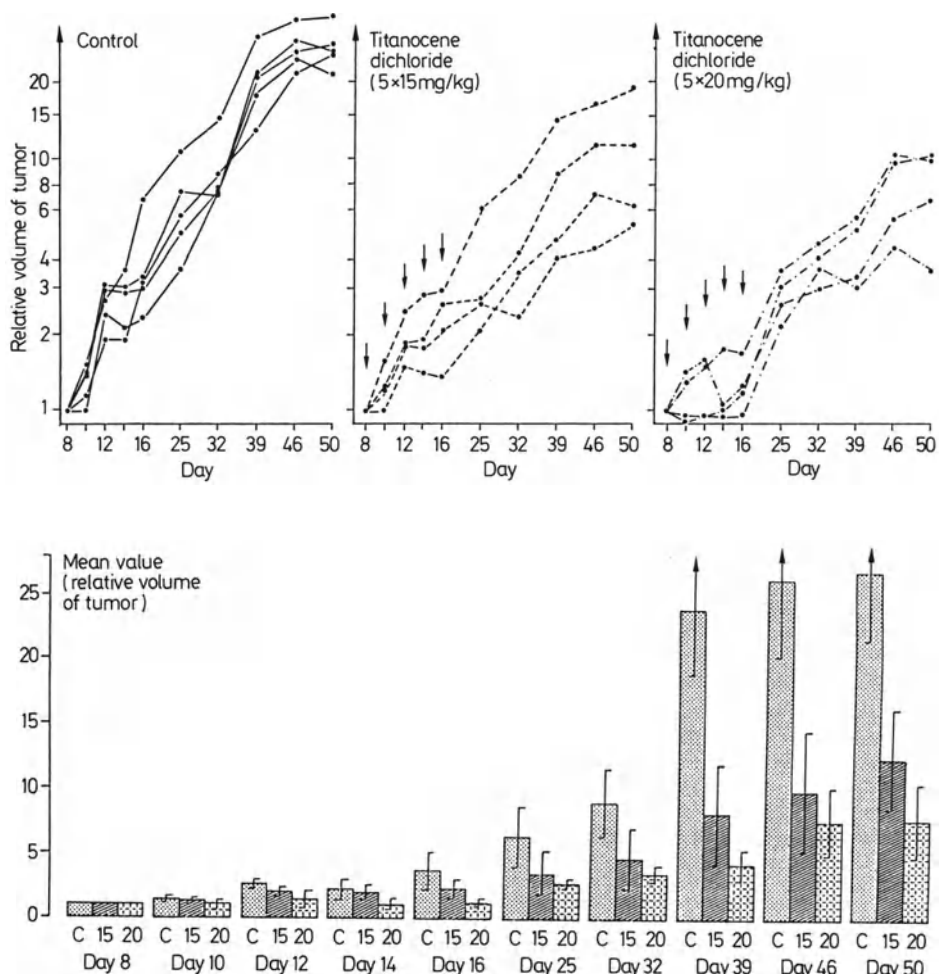


Fig. 14. Growth behavior of the xenografted human colon adenocarcinoma CX1 under treatment with titanocene dichloride, applied on days 8, 10, 12, 14, 16 after tumor transplantation. The schedule 5×20 mg/kg corresponds to a LD_{10} regimen. Upper part: growth curves of individual tumors; on abscissa, days after tumor implant on day 0; arrows indicate substance injections. Lower part: mean values of relative volume and standard deviations within control and treatment groups shown in the upper part

several weeks beyond the end of the treatment period (Fig. 14). Best activity was observed in the case of the colon adenocarcinoma C-Stg 2, the growth of which was inhibited nearly totally during the period of treatment with titanocene dichloride applied in doses of 5×15 mg/kg (Fig. 15). The temporal delay of tumor development which was effected by treatment with 5×10 or 5×15 mg/kg amounted to 13 and 31 days, respectively. Some other titanocene dihalides and carboxylates as well as ferrocenium complexes were also tested against the rectum carcinoma R85 and the sigma carcinoma S90⁴⁷⁾. Whereas titanocene dibromide and bis(hydrogenmaleinate) caused similar effects against S90 as titanocene dichloride, but were less active against R85,

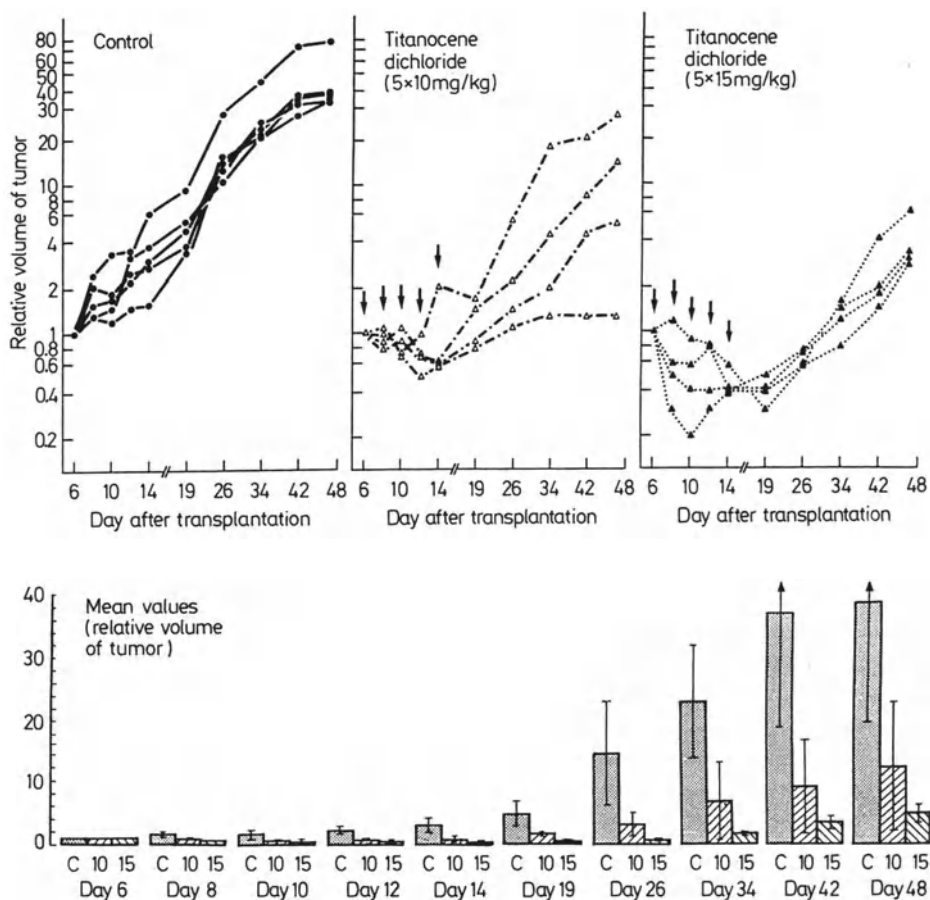


Fig. 15. Growth behavior of the xenografted human colon adenocarcinoma C-Stg2 under treatment with titanocene dichloride, applied at sublethal doses according to $Q2D \times 5$ ($D = 10$ or 15 mg/kg) on days 6, 8, 10, 12, 14. For further details, cf. legend to Fig. 14

ferricinium salts were generally characterized by an inverse behavior causing more pronounced growth suppression in R85 than in S90. For comparison purposes, cisplatin as well as 5-fluorouracil, one of the clinically approved cytostatic drugs against colorectal carcinomas, were administered in equitoxic doses in animals bearing the R85 or S90 tumor. Neither compound was able to induce more pronounced effects than titanocenes. Both compounds caused marginal activity and slowed down tumor proliferation at LD_{10} doses by 20–35% (tumor masses between 80 and 65% of controls).

On investigating morphologically colorectal carcinomas which had been treated with titanocene dichloride, the cytostatic action of the compound against this tumor type could be confirmed by the alteration pattern of the tumors⁵¹). There were pronounced histologic and cytologic alterations occurring after single application of titanocene dichloride in a dose of 40 mg/kg (Fig. 16). Within 24 h, there was a rapid

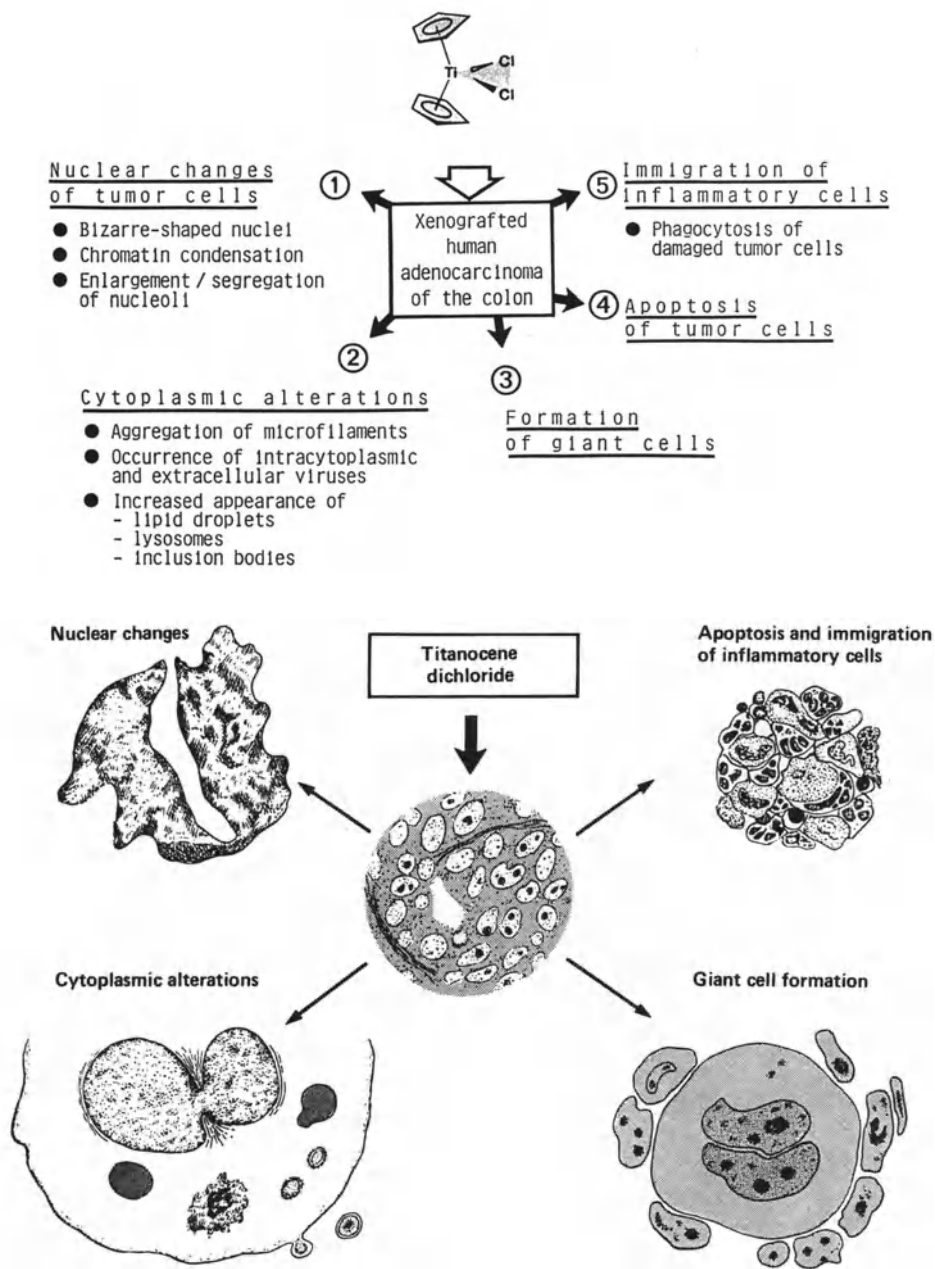


Fig. 16. Cytologic phenomena occurring in the xenografted human colon adenocarcinoma S90 after treatment with titanocene dichloride in nude mice

and pronounced decrease of the value of mitotic index of 2.5% (control value) to 0.3%, i.e., to about 10% of the initial value. During the same period, the nuclear chromatin of tumor cells condensed, the nuclear envelope enlarged resulting in the formation of segmented nuclei and structural aberrations developed within the nucleoli (Fig. 16). Cytoplasmic phenomena occurred 12 h later and were manifested by the appearance of lipid droplets and inclusion bodies, which often contained cellular debris. These phenomena indicated cytoplasmic degeneration in consequence to cellular injuries effected by treatment with titanocene dichloride. Moreover, some giant cells were observed 12–48 h after treatment, either containing one enlarged nucleus with a prominent nucleolus or several nuclei of different size. Beginning 24 h after application of titanocene dichloride, numerous inflammatory cells penetrated the tumor tissue and phagocytosed damaged tumor cells, so that necrotic cells progressively disappeared within 3 to 5 days (Fig. 16).

Summarizing the results obtained with titanocene complexes and ferricinium salts against xenografted human tumors, there is obviously antiproliferative activity of cyclopentadienyl metal complexes against diverse types of heterotransplanted human tumors. Because of the positive correlation between the response of human tumors xenografted into athymic mice and the clinical results obtained with the same drugs, the described experimental findings are remarkable in suggesting activity of cyclopentadienyl metal compounds against certain human tumors under clinical conditions. Finally the spectra of antitumor activity appear to be similar for both the titanocene and ferricinium complexes.

3 Other Biological Properties

For some cyclopentadienyl metal complexes, especially for titanocene dichloride, recent investigations have uncovered additional biological activities other than anti-tumor properties.

3.1 Radiosensitizing Properties

Pilot experiments performed during the past months pointed to possible radiosensitizing properties of titanocene dichloride⁵²⁾. This was shown in the case of a radio-resistant human lung adenocarcinoma cultured *in vitro*. The radioresistance of this tumor was partially reduced in a dose-dependent manner by combining radiation with application of titanocene dichloride (Table 4).

3.2 Antiviral Properties

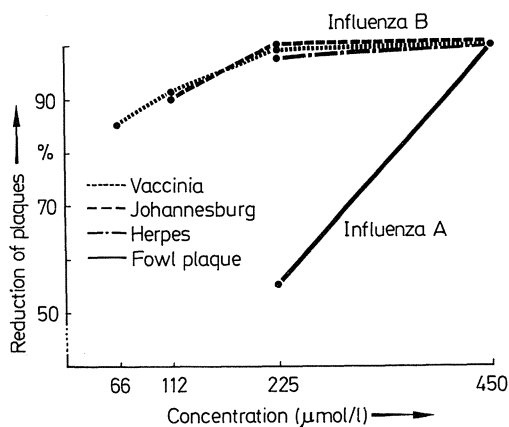
Significant antiviral efficacy was shown *in vitro* for titanocene dichloride against numerous DNA and RNA viruses in the extracellular phase⁵³⁾. Typical representatives of viruses, which were inhibited by direct contact with titanocene dichloride and

Table 4. In-vitro sensitivity of a human lung adenocarcinoma to titanocene dichloride, radiation, and a combination of both therapy modalities

Concentration of titanocene dichloride ($\mu\text{Mol/l}$)	Radiation dose (cGy)		
	200	400	800
—	83	82	45
0.001	70	64	57
0.01	61	55	44
0.1	1	1	0

The parameter evaluated is T/C ratio expressing clonogenic survival of treated populations related to controls given as percentage

apparently had lost their infectiousness, were vaccinia and herpes viruses as examples of DNA viruses, and influenza A and B as RNA viruses (Fig. 17). A comparable antiviral effect against herpes virus was detectable after application of ferricenium picrate⁵⁴, whereas molybdenocene dichloride failed to elicit antiviral activity under the same experimental conditions⁵³. When, in another series of experiments, mammalian cells that had been infected 1 h before with diverse types of viruses were treated with metallocene dichloro complexes, antiviral activity was observed. In the case of coxsackie virus, the number of plaques were reduced to 25% of the control value (100%) following application of titanocene dichloride (100 $\mu\text{g/ml}$)⁵⁴. Moreover, the reverse transcriptase of HIV viruses was inhibited significantly by vanadocene dichloride (20 $\mu\text{g/ml}$)⁵⁴. Future investigations are necessary to clarify whether this effect is combined with antiviral effectiveness of vanadocene dichloride against the intact AIDS virus.

**Fig. 17.** Antiviral efficiency of titanocene dichloride in vitro against some DNA and RNA viruses. Data from Ref.⁵³

3.3 *Antiinflammatory Properties*

An experimental study published in 1987 drew attention to the antiinflammatory activity of some cyclopentadienyl titanium(IV) complexes⁵⁵). Both titanocene dichloride and titanocene difluoride were shown to be potent antiedemic drugs and to exhibit significant acute antiinflammatory properties in rats. The effects observed were equivalent and even more pronounced than those occurring after application of aspirin. On the other hand, titanocene dichloride and titanocene dibromide were able to suppress the development of arthritis induced by Freund's adjuvant, when they were administered just before or after arthritic symptoms appeared. The effect of titanocene complexes in suppressing arthritis symptoms during their initial stage was similar to the action of phenylbutazone, whereas cisplatin and cyclophosphamide were shown to be effective prophylactic drugs, but were unable to suppress arthritic symptoms during their initial stage.

4 Toxicologic and Pharmacokinetic Properties

4.1 *Organ Toxicity*

The pattern of organ toxicity induced by *titanocene dichloride* was analyzed following a single intraperitoneal application of the compound at the ED₉₀ (40 mg/kg) and LD₁₀ (60 mg/kg) levels⁵⁶⁻⁵⁹).

Liver. Dose-limiting toxicity of titanocene dichloride was apparently caused by hepatotoxicity⁵⁶). The serum levels of typical liver enzymes, such as GOT (glutamic-oxaloacetic transaminase), GPT (glutamic-pyruvic transaminase), and GLDH (glutamate dehydrogenase), increased reversibly within 2 to 4 h to significantly elevated values which exceeded the control values by factors between 3 and 4 (Fig. 18). These findings indicate a short-lasting, reversible injury of the integrity of liver cells. Histological examinations confirmed these findings and uncovered the occurrence of small lipid droplets within the cytoplasm of liver cells furnishing evidence for ongoing fatty degeneration of liver parenchyma cells⁵⁷). At higher doses, single cell necroses were observed within the liver parenchyma. These structural alterations were also transient and reversible and disappeared within 16 to 32 days after substance application.

Endocrine glands. Alterations of the hormonal status of animals treated with titanocene dichloride represented other symptoms of organ toxicity⁵⁶). There were pronounced elevations of the serum concentrations of cortisol and glucagon by factors of 3 to 4 within 1 h after substance application, whereas the levels of other hormones such as insulin, aldosterone, catecholamines, and progesterone remained unaltered. Possibly, the initial decrease of glucose concentration in the peripheral blood occurring immediately after administration of the compound was the factor stimulating the regulative output of cortisol and glucagon from suprarenal glands and pancreatic islands.

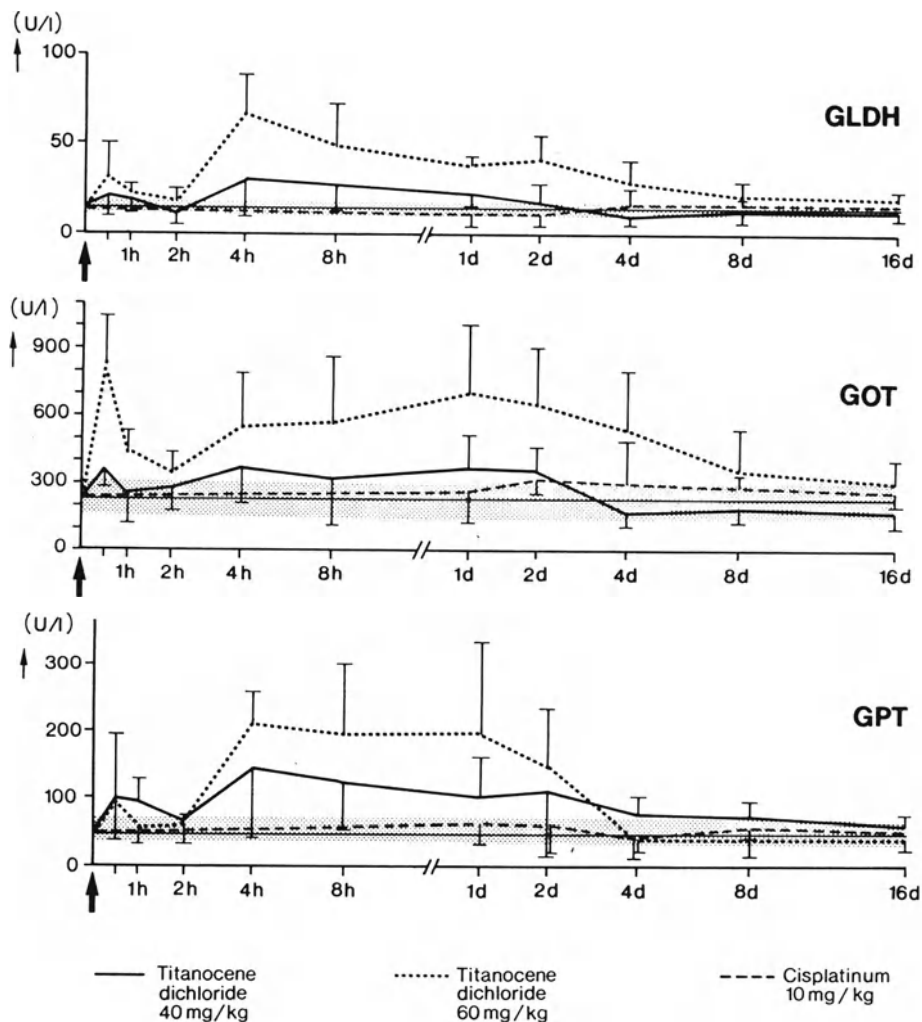


Fig. 18. Serum content of some enzymes at various intervals (given on abscissa) after administration of titanocene dichloride or cisplatin to mice on time 0. Given are mean values and standard deviations as +s or -s. Straight continuous lines and shaded areas represent mean values and ranges of standard deviations of control populations

Kidneys. In contrast to the heavy-metal complex cisplatin, titanocene and vanadocene dichloride did neither disturb renal function nor damage the structure of renal cells^{56,58}. No long-lasting elevations of blood retention values (BUN, creatinine), no changes in the composition of the urine, and no histologic and ultrastructural alterations within tubular or glomerular cells were detectable after application of metallocene dichloro complexes. This was documented after application of ED₉₀, LD₁₀, and even LD₅₀ doses of titanocene and vanadocene dichloride^{56,58}.

Bone marrow. Because of its vivacious proliferating activity, the bone marrow generally represents one of the target organs for the toxic action of common cytostatic drugs like alkylating agents, antimetabolites, and *vinca rosea* alkaloids. In the case of titanocene dichloride, however, only a slight and transient decrease of the count of circulating platelets beneath the control range was discernible 8 days after substance application, whereas the numbers of leukocytes and erythrocytes in the peripheral blood and the supply of young erythrocytes from bone marrow were apparently not influenced⁵⁹). The finding of an only very mild myelotoxicity following application of a cytostatic agent is quite unusual.

A similar pattern of organ toxicity was observed in the case of the analogous *vanadocene dichloride* complex. It also severely damaged the structure of liver parenchyma cells²⁶), but did not injure the histologic architecture of either the kidneys or the intestine^{58,26}).

4.2 Organ Distribution and Pharmacokinetics

The time-dependent organ distribution of titanium and vanadium following application of single doses of titanocene dichloride (60 mg/kg) and vanadocene dichloride (80 mg/kg) at time 0 was pursued by flameless atomic absorption spectroscopy in dried organ specimens^{60,63}).

Following injection of *titanocene dichloride*, the clearance of *titanium* from the blood showed a distinctly biphasic pattern with a rapid-phase half-time of about 5 h and a slow-phase half-time of several days⁶⁰). At 96 h after substance injection, 30% of the 1 h-value was still recovered in the blood (Fig. 19). Regarding the time-

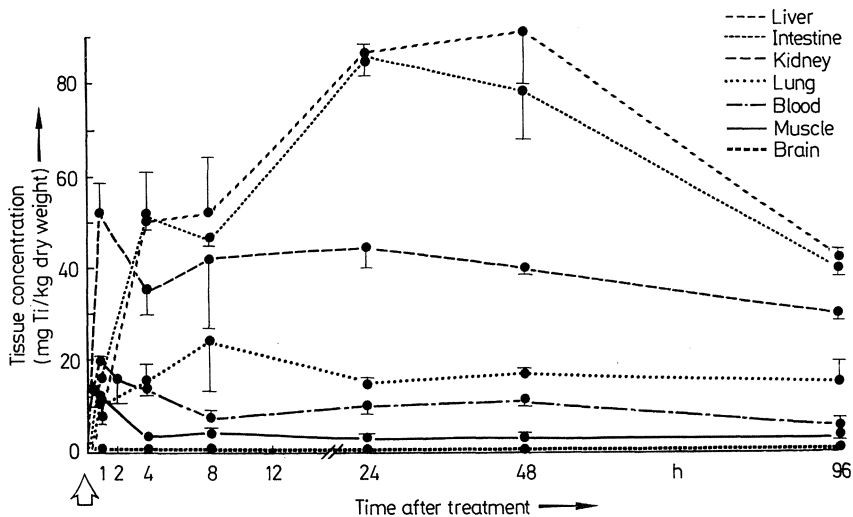


Fig. 19. Time-dependent organ distribution of Ti after single intraperitoneal application of titanocene dichloride (60 mg/kg) to NMRI mice at time 0. Control values ranging in all organs between 0.2 ± 0.05 and 0.6 ± 0.35

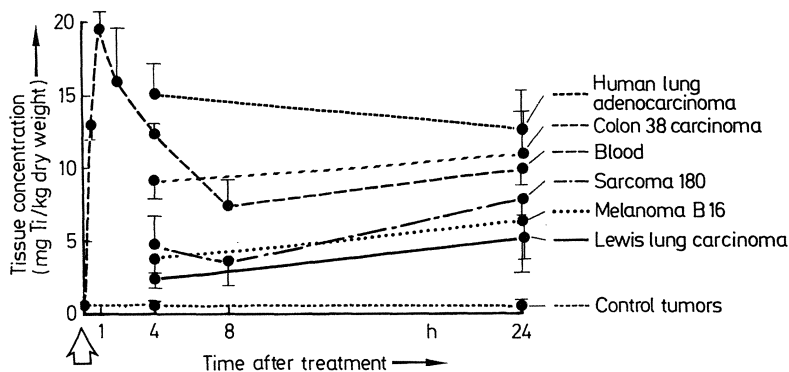


Fig. 20. Time-dependent disposition of Ti in various solid tumors growing subcutaneously after single intraperitoneal application of titanocene dichloride at time 0. Control values of untreated tumors ranging between 0.4 ± 0.10 and 0.7 ± 0.25

dependent organ distribution⁶⁰⁾, the initial organ concentration of titanium was highest in the kidneys at 1 h, but fell during the following hours (Fig. 19). The concentrations in the liver and the intestine exceeded the kidney values at 4 h and later. At 24 and 48 h, about 10% of total titanium injected was accumulated in the liver yielding a liver: blood ratio of 8–9. At 96 h, the liver: blood and intestine: blood ratios still amounted to about 5. No titanium values elevated over control values were measurable in the brain at any time during the experiment.

When pregnant mice were treated with single doses of titanocene dichloride at various days of gestation between the phase of organogenesis and late fetal period, there was no obvious transfer of titanium-containing metabolites into the embryonal compartment, after treatment on days 10, 12, and 14⁶¹⁾. On day 16, small amounts of titanium were found in the fetuses, the concentrations measured at 8 h after substance application amounting to 3.0 mg Ti/kg dry weight and, thus, being only threefold as high as control values determined in untreated animals (1.0 mg Ti/kg) and distinctly smaller than the values found in most maternal organs at the same time (e.g., 12.3 mg Ti/kg, maternal blood).

Investigation of the concentration of titanium in solid tumors growing subcutaneously, revealed no selective tumor uptake during the two days after substance application⁶⁰⁾ (Fig. 20). Thereafter, increasing concentrations of titanium were found in numerous experimental tumors exceeding the values in muscles and, at 96 h, in the blood. At this time, concentrations of 15–25 mg Ti/kg dry weight, corresponding to 40–60% of the liver concentration, were registered in all animal and human tumors which were analyzed.

These results point to the liver and the intestine as the main organs of excretion for titanocene complexes, whereas elimination via the kidneys seems to be less important. Titanocenes or their titanium-containing metabolites are apparently unable to traverse the blood-brain barrier as well as the placental barrier before the end of fetal period. The latter finding is in accord with the lack of malformations in fetuses when pregnant mice were treated with titanocene dichloride during the sensitive phase of organogenesis⁶²⁾.

In analogous experiments, the time-dependent distribution of *vanadium* was analyzed in mice after application of *vanadocene dichloride* ⁶³⁾. The differences in the distribution pattern of titanium following treatment with titanocene dichloride were striking. The main accumulation of vanadium was found in the kidneys, followed by the liver and the small intestine. On the other hand, similar to titanium, no vanadium was detectable in brain tissue over the temporal course of the experiment (24 h). The plasma levels of vanadium declined rapidly with a half-life of about 2 h, so that at 24 h no vanadium was measurable anymore in the plasma. After application of vanadocene dichloride in humans, electron spin resonance studies revealed an apparent binding of unaltered vanadocene dichloride to serum components for more than 12 h ⁶³⁾.

5 Cellular Mode of Action

Some cytobiological experiments were performed during the past years to gain some insights into the mode of action which probably leads to the antiproliferative properties of metallocene diacido complexes.

5.1 Precursor Incorporation Studies

Incorporation studies with tritium-labelled, specific precursors of DNA, RNA, and protein synthesis revealed pronounced and persistent inhibitions of nucleic acid synthesis activities following in-vivo and in-vitro application of titanocene or vanadocene dichloride ^{64,65)}. DNA synthesis was especially suppressed in a significant and long-lasting manner, with vanadocene dichloride effecting irreversible inhibition of DNA synthesis by 20% in vitro at doses as low as 5×10^{-6} mol/l (Fig. 21). Interestingly, an actual interaction between metallocenes and nucleic acids leading to an alteration of the secondary structure of the nucleic acids could be demonstrated in vitro by incubation of DNA or RNA with titanocene or vanadocene dichloride and UV-spectroscopic investigations. The latter revealed an increase of the absorbance maximum of the nucleic acids and its shifting to lower wavelengths ⁶⁶⁾.

5.2 Cytokinetic Studies

Cytokinetic investigations were performed with Ehrlich ascites tumor cells in vivo and in vitro to recognize treatment-induced alterations of the cellular transit through the cell cycle ^{67,68)}. The studies revealed the appearance of a premitotic G₂ block as a common result in vivo (Fig. 22) and in vitro, combined with marked mitotic depressions from 3.0–3.5% to 0–1.0% after application of therapeutic doses of titanocene and vanadocene dichloride. During in-vitro exposure, additional accumulations of cells at the G₁/S boundary were observed. Following short exposure periods, these cells escaped arrest at G₁/S and continued their transit through the cell cycle as a synchronized cell population. The comparison with the cytokinetic behavior after

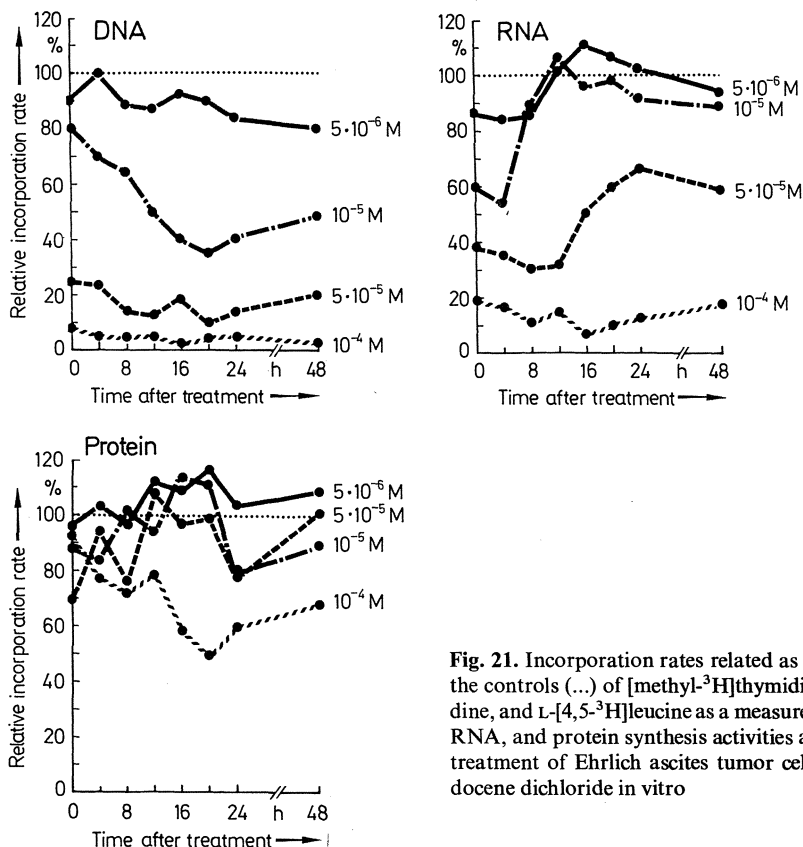


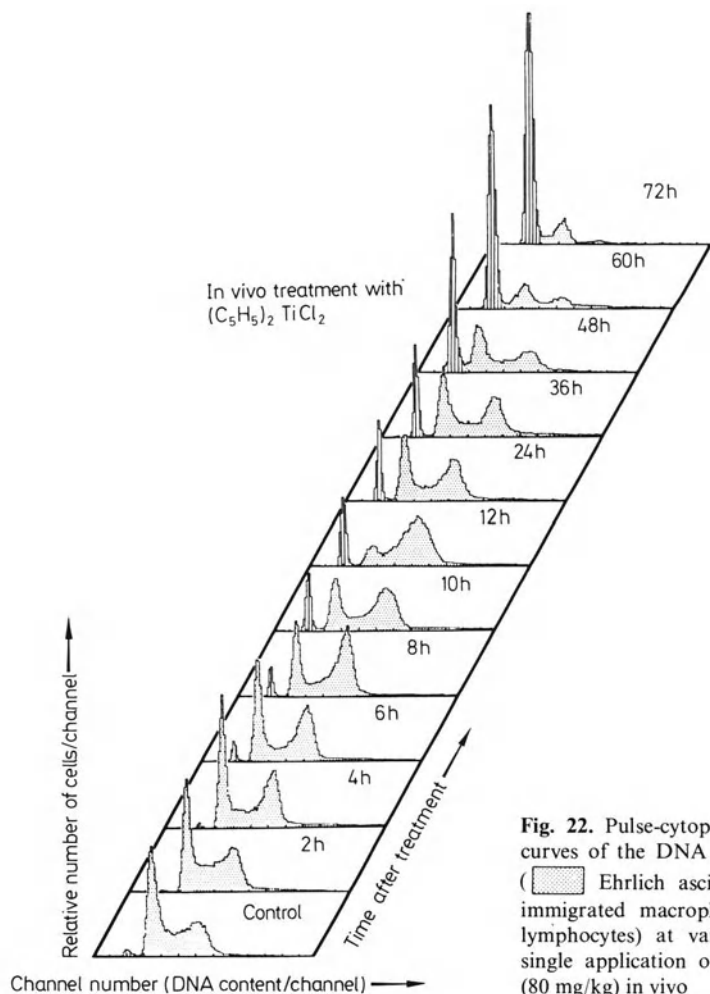
Fig. 21. Incorporation rates related as percentage to the controls (...) of [methyl- ^3H]thymidine, [^3H]uridine, and L-[4,5- ^3H]leucine as a measure of the DNA, RNA, and protein synthesis activities after a 90-min treatment of Ehrlich ascites tumor cells with vanadocene dichloride *in vitro*

treatment with other cytostatic drugs shows that many substances, for which molecular attack upon DNA molecules is generally assumed, provoked similar findings. Cisplatin, the anthracyclines, and alkylating agents such as cyclophosphamide and melphalan caused cell arrests in the G_2 phase, whereas cell accumulation at the G_1/S boundary were detected under the influence of antimetabolites and cisplatin [for Refs. cf. ⁶⁸].

5.3 Studies into Subcellular Distribution of Central Metal Atoms

All cytobiological experiments yet performed point to nucleic acid metabolism as the probable intracellular target for metallocene diacido complexes.

Some years ago, microanalytical studies of tumor cells which had been treated *in vivo* or *in vitro* with titanocene or vanadocene dichloride revealed that the central metal atoms Ti and V actually accumulate in those cellular regions that are



rich in nucleic acids⁶⁹). Highest concentrations were found in the nuclear heterochromatin, followed by the euchromatin and the nucleolus. However, in this connection it must be underscored that electron energy loss spectroscopy does not deliver information about the chemical composition of the metal-containing species accumulated in certain cellular regions and that the quantitative enrichment of the central metal atoms within certain cellular areas may be interpreted as a hint to the probable intracellular site of molecular action, but may not necessarily be identical with it.

Recently, similar experiments were performed using the newly developed electron spectroscopic imaging (ESI) method in the liver of mice, which had been treated with titanocene dichloride (80 mg/kg) 24 or 48 h before²⁵). This method allows a direct ultrastructural imaging of the elemental distribution within cellular organelles and

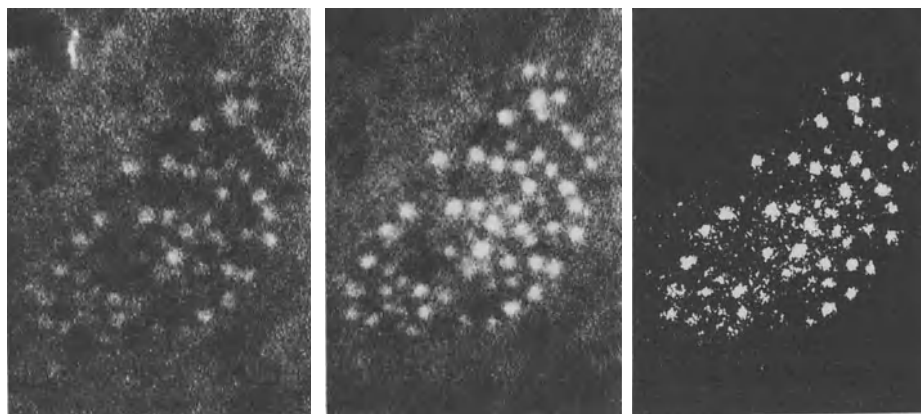


Fig. 23. Part of the nucleus of a hepatocyte of a mouse, treated with titanocene dichloride (80 mg/kg) 24 h before. The ultrathin sections were irradiated by electrons with an energy of 410 eV (a) corresponding to the underground, and 465 eV (b) corresponding to the $L_{2,3}$ edge of Ti. On the right (c), computer-calculated net distribution of Ti in the same area

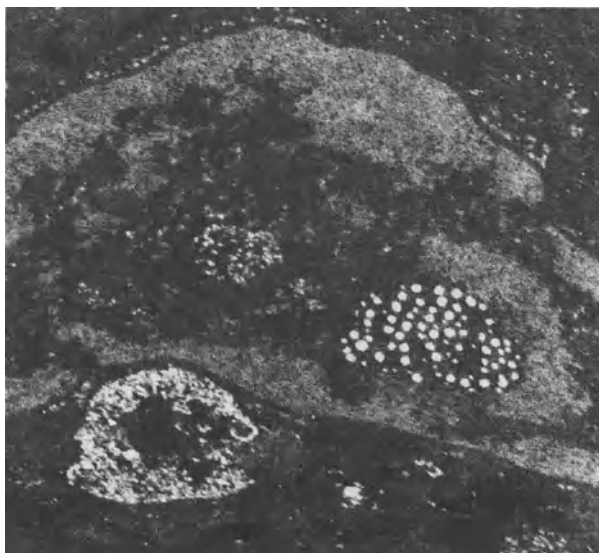


Fig. 24. Nucleus and cytoplasm of the hepatocyte shown in Fig. 23. Nuclear granules and cytoplasmic inclusion bodies, containing high concentrations of Ti, P, and O. Irradiation with electrons with an energy of 165 eV corresponding to the $L_{2,3}$ edge of P

compartments. One day after application of titanocene dichloride, titanium was found accumulated:

- i) in the cytoplasm of endothelial cells of liver sinusoids,
- ii) in the chromatin and the nucleolus of hepatocytes, where titanium was found condensed to granules of different size (Fig. 23) which moreover contained phosphorus and oxygen in similarly high concentrations, and
- iii) in the cytoplasm of hepatocytes, being obviously incorporated into cytoplasmic inclusion bodies and lysosomes (Fig. 24). Occasionally, the extrusion of the cytoplasmic inclusions into bile capillaries could be detected.

These observations confirm that titanium-containing species are actually able to enter the cells and the nuclei. There, they obviously form complexes with the phosphorus-rich nucleic acid molecules. Because of the resulting damage to nucleic acid molecules, it seems to be conceivable that parts of them are condensed to granules and eliminated from the nucleus, incorporated into cytoplasmic lysosomes and/or extruded into the bile.

6 Model Complexes

During the past years, several groups tried to synthesize model compounds of metallocene complexes with nucleic acid components⁷⁰⁻⁷⁶) to elucidate the molecular mode of action probably involving direct coordination of the metal-containing moiety to DNA or RNA donor sites. Though the synthesis turned out to be quite difficult especially under physiological conditions, some model compounds were successfully prepared since 1984. However, their value as models is limited by the fact that i) most model complexes were prepared in organic media, i.e., under non-physiological conditions, and that ii) as starting materials, not only titanocene, vanadocene, and molybdenocene dichloride, but also the low-valent titanium(III) or titanium(II) species $[(C_5H_5)_2TiCl]_2$ or $(C_5H_5)_2Ti(CO)_2$ were used. Thus, some of the model complexes contained titanium in +3 oxidation state as central metal atom.

Four main types of model compounds containing the titanium centre were isolated and characterized:

- a titanocene purinato derivative⁷⁰⁾ where titanium(IV) is bound by monofunctional bonding to the nitrogen-9 atom of the purinato ligand (Fig. 25);

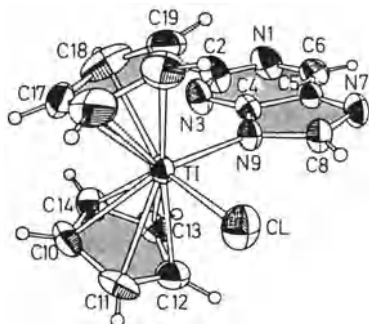


Fig. 25. Molecular structure of chlorobis(cyclopentadienyl)-purinatotitanium(IV). Modified according to Ref. 70)

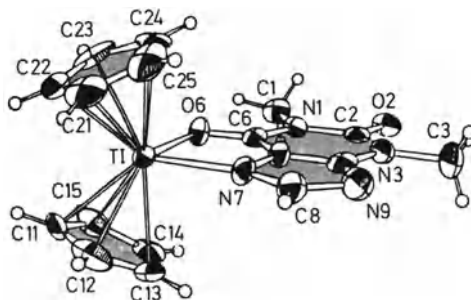


Fig. 26. Molecular structure of bis(cyclopentadienyl)(theophyllinato)titanium(III). Modified according to Ref. ⁷¹⁾

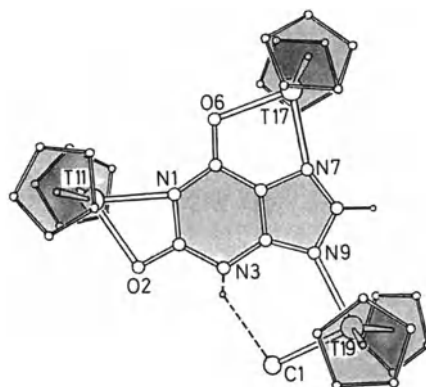


Fig. 27. Molecular structure of chloro-xanthinato(-2)-tris[bis(cyclopentadienyl)titanium(III)]. Modified according to Ref. ⁷²⁾

- a titanocene theophyllinato derivative ⁷¹⁾ where the titanium(III) atom of the bis(cyclopentadienyl)titanium unit is bound via bifunctional chelation to the nitrogen-7 and oxygen-6 atoms of the theophyllinato ligand (Fig. 26);
- a trinuclear complex with the xanthinato dianion ⁷²⁾ where two bis(cyclopentadienyl)titanium(III) units are bound bifunctionally to both the N-7 and O-6 and the N-1 and O-2 atoms of the xanthinato dianion and the third titanocene center is coordinated by a monodentate dative bond to the N-9 atom (Fig. 27);
- complexes of the type $[(C_5H_5)_2Ti(HNucl)(MeOH)]Cl_2$ and $[(C_5H_5)_2Ti(Nucl)]Cl$ with titanium(IV), where HNucl represents one of the nucleosides adenosine, guanosine, cytidine, or inosine and MeOH is methanol ⁷³⁾.

All these models demonstrate that, in principle, the titanocene center is able to coordinate to nucleobase-related purines and oxopurines by a single monodentate Ti-N bond or by bidentate O-Ti-N or N-Ti-N bonds.

Quite another kind of interaction was pointed out in the case of the paramagnetic $(C_5H_5)_2VCl_2$ with mononucleotides in aqueous solution near physiological pH by NMR and ESR methods, whereby the vanadocene moiety was bound in a labile outer-sphere complexation to the nucleotide phosphate group, the nucleotide-nucleotide Watson-Crick base-pairing not being disrupted by the binding of the vanadocene molecule ⁷⁴⁾. In a model complex using phospho-diester diphenylpho-

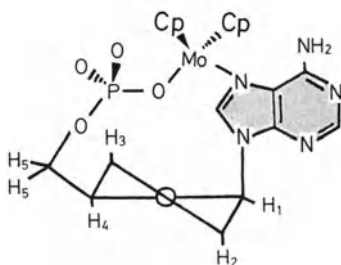


Fig. 28. Structure of bis(cyclopentadienyl)(5'-deoxyadenosinemonophosphate) molybdenum(IV) (Cp = C₅H₅). Modified according to Ref. ⁷⁵⁾

sphoric acid simulating the nucleotide phosphate group as ligand, a hydrogen-bonding interaction between the water molecules, coordinated in the vanadocene diaquo cation [(C₅H₅)₂V(OH₂)₂]²⁺, and the oxo oxygen atoms of the diphenylphosphate anions was actually established ⁷⁴⁾.

In the case of molybdenocene, a direct O(phosphate)-Mo bond and a N7(adenine)-Mo bond were observed in [(C₅M₅)₂Mo(5'-dAMP)], a complex obtained by titration of Na₂(5'-dAMP) with (C₅H₅)₂MoCl₂ in D₂O at pD 7.6–7.8 ⁷⁵⁾. Another molybdenum-containing metal complex, [(C₅H₅)₂Mo(9-MeAd)]PF₆, was isolated in two isomers from the reaction of (C₅M₅)₂MoCl₂ with 9-methyladenine (9-MeAdH) and NH₄PF₆. In one of both isomers, molybdenum was bound to the 9-MeAd anion via N-1 and N-6 in a four-membered chelate ring ⁷⁵⁾ (Fig. 28).

In all the mentioned model complexes, an intracellular interaction is anticipated between the bis(cyclopentadienyl)metal units and the nucleic acid components. On the other hand, it must also be considered that one of both cyclopentadienyl rings might be lost during the passage through the organism and that mono(cyclopentadienyl)metal complexes might react with cellular target molecules ⁷⁶⁾.

7 Conclusions and Outlook

Organometallic cyclopentadienyl metal complexes represent a group of non-platinum-group metal antitumor agents comprising complexes of different structural type:

- i) neutral bis(η⁵-cyclopentadienyl)metal (“metallocene”) diacido complexes (C₅H₅)₂MX₂ containing an early transition metal such as titanium(IV) or vanadium(IV) as central metal atom;
- ii) ionic metallocenium salts [(C₅H₅)₂M]⁺X⁻ including a medium transition metal, e.g., iron(III), as central atom;
- iii) uncharged decasubstituted metallocenes (C₅R₅)₂M with a main-group IV element, especially tin(II) or germanium(II), as central metal.

They effect growth-inhibition against various experimental and human tumors and are characterized by an unusual spectrum of antitumor activity and by toxicologic and pharmacokinetic properties which clearly differ from those of other inorganic, organometallic, and organic cytostatic agents.

These biological features qualify cyclopentadienyl metal complexes as an independent group of non-platinum-group metal antitumor agents, which are worth investigating in further experimental and clinical trials.

8 Acknowledgements

The author's work on cyclopentadienyl metal complexes was supported by financial grants of the Deutsche Forschungsgemeinschaft, the Medac GmbH, and the Trude Goerke foundation.

9 References

- Rosenberg B, VanCamp L, Trosko JE, Mansour VH (1969) *Nature* 222: 385
- Rosenberg B (1973) *Naturwiss.* 60: 399
- Prestayko AW, Crooke ST, Carter SK (eds) *Cisplatin: Current Status and New Developments*. Academic Press, New York 1980
- Hacker MP, Douple EB, Krakoff IH (eds) *Platinum Coordination Complexes in Cancer Chemotherapy*. Nijhoff, Boston 1984
- Nicolini M (ed) *Platinum and Other Metal Coordination Compounds in Cancer Chemotherapy*. Nijhoff, Boston 1988
- Bear JL, Gray HB, Rainen L, Chang IM, Howard R, Serio G, Kimball AP (1975) *Cancer Chemother. Rep. Part 1* 59: 611
- Giraldi S, Sava G, Bertoli G, Mestroni G, Zassinovich G (1977) *Cancer Res* 37: 2662
- Clarke MJ (1980) in: Martell EA (ed) *Inorganic Chemistry in Biology and Medicine*. American Chemical Society, Washington, pp 157–178
- Adamson RH, Canellos GR, Sieber SM (1975) *Cancer Chemother. Rep. Part 1* 59: 599
- Mulinos MG, Amin P (1980) *Fed. Proc. Fed. Am. Soc. Exp. Biol.* 39: 747
- Kumano N, Nakai Y, Ishikawa T, Koinumaru S, Suzuki S, Konno K (1978) *Sci. Rep. Res. Inst. Tohoku Univ., Ser. A* 25: 89
- Köpf H, Köpf-Maier P (1979) *Angew. Chem.* 91: 509; *Angew. Chem. Int. Ed. Engl.* 18: 477
- Köpf-Maier P, Köpf H (1979) *Z. Naturforsch.* 34b: 805
- Köpf H, Köpf-Maier P (1983) *ACS Symp. Ser.* 209: 315
- Keller HJ, Keppler B, Schmähl D (1982) *Arzneim.-Forsch./Drug Res.* 32: 806
- Keppler BK, Schmähl D (1986) *Arzneim.-Forsch./Drug Res.* 36: 1822
- Köpf-Maier P, Köpf H, Neuse EW (1984) *J. Cancer Res. Clin. Oncol.* 108: 336
- Sadler PJ, Nasr M, Narayanan VL (1984) *Dev. Oncol.* 17: 290
- Elo HO, Lumme PO (1985) *Cancer Treat. Rep.* 69: 1021
- Shaw CF, Beery A, Stocco GC (1986) *Inorg. Chim. Acta* 123: 213
- Mirabelli CK, Johnson RK, Sung CM, Faucette L, Muirhead K, Crooke ST (1985) *Cancer Res.* 45: 32
- Berners-Price SJ, Mirabelli CK, Johnson RK, Mattern MR, McCabe FL, Faucette LF, Sung CM, Mong SM, Sadler PJ, Crooke ST (1986) *Cancer Res.* 46: 5486
- Köpf-Maier P, Wagner W, Köpf H (1981) *Cancer Chemother. Pharmacol.* 5: 237
- Köpf-Maier P (1985) *Z. Naturforsch.* 40c: 843
- Köpf-Maier P, unpublished results
- Murthy MS, Rao LN, Kuo LY, Toney JH, Marks TJ (1988) *Inorg. Chim. Acta* 152: 117
- Köpf-Maier P, Hermann G (1984) *Virchows Arch. [Cell Pathol.]* 47: 107
- Köpf-Maier P, Hesse B, Köpf H (1980) *J. Cancer Res. Clin. Oncol.* 96: 43
- Köpf-Maier P, Hesse B, Voigtländer R, Köpf H (1980) *J. Cancer Res. Clin. Oncol.* 97: 31

30. Köpf-Maier P, Grabowski S, Liegener J, Köpf H (1985) *Inorg. Chim. Acta* 108: 99
31. Köpf-Maier P, Klapötke T, Köpf H (1988) *Inorg. Chim. Acta* 153: 119
32. Köpf-Maier P, Klapötke T, Neuse EW, Köpf H, *Cancer Chemother. Pharmacol.*, in press
33. Köpf-Maier P, Janiak C, Schumann H (1988) *Inorg. Chim. Acta* 152: 75
34. Köpf-Maier P, Janiak C, Schumann H (1988) *J. Cancer Res. Clin. Oncol.* 114: 502
35. Köpf-Maier P, Preiß F, Marx T, Klapötke T, Köpf H (1986) *Anticancer Res.* 6: 33
36. Köpf-Maier P, Wagner W, Hesse B, Köpf H (1981) *Eur. J. Cancer* 17: 665
37. Slavik M, Blanc O, Davis J (1987) *Invest. New Drugs* 1: 225
38. Köpf-Maier P, Köpf H (1987) *Arzneim.-Forsch./Drug Res.* 37: 532
39. Köpf-Maier P, Klapötke T (1989) *Arzneim.-Forsch./Drug Res.* 39: 369
40. Wolpert-De Filippes MK (1979) *Cancer Treat. Rep.* 63: 1453
41. Bellet RE, Danna V, Mastrangelo MJ, Berd D (1979) *J. Natl. Cancer Inst.* 63: 1185
42. Fiebig HH, Schuchhardt C, Heuss H, Fiedler L, Löhr G (1984) *Behr. Inst. Mitt.* 74: 343
43. Povlsen CO, Jacobsen GK, Rygaard J (1973) in Spiegel A (ed) *Laboratory Animals in Drug Testing*. Fischer, Stuttgart, pp 63–72
44. Kyriazis AA, Kyriazis AP, Kereiakes JG, Soloway MS, McCombs WB (1983) *Exp. Cell Biol.* 51: 83
45. Osieka R, Houchens DP, Goldin A, Johnson RK (1977) *Cancer* 40: 2640
46. Shorthouse AJ, Peckham MJ, Smyth JF, Steel GG (1981) in Bastert GBA, Fortmeyer HP, Schmidt-Matthiesen H (eds) *Thymusaplastic Nude Mice and Rats in Clinical Oncology*. Fischer, Stuttgart, pp 365–371
47. Köpf-Maier P (1988) in Winograd B, Peckham MJ, Pinedo HM (eds) *Human Tumour Xenografts in Anticancer Drug Development*. Springer, Berlin, pp 85–88
48. Köpf-Maier P (1987) *J. Cancer Res. Clin. Oncol.* 113: 342
49. Köpf-Maier P, Moormann A, Köpf H (1985) *Eur. J. Cancer Clin. Oncol.* 21: 853
50. Köpf-Maier P (1989) *Cancer Chemother. Pharmacol.* 23: 225
51. Köpf-Maier P (1988) *J. Cancer Res. Clin. Oncol.* 114: 250
52. Köpf-Maier P, Hinkelbein W, submitted für publication
53. Tonew E, Tonew M, Heym B, Schröer HP (1981) *Zbl. Bakt. Hyg., I. Abt. Orig. A* 250: 425
54. Taylor C, personal communication
55. Fairlie DP, Whitehouse MW, Broomhead JA (1987) *Chem. Biol. Interact.* 61: 277
56. Köpf-Maier P, Gerlach S (1986) *J. Cancer Res. Clin. Oncol.* 111: 243
57. Köpf-Maier P, Köpf H (1986) *Anticancer Res.* 6: 227
58. Köpf-Maier P, Funke-Kaiser P (1986) *Toxicol.* 38: 81
59. Köpf-Maier P, Gerlach S (1986) *Anticancer Res.* 6: 235
60. Köpf-Maier P, Brauchle U, Henßler A (1988) *Toxicol.* 51: 291
61. Köpf-Maier P, Brauchle U, Henßler A (1988) *Toxicol.* 48: 253
62. Köpf-Maier P, Erkenwick P (1984) *Toxicol.* 33: 171
63. Toney JH, Murthy MS, Marks TJ (1985) *Chem. Biol. Interact.* 56: 45
64. Köpf-Maier P, Köpf H (1980) *Naturwiss.* 67: 415
65. Köpf-Maier P, Wagner W, Köpf H (1981) *Naturwiss.* 68: 272
66. Köpf H, Köpf-Maier P (1981) *Nachr. Chem. Tech. Lab.* 29: 154
67. Köpf-Maier P, Wagner W, Liss E (1981) *J. Cancer Res. Clin. Oncol.* 102: 21
68. Köpf-Maier P, Wagner W, Liss E (1983) *J. Cancer Res. Clin. Oncol.* 106: 44
69. Köpf-Maier P, Krahl D (1983) *Chem. Biol. Interact.* 44: 317
70. Beauchamp AL, Cozak D, Mardhy A (1984) *Inorg. Chim. Acta* 92: 191
71. Cozak D, Mardhy A, Olivier MJ, Beauchamp AL (1986) *Inorg. Chem.* 25: 2600
72. Beauchamp AL, Bélanger-Gariépy F, Mardhy A, Cozak D (1986) *Inorg. Chim. Acta* 124: L23
73. Pneumatikakis G, Yannopoulos A, Markopoulos J (1988) *Inorg. Chim. Acta* 151: 125
74. Toney JH, Brock CP, Marks TJ (1986) *J. Am. Chem. Soc.* 108: 7263
75. Kuo LY, Kanatzidis MG, Marks TJ (1987) *J. Am. Chem. Soc.* 109: 7207
76. Köpf H, Tekes Z, Grabowski S, unpublished results; cf. Tekes Z, *Dissertation Techn. Univ. Berlin*, 1985
77. Heeg MJ, Janiak C, Zuckerman JJ (1984) *J. Am. Chem. Soc.* 106: 4259
78. Schumann H, Janiak C, Hahn E, Kolax C, Loebel J, Rausch MD, Zuckerman JJ, Heeg MJ (1986) *Chem. Ber.* 119: 2656

NMR Relaxation Footprinting: The $[\text{Cr}(\text{NH}_3)_6]^{3+}$ Cation as a Probe for Drug Binding Sites on Oligonucleotides

Elwood V. Scott¹, Gerald Zon², and Luigi G. Marzilli¹

¹ Department of Chemistry, Emory University, Atlanta, Georgia 30322, USA

² Applied Biosystems, 850 Lincoln Centre Drive, Foster City, California 94404, USA

$[\text{Cr}(\text{NH}_3)_6](\text{NO}_3)_3$ was used to probe structural features of the oligonucleotide, $d(\text{ATGCGCAT})_2$ (numbering of strand: 5' $A_1T_2G_3C_4G_5C_6A_7T_8$ 3') and to footprint the binding site of actinomycin D (ActD) in the unique 2:1 ActD/ $d(\text{ATGCGCAT})_2$ complex by proton longitudinal relaxation (T_1) studies. Longitudinal relaxation rates ($1/T_1$) of the ^1H NMR signals were measured before and after the addition of the $[\text{Cr}(\text{NH}_3)_6]^{3+}$ solution to determine the paramagnetic longitudinal relaxation rate ($1/T_{1p} = 1/T_{1(\text{Cr})} - 1/T_{1(\text{noCr})}$). The chromium complex seems to prefer the center of the duplex, since signals for protons on nucleotides in the center of the duplex have the largest $1/T_{1p}$ s. Larger $1/T_{1p}$ values are observed for signals of major groove base protons on G_3 , C_4 , G_5 and C_6 and also for signals of deoxyribose $H1'$ and $H3'$ protons which are close to the phosphate backbone ($H3'$ closer than $H1'$). We believe that electrostatic forces and hydrogen bonding are the main interactions between the chromium hexaammine cation and $d(\text{ATGCGCAT})_2$. To interpret our data we used distances from computer-generated models for five major binding modes. Four of these involved hydrogen bonding of the ammonia ligands to various sites on the oligonucleotide (phosphate oxygens, base oxygens and base nitrogens). One mode involved the approach of the $[\text{Cr}(\text{NH}_3)_6]^{3+}$ cation into the minor groove of the duplex with no hydrogen bonding. Neither a single binding mode nor an equal weighting of all binding modes appeared to explain the results. Two modes appeared to have the greatest influence. One involved major groove interstrand binding at G_3 and G_5 . The other involved interaction of the cation with a single phosphate group, with all phosphate groups exhibiting this binding mode. Other modes most likely do occur, but from modeling studies these modes appear to be less important. This relatively non-selective binding suggested the possibility of using the $[\text{Cr}(\text{NH}_3)_6]^{3+}$ cation as a paramagnetic probe for NMR footprinting of drug binding sites on oligonucleotides. Examination of the 2:1 ActD/ $d(\text{ATGCGCAT})_2$ complex showed that the signals of $H1'$ protons in the center of the duplex were protected from the $[\text{Cr}(\text{NH}_3)_6]^{3+}$ cation, most likely by the ActD cyclic peptides. Also, the $[\text{Cr}(\text{NH}_3)_6]^{3+}$ cation had a large effect on the ActD-H8 signal, as expected since it is located between G_5 and C_6 . Base proton signals of these nucleotides are affected significantly by the $[\text{Cr}(\text{NH}_3)_6]^{3+}$ cation. Furthermore, the signals of protons on terminal nucleotides appear to be influenced relatively more in the drug adduct than in the parent oligonucleotide. These preliminary results demonstrate the feasibility of using paramagnetic metal complexes as NMR footprinting agents.

1 Introduction	186
2 Experimental	188
3 Results	189
3.1 $d(\text{ATGCGCAT})_2$	189
3.2 $d(\text{ATGCGCAT})_2$ with $[\text{Cr}(\text{NH}_3)_6](\text{NO}_3)_3$	190
3.3 2:1 ActD: $d(\text{ATGCGCAT})_2$ Complex	192
4 Discussion	195
5 Abbreviations	203
6 Acknowledgements	203
7 References	203

1 Introduction

To understand the interactions of DNA-binding drugs with DNA it is important to evaluate the solution structure of the DNA-drug adduct. A valuable approach has been to use metal species as probes for structural information in solution¹⁻⁴. These studies of metal ions as structural probes have involved both inner-sphere and outer-sphere coordination of the metal complex to the DNA. The outer-sphere binding metal complexes act as DNA-cleaving agents (monitored by gel electrophoresis). Metal species that bind directly have been monitored by NMR spectroscopy¹. Parameters of the NMR signals that can be useful to assess the metal binding site are the chemical shift, longitudinal relaxation time (T_1), transverse relaxation time (T_2), and line width^{5,6}. Changes in any of these parameters may indicate that the nuclei under observation are spatially close to the metal binding site. However, complications do arise, especially in the interpretation of T_2 data and chemical shifts⁶.

One of the most useful NMR parameters is T_1 since there is a direct relationship between the effect of the metal and the distance to the resonating nucleus. Inner-sphere coordination to the paramagnetic complexes is not necessary for NMR relaxation effects; for example, tris(acetylacetonato)chromium(III) is used in solution to shorten the longitudinal relaxation time of nuclei with unusually long T_1 's⁷. The resulting decrease in T_1 allows acquisition of more transients per unit time, thus shortening the NMR experiment. It is conceivable that inert paramagnetic metal complexes can be used as NMR probes for DNA structural analysis by exploiting the enhancement of longitudinal relaxation rates of nuclei close to the paramagnetic metal. The use of inert complexes minimizes the problems typically encountered with labile metal species such as signal line broadening from contact interactions and highly selective binding at a single site⁶. Also, outer-sphere interactions should lead to less structural distortion of the DNA being probed.

To test the feasibility of using inert paramagnetic metal complexes as NMR probes for structural information, we decided to investigate the use of $[\text{Cr}(\text{NH}_3)_6](\text{NO}_3)_3$ on the well characterized, self-complementary oligonucleotide, $d(\text{ATGCGCAT})_2$ ⁸. $[\text{Cr}(\text{NH}_3)_6](\text{NO}_3)_3$ was chosen because Cr(III) complexes have been used successfully as relaxation agents, as mentioned above, and because the ammonia ligands on the chromium are relatively inert. Since a goal of this initial study was to gain footprinting type information (see below), we wished to examine a simple achiral complex, which is unlikely to bind with high site selectivity. Recent studies in Barton's laboratory reveal that chiral systems may bind in a highly selective manner to different forms of DNA^{3,9}. On the other hand, studies with the analogous diamagnetic cobalt hexaammine cation revealed it binds to DNA with little site selectivity¹⁰. The oligonucleotide duplex, $d(\text{ATGCGCAT})_2$, was chosen because it has been shown by 2D NMR techniques (proton assignments made for all oligonucleotide protons except deoxyribose 4', 5', and 5'' protons) to be a standard B-form helix (right-handed helix, C2'-endo sugar puckers, ⁸).

A major goal of this research was to explore the feasibility of using the $[\text{Cr}(\text{NH}_3)_6]^{3+}$ cation for footprinting the position of a drug on a DNA strand. Tullius has used $[\text{Fe}(\text{EDTA})]^{2-}$ to carry out footprinting studies with the HSV-1 tk DNA fragment². Sigman and co-workers exploited the 1,10-phenanthroline-copper

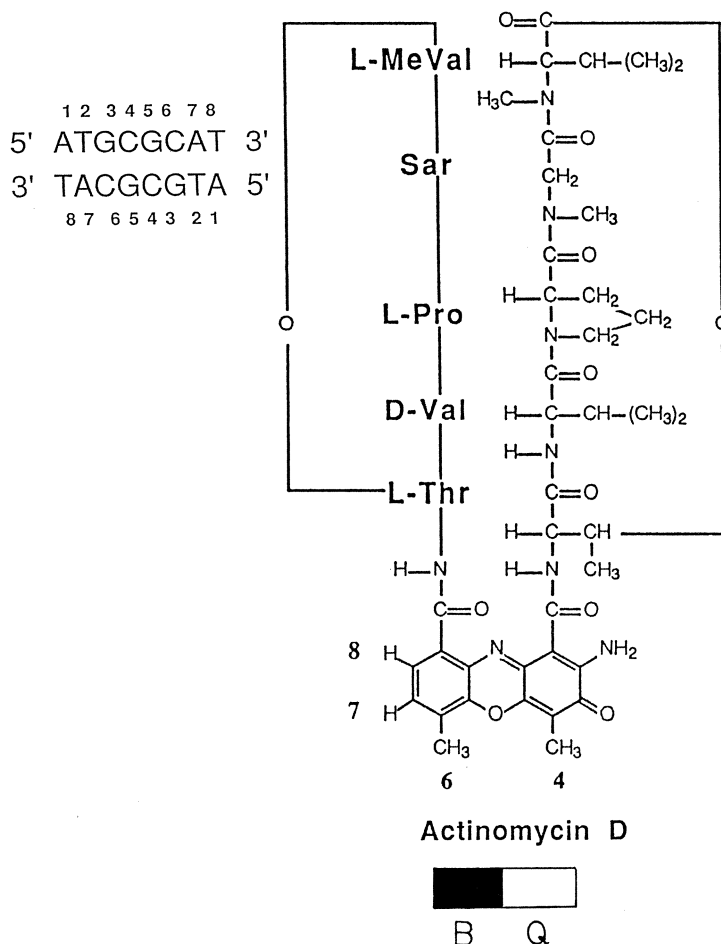


Fig. 1. *Left:* numbering scheme for the self-complementary oligonucleotide $d(ATGCGCAT)_2$.
Right: structure of actinomycin D

ion in similar studies⁴⁾. For this purpose, we chose to examine the adduct formed between $d(ATGCGCAT)_2$ and two actinomycin D (ActD) molecules using the $[Cr(NH_3)_6]^{3+}$ cation. Structural features of the unique 2:1 complex have already been determined (assignments of most proton signals for the duplex and for ActD are known⁸⁾) such that the duplex is in a distorted right-handed helix with C3'-*endo* conformation for the sugars on T₂, C₄, and C₆ (see Fig. 1 for the numbering scheme of duplex and the ActD structure). The phenoxazone rings are intercalated at the adjacent-GpC-sites in the orientation shown in Fig. 2. Note that the cyclic peptides of the ActD molecules are along the minor groove of the duplex.

The Mn^{2+} cation has been used to gain structural information of ActD-oligonucleotide complexes in which NMR signals were examined for paramagnetic broadening to determine the metal-binding sites¹⁾. However, the mode of binding of the Mn^{2+} cation to DNA is complex⁵⁾ and the elegant method of Chiao and Krugh¹⁾ is limited to species close to a dianionic phosphate monoester group.

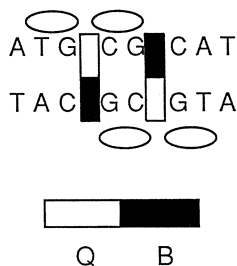


Fig. 2. Orientation of the intercalated phenoxazine moiety of the actinomycin D molecule in the 2:1 ActD/d(ATGCGCAT)₂ complex. Q is the quinoid portion of the phenoxazine ring and B is the benzenoid portion of the phenoxazine ring

2 Experimental

The oligonucleotide dATGCGCAT was prepared by the phosphoramidite method and purified as previously described¹¹. [Cr(NH₃)₆](NO₃)₃ was prepared as previously described,¹² its identity was determined by adsorption spectroscopy, and its purity was confirmed by elemental analysis [Anal. Calcd for Cr₁H₁₈N₉O₉: N, 37.06; H, 5.33. Found: N, 37.00; H, 5.35]. Actinomycin D (ActD) was purchased from Sigma and used without further purification.

¹H NMR data were obtained at 361.02 MHz on a Nicolet 360NT FT spectrometer at 15 °C, spectral width of 3436 Hz, 16 K data points, typically 96 transients, applying 0.1 Hz line broadening to the FID before Fourier transformation. All chemical shifts were referenced to sodium 3-(trimethylsilyl)tetradeuteriopropionate (TSP). Longitudinal relaxation data were obtained using the inversion-recovery method with a modified pulse sequence that incorporates phase shifting of the pulses ($90^{\circ}_{+x} - 180^{\circ}_{+y} - 90^{\circ}_{+x-t} - 90^{\circ}_{+/-x} - \text{Acq.}_{+/-}$;¹³). Peak heights were used to make the relaxation curve and a line fitting program was then used to calculate the best fit of the curve from which T₁ values were calculated (NMR-1280 software (version 9) from GE Corp.;¹⁴). ³¹P NMR data were collected at 80.1 MHz on an IBM WP-200SY spectrometer under the following conditions: 12,000 scans, 45° pulse, 2-s pulse repetition, broadband proton decoupling, 1 Hz line broadening applied before Fourier transformation.

NMR samples of 0.5 ml in a 5-mm NMR tube were prepared in 99.96% D₂O (KOR, Inc.), 0.1 M NaCl, 1.0 mM EDTA, 35 mM bases (dATGCGCAT), and pH 7.0. ActD was added to the oligonucleotide solution as previously described¹⁵. For ³¹P studies, the 5-mm NMR tubes were placed in 10-mm tubes containing 0.1 M NaCl and 1.0 mM EDTA in D₂O (pH 7.0) with trimethyl phosphate as a reference. In the titrations, 15- μ l aliquots of a [Cr(NH₃)₆](NO₃)₃ solution in D₂O (1×10^{-3} M) were added for each titration point to the oligonucleotide solutions. ¹H relaxation data for only the last three titration points (Cr(III) concentrations of 9×10^{-5} M, 12×10^{-5} M, and 15×10^{-5} M) are reported here since only small non-linear rate increases were observed for the first two additions.

Modeling studies were done using MacroModel (version 2.0, generously supplied by Prof. Clark Still, Columbia University, Dept. of Chem., New York, NY, 10027) on a DEC VAXstation II computer with an Evans and Sutherland PS-390 work station. B-form coordinates for the DNA model were part of the MacroModel program and were derived from Arnott et al.¹⁶.

3 Results

3.1 $d(ATGCGCAT)_2$

The T_1 values for most of the resolved ^1H signals of this duplex are presented in Table 1 as the longitudinal relaxation rate, $1/T_1$. In general, the standard deviation was 1 to 3% of T_1 and the T_1 values appeared reasonable in reference to previous

Table 1. $1/T_{1p}$ ^a values for selected protons of duplexed $dATGCGCAT$ (35 mM in bases) at different concentrations of $[\text{Cr}(\text{NH}_3)_6]^{3+}$ cation

Resonance ^b	$1/T_1$ (s^{-1}) (no chromium)	$1/T_{1p}$ (s^{-1}) $[\text{Cr}(\text{NH}_3)_6]^{3+}$		
		9×10^{-5} M	12×10^{-5} M	15×10^{-5} M
A ₁ H8	0.61	0.15	0.48	0.55
A ₁ H2	0.22	0.22	0.52	0.72
A ₁ H1'	0.76	0.25	0.57	0.64
A ₁ H3'	0.76	0.36	2.46 ^d	1.56
T ₂ H6	0.84	0.38	0.87	1.71
T ₂ -CH ₃	0.70	0.39	0.99	1.73
T ₂ H1'	0.69	0.28	0.58	1.43
T ₂ H3'	^c			
G ₃ H8	0.69	0.43	1.26	2.24
G ₃ H1'	0.68	0.28	0.74	2.02
G ₃ H3'	0.76	0.36	2.46 ^d	1.56
C ₄ H6	0.75	0.43	1.00	1.88
C ₄ H5	0.58	0.52	2.20	4.18
C ₄ H1'	0.69	0.28	0.58	1.43
C ₄ H3'	^c			
G ₅ H8	0.70	0.50	1.26	2.63
G ₅ H1'	0.68	0.39	1.24	2.26
G ₅ H3'	0.76	0.36	2.46 ^d	1.56
C ₆ H6	0.73	0.43	1.02	1.90
C ₆ H5	0.53	0.25	0.86	1.64
C ₆ H1'	0.69	0.43	0.63	1.87
C ₆ H3'	^c			
A ₇ H8	0.76	0.34	0.78	1.28
A ₇ H2	0.22	0.20	0.49	0.79
A ₇ H1'	0.75	0.27	0.65	1.00
A ₇ H3'	0.76	0.36	2.46 ^d	1.56
T ₈ H6	0.71	0.29	0.54	0.75
T ₈ -CH ₃	0.69	0.25	0.59	0.85
T ₈ H1'	0.64	0.20	0.50	0.95
T ₈ H3'	0.85	0.04	0.03	0.09

^a $1/T_{1p} = 1/T_1$ (with $[\text{Cr}(\text{NH}_3)_6]^{+3}$) $- 1/T_1$ (without $[\text{Cr}(\text{NH}_3)_6]^{+3}$).

^b Assignments were made previously⁸⁾.

^c T₁'s of H3' protons on T2, C4, and C6 were not measureable as they were located under the HDO signal.

^d Fluctuation in value presumably due to overlap of 3' signals for A₁, G₃, G₅, and A₇ as well as closeness to water signal; value is not reliable

studies^{17,18}). The numbering scheme for the oligonucleotide, dA₁T₂G₃C₄G₅C₆A₇T₈, is the same as that used in the ¹H NMR assignment⁸).

3.2 *d(ATGCGCAT)₂ with [Cr(NH₃)₆] (NO₃)₃*

The addition of a [Cr(NH₃)₆]³⁺ solution to the solution of the oligonucleotide resulted, as expected, in a decrease in the T₁'s of the signals of the duplex. The order of most affected to least affected signal was consistent for each addition (Table 1). Unexpectedly, the effect was not linear for the initial Cr(III) additions, presumably due to adsorption on the surface of the NMR tube and/or trace amounts of other anions in solution. Linear 1/T₁ increases were observed for most signals at the Cr(III) concentrations of 9 × 10⁻⁵ M, 12 × 10⁻⁵ M, and 15 × 10⁻⁵ M. Linear increases of 1/T₁ of water protons in the presence and absence of DNA by the addition of metal ions (Mn²⁺ and Co²⁺) were also observed by Granot and Kearns⁵) in their examination of the extent and modes of binding of divalent metal ions to DNA. In Table 1, the data are presented as 1/T_{1p} = 1/T₁ (presence of Cr) - 1/T₁ (no Cr). The propagated deviation of 1/T_{1p} is on the order of 6 to 9%. A list of some of the most affected proton signals of the duplex appears in Scheme 1.

C₄H5 ≫

G₅H8 > G₅H1' > G₃H8 > G₃H1' ≫

C₆H6 > C₄H6 > C₆H1' > T₂-CH₃ > T₂H6 > C₆H5 > A₇H3', A₁H3', G₅H3' ≫

C₄H1', T₂H1'

Scheme 1

The T₁'s of protons on nucleotides in the center of the duplex are affected more than the T₁'s of protons on terminal nucleotides, i.e., compare the 1/T_{1p} values of

Table 2. 1/T_{1p} values for signals of protons in the deoxyribose 4', 5' and 5'' region of duplexed dATGCGCAT (35 mM in bases) at different concentrations of [Cr(NH₃)₆]³⁺ cation

Resonance ^a	1/T ₁ (s ⁻¹) (no chromium)	1/T _{1p} (s ⁻¹) [Cr(NH ₃) ₆] ³⁺		
		9 × 10 ⁻⁵ M	12 × 10 ⁻⁵ M	15 × 10 ⁻⁵ M
4.25 ppm	0.71	0.40	1.01	1.97
4.21 ppm	0.69	0.56	0.92	1.50
4.12 ppm	0.87	0.29	0.79	1.24
4.05 ppm	0.76	0.45	1.19	2.94
3.99 ppm	0.82	0.49	1.13	1.80
3.87 ppm	0.84	0.38	0.79	1.43
3.64 ppm	1.30	0.45	1.97 ^b	1.74

^a Signals are not assigned and are therefore listed by chemical shift.

^b Fluctuation in 1/T₁ is presumably due to overlap of signals; value is not very reliable

G_3H8 (2.24 sec^{-1}) and G_5H8 (2.26 sec^{-1}) to those of A_1H8 (0.55 sec^{-1}) and A_2H8 (1.28 sec^{-1}) in Table I ($15 \times 10^{-5} \text{ M } [Cr(NH_3)_6]^{3+}$). Although assignments for deoxyribose 4', 5' and 5'' resonances were not made previously because of overlap of the signals, we did calculate a T_1 value for the maxima in the 4', 5' and 5'' spectral region of the NMR spectrum (3.5 to 4.5 ppm). Table 2 shows the $1/T_{1p}$ values for these overlapped peaks and some of these values are comparable to those of the most affected signals listed in Scheme 1. The 5' and 5'' protons are very close to the phosphate groups and the T_1 data suggest that the chromium hexaammine cation does have an affinity for the phosphate groups on the duplex.

The ^{31}P NMR spectrum of the oligonucleotide solution was examined at the final chromium addition ($15 \times 10^{-5} \text{ M } [Cr(NH_3)_6](NO_3)_3$, 233 bases/chromium). There were no observable changes (extreme line broadening or shifted signals) of the phosphorus signals compared to ^{31}P NMR spectra of solutions without added chromium hexaammine cation.

Table 3. $1/T_{1p}$ values for dATGCGCAT protons of 2:1 complex of ActD/dATGCGCAT at different concentrations of $[Cr(NH_3)_6]^{3+}$ cation

Resonance ^a	$1/T_1$ (s^{-1}) (no chromium)	$1/T_{1p}$ (s^{-1}) $[Cr(NH_3)_6]^{3+}$		
		$9 \times 10^{-5} \text{ M}$	$12 \times 10^{-5} \text{ M}$	$15 \times 10^{-5} \text{ M}$
A_1H8	0.69	0.07	0.03	0.12
A_1H2	0.36	0.04	0.00 ^b	0.09
A_1H1'	0.78	0.12	0.09	0.22
T_2H6	0.73	0.24	0.25	0.67
T_2-CH_3	0.75	0.08	0.07	0.15
T_2H1'	0.78	0.12	0.09 ^b	0.22
G_3H8	0.70	0.65	0.81	1.42
G_3H1'	0.64	0.37	0.33	0.54
C_4H6	0.54	0.87	1.36	^c
C_4H5	0.47	0.45	0.52	1.11
C_4H1'	0.51	0.32	0.14 ^b	0.56
G_5H8	0.67	0.31	0.45	0.91
G_5H1'	0.57	0.27	0.28	0.55
C_6H_6	0.47	0.15	0.16	0.38
C_6H5	0.51	0.00	0.06	0.24
C_6H1'	0.51	0.32	0.14 ^b	0.56
A_7H8	0.69	0.17	0.14 ^b	0.35
A_7H2	0.51	~0	~0	~0
A_7H1'	0.78	0.19	0.19	0.32
T_8H6	0.91	0.07	0.04 ^b	0.19
T_8-CH_3	0.51	0.03	0.13	0.18
T_8H1'	0.64	0.37	0.33 ^b	0.54

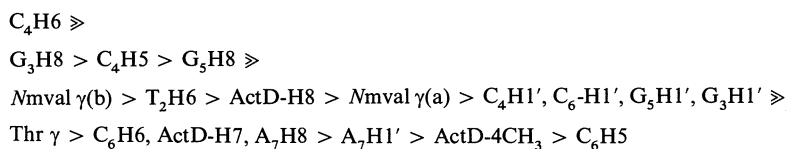
^a Assignments were made previously ⁸⁾.

^b Fluctuation in $1/T_1$ value is presumably due to overlap of signals except in the case of A_7H8 , A_7H2 , A_1H2 , and T_8H6 .

^c Calculated T_1 deviation was too high for value to be reliable (relaxation rate was too fast)

3.3 2:1 ActD:d(ATGCGCAT)₂ Complex

The $1/T_1$ results obtained for the 2:1 ActD:d(ATGCGCAT)₂ complex before the addition of $[\text{Cr}(\text{NH}_3)_6]^{3+}$ are presented in Table 3, along with the $1/T_{1p}$ values obtained for several additions of the $[\text{Cr}(\text{NH}_3)_6]^{3+}$ solution. As for the free duplex, signals for protons on nucleotides in the center of the duplex are again affected the most. The final T_1 value (15×10^{-5} M $[\text{Cr}(\text{III})]$) for C₄H6 was not reliable since the signal relaxed so quickly, causing a large deviation in its calculated value, but the trend of the C₄H6 signal being the most affected in the previous titration, points can be extrapolated to the results of the last titration point. Scheme 2 shows the order of the most affected signals in the 2:1 complex for both oligonucleotide protons (Table 3) and ActD protons (Table 4).



Scheme 2

Table 4. $1/T_{1p}$ values for ActD protons of 2:1 complex of ActD/dATGCGCAT at different concentrations of $[\text{Cr}(\text{NH}_3)_6]^{3+}$ cation

Resonance ^a	$1/T_1$ (s ⁻¹) (no chromium)	$1/T_{1p}$ (s ⁻¹) $[\text{Cr}(\text{NH}_3)_6]^{3+}$		
		9×10^{-5} M	12×10^{-5} M	15×10^{-5} M
H8	0.50	0.18	0.20	0.60
H7	0.41	0.03	0.11	0.35
4-CH ₃	0.51	0.15	0.21	0.31
6-CH ₃	0.48	0.09	0.17	0.20
Thr β (Q) ^b	0.85	0.50	0.00	0.39
Thr β (B) ^b	0.61	0.69	0.19	0.51
Thr γ (Q & B)	0.77	0.21	0.30	0.46
DVal γ (Q & B)	0.98	0.09	0.15	0.28
Pro α (Q) ^b	0.73	0.25	0.20	0.30
NmVal <i>N</i> -CH ₃ (Q) ^b	0.69	0.32	0.14	0.21
NmVal <i>N</i> -CH ₃ (B)	0.79	0.10	0.14	0.20
Sar <i>N</i> -CH ₃ (Q)	0.70	0.03	0.08	0.11
Sar <i>N</i> -CH ₃ (B) ^b	0.70	0.08	0.07	0.15
NmVal γ (a) ^c	1.39	0.13	0.25	0.53
NmVal γ (b)	1.79	0.14	0.30	0.65

^a Assignments were made previously⁸⁾.

^b Inconsistencies of chromium effect on the longitudinal relaxation rates are presumably due to overlap of signals and in the case of the Thr β protons most likely a result of closeness of the signal to the water signal. Q and B are for the cyclic peptide chains on the quinoid and benzenoid side of the ActD phenoxazone ring, respectively.

^c Two signals for NmVal γ protons are observed but not assigned

The order of affected DNA signals is slightly different in the free and the 2:1 complex, but the major significant relative differences are best appreciated by the examination of the ratio of the $1/T_{1p}$ (H1') to $1/T_{1p}$ (base proton, H8 or H6) on the same nucleotide. These ratios are listed in Table 5 for the free duplex and the 2:1 ActD complex. For T_2 , G_3 , C_4 and G_5 the ratios are less for the 2:1 complex than for the free duplex, giving evidence that the H1' for these nucleotides are being somewhat protected from the chromium complex. The ratios for A_1 , C_6 , A_7 and T_8 are larger for the 2:1 complex than for the free duplex. The increase in these ratios could be a result of the chromium cation's relatively greater occupation of binding sites on the duplex not blocked by the ActD drug. These are typically at the end of the duplex. It is unlikely that the C3'-endo conformation adopted by some of the nucleotides in the 2:1 complex is responsible for the smaller $1/T_{1p}$ (H1') to $1/T_{1p}$ (base proton) ratio since this ratio is larger for C_6 and smaller for T_2 and C_4 in the 2:1 complex. These three nucleotides adopt the C3'-endo conformation.

The effect of the chromium cation on some of the ActD signals in the 2:1 complex (Table 4) is inconsistent at the chromium cation concentration of 12×10^{-5} M for the following protons: Thr β (quinoid and benzenoid), Pro α (quinoid), an NmVal $N\text{-CH}_3$, and a Sar $N\text{-CH}_3$ (Table 4). We believe this problem is a result of either overlap of signals and/or closeness of the signal to the large HDO signal. For this reason we will not discuss the effect of the chromium on these ActD signals but will concentrate on the ActD signals that exhibit a normal incremental longitudinal relaxation rate increase with the addition of the chromium hexaammine cation.

The most affected of the ActD signals are those for the NmVal γ protons (Scheme 2) which are on cyclic peptides on the minor groove side of the duplex. These NmVal γ protons are pointing towards the phosphate backbone of the duplex, one of the likely binding sites of the $[\text{Cr}(\text{NH}_3)_6]^{3+}$ cation. The DVal γ protons are pointing into the solvent away from the DNA and their signals are marginally affected by the $[\text{Cr}(\text{NH}_3)_6]^{3+}$ cation. The $N\text{-CH}_3$ groups of both NmVal residues, which are pointing directly into the minor groove, are protected from access by the cation. As expected, their signals are negligibly affected by the Cr(III). The $N\text{-CH}_3$ moieties of Sar are

Table 5. Ratio of paramagnetic effect on H1' protons to base H8 (purine) or H6 (pyrimidine) protons for nucleotides in duplexed dATGCGCAT derived from the T_1 values at the final chromium addition (15×10^{-5} M, see Tables 1 and 3)

Residue	$[1/T_{1p}(\text{H1}')]/[1/T_{1p}(\text{H8 or H6})]$	
	Free dATGCGCAT	2:1 ActD/dATGCGCAT
A_1	1.16	1.83
T_2	0.84	0.33
G_3	0.90	0.38
C_4	0.76	0.13
G_5	0.86	0.60
C_6	0.98	1.47
A_7	0.78	0.91
T_8	1.27	2.84

directed away from the DNA and into the solvent and their signals also experience little to no enhanced relaxation. The ActD-H8 is the second most affected ActD signal. We would expect to see a large effect on ActD-H8 and ActD-H7 since the orientation of the phenoxazine ring brings both protons close to G₅H8 (confirmed by NOE data⁸⁾). The fourth signal most affected by the Cr(III) is G₅H8 (Scheme 2, Tables 3 and 4). Thus, the chromium should be close to ActD-H8 and ActD-H7 since these protons are close to G₅H8. The ActD-4CH₃ signal seems also to be substantially influenced by the chromium in comparison to other ActD signals and this also is expected since the ActD-4CH₃ group is in the major groove, very close to C₄ and G₃ whose base protons are affected the most by the Cr(III). Other ActD signals are not substantially influenced by the [Cr(NH₃)₆]³⁺ cation.

³¹P NMR spectra of the 2:1 ActD:d(ATGCGCAT)₂ complex were examined as a function of added chromium hexaammine cation starting at the final addition for the proton T₁ data (233 bases/chromium, 15 × 10⁻⁵ M [Cr(NH₃)₆](NO₃)₃) because of the potential hydrogen bonding between the duplex phosphates and the chromium hexaammine cation. The ³¹P NMR spectrum of the 2:1 complex has two downfield shifted phosphorus signals (-2.3 ppm and -2.7 ppm) outside of the main signals (-3.8 ppm to -4.4 ppm, see Fig. 3) that have been assigned to G_{3p}C₄ and G_{5p}C₆, respectively, in a related 2:1 complex, ActD:d(TGCGCA)₂¹⁹⁾. We compared the relative broadening of the ³¹P signals. Such broadening allows a qualitative assessment of selective binding of the chromium complex. We found that all the phosphorus signals broadened similarly with the addition of chromium hexaammine cation up

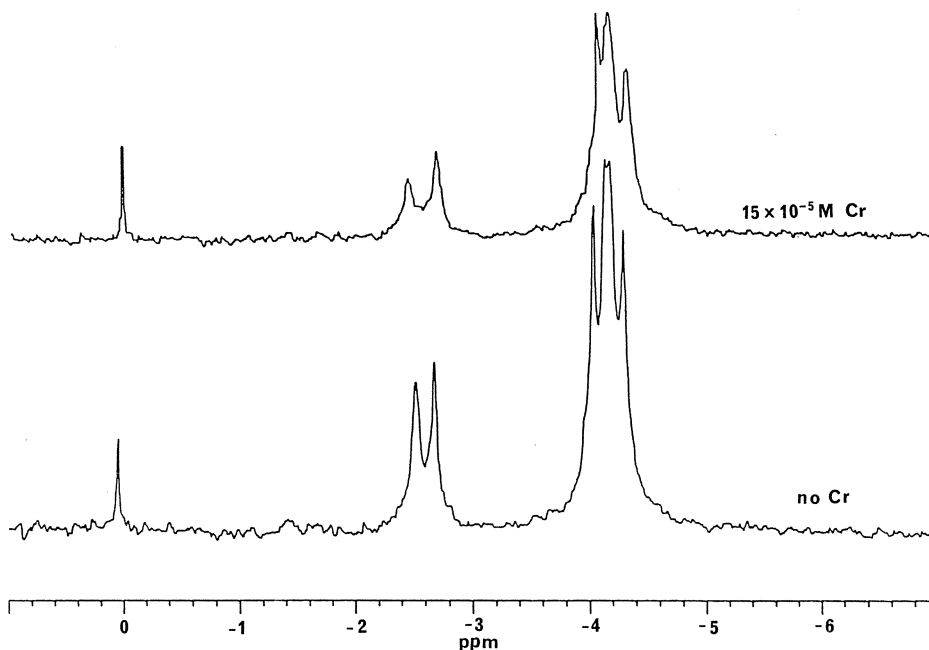


Fig. 3. ³¹P NMR spectra of 2:1 ActD/d(ATGCGCAT)₂; Bottom spectrum: no [Cr(NH₃)₆]³⁺; Top spectrum: 15 × 10⁻⁵ M [Cr(NH₃)₆]³⁺

to the ratio of 61 bases/chromium. At this ratio we clearly observed a slight down-field shift for the G_3pC_4 signal originally located at -2.3 ppm (Figure 3). This signal also broadens slightly more than the other signals. These results suggest that we have reached ratios of chromium to duplex (1:3.8) that can induce conformational changes in the duplex. However, at low ratios, there appear to be no selective interactions with any of the phosphate groups.

4 Discussion

Modeling Studies

In an effort to understand qualitatively the $1/T_{1p}$ data for dATGCGCAT in the free form, we examined models of the duplex and the chromium hexaammine cation using the MacroModel modeling program and a graphics terminal. The $[Cr(NH_3)_6]^{3+}$ computer model was constructed using crystal structure data²⁰⁾ and the duplex structure was made using data for B-form DNA contained within MacroModel. We assume the most important interactions of the duplex and the chromium complex are 1) the electrostatic attraction of the positively charged $[Cr(NH_3)_6]^{3+}$ cation to the negatively charged phosphates and 2) hydrogen bonding of the ammonia ligands on the chromium complex to phosphate oxygens as well as to base oxygens and nitrogens. In the examination of our computer models for important hydrogen bonding modes, we utilized the hydrogen bonding distances between hetero-atoms (~ 3.0 Å) observed in the structure of the cobalt hexaammine adduct of the Z-form duplex, $d(CGCGCG)_2$ ²¹⁾.

Based on this modeling approach, we were able to determine that the $[Cr(NH_3)_6]^{3+}$ cation is able to access the floor of the major groove easily. However, the metal

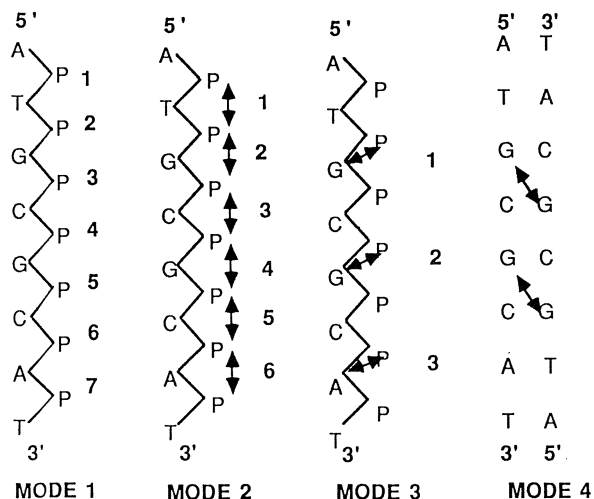


Fig. 4. Representations of the DNA-binding sites for the four $[Cr(NH_3)_6]^{3+}$ cation-DNA hydrogen bonding modes. The arrows and the numbers indicate the binding sites

complex cannot fit into the minor groove. This might be expected since minor groove binders such as netropsin, distamycin and Hoechst 33258, which have aromatic ring systems with a thickness of approximately 3.5 Å, were found to fit tightly into the minor groove of DNA²²⁻²⁵). The chromium hexaammine cation, calculated from crystal structure data²⁰) to span ca. 6 Å from *trans*-to-*trans* ammonia ligands, is too large to fit completely into the minor groove. Even the insertion of two *cis* ammonias into the minor groove is not very likely since the other two ammonias that are *cis* to these ammonias do not allow close enough access to atoms in the minor groove for hydrogen bonding. In any case, the thickness of the ammonia ligand is ca. 3.5 Å, the maximum value for insertion into an undistorted minor groove.

In the following assessment of likely modes of interaction, we therefore ruled out tight minor groove binding by the insertion of two ammonia ligands. However, we did consider the closest approach of the chromium complex to the minor groove by the insertion of one ammonia ligand into the minor groove along with analysis of the more likely major groove and phosphate backbone hydrogen bonding sites on the DNA. The various binding sites can be classified into five modes as follows (Fig. 4 shows examples of the sites for hydrogen bonding modes 1 through 4): 1) mode 1 — interaction with oxygens on a single phosphate, seven sites/strand; 2) mode 2 — in-

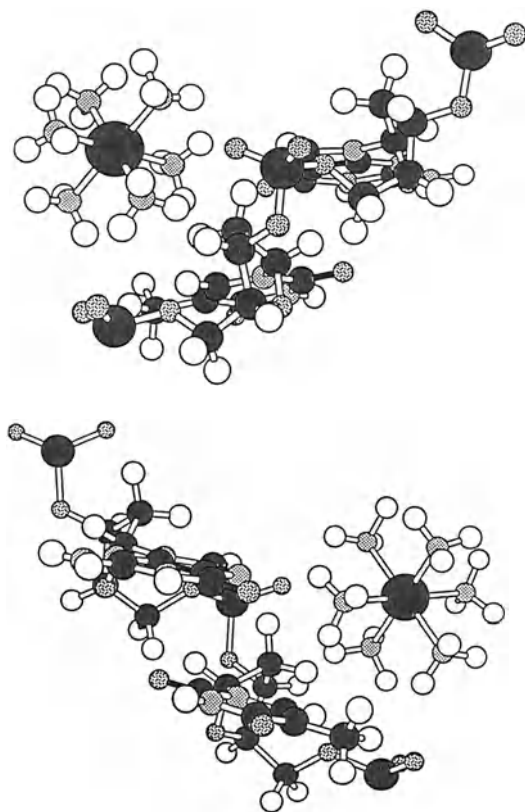


Fig. 5. Model of mode 2 developed using Macro Model (described in experimental). Two different views of the same site are shown of the $[\text{Cr}(\text{NH}_3)_6]^{3+}$ cation placed across two phosphates of the strand at T_2 and G_3

trastrand interactions with oxygens of any two neighboring phosphates, six possible sites/strand; 3) mode 3 — intrastrand interactions with any purine N7 and the adjacent 5' phosphate oxygens, three possible sites/strand; 4) mode 4 — a major groove inter-strand interaction with N7 and O6 of G₃ to N7 and O6 of G₅, two sites/duplex; and 5) mode 5 — closest approach to the minor groove with a single ammonia inserted into the minor groove; eight sites/strand. Model examples of mode 2 and mode 4 are shown in Fig. 5 and 6, respectively.

Approximate distances (Å) for the computer-generated models can be obtained from the chromium atom to protons of interest in the duplex using the modeling program. However, distances were considered “close” only when the chromium was within 10 Å of a base, an H1' or an H3' proton. Then the $1/r^6$ values for all relevant hydrogen bonding modes for each proton (to be discussed below) were added together (Table 6). Since the paramagnetic effect of the Cr(III) should follow a $1/r^6$

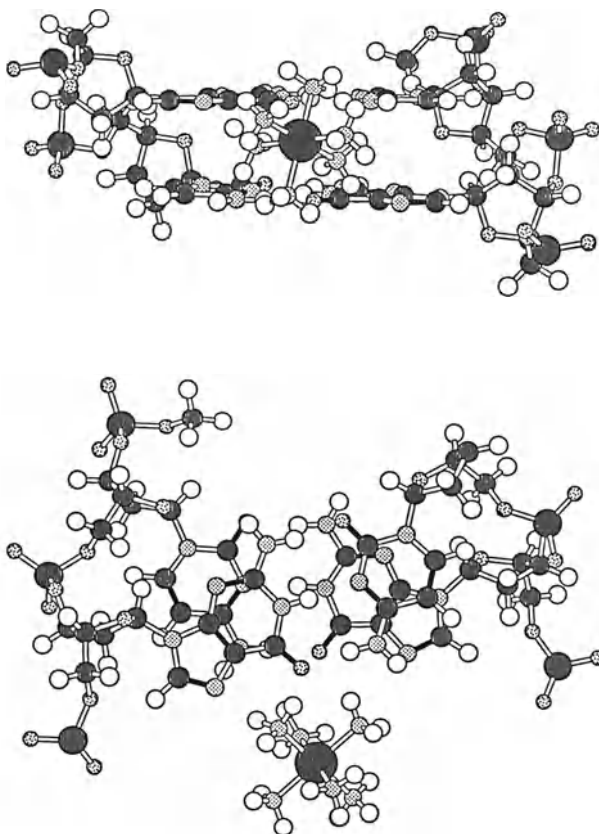


Fig. 6. Model of mode 4 developed using Macro Model (described in experimental). Two views of the same site are shown with the $[\text{Cr}(\text{NH}_3)_6]^{3+}$ cation placed in the major groove where hydrogen bonding to G residues on each strand at the same time is possible. The nucleotides shown are G₃ and C₄ of one strand and G₅ and C₆ of the complementary strand

dependence^{26,27}), these total values could be viewed as a rough guide for the relative effects of the $[\text{Cr}(\text{NH}_3)_6]^{3+}$ cation if it is distributed equally among all sites.

In the discussion to follow, it will become evident that multiple binding modes are present. Furthermore, we used ideal B-form DNA and did not carry out energy minimization calculations in the presence of the $[\text{Cr}(\text{NH}_3)_6]^{3+}$ cation. In addition, several slightly different locations often appeared feasible. Consequently, the distances employed should be considered to be no more than an approximate guide.

Mode 1 hydrogen bonding of the $[\text{Cr}(\text{NH}_3)_6]^{3+}$ cation to a single phosphate brings the chromium within 10 Å of base protons and deoxyribose protons of the

Table 6. Values of $1/r^6 \times 10^5$ using distances (Å) of the chromium to selected protons of duplexed dATGCGCAT from the hydrogen bonding modes in the model studies

Resonance	$1/r^6 \times 10^5$ (Å ⁻¹) ^a ΣMODES ^b					Σ $1/r^6 \times 10^5$ all modes
	1	2	3	4	5	
A ₁ H8	1.7	0.1	0.4	0.1		2.3
A ₁ H2					2.1	2.1
A ₁ H1'	0.7	0.5	1.1	0.1	0.8	3.2
A ₁ H3'	5.7	0.6				6.3
T ₂ H6	1.9	5.3	33.2	0.9		41.3
T ₂ -CH ₃	1.5	1.2	21.5	2.6		36.8
T ₂ H1'	1.0	2.0	3.2	0.3	0.8	7.3
T ₂ H3'	6.5	18.8	0.4			25.7
G ₃ H8	1.9	8.7	14.1	1.4		26.1
G ₃ H1'	1.0	2.0	1.2	0.4	0.8	5.4
G ₃ H3'	6.5	19.3	2.1			27.9
C ₄ H6	1.9	8.7	18.4	2.1		31.1
C ₄ H5	1.5	8.5	8.7	8.2		26.9
C ₄ H1'	1.0	1.9	2.4	0.4	0.8	6.5
C ₄ H3'	6.5	19.3	0.8			26.6
G ₅ H8	1.9	9.5	14.1	1.1		26.6
G ₅ H1'	1.0	2.0	1.1	0.2	0.8	5.1
G ₅ H3'	6.5	19.3	2.1			27.9
C ₆ H6	1.9	8.7	18.4	0.1		29.1
C ₆ H5	1.5	8.8	9.4	0.6		20.3
C ₆ H1'	1.0	1.8	2.4		0.8	6.0
C ₆ H3'	6.5	19.3	0.8			26.6
A ₇ H8	1.5	6.4	12.0			19.9
A ₇ H2					2.1	2.1
A ₇ H1'	1.0	1.0	0.3		0.8	3.1
A ₇ H3'	6.5	18.8	2.1			27.4
T ₈ H6		1.8	0.2			2.0
T ₈ -CH ₃	0.4	8.7	4.0			13.1
T ₈ H1'	0.3	0.1			0.8	1.2
T ₈ H3'	0.9	0.6	0.4			1.9

^a Distances measured from the chromium to duplex protons (if less than 10 Å) were multiplied by $1/r^6$ and then these values for relevant hydrogen bonding modes for each proton were added together. Missing numbers in the table indicate that the proton is greater than 10 Å away from the chromium for hydrogen bonding sites of that mode.

^b See²⁸⁾

immediate nucleosides on the 5' and 3' side of the phosphate²⁸). The distances are large in all cases (\geq ca. 6 Å) and the paramagnetic effect of the chromium per binding event is not expected to be substantial compared to some of the other hydrogen bonding modes (see Table 6 and²⁸).

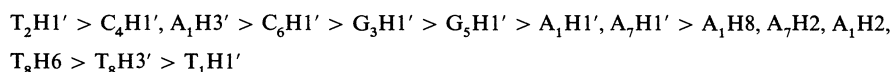
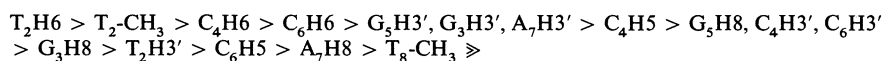
At four of the six possible hydrogen bonding sites for mode 2 (site 1, 2, 3, and 5, Fig. 4) the chromium is within 10 Å of protons on four nucleotides of the strand²⁸). These include three nucleotides bridged by the two phosphates as well as the nucleotide toward the 3' direction. So when the chromium is at site 1 of mode 2 (Fig. 4), the nucleotides A₁, T₂, G₃ and C₄ have protons within 10 Å of the chromium. At site 6 of mode 2, the chromium is close to protons on only three nucleotides, C₆, A₇, and T₈, since T₈ does not have a nucleotide on its 3' side. At site 4 of mode 2, the chromium is close to protons on the four nucleotides of the strand (C₄, G₅, C₆ and A₇) as well as within 10 Å of the methyl protons on T₂ of the complementary strand.

In mode 3, the chromium is within 10 Å of protons on four nucleotides of the strand which include the directly hydrogen bonded nucleotide as well as the two adjacent nucleotides in the 5' direction and the adjacent nucleotide in the 3' direction (Fig. 4 and²⁸). Also, site 1 and site 2 of mode 3 are close to protons on nucleotides of the complementary strand. At site 1 of mode 3, the chromium is close to protons on A₁, T₂, G₃, and C₄ of the strand and also C₄ of the complementary strand. Protons of G₃, C₄, G₅, and C₆ as well as T₂ on the complementary strand are close to the chromium at site 2 of mode 3. At site 3 of mode 3, the chromium is close to protons on G₅, C₆, A₇, and T₈.

In mode 4, the [Cr(NH₃)₆]³⁺ cation is in the major groove and bridges G₃ and G₅ on different strands (Fig. 4). The chromium complex can tilt towards G₃ (mode 4A, in the direction of the end of the duplex) or towards G₅ (mode 4B, in the direction of the center of the duplex). Nucleotides on both strands have protons within 10 Å of the chromium and, for both tilt orientations (A and B), the same nucleotides of both strands of the duplex have protons close to the chromium²⁸). The nucleotides are: strand 1 — A₁, T₂, G₃, and C₄; strand 2 — G₃, C₄, G₅ and C₆. It is unlikely that hydrogen bonding (mode 4 type) of the chromium hexaammine cation will occur in the major groove at A-T base pairs. The T-methyl group points towards the T-O(4) and sterically hinders the approach of the chromium cation, thus preventing H-bond formation to O(4).

The chromium in mode 5 (one ammonia ligand is inserted into the minor groove of the duplex) is close to only AH₂ protons and H₁' protons but the distance is large enough that the chromium would have very little effect on these protons (see Table 6 and²⁸). This mode is important in explaining the minor effects that are observed for the AH₂ signals (Tables 1 and 3).

Scheme 3 shows the hierarchy of affected signals as predicted from the above distance considerations, assuming equal distribution of the modes as calculated in Table 6.



Scheme 3

Scheme 3 predicts that the T_2 base signals should be the most affected DNA signals but in Scheme 1 (also see Table 1) we see that the T_2 base signals are not affected as much by the chromium as those for the G_3 , C_4 , G_5 , and C_6 base protons. Also, from distance considerations only (Scheme 3), it is predicted that the chromium will have a greater effect on the signals of all the T_2 , G_3 , C_4 , G_5 , and C_6 base protons than on the $H1'$ signals but this is not observed (Scheme 1, Table 1). The small effect of the chromium on signals of terminal nucleotides, as predicted by the statistical distribution of the $[\text{Cr}(\text{NH}_3)_6]^{3+}$ across all sites, does correlate well with the $1/T_{1p}$ results for these signals (Table 1). Studies of the binding of the similar cation, $[\text{Co}(\text{NH}_3)_6]^{3+}$, to DNA suggested nonselective binding by the cation¹⁰. Obviously, an equal distribution of $[\text{Cr}(\text{NH}_3)_6]^{3+}$ cation to all binding sites does not explain our T_1 results.

To further refine our analysis of the influence of $[\text{Cr}(\text{NH}_3)_6]^{3+}$, we must consider the likely possibility that the $[\text{Cr}(\text{NH}_3)_6]^{3+}$ cation favors some of the hydrogen bonding modes over others. If we consider only mode 1 (Table 6 and²⁸), the $1/r^6$ values do not correlate well with the $1/T_{1p}$ values for the protons on nucleotides in the interior of the duplex. Mode 1 predicts the $H3'$ signal would be the most affected signal for all the interior nucleotides but this is not observed (Table 1). Mode 1 also predicts that all purine $H8$ and pyrimidine $H6$ signals for interior nucleotides would be affected similarly and, again, this is not observed (Table 1). However, mode 1 does predict T_8H3' to be the least affected of all the $H3'$ signals considering the available data (average $H3'$ relaxation data for A_1 , G_3 , A_7 , and T_8). It does not account for the medium effect on T_8H1' and the large effects on G_3H1' , C_4H5 , G_5H1' and C_6H1' . Thus, mode 1 alone does not explain all the relaxation data.

In mode 2, as in mode 1, the $H3'$ protons of all interior nucleotides should have the most affected signals²⁸) but this is not observed (Table 1). Mode 2 also does not account for the effects on the $H1'$ signals, particularly G_5 , C_6 and T_8 . It also fails to account for differences between C_4 and C_6 and for the large differences in enhancement of C_4H5 and C_4H6 . For these reasons, we can rule out mode 2 as the major contributing hydrogen bonding mode.

Mode 3 predicts that the T_2H6 and $T_2\text{-CH}_3$ signals will be the most affected by the $[\text{Cr}(\text{NH}_3)_6]^{3+}$ but the relaxation rates for signals of base protons on C_4 , C_6 , G_3 , and G_5 are much more affected by Cr(III) . This mode could better explain much of the trends we observe if the occupancy of site 2 was greater than site 3, which in turn was greater than site 1. As for the previous modes, mode 3 alone does not explain the relaxation data, especially the $H1'$ relaxation results.

In the consideration of mode 4 (Table 6), the prediction that the C_4H5 signal will be the most affected signal correlates well with the relaxation data (Table 1). However, mode 4 is localized to part of the duplex and does not account for the remaining observed order of affected signals. Although it appears to be an important mode to consider, it is by no means the sole contributing binding mode. Also, form B of Mode 4 correlated better with the observed relaxation data than form A, so distances from form B were used in Table 6.

Mode 5 would account for the enhanced relaxation of the $AH2$ signals. It would also explain $1/T_1$ enhancement of all $H1'$ signals of the end nucleotides, although the enhancement would be small since the Cr(III) to $H1'$ distances are ca. 7 Å (Table 6).

No other nucleotide protons are close enough to chromium in mode 5 to be affected.

Neither a single binding mode we have considered nor the unweighted sum of these modes fully explains the trends observed on the addition of the $[\text{Cr}(\text{NH}_3)_6]^{3+}$ cation. However, the greater effect on signals for interior nucleotides is explained. The modeling studies are approximate. Nevertheless, it is clear that a combination of interactions between the $[\text{Cr}(\text{NH}_3)_6]^{3+}$ cation and the duplex is taking place. Our studies allow us to suggest confidently that the chromium cation is most likely spending more time in the vicinity of the interior of the duplex since protons on interior nucleotides are affected the most. Also, the chromium appears to have greater access to the major groove over the minor groove since major groove base signals (H8, H6, H5 and CH_3) of interior nucleotides are affected much more than the minor groove base signal, AH2.

The selective effects we have observed appear to rule out a totally loose arrangement of the $[\text{Cr}(\text{NH}_3)_6]^{3+}$ cation in an ion atmosphere. On the other hand, a tight interaction of one site or even a high degree of preferential residency at one site appears to be unlikely. This conclusion agrees with previous conclusions from studies of $[\text{Co}(\text{NH}_3)_6]^{3+}$ binding to DNA¹⁰. Therefore, the $[\text{Cr}(\text{NH}_3)_6]^{3+}$ cation appears suitable for footprinting type studies since nonselective agents are necessary for such experiments.

The relative paramagnetic effect on the longitudinal relaxation rates of nucleotide protons in the 2:1 ActD:d(ATGCGCAT)₂ complex and the free duplex was noticeably different. Differences between the $1/T_{1p}$ results of the free duplex and the 2:1 ActD complex are expected since the duplex in the drug complex, although still a right-handed helix, is severely distorted⁸. Although all nucleotide signals in the 2:1 complex experienced an increase in their longitudinal relaxation rate with one exception, the rate increase was not as much as that seen for the analogous protons in the free duplex. The only exception was the C₄H6 signal which was affected more by the chromium in the 2:1 complex than in the free duplex (see Scheme 1 and 2).

Other differences in the T₁ data between the free duplex and 2:1 complex nucleotide signals include the order of affected signals (Scheme 1 and 2) as well as a noticeably decreased relative effect on the H1' protons compared to the base protons of interior nucleotides (Table 5).

The slight difference in the order of affected protons of the duplex from the free to 2:1 complex (Tables 1 and 3, Schemes 1 and 2) can be explained in part by the inability of the duplex in the 2:1 species to form the mode 4 hydrogen bond. The intercalation of the ActD phenoxazone ring separates G₃ and G₅ of opposing strands enough to prevent hydrogen bonding to both bases at the same time and it is in mode 4 that the chromium is positioned closer to C₄H5 than to C₄H6 (see Table 6). Without mode 4, the chromium hexaamine cation can hydrogen bond only by modes 1–3, which in all cases would bring the chromium closer to C₄H6 than to C₄H5. However, only in the case of mode 3 is the C₄H6 expected to be influenced to a greater extent than the C₄H5 signal. As for the free duplex, site 2 of mode 3 appears to be most important.

The decreased effect of the chromium on the deoxyribose H1' protons on nucleotides in the center of the duplex in the 2:1 complex (Table 5) can be explained by the presence of the cyclic peptides which have been shown to be in the minor groove of the duplex⁸. The approach of the chromium hexaamine cation to the H1' protons

is sterically impeded by the cyclic peptides. We believe that the bulky cyclic peptides are responsible for the conformational changes in the sugar puckers ($C2'$ -endo to $C3'$ -endo) of T_2 , C_4 and C_6 of the 2:1 complex⁸⁾. The conformational changes of the sugar puckers from $C2'$ -endo to $C3'$ -endo widen the minor groove and allow for the accommodation of the large cyclic peptides. The chromium has in a sense acted as a probe for confirming the location of the cyclic peptide chains along the minor groove of the duplex by the decreased paramagnetic effect observed for the minor groove $H1'$ protons.

This study of the effect of the chromium hexaamine cation on duplexed dATGCGCAT and its 2:1 ActD complex has shown that paramagnetic transition metal complexes that have only outer-sphere interactions with biopolymers such as DNA may be potentially useful as NMR probes for structure and for drug binding sites. Our T_1 measurements of the protons in the duplex showed the chromium to have a greater paramagnetic effect on nucleotides in the center of the duplex. Modeling studies suggest that the chromium hexaamine cation can hydrogen bond to a number of locations on a particular oligonucleotide strand as well as across the complementary strands of the duplex. By disrupting the normal structure of a DNA duplex with the addition of a DNA-binding drug, the accessibility of the $[Cr(NH_3)_6]^{3+}$ cation to available sites changes as evidenced by T_1 measurements on $d(ATGCGCAT)_2$ and the 2:1 ActD: $d(ATGCGCAT)_2$ complex. In this way, it may be possible eventually to determine structural features of the DNA-drug complexes. More likely, our approach may prove to be a higher resolution method than footprinting methods based on enzymatic degradation²⁹⁾. Other methods based on DNA degradation are limited to providing insight into accessibility to protons abstracted in the degradation reaction^{2,4)}. However, these chemical footprinting methods are applicable to much larger pieces of DNA than is feasible by our method. It is clear that each of these methods offer complementary information, and together they should provide a more complete picture of drug binding.

Our preliminary results on the affinity of chromium hexaamine cation for duplexed $d(ATGCGCAT)_2$ and its ActD 2:1 complex have given us insights as to probable binding sites of the paramagnetic metal complex to DNA. The next steps in this area of research involve examining the usefulness of the $[Cr(NH_3)_6]^{3+}$ cation in studying other types of DNA-binding agents, particularly cationic species, and with longer strands of DNA as well as on oligonucleotides with different sequences. Finally, in the early seventies, Pispisa and colleagues^{30, 31)} explored the use of both Δ and Λ forms of tris(ethylenediamine)cobalt(III) cations to examine the effects of chirality on DNA-binding specificity. Interestingly, they found no differences between the optical isomers but did conclude that the cations were binding in the major groove. They also suggested that the complex could span the phosphate chains on both strands, possibly with distortion of the DNA structure. Indeed, a relatively large increase can be observed at 275 nm in the circular dichroism spectrum of native calf thymus DNA. The resulting nonconservative spectrum appeared similar to that expected from A-form DNA, and the change was cooperative. In contrast, the cobalt cations had relatively little effect on the circular dichroism spectrum of denatured DNA. These types of phenomena are intriguing and suggest that NMR studies on oligonucleotides with diamagnetic complexes, such as the $[Co(III)(NH_3)_6]^{3+}$ cation, may reveal interesting changes in DNA conformation.

5 Abbreviations

DNA	deoxyribonucleic acid
DVal	D-valine
EDTA	ethylenediaminetetraacetic acid
FID	free induction decay
FT	Fourier transformation
Pro	proline
NmVal	<i>N</i> -methylvaline
Sar	sarcosine (<i>N</i> -methylglycine)
Thr	threonine
2D	two-dimensional

6 Acknowledgements

This work was supported by NIH Grant GM 29222 to L. G. M.

7 References

1. Chiao YC, Krugh TR (1977) *Biochemistry* 16: 747
2. Tullius TD, Dombrowski BA (1985) *Science* 230: 679
3. Fleisher MB, Waterman KC, Turro NJ, Barton JK (1986) *Inorg. Chem.* 25: 3549
4. Kuwabara M, Yoon C, Goynes T, Thederahn T, Sigman DS (1986) *Biochemistry* 25: 7401
5. Granot A, Kearns DR (1982) *Biopolymers* 21: 203
6. Marzilli LG (1977) *Prog. Inorg. Chem.* 23: 255
7. Derome AE In: Bardwin JE (ed) (1987) *Modern NMR techniques for chemistry research*. Pergamon, Oxford, p 89
8. Scott EV, Zon G, Marzilli LG, Wilson WD (1988) *Biochemistry* 27: 7490
9. Barton JK (1988) *Chemical and Engineering News* 66 (39): 30
10. Braunlin WH, Anderson CF, Record MT (1987) *Biochemistry* 26: 7724
11. Stec WJ, Zon G, Egan W, Byrd RA, Phillips LR, Gallo KA (1985) *J. Org. Chem.* 50: 3908
12. Oppegard AL, Bailar JC (1950) *Inorg Syntheses* 3: 153
13. Cutnell JD, Bleich HE, Glasel JA (1976) *J. Magn. Reson.* 21: 43
14. Levy G, Peat I (1975) *J. Magn. Reson.* 18: 500
15. Jones RL, Scott EV, Zon G, Marzilli LG, Wilson WD (1988) *Biochemistry* 27: 6021
16. Arnott S, Campbell Smith PJ, Chandrasekaran R (1976) In: Fasman GD (ed) *CRC Handbook of biochemistry and molecular biology*. CRC, Ohio, p 411
17. Tran-Dinh S, Neumann J-M, Huynh-Dinh T, Igolen J, Kan SK (1982) *Org. Magn. Reson.* 18: 148
18. Fouts CS (1987) Ph. D. Thesis, Emory University, Atlanta, GA
19. Wilson WD, Jones RL, Zon G, Scott EV, Banville DL, Marzilli LG (1986) *J. Am. Chem. Soc.* 108: 7113
20. Raymond KN, Meek DW, Ibers JA (1968) *Inorg. Chem.* 7: 1111
21. Gessner RV, Quigley GJ, Wang A, Van der Marel GA, van Boom JH, Rich A (1985) *Biochemistry* 24: 237
22. Kopka ML, Yoon C, Goodsell D, Pjura P, Dickerson RE (1985) *Proc. Natl. Acad. Sci. USA* 82: 1376
23. Coll M, Frederick CA, Wang A, Rich A (1987) *Proc. Natl. Acad. Sci. USA* 84: 8385
24. Teng M, Usman N, Frederick CA, Wang A (1988) *Nucleic Acids Res.* 16: 2671
25. Pjura P, Grzeskowiak K, Dickerson RE (197) *J. Mol. Biol.* 197: 257

26. Bloembergen N (1957) *J. Chem. Phys.* 27: 572
27. Solomon I (1955) *Phys. Rev.* 99: 559
28. Values of $1/r^6$ for each site of modes 1–5 can be found in Scott EV (1988) Ph. D. Thesis, Emory University, Atlanta, GA
29. Fox KR, Waring MJ (1984) *Nucl. Acids Res.* 12: 9271
30. Ascoli F, Branca M, Mancini C, Pispisa B (1972) *J. Chem. Soc., Faraday Trans I* 68: 1213
31. Ascoli F, Branca M, Mancini C, Pispisa B (1973) *Biopolymers* 12: 2431

Antitumor Activity of Bis[Bis(Diphenylphosphino)Alkane and Alkene] Group VIII Metal Complexes

John E. Schurig¹, Harry A. Meinema², Klaas Timmer², Byron H. Long¹,
and Anna Maria Casazza¹

We have prepared a broad series of group VIII transition metal complexes of the general type $[L_2MX_m]^{n+} nX^-$ [$L = Ph_2P-A-PPh_2$, $A = (CH_2)_2$, $(CH_2)_3$ or *cis*- $CH=CH$; $M = Fe, Co, Rh, Ir, Ni, Pd$; $X = Cl, Br, I, NO_3, C_10_4, CF_3SO_3$; $m = 0-2$; $n = 0-3$]. Presented here are the results of evaluations of these metal complexes for in vitro cytotoxicity, in vivo antitumor activity in murine tumor models and mechanism of action. Of 21 complexes tested in vitro against a panel of murine and human tumor cell lines, 10 were cytotoxic with IC₅₀ values of 0.8 to 491 μ g/ml. Many of the complexes investigated had antitumor activity against ip implanted P388 murine leukemia and ip implanted B16 melanoma. The mechanism of action of these complexes appears different from that of cisplatin based on effects on DNA and lack of cross resistance with L1210/DDP, a line of L1210 murine leukemia resistant to cisplatin. These complexes are deficient in antitumor activity against tumors located distal to the site of drug injection (e.g., iv P388 leukemia, sc B16 melanoma, sc M5076 reticulum cell sarcoma and sc 16/c mammary adenocarcinoma). It appears that the poor solubility of these compounds contributes to this type of deficiency. Therefore, future efforts with this class of group VIII metal complexes will focus on increasing solubility.

1 Introduction	206
2 Synthesis of the Metal Complexes	206
3 Biological Evaluations	207
3.1 In Vitro Cytotoxicity	207
3.2 In Vivo Antitumor Activity	208
3.3 Mechanism of Action	208
4 Results and Discussion	208
4.1 In Vitro Cytotoxicity	208
4.2 Antitumor Activity: Ip-Implanted Tumors	209
4.3 Antitumor Activity: Distal Site Tumors	211
4.4 Mechanism of Action	213
5 Conclusions	214
6 Acknowledgements	215
7 Abbreviations	215
8 References	215

¹ Pharmaceutical Research and Development Division, Bristol-Myers Co., Wallingford, CT, USA

² Institute of Applied Chemistry, TNO, Zeist, The Netherlands

1 Introduction

Prior to the discovery of the antitumor activity of cisplatin¹⁾ most of the anticancer agents were organic compounds. That discovery has stimulated numerous searches for non-platinum metal complexes with potential utility as anticancer agents. This period has been termed the “era of inorganic cytostatics” by Köpf-Maier and co-workers²⁾. Antitumor activity has been reported for a variety of compounds involving metals such as titanium, vanadium, iron, gold, silver, copper, palladium, ruthenium, germanium and tin²⁻¹⁷⁾. However, we are aware of only one non-platinum metal compound, a titanium complex¹⁸⁾, that is currently in clinical trials.

We initiated a collaborative effort to identify novel heavy metal complexes with antitumor activity. The focus was on group VIII transition metals complexed with bis(diphenylphosphino)alkane and -alkene ligands¹⁹⁾. A broad series of metal complexes of iron, cobalt, rhodium, iridium, nickel and palladium were prepared and evaluated for *in vitro* cytotoxicity against murine and human tumor cell lines and *in vivo* antitumor activity in murine tumor model systems. In addition preliminary mechanism of action studies were performed in comparison with cisplatin. Presented here are the results of these investigations.

2 Synthesis of the Metal Complexes

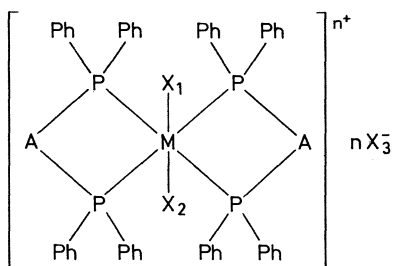
The bis[bis(diphenylphosphino)alkane and -alkene] group VIII metal complexes were synthesized via reaction of suitable group VIII metal precursors with two equivalents of bis(diphenylphosphino)ethane, -ethene or -propane following procedures described in the literature¹⁹⁾. The resulting complexes were characterized by elemental analysis (C, H, P, halogen, O) and NMR (¹H, ³¹P). The structures of these complexes are shown in Table 1.

3 Biological Evaluations

The experimental systems used to evaluate the metal complexes are briefly described. The detailed methodologies can be found in the references cited for each system.

3.1 *In Vitro* Cytotoxicity

The complexes were tested for cytotoxicity against a tumor cell line panel composed of murine and human tumor cell lines. The specific tumor cell lines in the panel were varied at approximately 6 month intervals. The tumor cell lines available for inclusion in the panel at any given time are listed in Table 2. The methods used for cytotoxicity testing have been described in detail by Catino and coworkers^{20,21)}.

Table 1. Structures of Bis[Bis(diphenylphosphino)alkane and alkene] group VIII transition metal complexes

Complex	M	A	X ₍₁₎	X ₍₂₎	X ₍₃₎	n
396	Fe II	<i>cis</i> -CH=CH	Cl	Cl	—	0
405	Fe III	<i>cis</i> -CH=CH	Cl	Cl	FeCl ₄	1
346	Co II	(CH ₂) ₂	Br	—	Br	1
347	Co II	(CH ₂) ₂	NO ₃	—	NO ₃	1
358	Co II	(CH ₂) ₂	—	—	ClO ₄	2
302	Rh I	(CH ₂) ₂	—	—	CF ₃ SO ₃	1
316	Rh I	(CH ₂) ₂	—	—	ClO ₄	1
355	Rh III	(CH ₂) ₂	Cl	Cl	ClO ₄	1
363	Rh III	(CH ₂) ₂	Cl	Cl	Cl	1
379	Rh I	<i>cis</i> -CH=CH	—	—	ClO ₄	1
344	Ir I	(CH ₂) ₂	—	—	ClO ₄	1
413	Ir III	(CH ₂) ₂	—	Peroxo	ClO ₄	1
354	Ni II	(CH ₂) ₂	—	—	NO ₃	2
404	Ni II	(CH ₂) ₂	—	—	ClO ₄	2
306	Pd II	(CH ₂) ₂	—	—	Cl	1
342	Pd II	(CH ₂) ₂	I	I	—	0
343	Pd II	(CH ₂) ₂	—	—	ClO ₄	2
345	Pd II	(CH ₂) ₂	—	—	NO ₃	2
357	Pd II	<i>cis</i> -CH=CH	—	—	Cl	2
376	Pd II	(CH ₂) ₂	—	—	Br	2
383	Pd II	(CH ₂) ₃	—	—	Cl	2

Table 2. In vitro tumor cell line panel

Derivation	Cell line
Murine Melanoma	B16-F10
Lung	M109
Human Colon	HCT 116
Colon	RCA
Colon	Moser
Lung	A549
Lung	SW 1271
Nasopharyngeal	KB

3.2 *In Vivo* Antitumor Activity

The experimental tumor models used to assess antitumor activity are shown in Table 3.

Table 3. Murine tumor models

A. IP Implanted tumors P388 leukemia L1210 leukemia L1210/DDP leukemia ^a B16 melanoma	B. Distal site tumors iv P388 leukemia sc B16 melanoma sc 16/c mammary adenocarcinoma ^b sc M5076 reticulum cell sarcoma
---	---

^a Resistant to cisplatin;

^b studies involving 16/c mammary adenocarcinoma were performed by Southern Research Institute, Birmingham, AL

These models are routinely used to evaluate drugs for antitumor activity and have been described in previous publications^{22–25}. Most of the group VIII metal complexes have to be administered ip due to poor aqueous solubility. The ip treatment of ip tumors provides an initial indication of antitumor activity of the complexes at tolerated doses without much concern for metabolism and pharmacokinetics. However, it is essential that a complex with activity against ip tumors also has activity against tumors located distal to the site of drug administration. Therefore distal site tumor models are used for advanced evaluations of complexes to select lead compounds for further preclinical development. The use of an iv implanted murine leukemia as a distal site tumor model is based on the dissemination of the tumor to the spleen, liver and marrow 24 hours after inoculation²⁶.

3.3 *Mechanism of Action*

The ability of the group VIII metal complexes to cause single and double strand DNA breaks was determined by standard alkaline elution techniques²⁷) using HCT 116 human colon carcinoma cells, prelabeled with 0.01 μ ci/ml ¹⁴C-thymidine, exposed to various concentrations of drug for 1 hour. Interstrand DNA cross link formation was assessed using a procedure similar to that used for measuring single strand DNA breaks as previously described²⁸).

4 Results and Discussion

4.1 *In Vitro* Cytotoxicity

Ten of the 21 complexes were cytotoxic to the tumor cell lines with IC₅₀ values ranging from 0.8 to 491 μ g/ml (Table 4). Of the complexes that were cytotoxic, Pd-345 and Ni-354 were the most potent across all the cell lines in the panel. The other 11 compounds were considered “noncytotoxic” because their IC₅₀ values were > 500 μ g/ml in all cell lines.

Table 4. Invitro cytotoxicity

Metal	Complex No.	IC50 — µg/ml ^a							
		B16-F10	M109	HCT116	RCA	MOSER	A549	SW1271	KB
Fe	396	452	^b	383		> 500	466	460	
	405	30		277		> 500	372	> 500	
Co	347	415	248	> 500	322	491			389
Ir	413	367		374		> 500	456	> 500	
Ni	354	4.1	115	1.3	2.8	25			5.5
	404	6.9		155		413	277	> 500	
Pd	306	91	225		278	204			14
	345	4.5	19.4	12.5	19.3	27.8			1.6
	357	28	145	16	43	82			324
	376	1.2		0.8			2.8	329	

^a Microtiter assay, 72 hour drug exposure;

^b absence of IC50 value indicates cell line not included in the panel used for that drug

The apparent lack of cytotoxicity of the 11 complexes in these assays does not necessarily indicate an intrinsic lack of cytotoxicity. As pointed out before, most of these compounds have limited solubility. Because of the potential for reactivity with solvents such as DMSO, only saline was used as the vehicle for the in vitro assays which resulted in suspensions being tested. Therefore, the actual drug concentration in each well of the microtiter plate could be less than the calculated concentration.

4.2 Antitumor Activity: *Ip-Implanted Tumors*

The activities of the complexes against ip implanted P388 are summarized in Table 5. The best effect observed with each complex and the dose at which that effect was obtained (i.e., the "optimal dose") are presented in the table. Fifteen of the compounds were active with T/C values ranging from 133% (Rh-363) to 240% (Ni-404). The optimal doses of the active complexes were quite varied, ranging from 4 mg/kg to 200 mg/kg. The Pd complexes 306, 345, 357 and 376 were the least tolerated and none of them were active; however, the better tolerated Pd complex (343) exerted good antitumor activity.

We were interested in determining if the in vitro cytotoxicity of the complexes predicted for their in vivo antitumor activity against P388. The last column in Table 5 lists the IC50 for each complex against B16-F10, the only tumor cell line in which all of the complexes had been tested (also the most sensitive in most cases). The most active complex in vivo, Ni-404, was also one of the most potent in vitro. However, with the palladium complexes, high in vitro potency was not associated with in vivo activity. Conversely, complexes such as the cobalts and iridiums had very low potency in vitro but were quite active in vivo. Thus, no relationship was apparent between in vitro potency and level of in vivo antitumor activity (% T/C)

Table 5. Antitumor activity against P388 murine leukemia^a

Metal	Complex No.	Max % T/C ^b	Optimal dose (mg/kg) ^c	In vitro IC50 (µg/ml) vs. B16-F10
Fe	396	150	200	452
	405	160	100	30
Co	346	167	100	> 500
	347	161	100	415
	358	144	100	> 500
Rh	302	153	4	> 500
	316	150	12.5	> 500
	355	167	100	> 500
	363	133	50	> 500
	379	106	200	> 500
Ir	344	167	200	> 500
	413	170	200	367
Ni	354	139	50	4.1
	404	240	25	6.9
Pd	306	100	2.5	91
	342	139	5	> 500
	343	178	200	> 500
	345	100	1.6	4.5
	357	117	1.6	28
	376	107	1	1.2
	383	107	25	> 500

^a 1×10^6 cells implanted ip, Day 0;

^b % T/C = $\frac{\text{median survival time (MST) of treated (T) mice}}{\text{MST of control (C) mice}} \times 100$;

^c single treatment ip, Day 1

against P388. This result differs in part from that reported by Mirabelli and coworkers²⁹). These authors reported that with a series of gold (I) phosphine coordination complexes lack of potency in vitro correlated well with lack of antitumor activity against ip P388. However, they also reported that potent cytotoxicity in vitro was not necessarily predictive of activity in vivo which does agree with our observation.

The data in Table 5 do suggest some relationship between potency in vitro and potency (optimal dose) in vivo. In several instances IC50 values below 100 µg/ml were associated with optimal doses below 100 mg/kg whereas IC50 values ≥ 100 µg/ml were associated with optimal doses above 100 mg/kg. Thus, we could use the IC50 value of a complex as a guide for selecting dose ranges of that complex to test against P388.

Nine of the complexes active against ip P388 were evaluated against ip B16. The results, reported in Table 6, show that all of these compounds were also active against ip B16. The level of activity observed for a particular complex against P388 did not necessarily predict its level of activity against B16. The last column in Table 6 lists the IC50 values for each complex against B16-F10. It is readily apparent that the IC50 values do not correlate with the level of antitumor activity against B16 or the in vivo potency of the complex.

Five of the complexes active against ip P388 and ip B16 were evaluated for activity against ip L1210 and ip L1210/DDP. The results, summarized in Table 7,

Table 6. Antitumor activity against B16 melanoma^a

Metal	Complex No.	Max % T/C ^b	Optimal dose (mg/kg/inj) ^c	In vitro IC50 (µg/ml) vs. B16-F10
Co	347	171	20	415
	358	150	20	> 500
Rh	302	150	3.2	> 500
	316	131	16	> 500
	355	171	30	> 500
Ir	344	150	20	> 500
Ni	354	183	30	4.5
	404	179	16	6.9
Pd	343	204	60	> 500

^a 0.5% of a 10% tumor brei implanted ip, Day 0;

^b % T/C = $\frac{\text{median survival time (MST) of treated (T) mice}}{\text{MST of control (C) mice}} \times 100$;

^c treatment administered ip, Days 1–9

show that four of the complexes were active against L1210/DDP whereas Rh-355 was not active against L1210/DDP or L1210. Cisplatin was tested in parallel and was always active against L1210, inactive against L1210/DDP (data not shown). These results indicate that these group VIII metal complexes are not cross-resistant with cisplatin when tested on L1210/DDP. Interestingly, 2 of the 4 complexes active against L1210/DDP were inactive against the parent tumor line whereas the other two were essentially equally active against both tumor lines.

4.3 Antitumor Activity: Distal Site Tumors

The complexes Pd-343, Ir-344, Co-347, Ni-354 and Rh-355 were evaluated for activity against iv implanted P388 leukemia. Although these compounds were active against

Table 7. Antitumor activity against L1210 and L1210/DDP murine leukemia^a

Metal	Complex No.	L1210		L1210/DDP ^d	
		Max % T/C ^b	Optimal dose (mg/kg) ^c	Max % T/C	Optimal dose (mg/kg) ^c
Co	347	100	100	150	50
	358	142	120	143	100
Rh	316	133	160	157	120
	355	114	80	119	40
Ni	354	100	80	138	80

^a 1×10^6 cells implanted ip, Day 0;

^b % T/C = $\frac{\text{median survival time (MST) of treated (T) mice}}{\text{MST of control (C) mice}} \times 100$;

^c single treatment ip, Day 1;

^d L1210 resistant to cisplatin

Table 8. Antitumor activity against SC implanted murine tumors

Tumor	Metal	Complex No.	Max. MST % T/C, ^a (MTW % T/C) or [T-C]	Optimal dose (mg/kg/inj) ^b
B16	Co	347	105 (41)	60
	Rh	355	111 (78)	80
	Ni	354	100 (28)	40
16/c Mam.	Ir	344	117 [1.5]	40
	Ni	354	110 [0.5]	40
	Pd	343	117 [3.9]	80
M5076	Co	346	131 [3]	30
	Co	347	86 [0]	30
	Rh	316	104 [2]	30
	Rh	355	91 [0]	60
	Ir	344	139 [7]	60
	Pd	343	114 [2.3]	24

$$^a \text{MST \% T/C} = \frac{\text{median survival time (MST) of treated (T) mice}}{\text{MST of control (C) mice}} \times 100;$$

$$\text{MTW \% T/C} = \frac{\text{median tumor weight (MTW) of treated mice}}{\text{MTW of control mice}} \times 100;$$

T-C = treated mice — control mice, days for tumor to reach 1 gm

^b Treatment schedules (all ip): B16 — Days 1, 5 & 9;

16/C Mam. — Days 2, 6 & 10;

M5076 — Days 5, 9, 13 & 17

The following values were considered significant antitumor activity:

Tumor	MST % T/C	MTW % T/C	T-C days
sc B16	140	≤ 42	—
sc 16/C Mam.	125	—	8
sc M5076	125	—	13

ip P388 (Table 5), none was active against iv P388 following single dose ip administration (data not shown).

Selected complexes were also tested against sc implanted murine tumors. The results, summarized in Table 8, show that Co-347 and Ni-354 were active against sc B16 in terms of inhibition of primary tumor growth but did not cause an increase in lifespan. The other complexes were inactive. None of the complexes evaluated against sc 16/c mammary adenocarcinoma achieved an active result in terms of survival or inhibition of the growth of the primary tumor. Against sc M5076, Ir-344 and Co-356 caused modest increases in lifespan whereas the other complexes were inactive.

All of the distal site tumor studies involved ip administration of the complexes because of their poor solubility. The complexes tested against iv P388 and sc B16 had shown good activity against these tumors implanted ip indicating the tumors were sensitive to those complexes. It appears likely that the inactivity of these complexes against iv P388 and the minimal to no activity against sc B16 may be related to poor bioavailability after ip administration. This situation could be due to first pass effects and/or inadequate blood levels following ip administration. Additional studies are needed to examine these possibilities more thoroughly.

4.4 Mechanism of Action

The effects of selected complexes on interstrand DNA crosslink formation in HCT 116 human colon tumor cells are shown in Table 9. Only cisplatin produced a high level of interstrand DNA crosslinks upon incubation with the cells for 1 hour. The number of crosslinks continued to increase with continued incubation. Complexes Pd-306 and Pd-343 produced only low levels of crosslinks that did not continue to accumulate with time. Complex Ir-344 caused no interstrand DNA crosslinks.

Table 9. Interstrand DNA crosslink formation in HCT 116 human colon tumor cells

Incubation (hr)	DNA Crosslinks/ 10^8 Nucleotides			
	Cis DDP	Pd-306	Pd-343	Ir-344
1	178.4	14.2	14.2	—
2	484.9	13.7	13.	—4.4
4	^a	19.4	13.2	—0.6

^a Unable to calculate

The ability of these same complexes to produce DNA strand breaks is shown in Table 10. Substantial single strand DNA breakage was induced after a 1 hour incubation of the cells with 100 μ M concentrations of Pd-306 and Ir-344 but not Pd-343. These breaks continued to increase upon continued incubation of the cells with Ir-344 but not Pd-306. The relative amount of double-strand DNA breakage produced by these drugs can be assessed by comparing the percentage of DNA appearing in the cell lysis fractions after drug treatment. Complex Pd-306 clearly produced double-strand DNA breaks and Ir-344 produced double-strand breaks after incubation for 4 hours.

The objective of these preliminary mechanism of action studies was to determine differences between the effects of these group VIII metal complexes and cisplatin on DNA. Our results indicate that some of the complexes differ from cisplatin in that they do not cause interstrand crosslinking and they do cause DNA strand breaks. These results together with the lack of cross resistance observed with L1210/DDP provide substantial support for considering the group VIII metal complexes as novel agents relative to cisplatin.

Table 10. Effect on DNA integrity in HCT 116 human colon tumor cells

Incubation (hr)	Control		Pd-306		Pd-343		Ir-344	
	SSDB ^a	% Lysis ^b	SSDB	% Lysis	SSDB	% Lysis	SSDB	% Lysis
1	0.1	1.8	18.3	11	0.5	2.0	13.5	1.5
2	0.1	2.7	17.7	11.3	0.8	2.1	11.0	2.3
4	0.1	2.1	18.2	15.3	4.8	4.6	178.3	6.9

^a Single-strand DNA breaks/ 10^7 nucleotides;

^b indication of double-strand DNA breaks

These data are in agreement with those previously reported by other authors. Production of DNA strand breakage as well as DNA-protein crosslinks have been reported for a bis[bis(diphenylphosphino)ethane] gold complex⁹⁾. Subsequent studies suggested that DNA-protein crosslinks are the relevant DNA lesions produced by this complex at cytotoxic concentrations³⁰⁾. Additional studies reported by Mirabelli and coworkers³¹⁾ demonstrated that this complex causes depletion of ATP from P388 leukemia cells and they suggested mitochondria as the subcellular target for this complex. McCabe and coworkers³²⁾ developed a subline of P388 leukemia that was induced resistant to the bis(diphenylphosphino)ethane ligand *in vivo*. This subline was also resistant to the bis[bis(diphenylphosphino)ethane]gold complex but was not cross resistant to cisplatin. The results of these studies with the gold complex provide additional evidence differentiating bis[bis(diphenylphosphino)alkane and -alkene] heavy metal complexes from cisplatin in terms of mechanism of action.

5 Conclusions

These studies indicate that many of the bis[bis(diphenylphosphino)alkane and -alkene] group VIII metal complexes investigated were cytotoxic *in vitro* and had antitumor activity against *ip* implanted murine tumors. These complexes were, however, deficient in antitumor activity against tumors located distal to the site of drug injection. They were inactive against *iv* P388 leukemia and *sc* 16/c mammary adenocarcinoma, and had only marginal activity against *sc* B16 melanoma and *sc* M5076 reticulum cell sarcoma. Previously reported results of distal tumor testing of a bis[bis(diphenylphosphino)ethane] gold complex are in general agreement with our results in that the gold complex was inactive against *iv* P388 and marginally active against *sc* M5076⁹⁾. However, this gold complex was active against *sc* 16/c mammary whereas the group VIII metal complexes we tested against this tumor were inactive. We believe the poor solubility of the group VIII metal complexes contributes significantly to their lack of good activity against distal tumors. Therefore, future efforts with this class of metal complexes will focus on increasing solubility.

The mechanism of action of these group VIII metal complexes differs from that of cisplatin, based on the results of our studies and the results reported by others investigating the gold complex^{9,30-32)}. It has been suggested that the active moiety of bis[bis(diphenylphosphino)alkane and -alkene] metal complexes could be the bis(diphenylphosphino)alkane or -alkene ligand¹¹⁾. Metal-free phosphine ligands have been shown to be cytotoxic to tumor cell lines *in vitro* and active *in vivo* against murine tumors^{10,11)}. However, the free ligands are unstable due to their susceptibility to oxidation. Therefore, it has been proposed that the role of the metal in the complex could be to protect the ligand from oxidation until it can interact with the tumor cells⁹⁾. In our extensive studies with a large member of metal complexes the variations in potency and activity of the group VIII metal complexes observed with the variation of the metal in the complex suggest that, in the cytotoxic event, the role of the metal may be more than just providing protection of the ligand.

6 Acknowledgements

The authors wish to thank Dr. Jerzy Golik and Brenda Skonieczny for their assistance in preparing this manuscript.

7 Abbreviations

ip intraperitoneally
sc subcutaneously
iv intravenously

8 References

1. Rosenberg B, Van Camp L, Trosko JE, Mansoar VH (1969) *Nature* 222: 385
2. Köpf-Maier P, Köpf H, Neuse EW (1984) *J. Cancer Res. Clin. Oncol.* 108: 336
3. Köpf-Maier P, Hesse B, Voigtländer R, Köpf H (1980) *J. Cancer Res. Clin. Oncol.* 97: 43
4. Köpf H, Köpf-Maier P (1983) *Am. Chem. Soc. Symp. Ser.* 209: 805
5. Köpf-Maier P, Köpf H (1987) *Arzneim-Forsch./Drug Res.* 37: 532
6. Keller HJ, Keppler B, Schmöhl D (1983) *J. Cancer Res. Clin. Oncol.* 105: 109
7. Köpf-Maier P, Köpf H (1979) *Z. Naturforsch.* 34: 805
8. Mirabelli CK, Johnson RK, Sung CM, Faucette L, Muirhead K, Crooke ST (1985) *Cancer Res.* 45: 32
9. Berner-Price SF, Mirabelli CK, Johnson RK, Maltern MR, McCabe FL, Faucette LF, Sung CM, Mong S, Sadler PJ, Crooke ST (1986) *Cancer Res.* 46: 5486
10. Mirabelli CK, Hill DT, Faucette LF, McCabe FL, Girard GR, Bryan DB, Sutton BM, Bartus JO, Crook ST, Johnson RK (1987) *J. Med. Chem.* 30: 2181
11. Snyder RM, Mirabelli CK, Johnson RK, Sung CM, Faucette LF, McCabe FL, Zimmerman JP, Hempel JC, Crooke ST (1986) *Cancer Res.* 46: 5054
12. Gills DS (1984) In: Hacker MP, Douple EB, Krakoff IH (eds) *Platinum coordination complexes in cancer chemotherapy.* Martinus Nijhoff, Boston p 267
13. Sava G, Zorzet S, Giraldi T, Mestroni G, Zassinovich G (1984) *Eur. J. Cancer Clin. Oncol.* 20: 841
14. Clarke MJ (1988) In: Nicolini M (ed) *Platinum and other metal coordination compounds in cancer chemotherapy.* Martinus Nijhoff, Boston p 582
16. Crowe AJ, Smith PJ, Atassi G (1980) *Chem. Biol. Interact* 32: 171
17. Meinema HA, Liebrechts AMJ, Budding HA, Bulten EJ (1985) *Rev. Si, Ge, Sn and Pb Comp.* 8: 157
18. Heim ME, Flechtner H, Keppler BK (1988) *J. Cancer Res. Clin. Oncol.* 114 (Suppl): 531
19. Timmer K, Meinema HA, Schurig JE (1986) [Nederlandse Centrale Organisatie voor Toegepast Natuurwetenschappelyk Onderzoek], *Eur Pat Appl* 86201853.8
20. Catino JJ, Francher DM, Edinger KJ, Stringfellow DA (1985) *Cancer Chemother. Pharmacol.* 15: 240
21. Catino JJ, Francher DM, Schurig JE (1986) *Cancer Chemother. Pharmacol.* 18: 1
22. Geran RI, Greenberg NH, MacDonald MM, Schumacher AM, Abbott BJ (1972) *Cancer Chemother. Rep.* 3: 1
23. Rose WC, Schurig JE, Huftalen JB, Bradner WT (1983) *Cancer Res.* 43: 1504

24. Rose WC (1986) *Anticancer Res.* 6: 557
25. Corbett TH, Griswold DP, Roberts BJ, Peckham JC, Schabel FM (1978) *Cancer Treat. Rep.* 62: 1471
26. Schabel FM, Skipper HE, Laster WR, Trader MW, Thompson SA (1966) *Cancer Chemother. Rep.* 50: 55
27. Kohn KW, Ewig RAG, Erickson LC, Zwelling LA (1981) In: Friedberg EC, Hanault PC (eds) *DNA repair: a laboratory manual of research techniques.* Marcel Dekker, NY, p 379
28. Long BH, Musial ST, Brattan MG (1984) *Biochem.* 23: 1183
29. Mirabelli CK, Johnson RK, Hill DT, Faucette LF, Girard GR, Kew GY, Sung CM, Croke ST (1986) *J. Med. Chem.* 29: 218
30. Johnson RK, Jarrett PS, Mong SM, Sadler PJ, Bartus JO, Croke ST, Mirabelli CK, Mattern MR (1987) *Proc. Amer. Assoc. Cancer Res.* 28: 316
31. Mirabelli CK, Rush GF, Jensen BD, Bartus JO, Sung CM, Reberts DW, Gennaro DE, Hoffstein ST, Johnson RK, Croke ST (1987) *Proc. Amer. Assoc. Cancer Res.* 28: 313
32. McCabe FL, Faucette LF, Bartus JO, Sung CM, Jensen BD, Rush GF, Mirabelli CK, Johnson RK (1987) *Proc. Amer. Assoc. Cancer Res.* 28: 315

Clinical Studies with Budotitane — A New Non-Platinum Metal Complex for Cancer Therapy

Manfred E. Heim¹, Henning Flechtner¹, and Bernhard K. Keppler²

¹ Onkologisches Zentrum, Klinikum Mannheim, Universität Heidelberg, Theodor-Kutzer-Ufer, D-6800 Mannheim, FRG

² Anorganisch-Chemisches Institut der Universität Heidelberg, Im Neuenheimer Feld 270, D-6900 Heidelberg, FRG

The new antitumor-active transition metal complex diethoxybis(1-phenylbutane-1,3-dionato)titanium(IV) (INN Budotitane, DBT) has demonstrated antitumor activity in several experimental tumor models. The cytotoxic activity of DBT in the AMMN-induced autochthonous colorectal carcinoma in the rat appeared especially promising. In the preclinical toxicity studies, liver toxicity, mild nephrotoxicity, but no myelosuppression was observed.

In a phase-I study patients with histologically confirmed malignant tumors no longer amenable to standard treatments were treated with DBT to determine the maximum tolerated single and repeated dose. The starting dose was chosen as $1/10$ of the acute LD_{10} in rats. Three patients were treated at each nontoxic dose level. Dose escalation was performed with initial dose increments of 100%, subsequent 50% as long as no toxicity was observed and 25% in the case of mild toxicity. Safety laboratory controls and pharmacokinetic studies were performed during treatments. Single dose levels of 1, 2, 4, and 6 mg/kg body weight as short i.v. infusion could be given without toxicity. At a dose of 9 mg/kg a reversible impairment of the gustatory sense was observed, at 14 mg/kg a moderate increase of liver enzymes and LDH was seen. Two of the three patients receiving 21 mg/kg developed a dose-limiting nephrotoxicity. The repeated dose application of 100, 120, and 150 mg/m² twice a week for a 4 week period (3 patients at each dose level) was well tolerated and further dose escalation is planned.

1 Introduction	218
2 Patients and Methods	219
3 Results	220
4 Discussion	222
5 References	222

1 Introduction

The introduction of the inorganic metal complex *cis*-diamminedichloroplatinum(II) (INN: cisplatin) into cancer therapy in the late seventies was a major progress in clinical oncology ¹⁾.

Besides the platinum complexes, only three other inorganic metal complexes, the germanium complexes (spirogermanium, germanium-132), gallium nitrate, and budotitane were evaluated in clinical trials for their antitumor activity ^{2,3,4)}. While the other drugs mentioned have already been tested in several phase I and II studies, the first clinical dose-finding and tolerability studies with budotitane have just begun.

The antitumor activity of the bis- β -diketonato metal complexes was first described in 1982 ⁵⁾. Of this class of metal complexes budotitane (diethoxybis(1-phenylbutane-1,3-dionato)titanium) was selected for further development (Fig. 1). The antitumor activity of budotitane was examined in numerous tumor systems (Table 1) ⁵⁻⁹⁾. The survival time of sarcoma 180 ascitic tumor-bearing mice could be tripled. The subcutaneously transplanted sarcoma 180 can be cured in a similar way, while the intramuscularly transplanted sarcoma 180 is a little less sensitive to chemotherapy. There is only marginal activity in P 388 and L 1210 leukemia.

Excellent activity was seen in the MAC 15 A colon adeno-carcinoma and in the autochthonous AMMN-induced colorectal tumors. This tumor model seems especially relevant to the human situation, as only 5-fluorouracil (5-FU) shows some activity. Budotitane was significantly more active than 5-FU and cisplatin in this model. Preclinical toxicity studies showed that the LD₅₀ in female SD rats was 60–80 mg/kg i.v. single dose, and twice as high for mice. Main side effects were hepatotoxicity (liver necroses) and hemorrhagic pleural effusions. Other findings were hyaline thrombi in the kidney glomeruli and increase of urea and creatinine after chronic application (up to 18 mg/kg 2x/week over 12 weeks). No myelosuppression or emesis was observed ⁸⁾. Studies on the mutagenicity of budotitane, using the *Salmonella thyphimurium* mammalian microsome assay of Ames, did not produce signs of

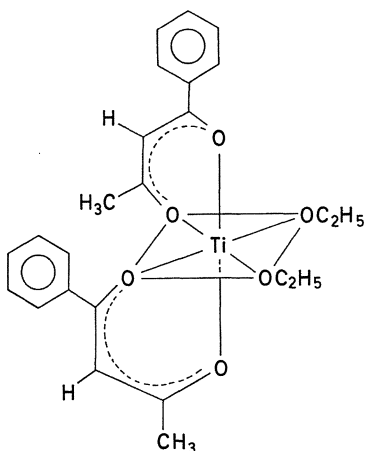


Fig. 1. Diethoxybis(1-phenylbutane-1,3-dionato)titanium(IV), INN: Budotitane

Table 1. Activity of budotitane in experimental tumor models

Tumor model	Evaluation parameter 1	Optimum T/C value ² (%)
Sarcoma 180 ascitic tumor	ST	300
Sarcoma 180 tumor, Subcutaneously growing	TW	0
Sarcoma 180 tumor, Intramuscularly growing	TW	30
Walker 256 carcinosarcoma	ST	200
L 1210 leukemia	ST	130
P 388	ST	130
Colon ascitic adenocarcinoma MAC 15A	ST	200
Autochthonous AMMN-induced colorectal	ST	146
	TW	20

¹ ST = survival time,

TW = tumor weight;

² T/C (%) = median tumor weight or survival time of treated animals versus control animals \times 100.

mutagenic potential¹⁰). A clinical phase I study with cancer patients was started in 1986. The aim of this phase I study was to determine the maximum tolerated dose (MTD), the most frequent toxic effects, and the dose-limiting toxicity of this new compound.

2 Patients and Methods

Only those patients with histologically confirmed malignant tumors for whom no other standard treatment procedure was available were candidates for this phase I study. Other criteria were: age between 18 and 75, Karnofsky performance index of 40 or better, no major organ dysfunctions, no cytotoxic treatment during the last four weeks, an estimated life expectancy of at least three months. Informed consent following a full explanation of the purpose and the limited expectations of the study was obtained before starting treatment. Three patients were treated at each dose level. Dose escalation was performed with initial dose increments of 100%, subsequent 50% as long as no toxicity was observed, and 25% if mild toxicity was observed (Gottlieb method)¹¹).

In the first part of the study single dose administration was evaluated. In the second part budotitane was given twice a week over four weeks. The maximum tolerated dose was defined as that dose which was not followed by toxicity of grade 2 according to WHO criteria or other toxicities of comparable intensity¹²).

To assess the toxicity of the drug, the following laboratory safety parameters were determined before, and one and seven days after treatment:

- differential blood count, reticulocytes
- blood chemistry (Ca, Na, K, LDH, SGOT, SGPT, AP, γ -GT, lipase, amylase, bilirubin, uric acid, creatinine, total protein, albumin, glucose)

- coagulation analysis
- urinalysis.

For pharmacokinetic studies, blood was drawn 10 minutes, 1, 2, 8, 24 hours, and 7 days after the budotitane infusion. The titanium concentration in serum and red blood cells was detected by atomic absorption spectroscopy.

Budotitane was applied in the form of a cremophorEL/propylene glycol coprecipitate. The substance was given as a short infusion into a peripheral or a central vein over a period of 30 minutes.

3 Results

The starting dose was chosen according to animal toxicity studies as $1/10$ acute LD₁₀ in rats. In the single dose application, 7 dose levels of 1, 2, 4, 6, 9, 14, and 21 mg/kg of body weight have been evaluated. All patients were pretreated with different chemotherapy regimens. A few patients were treated over two or three dose levels with at least a six-week interval between applications (Table 2).

The first drug-related toxicity was observed at a dose of 9 mg/kg, when a patient complained about a reversible impairment of the sense of taste shortly after the infusion. A moderate increase in liver enzymes and LDH was observed at a dose of 14 mg/kg. Nephrotoxicity with an increase in urea and creatinine of grade 2 WHO was dose-limiting at the 21 mg/kg dose level in two patients. In both patients pretreat-

Table 2. Patient characteristics single dose application

7 Dose levels	21 Dose applications
	N = 14
Single dose	: 9
Dose escalation	
— 2 levels	: 3
— 3 levels	: 2
Median age in years (range)	: 57 (43–75)
Sex: female: 9	
Male: 5	
Number of prior chemotherapy-regimen:	
One	: 2
Two	: 5
Three	: 5
Four	: 2
Primary tumor: colorectal	: 9
lung	: 1
breast	: 1
melanoma	: 1
renal cell	: 1
soft-tissue sarcoma	: 1
Multiple dose application:	
3 dose levels (100, 120, 150 mg/m ² × 8 in 4 weeks)	
8 patients (5 colorectal carcinoma, 2 melanoma,	
1 renal cell carcinoma).	

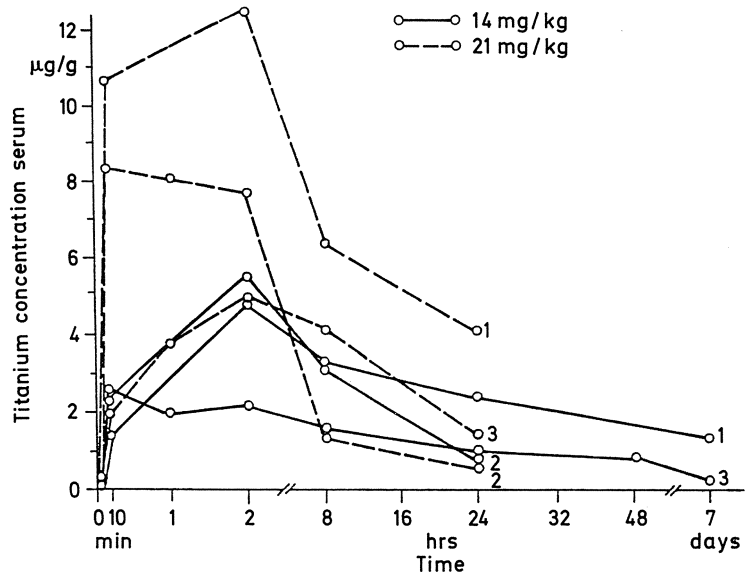
Table 3. Budotitane human toxicity

Tumor	Dose level (mg/kg)	Dose (mg)	Toxicity
Soft tissue sarcoma	9	630	None
Breast-CA	9	500	None
Malignant melanoma	9	730	Ageusia
M. melanoma	14	1000	Ageusia
Colorectal CA	14	720	Nausea, increase in liver enzymes
Renal cell CA	14	800	LDH Increase, Hypogeusia
M. melanoma	21	1500	Ageusia
Renal cell CA	21	1900	Increased Creatinine (WHO 2), Liver enzymes
Colorectal CA	21	1200	Increased Creatinine (WHO 2)

ment creatinine clearance had been normal. Urea and creatinine returned to normal values over a period of 10 weeks.

Nephrotoxicity was accompanied by nausea, weakness, and malaise. Myelosuppression was not observed at any of the tested dose levels (Table 3).

The maximum tolerated single dose of budotitane thus was between 14 and 21 mg/kg. The recommendation for the repeated dose application is 21 mg/kg (800 mg/m²) total dose divided into 8 applications of 100 mg/m² twice a week over a four-week period. So far 3 patients at each dose level were treated with 100, 120, and 150 mg/m² BSA 8 times in 4 weeks. No hepatotoxicity or nephrotoxicity were

**Fig. 2.** Titanium concentration in the serum after single dose application

observed at these dose levels, while all patients experienced the described gustatory changes.

At a dose of 14 mg/kg of budotitane titanium concentration in the serum reached values between 2 and 5 $\mu\text{g/g}$, and at a dose of 21 mg/kg values between 5 and 12 $\mu\text{g/g}$. Titanium could be detected in the serum 7 days and, in one case, even four weeks after a single dose application (Fig. 2). In red blood cells titanium was detected at concentrations of 1–2 $\mu\text{g/g}$.

4 Discussion

In these preliminary results of an ongoing phase I study the spectrum of observed adverse reactions was similar to preclinical toxicological studies. For the single dose application, nephrotoxicity was dose-limiting. A prophylactic hyperhydration and diuresis might prevent nephrotoxicity, as is well known for the cisplatin-induced renal damage. The clinical studies did not show any emetic potential of the drug budotitane except in one patient. In contrast to animal toxicity studies no local toxicity could be observed in man, not even in a few cases with accidental paravenous injection. The fact that there was no myelosuppression at all is of special interest to the clinical situation as it facilitates combination chemotherapy with other cytotoxic drugs.

As a rather unusual side effect, patients complained about a reversible impairment of the sense of taste shortly after budotitane infusion. The mechanism of this toxicity is still unclear.

The detection of titanium in the serum and in the red blood cells did not yet produce sufficient pharmacokinetic data. Further pharmacokinetic studies are necessary to obtain more information about the fate of the drug, its metabolism, and organ distribution.

The optimum dose schedule for clinical phase II studies with repeated applications has not yet been exactly determined. Experiences with a multiple dose schedule do suggest that the total dose can be increased considerably without any severe toxicity.

5 References

1. Prestayko AW, Crooke ST, Carter SK (eds) (1980) Cisplatin — current status and new developments. Academic Press, Inc. New York
2. Slavik M, Blanc O, Davis J (1983) Spirogermanium: A new investigational drug of novel structure and lack of bone marrow toxicity. *Invest New Drugs* 1: 225
3. Miyao K, Onishi T, Asai K, Tomizawa S, Suzuki F (1980) Toxicology and phase I studies on a novel organogermanium compound, Ge-132. In: Current chemotherapy and infectious disease, Vol II. Nelson JD, Grassi C (eds) The American Society for Microbiology: Washington, pp 1527
4. Hopkins SJ (1981) Gallium Nitrate. *Drugs of the Future* IV: 228
5. Keller HJ, Keppler BK, Schmähl D (1982) Antitumor activity of *cis*-dihalogenobis(1-phenyl-1,3-butane-dionato)titanium(IV) compounds against Walker 256 carcinosarcoma. *Arznei-Forsch/Drug Res* 32 (II) 8: 806
6. Keppler BK, Heim ME (1988) Antitumor-active bis- β -diketonato metal complexes: budotitane — a new anticancer agent. *Drugs of the Future* 13: 637

7. Keppler BK, Michels K (1985) Antitumor activity of 1,3-diketonato zirconium(IV) and hafnium(IV) complexes. *Arzneim-Forsch/Drug Res* 35 (II) 12: 1837
8. Keppler BK, Schmähl D (1986) Preclinical evaluation of dichlorobis(1-phenylbutane-1,3-dionato)-titanium(IV) and budotitane. *Arzneim-Forsch/Drug Res* 36 (II) 12: 1822
9. Bischoff H, Berger MR, Keppler BK, Schmähl D (1987) Efficacy of β -diketonato complexes of titanium, zirconium, and hafnium against chemically induced autochthonous colonic tumors in rats. *J Cancer Res Clin Oncol* 113: 446
10. Keppler BK, Heim ME, Flechtner H, Wingen F, Pool BL (in press) Antitumor activity of budotitane in three different transplantable tumor systems, its mutagenicity, and first results of clinical phase I studies. *Drug Res*
11. EORTC New Drug Development Committee (1985) EORTC guidelines for phase I trials with single agents in adults. *Eur J Cancer Clin Oncol* 21: 1005
12. WHO Handbook for reporting results of cancer treatment (1979) WHO publication No 48, Geneva

Author Index Volumes 1–10

The volume numbers are printed in italics

- Artur, Y., Siest, G., Sanderink, G. J., Wellman, M., Galteau, M. M., Schiele, F.: Reference Values and Drug Effects on Hepatic Enzymes. *8*, 75–92 (1989).
- Azria, M.: Calcitonins — Physiological and Pharmacological Aspects. *9*, 1–34 (1989).
- Bartle, W. R., Walker, S. E., Winslade, N. E.: Pharmacokinetic Drug Interaction. *5*, 101–132 (1987).
- Blanckaert, N., Fevery, J., Vanstapel, F., Muraca, M.: Clinical Significance of Recent Developments in Serum Bilirubins. *8*, 105–128 (1989).
- Boehm, T. L. J.: Oncogenes and the Genetic Dissection of Human Cancer: Implications for Basic Research and Clinical Medicine. *2*, 1–48 (1985).
- Botdorf, M. B., Evans, W. E.: Drug Concentration Monitoring. *7*, 1–16 (1988).
- Braun, V. and Winkelmann, G.: Microbial Iron Transport — Structure and Function of Siderophores. *5*, 67–100 (1987).
- Farrell, N.: Metal Complexes as Radiosensitizers. *10*, 89–110 (1989).
- Flückiger, R., Berger, W.: Monitoring of Metabolic Control in Diabetes Mellitus: Methodological and Clinical Aspects. *3*, 1–27 (1986).
- Clarke, M. J.: Ruthenium Chemistry Pertaining to the Design of Anticancer Agents. *10*, 25–40 (1989).
- Costa, M., Kraker, A. J., Patierno, S. R.: Toxicity and Carcinogenicity of Essential and Nonessential Metals. *1*, 1–45 (1984).
- Griffiths, J.: Enzymatic Profiles of Hepatic Disease Investigated by Alkaline Phosphatase Isoenzymes and Isoforms. *8*, 63–74 (1989).
- Grossmann, Ch. J. and Roselle, G. A.: The Control of Immune Response by Endocrine Factors and the Clinical Significance of Such Regulation. *4*, 1–56 (1987).
- Grünwald, S. and Pfeifer, G. P.: Enzymatic DNA Methylation. *9*, 61–104 (1989).
- Heim, M. E., Flechtner, H., Keppler, B. K.: Clinical Studies with Budotitan — A New Non — Platinum Metal Complex for Cancer Therapy. *10*, 217–224 (1989).
- Hidaka, H. and Hagiwara, M.: Biopharmacological Regulation of Protein Phosphorylation. *5*, 25–42 (1987).
- Hubbich, A., Debus, E., Linke, R., Schrenk, W. J.: Enzyme-Immunoassay: A Review. *4*, 109–144 (1987).
- Johnson, N. P., Butour, J.-L., Villani, G., Wimmer, F. L., Defais, M., Pierson, V., Brabec, V.: Metal Antitumor Compounds: The Mechanism of Action of Platinum Complexes. *10*, 1–24 (1989).
- Keppler, B. K., Henn, M., Juhl, U. M., Berger, M. R., Niebl, R., Wagner, F. E.: New Ruthenium Complexes for the Treatment of Cancer. *10*, 41–70 (1989).
- Kirchner, H.: Interferon Gamma. *1*, 169–203 (1984).
- Köpf-Maier, P.: The Antitumor Activity of Transition and Main-Group Metal Cyclopentadienyl. *10*, 151–184 (1989).
- Köppe, H. G.: Recent Chemical Developments in the Field of Beta Adrenoceptor Blocking Drugs. *3*, 29–72 (1986).
- Klotz, U.: Clinical Pharmacology and Benzodiazepines. *1*, 117–167 (1984).

- Kuhns, W. J. and Primus, F. J.: Alteration of Blood Groups and Blood Group Precursors in Cancer. *2*, 49-95 (1985).
- Meddings, J. B. and Dietschy, J. M.: Regulation of Plasma Low Density Lipoprotein Levels: New Strategies for Drug Design. *5*, 1-24 (1987).
- Mestroni, G., Alessio, E., Calligaris, M., Attia, W. M., Quadrifoglio, F., Cauci, S., Sava, G., Zorzet, S., Pacor, S., Monti-Bragadin, C., Tamaro, M., Dolzani, L.: Chemical, Biological and Antitumor Properties of Ruthenium (II) Complexes with Dimethylsulfoxide. *10*, 71-88 (1989).
- Moss, D. W.: Alkaline Phosphatase in Hepatobiliary Disease. *8*, 47-62 (1989).
- Mountford, C. E., Holmes, K. T., Smith, I. C. P.: NMR Analysis of Cancer Cells. *3*, 73-112 (1986).
- Nickoloff, E. L.: The Role of Immunoassay in the Clinical Laboratory. *3*, 113-155 (1986).
- Niemeyer, U., Engel, J., Hilgard, P., Peukert, M., Pohl, J., Sindermann, H.: Mafosfamide — A Derivative of 4-Hydroxycyclophosphamide. *9*, 35-60 (1989).
- Obermeier, R. and Zoltobrocki, M.: Human Insulin — Chemistry, Biological Characteristics and Clinical Use. *2*, 131-163 (1985).
- Percy-Robb, I. W.: The Clinical Biochemistry of Hepatobiliary Diseases. *8*, 1-16 (1989).
- Roda, A., Festi, D., Armanino, C., Rizzoli, R., Simoni, P., Minutello, A., Roda, E.: Methodological and Clinical Aspects of Bile Acid Analysis in Biological Fluid. *8*, 129-174 (1989).
- Rosalki, S. B.: Plasma Amylase in Pancreatic and Hepatobiliary Disease. *8*, 93-104 (1989).
- Rubinstein, A. and Robinson, J. R.: Controlled Drug Delivery. *4*, 71-108 (1987).
- Sacchetti, L., Castaldo, G., Salvatore, F.: The Serum Gamma-glutamyltransferase Isoenzyme System and its Diagnostic Role in Hepatobiliary Disease. *8*, 17-46 (1989).
- Schurig, J. E., Meinema, H. A., Timmer, K., Long, B. H., Casazza, A. M.: Antitumor Activity of Bis[Bis(Diphenylphosphino) Alkane and Alkene] Group VIII Metal Complexes. *10*, 205-216 (1989).
- Scott, E. V., Zon, G., Marzilli, L. G.: NMR Relaxation Footprinting: The $[\text{Cr}(\text{NH}_3)_6]^{3+}$ Cation as a Probe for Drug Binding Sites on Oligonucleotides. *10*, 185-204 (1989).
- Smith, R. D., Wolf, P. S., Regan, J. R., and Jolly, S. R.: The Emergence of Drugs which Block Calcium Entry. *6*, 1-152 (1988).
- Srivastava, S. C., Mausner, L. F., Clarke, M. J.: Radioruthenium-Labeled Compounds for Diagnostic Tumor Imaging. *10*, 111-150 (1989).
- Trager, W., Perkins, M. E., Lanners, H. N.: Malaria Vaccine. *4*, 57-70 (1987).
- Suzuki, K., Ohno, Sh., Emori, Y., Imajoh, Sh., Kawasaki, H.: Calcium-Activated Neutral Protease (CANP) and its Biological and Medical Implications. *5*, 43-66 (1987).
- Truscheit, E., Hillebrand, I., Junge, B., Müller, L., Puls, W., Schmidt, D. D.: Microbial Alpha-Glucosidase Inhibitors: Chemistry, Biochemistry and Therapeutic Potential. *7*, 17-99 (1988).
- Wenger, R. M., Payne, T. G., Schreier, M. H.: Cyclosporine: Chemistry, Structure-Activity Relationships and Mode of Action. *3*, 157-191 (1986).
- Werner, M.: Strategies to Integrate Laboratory Information into the Clinical Diagnosis of Hepatic and Acute Pancreatic Disease. *8*, 175-186 (1989).
- Werner, R. G.: Secondary Metabolites with Antibiotic Activity From the Primary Metabolism of Aromatic Amino Acids. *1*, 47-115 (1984).
- Weser, U. and Deuschle, U.: Copper in Inflammation. *2*, 97-130 (1985).
- Will, H.: Plasminogen Activation: Molecular Properties, Biological Cell Function and Clinical Application. *7*, 101-146 (1988).